Republic of Iraq

Shiite Endowment Diwan

AL AABIA

PRINT ISSN
2312-5721
ONLINE ISSN
2313-0083

Quarterly Refereed Journal for Natural and Engineering Sciences

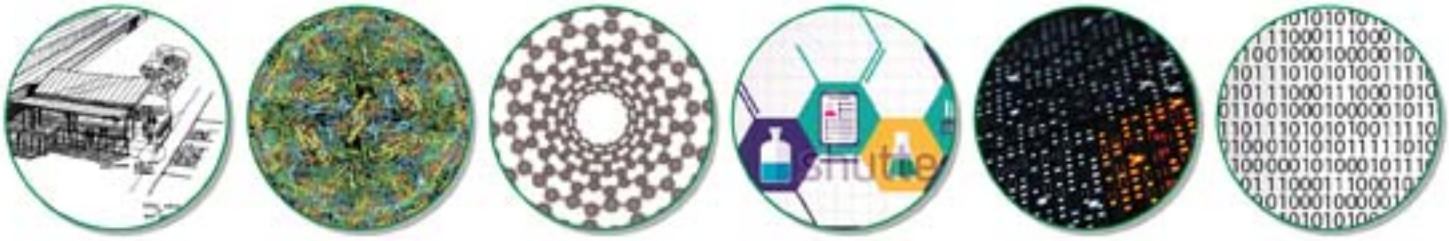

The influence of some additives on flammability and mechanical properties of modified polyester containing heterocyclic ring composites

Molecular and bioinformitic analysis of ITS1 region of three Eimeria species in Kerbala and Babylon provinces , Iraq

Spectroscopic Properties of Different Concentration Xanthene's Dye Mixture (6G, 3GO, B & C) Solution in Chloroform

Computation of inheritance share in Islamic Law by an expert system using Decision Tables

Fourth Year, Fourth Volume, Issue 1 and 2
Shaaban 1436, June 2015

Republic of Iraq
Shiite Endowment Diwan

AL BAHIA

Quarterly Refereed Journal
for Natural and Engineering Sciences

Issued by
Al-`Abbas Holy Shrine
International Al-`Ameed Centre for Research and Studies

Licensed by
Ministry of Higher Education
and Scientific Research

Fourth Year, Fourth Volume, Issue 1 and 2
Shaaban 1436, June 2015

Al-Ameed International Center

for Research and Studies

Print ISSN: 5721 – 2312
Online ISSN: 0083 – 2313
Consignment Number in the Housebook and Iraqi Documents: 1996, 2014

Iraq - Holy Karbala

Tel: +964 032 310059
Mobile: +964 760 235 5555
http://albahir.alkafeel.net
Email: albahir@alkafeel.net

Publication Conditions

Inasmuch as Al-`Bahir- effulgent- Abualfadhal Al-`Abbas cradles his adherents from all humankind, verily Al-Bahir journal does all the original scientific research under the conditions below:

1. Publishing the original scientific research in the various scientific sciences keeping pace with the scientific research procedures and the global common standards; they should be written either in Arabic or English and have never been published before.

2. Being printed on A4 using Word Program, delivering a copy and CD having, approximately, 10,000 - 15,000 words under simplified Arabic or times new Roman font witout using scan for the figures.

3. Delivering the abstracts, Arabic or English, not exceeding a page, 350 words, with the research title.

4. The front page should have the title; the name of the researcher / researchers, occupation, address, telephone number and email, and taking cognizance of averting a mention of the researcher / researchers in the context.

5. Making an allusion to all sources in the endnotes,and taking cognizance of the common scientific procedures in documentation; the title of the book, editor, publisher, publication place, version number, publication year and page number. Such is for the first mention to the meant source, but if being iterated once more, the documentation should be only as; the title of the book and the page number.

6. The references of the paper have to be mentioned by using the numbers according to their mentioning in the paper itself .These references have to be mentioned at the end of the paper.

7. Printing all tables, pictures and portraits on attached papers, and making an allusion to their sources at the bottom of the caption, in time there should be a reference to them in the context.

8. Attaching the curriculum vitae, if the researcher cooperates with the journal for the first time, so it is to manifest whether the actual research submitted to a conference or a symposium for publication or not. There should be an indication to the sponsor of the project, scientific or nonscientific, if any.

9. The research should never have been published previously, or submitted to any means of publication; in part, the researcher is to make a covenant certifying the abovementioned cases.

10. In the journal all the published ideas manifest the viewpoints of the researcher himself / herself it is not necessary to come in line with the issuing vicinity, in time, the research stratification is subject to technical priorities.

11. All research should be exposed to Turnitin processes and a confidential revision to state their reliability for publication. No research retrieved to researchers; whether they are approved or not; it takes the procedures below:

A: A researcher should be notified to deliver the meant research for publication

B: A researcher whose paper approved is to be apprised of the edition chief approval and the eminent date of publication.

C: With the rectifiers reconnoiters some renovations or depth,before publishing, the research has to be retrieved to the researchers to accomplish them for publication.

12: A researcher bestowed a version in which the meant research published, and a financial reward.

13. Taking into consideration some points for the publication priorities, as follows:

A: Research participated in conferences adjudicated by the issuing vicinity.

B: The date of research delivery to the edition chief.

C: The date of the research that has been renovated.

14. The Researcher can deliver her/his research paper to us either via Journal website http:// albahir.alkafeel.net , she/he/has to fill the standard format , or Al-Ameed Journal building (Al-Kafeel Cultural Association), behind Al-Hussein (PBUH) Amusement City, Al-Hussein (PBUH) Quarter, Holy Karbala, Iraq

In the Name of Allah
Most Compassionate, Mort Merciful

Edition Word

Thanks be to Allah, the Evolver of the Universe, most fragrant peace and greatest salute be upon our master Mahammad and his benevolent chaste posterity.

Now…

It is of certitude for the International Al-`Ameed Centre for Studies and Research personnel pertinent to the Holy Al-`Abbas Shrine to be in the heart of delectation for two reasons: the center pertains to our master Al-`Abbas Ibn Ali Abitalib (Peace be upon them all) , such pertinence incarnates many a shade of interpretations and gives whatsoever surges from the center a tinge of such a divine light emitting from the blessed tree of Mohammad people and from the truth tree whose roots are germinated and branch lurks in heaven.

The second reason bursts onto the scene as having the honest competition between the Al-`Ameed Centre cadre , that leads to various scientific products that run unequal in colour but equal in target and in the soul of its mission to the scientific knowledge.

As such Al-Bahir Journal heaves into aura as a pride in such a scientific atmosphere. As it is inspired for the journal to be an oasis to those who delve into the independent paper apart from the red lines “detriment to” the prolific abstract knowledge.

Issuing the current edition, a dream grows momentum, as inspired, to be in the avant garde of journals in having the Impact Factor and scientific repute the people in charge never fall short of having such targets.

Ultimately, the journal cuddles all the ardent researcher whose morale escalates to envision the products of the people of his and exerts himself in competing the other world researchers, it is not impossible as he reminiscences a history of brilliance of our nation whose monoliths are of scientific enlightened development.

The last we do pray thanks be upon Allah the Evolver of the universe, peace be upon Mohammad and his chaste benevolent posterity.

Consultation and Editaril

Molecular and bioinformitic analysis of ITS1 region of three Eimeria species in Kerbala and Babylon provinces, Iraq

***Dhamiaa Make Hamza, **Hadi Rasol Hasan Al-Massodi and *Zuhair Muhammad Ali Jeddoa**
***Collage of Medicine, University of Kerbala, Iraq.**
****Collage of Pharmacy, University of Kerbala, Iraq.**
Received Date: 10/May/2015
Accepted Date: 16/Aug/2015

الخلاصة

الانتاج العالمي للدواجن قد ازداد بمقدار ثلاثة اضعاف خلال العقدين الماضيين ويعتبر الان من المصادر الرئيسية لانتاج البروتينات الغذائية حيوانية المنشا على المستوى العالمي. تتعرض الدواجن للعديد من الامراض التي تسببها الاحياء المجهرية والتي تقلل من فعاليتاها الحيوية والانتاجية، مرض Coccidiosis الذي يسببة نوع من البدائيات apicomplexan protozoa العائدة الى جنس Eimeria يعتبر واحدا من اهم الامراض التي تصيب الدواجن. ان فهم طفيليات ال Eimeria على المستوى الحياتي يعزز في تطوير عقارات ولقاحات جديدة والذي بدوره يؤدي الى تحسين الامن الغذائي العالمي.

خمسه عشر عينة من الدنا DNA بواقع خمس عينات لكل واحدة من الانواع الثلاث من Eimeria تم تحديد تسلسل القواعد النتروجينيه اعتمادا على صف التسلسل التتابعات المتعددة باستخدام قواعد التحليل عبر الشبكة الدولية للمعلومات للجين المحدد ITS1 (Internal Transcribed Spacer 1) والذي سبق ان تم تضخيمة بعملية تفاعل انزيم البلمرة التسلسلي المقارنة بين تتابعات القواعد النتروجينية للعزلات المحلية لعزلة ال Eimeria مع العزلات العالمية والموثقة في بنك الجينات Gene bank ومقارنة الغربلة الجزيئية في الدراسة الحالية اظهرت صحة ودقة التشخيص لثلاثة انواع من Eimeria تحليل الشجرة التطورية phylogenetic tree باستخدام برنامج الحاسوب المعروف ب (MEGA6) تم اعتمادها لتحليل الشجرة الوراثية Genetic tree لتحليل الانواع لغرض مقارنة الانواع المحلية الثلاثة مع السلالات العالمية لل Eimeria وجد تشابة في تطابق التسلسلات للعزلات المحلية لل Eimeria tenella مقارنة مع بنك الجينات NCBI-Gene bank Eimeria tenella (JX853830) وباستخدام ال NCBI-BLASTE اظهرت النتائج 99% ،98% بينما التشابة في تطابق التسلسلات للعزلة المحلية Eimeria necatrix بالمقارنة مع عزلة بنك الجيناتNCBI-Gene bank Eimeria necatrix (JX83832.1) كانت 100% ،91% والتشابة في تطابق التسلسلات للعزلة المحلية Eimeria maxima الى عزلة بنك الجينات NCBI-Gene bank Eimeria maxima (JX853828.1) كانت 98%.

الكلمات المفتاحية

الإنتاج العالمي للدواجن، الأمراض التي تصيب الدواجن، طفيليات الـ(Eimeria).

Abstract

Global production of chickens has trebled in the past two decades and they are now the most important source of dietary animal protein worldwidE.Chickens are subject to many infectious diseases that reduce their performance and productivity. Coccidiosis, caused by apicomplexan protozoa of the genus Eimeria, is one of the most important poultry diseases. Understanding the biology of Eimeria parasites underpins development of new drugs and vaccines needed to improve global food security.

A Fifteen of DNA samples (five samples for each one of three species) of Eimeria has been sequenced and analyzed in which multiple sequence alignment online based analysis for the ITS1 (Internal Transcribed Spacer 1) region that previously amplified by polymerase chain reaction, A comparison between the sequences of bases of local isolates of Eimeria with global isolates that recorded in Gens Bank and the comparative molecular screening of the present study results revealed the Validity and accuracy of diagnosis of three Eimerian species.

Phylogenetic tree analysis using the program (MEGA 6) were adopted to determine genetic tree of the species analysis to compare the three of local species with global strains of Eimeria and found the Homology sequence identity of Eimeria tenella local isolates in comparison with NCBI-Gen bank Eimeria tenella (JX853830). Using NCBI-BLAST the results showed 98% and 99%, while the Homology sequence identity of Eimeria necatrix of local isolates in comparison with NCBI-Genbank Eimeria necatrix (JX853832.1) were 91% and 100 % and the Homology sequence identity of Eimeria maxima of local isolates to NCBI-Genbank Eimeria maxima (JX853828.1) was 98%.

Key words

Poultry Coccidiosis, Eimeria species, ITS1, PCR, DNA sequencing, Iraq.

Introduction

Chickens are the world's most popular food animal and the development of improved drugs and vaccines to eliminate poultry diseases are vital for worldwide food security. Protozoan parasites of the genus Eimeria cause coccidiosis, a ubiquitous intestinal disease of live stock that has major impacts on animal welfare and agro-economics [1].

It is a particularly acute problem in poultry where infections can cause high mortality and are linked to poor performance and productivity. Eimeria belong to the phylum Apicomplexa, which includes thousands of parasitic protozoa such as Plasmodium species that cause malaria, and the widely zoonotic pathogen Toxoplasma gondii [2]. Eimeria species have a direct oral-faecal life cycle that facilitates their rapid spread through susceptible hosts especially when these are housed at high densities [3]. Unsurprisingly, resistance to anticoccidial drugs can evolve rapidly under these conditions and there is a continuing need to develop novel therapies [4].

More than 1200 species of Eimeria are described [2] and virtually all of these are restricted to a single host species. The chickens can be infected by nine Eimeria species, each of which colonises a preferred region of the intestine causing symptoms of differing severity [5]. Five species induce gross pathological lesions and four of these are the most important in terms of global disease burden and economic impact (E.acervulina, E.maxima, E.necatrix and E.tenella) [6].

Diagnosis of coccidiosis is based on clinical features and pathology of host, parasite characteristics such as morphology at different

stages of parasitism, and the pre-patent period [7,8]. Analysis of these characteristics is labor intensive for diagnosis and does not provide accurate data for identification of the Eimeria species [9].

Identification and genetic characterization of different species of Eimeria genus are central to prevention, surveillance, and control of coccidiosis. This is particularly important with regard to the appearance of a widespread anticoccidial resistance of Eimeria species and the complications associated with drug residues [10].

Due to difficulties in the morphologic identification of some of chicken Eimeria spp., diagnostic laboratories are increasingly utilizing DNA-based technologies for the specific identification of the parasite [8].

So far, there is limited knowledge on the epidemiology of Eimeria infections under different rearing conditions in Iraq. In The present study, together with morphometric diagnosis, PCR assay, based on the amplification of internal transcribed spacer 1 (ITS1) regions of ribosomal DNA (rDNA) [11], and that amplified DNA would used in sequencing and Phylogenetic tree analysis using (MEGA 6) program were adopted to determine genetic tree of the species analysis (Test UPGMA tree) (Unweighted Pair Group Method with Arithmetic) to compare the local species with global strains of Eimeria which recorded in the Genbank in the Website (www.genome.jp).

1. Materials and methods

2. 1. Stool sample collection

From August 2013 to July 2014 about 200 samples of fresh fecal droppings and intestines were collected from suspected infected chickens with coccidiosis attending to the veterinary hospital and veterinary clinics were spread in Kerbala and Babylon provinces, Iraq for the examination and treatment.

The oocysts were isolated from intestines and stool of infected chickens and collected in Eppendrof tubes and stored in freezing (-80 C˚) until used in DNA extraction. [12]

DNA extraction from stool

Genomic DNA was extracted from stool samples of chicken by using AccuPrep® Stool DNA Extraction Kit (pioneer, Korea) Table (1) and done according to company instructions.

2. 2. DNA profile

For detection of DNA that extracted from stool samples through the use of a Nanodrop spectrophotometer (THERMO. USA) detects the percentage of purity and measuring the concentration of nuclic acids (DNA and RNA), Where is detected DNA concentration (ng / µl) and measuring the purity of the DNA by reading the absorbance at a wavelength at (280-260 nm).

2. 3. PCR- protocols

The DNA samples which extracted from stool samples would used in thermal cycler machine to amply the ITS1 region of rDNA using the forward and reverse primers which designed by NCBI site Table (1), according to the PCR program shown in the Table (2).

In which 50 µl of PCR master mix used for amplification of ITS1 region.

Also (5µl) of DNA template that extracted from stool samples was added then 1.5 µl of each type of Primers (forward and reverse) added to the master mix and then blend well using Exispin vortex centrifuge, then this tubes would transferred to the thermocycler machine, which has been programmed by the previous program for amplified of ITS1 region. The PCR products were electrophoresed in agarose gel and visualized on UV transllluminator and then photographed using photo documentation system.

Table (1): The sequence of the forward and reverse primers that used in the present study with their PCR product sizE.

Primer	Sequence (¯5-¯3)		Amplicon Bp
E.tenella	F	TGCAAAAGTCGTAACACGGT	525
	R	TCCAAGCAGCATGTAACGGA	
E.necatrix	F	TGCTGCTGGACTTACAGGTT	501
	R	TTCGAGCAAAAGAGTATCGCC	
E.maxima	F	AGAGCCCTCTAAAGGATGCA	503
	R	AATGCAAGACACTTCATACAGC	

Table (2): Thermal cycler program of PCR technique

Step	Temperature and duration	
Initial denaturation	95oC for 4 min	
Denaturation	94oC for 30sec	30 cycles
Annealing	59oC for 30 sec	
Elongation	72oC for 1 min	
Final elongation	72oC for 5 min	

2. 4. Measurement of DNA concentration

The DNA concentration Of the all fifteen samples were measured by Nanodrop machinE. All selected samples gave more than 100 concentration ng/ml, which consider the lowest concentration required in the process of identifying DNA sequences [13].

2. 5. DNA sequencing methods

DNA sequencing method performed for confirmative detection and Phylogenetic analysis of three local species of Eimeria that responsible for coccidiosis based on ITS1 region by Phylogenetic tree analysis using the program (MEGA 6), while the Test type was UPGMA treE.(525 bp) PCR product of the species *E.tenella*, (501 bp) PCR product of species *E.necatrix* and (503 bp) PCR product of the species *E.maxima* were purified from agarose gel by using (EZ EZ-10 Spin Column DNA Gel Extraction Kit, Biobasic. Canada). The purified DNA from PCR product samples were sent to Bioneer Company in Korea for performed the DNA sequencing (AB DNA sequencing system).

3. Statistical analysis

The results of present study analyzed statistically by Program The Statistical Analysis System (SAS) by using of the Lest Significant Difference (LSD) test and Duncan test depending on the level of probability P <0.05 to find the significant differences. [3]

Results

Out of 200 DNA samples that extracted from stool and intestins collected from chickins that clinically suspected coccidiosis were tested by convential PCR assay, only 160 samples which appeared positive and identified three species of Eimeria in both of Kerbala and Babylon provinces in Iraq. The identified species were *E.tenella* with 525 bp PCR product of ITS 1 region (Fig. 1).

Also *E.necatrix* was identified at 501 bp PCR product of ITS1 region on agarose gel electrophosis (Fig. 2).

While the last species diagnosed was *E.maxima* at 503 bp PCR product of ITS1 region as shown in the (Fig. 3).

Sequence analysis of fifteen positive samples from three species of Eimeria (Five samples for each one) were performed to confirm the PCR results. The Multiple sequence alignment analysis of ITS1 region of *E.tenella* was shown in the (Fig. 4)

while the Phylogenetic relationship tree analysis was constructed based on the five local samples of species *E.tenella* compare with other species of Eimeria through MEGA 6 program used of the test from type (UPGMA tree) as shown in the (Fig. 4).

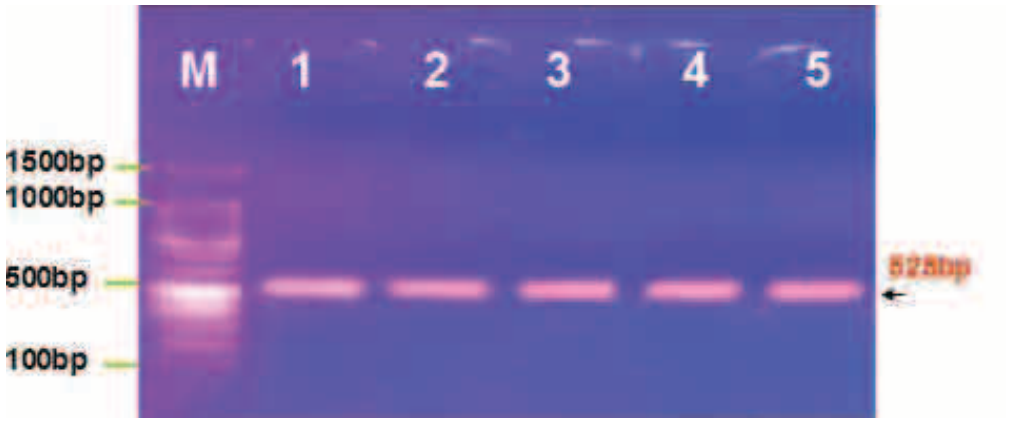

Fig. [1]: Agarose gel electrophosis show the PCR product results for E.tenella of ITS1 region where M: 1500bp ladder, Lane [1-5] are 525pb positive samples.

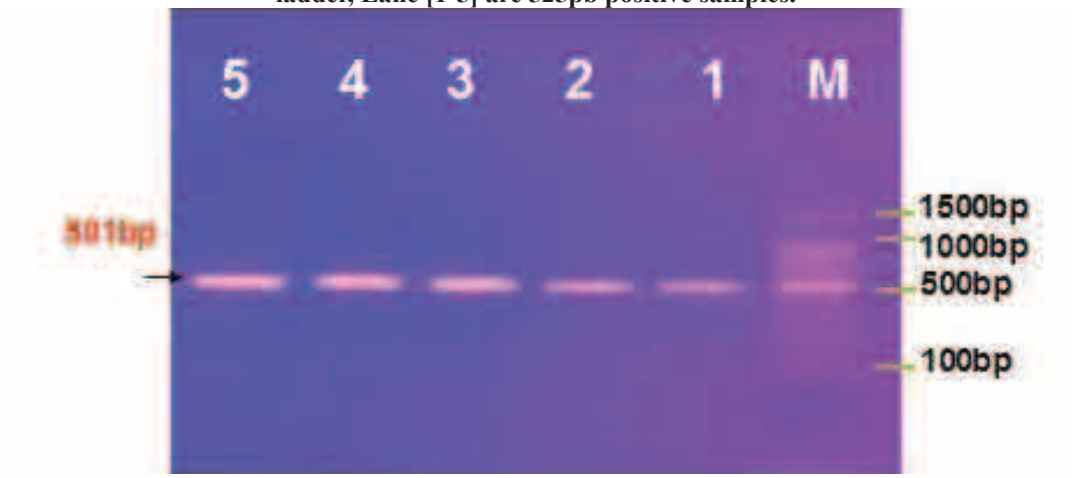

Fig. [2]: Agarose gel electrophosis show the PCRproduct results for E.necatrix of ITS1 region where M: 1500bp Ladder, Lane [1-5] are 501 bp positive samples.

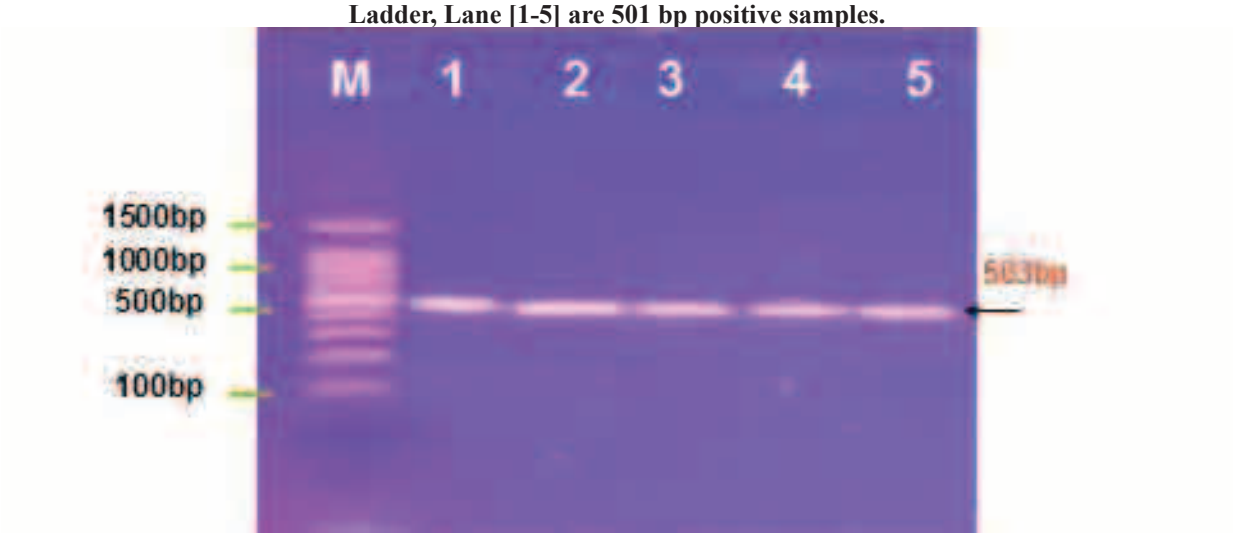

Fig. [3]: Agarose gel show the PCR product results for E.maxima of ITS1 region where M: 1500bp Ladder, Lane [1-5] are 503bp positive samples.

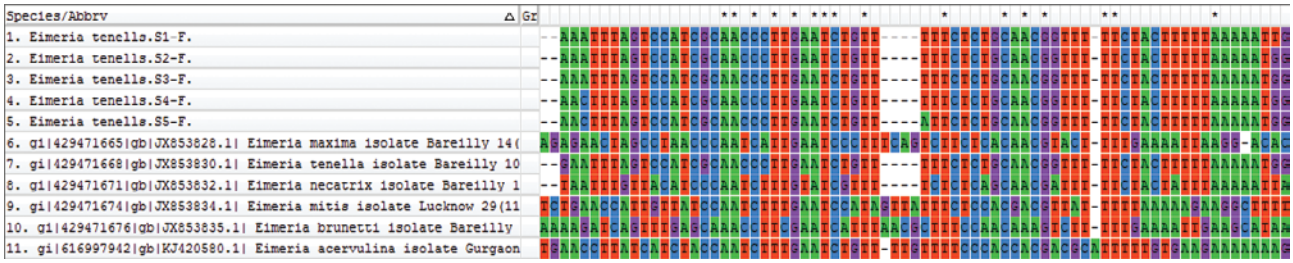

Fig. 4: The multiple alignment analysis of five local positive samples [S1, S2, S3, S4, S5] of E.tenella Comparison with other species of Eimeria.

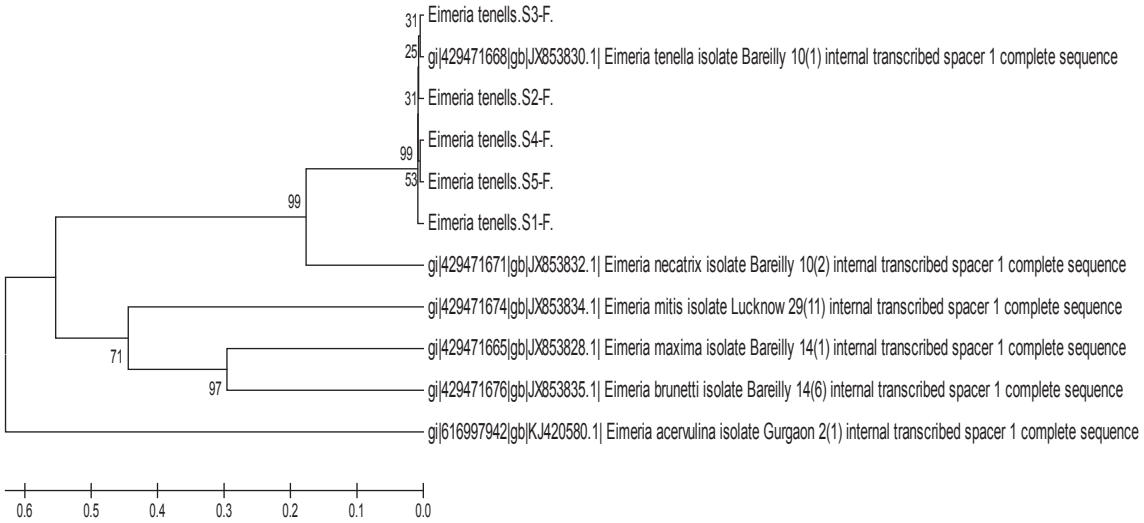

Fig. 5: The comparison between the phylogenetic Tree analysis of five local samples [S1, S2, S3, S4, S5] of E.tenella with other Eimerian species.

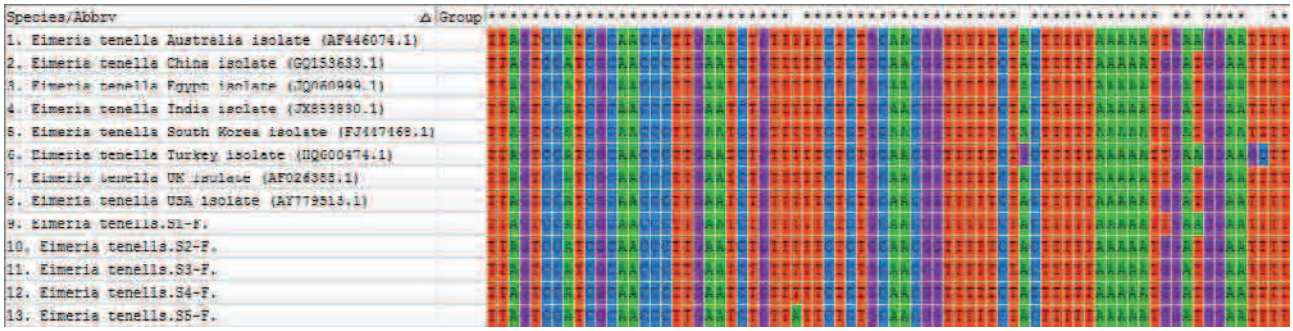

Fig. 6: The comparison in the multiple alignment analysis five local positive samples [S1, S2, S3, S4, S5] of E.tenella with global strains of species E.tenella.

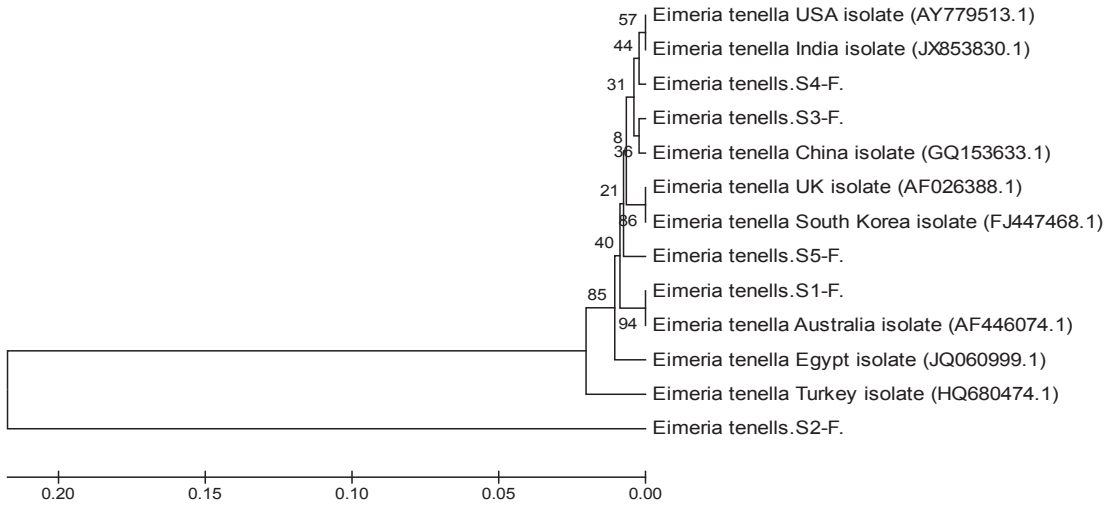

Fig. 7:The comparison between the phylogenetic tree analysis of five local samples of E.tenella with global strains of E.tenella by used of program [MEGA 6].

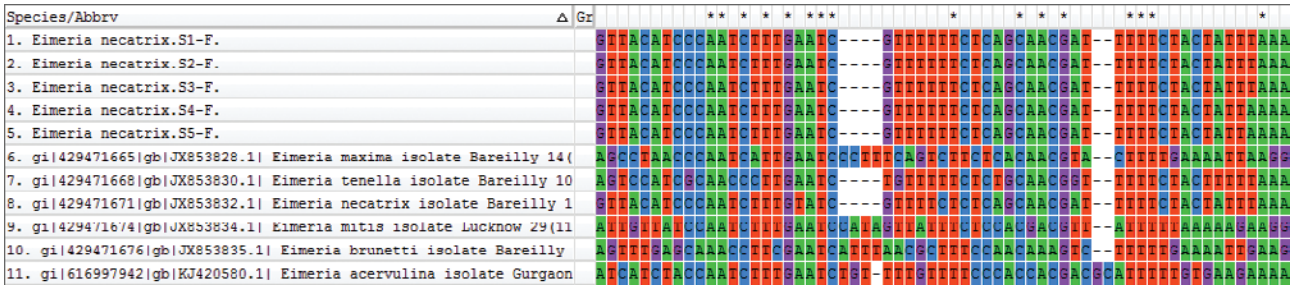

Fig. 8: The multiple alignment analysis of five local positive samples [S1, S2, S3, S4, S5] of E.necatrix comparison with other species of Eimeria.

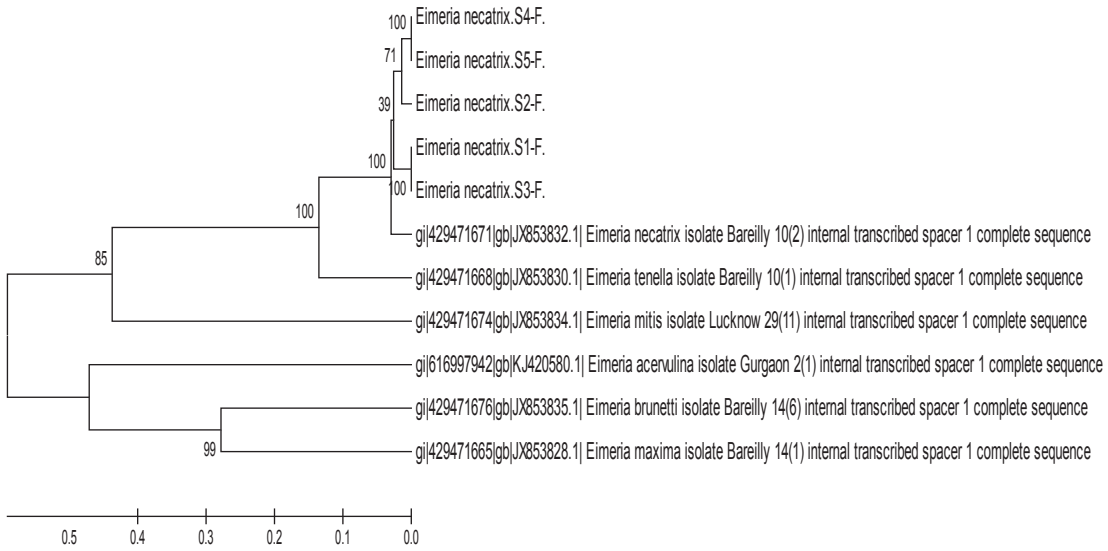

Fig. 9: The comparison between the phylogenetic tree analysis of five local samples [S1, S2, S3, S4, S5] of E.necatrix and the other Eimerian species.

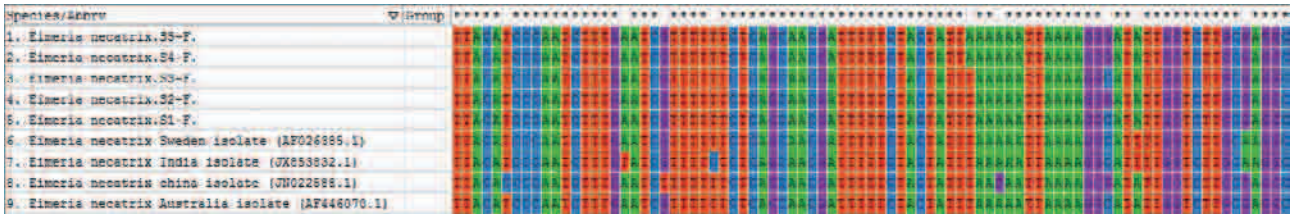

Fig. 10: The comparison of the multiple alignment analysis of five local positive samples [S1, S2, S3, S4, S5] of E.necatrix with global strains of species E.necatrix

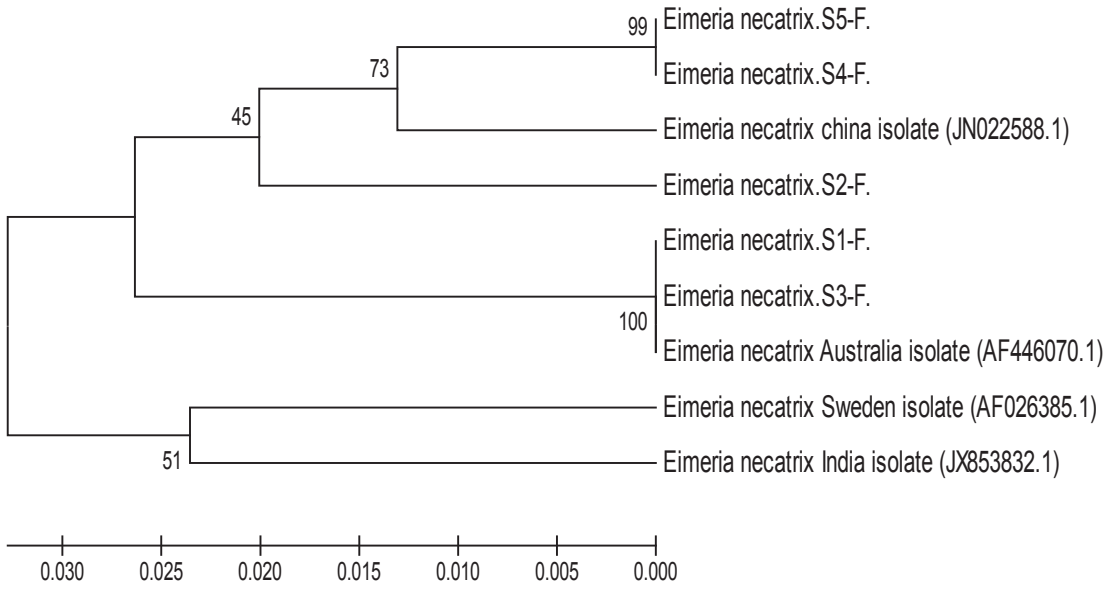

Fig. 11: The comparison between the phylogenetic tree analysis of five local samples of E.necatrix with global strains of *E.necatrix* by used of program [MEGA 6].

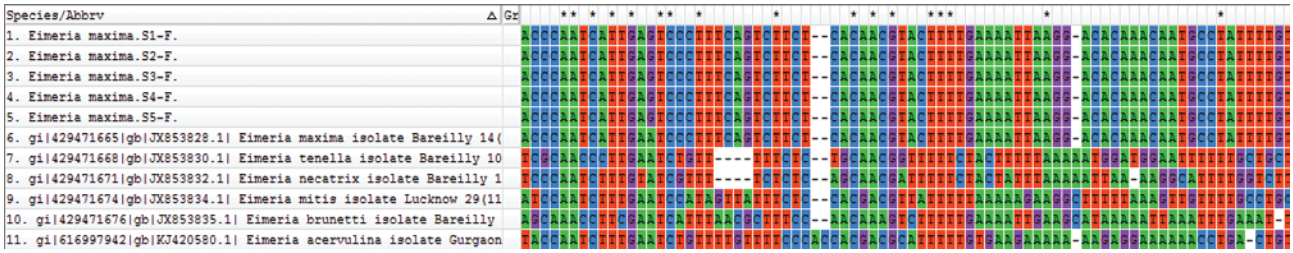

Fig. 12: Shows the multiple alignment analysis of five local positive samples [S1, S2, S3, S4, S5] of E.maxima comparison with other species of Eimeria.

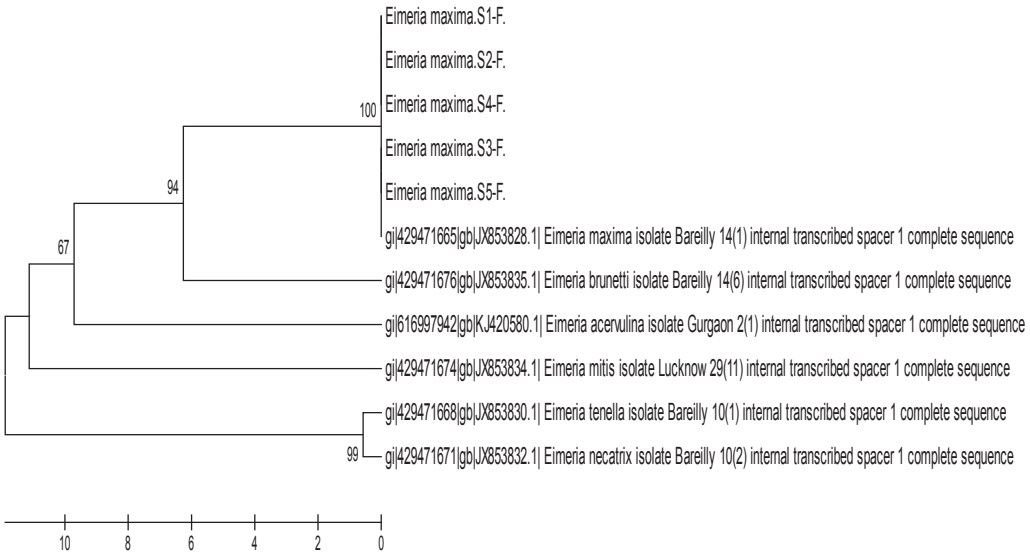

Fig. 13:The comparison between the phylogenetic Tree analysis of five local samples [S1, S2, S3, S4, S5] of E.maxima and the other Eimerian species.

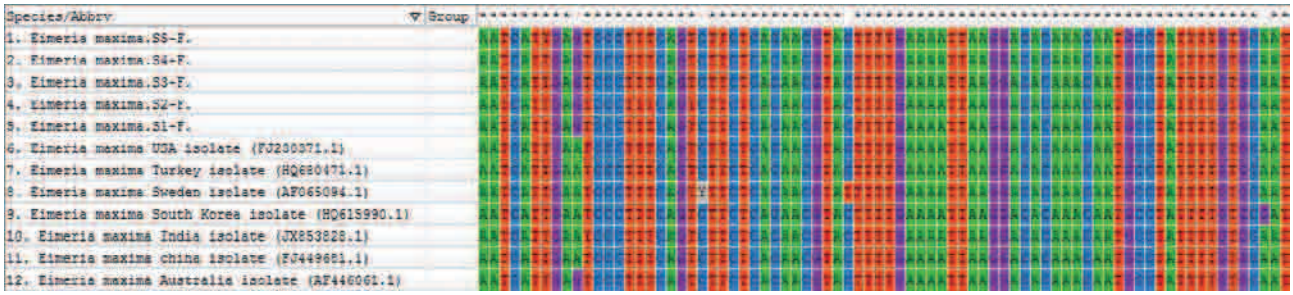

Fig. 14:The comparison of the multiple alignment analysis of five local positive samples [S1, S2, S3, S4, S5] of E.maxima with global strains of species E.necatrix.

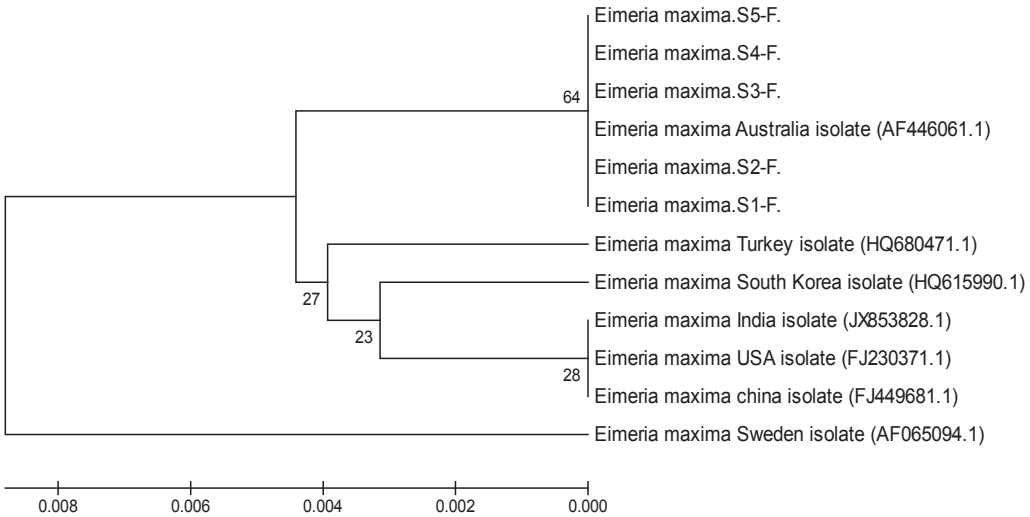

Fig. 15:The comparison between the phylogenetic tree analysis of five local samples of E.maxima with global strains of E.maxima by useing of MEGA 6 program.

4. Discussion

The specific diagnosis of Eimeria infections in chickens is clearly central to a better understanding of epidemiology and dynamics of the disease in intensive and extensive chicken establishments. This is particularly important for planning an effective prevention and control program of coccidiosis. Traditionally, diagnosis has been achieved by detecting Eimeria oocysts excreted in the feces of chickens by measuring oocyst and sporocyst dimensions or assessing the site and extent of the pathological lesions in the intestine of chickens [14].

Although the microscopic examinations can absolutely show the negative fecal samples, such traditional methods have generally had major limitations in the specific diagnosis of coccidiosis and identification of Eimeria species. These approaches are unreliable, particularly when multiple species of Eimeria simultaneously infect a single host and there is overlap in the size and shape of oocysts and the sites of infection in the intestines [8].

During recent years, there have been significant advances in the development of molecular-diagnostic tools. Several PCR based assays targeting different regions of the Eimeria genome have been described, such as the 5S rRNA, the small subunit rRNA [12, 21], the sporozoite antigen gene EASZ240/160 [14] and ITS-1 [8, 15, 17] and ITS-2 [18, 20] genomic regions. Since the ITS regions are less conserved than the rRNA genes, detecting variations in this region of DNA sequence, makes the design of primers straightforward and reduces the risk of cross reactions among different species [15].

Apart from an accurate identification of Eimeria species, molecular methods can also be helpful in epidemiological study of the parasite, an aspect that has been less investigated to datE.

At yet, there has not been any documentary report related to the occurrence and epidemiological pattern of the pathogenic Eimeria species of chickens in Iraq. Therefore, the results of the present study are the first on the prevalence of Eimeria species in the region, based on the molecular methodes.

In the present study, 200 samples of stool and intestines were collected from suspected infected chickens with coccidiosis 160 samples (80%) were positive which identified by used of molecular techniques, including Conventional PCR, by followed this technique three species of poultry Eimeria were diagnosed in the Kerbala and Babylon provinces and that species are E.tenella, E.necatrix and E.maxima the results of present study did not compare with any local studies and that due to the lack of a similar study.

Nowzari et al. in a large study including 5 provinces of Iran showed that E.maxima, E.mitis, E.brunetti, E.tenella and Eacervulina were distributed all over Iran. They identified E.mitis and E.brunetti for the first time by PCR [16]. E.brunettihas been found uncommon in broiler flocks [17]. In our study, E.tenella was the dominant species. This finding suggests that in poor management conditions, poultry houses may encounter acute coccidiosis in Kerbala and Babylon provinces due to highly pathogenic species, E.tenella.

Razmi et al, reported that prevalence of subclinical coccidiosis was 38% in Mashad,

north east of Iran and E.acervulina was the most prevalent species in broiler chicken farms [19]. In north-west of Iran, Tabriz, five Eimeria spp., E.acervulina, E.tenella, E.necatrix, E.maxima and E.mitis, were identified by morphometric study and E.acervulina was the most prevalent species [20].

Three species of Eimeria (E.acervulina, E.maxima and E.praecox (has been identified in Carolina in North America depending on PCR technique by used the amplified ITS1 of DNA that excreted from oocyst, Where the researcher recorded E.acervulina species the largest proportion compared to other species which is usually a medium pathogenesis [11].

In Australia, the researcher used PCR technique for diagnosis and detection the sequences of ITS1 region of rDNA of chickens Eimerian so, seven species were identified (E.tenella, E.necatrix, E.maxima, E acervulina, E.brunetti, E.mitis and E.praecox). The DNA sequences for each species analyzed and compared with European strains [7].

The traditional methods are not sufficiently reliable for specific diagnosis of Eimeria species in chickens. Moreover, occurrence of multiple infections in a single bird and the fact that, Eimeria species with low oocysts frequency in the mixture maybe missed, indicates that PCR based amplification of DNA sequence of parasite, could resolve this problem and overcame the limitation in analysis of small amounts of oocysts in mixed infections. On the other hand, this protocol can even identify strains of Eimeria species, characterized by different drugs resistance phenotypes [16, 18].

In Norway the samples collected from waste and chickens stool from 85 poultry farm and the researcher compared between two methods of diagnosis the first method depend upon the oocysts morphology while the other method is molecular assay (PCR) in which the oocysts isolated and identified depend on ITS1 region for rDNA, five species of Eimeria were identified E.acervulina, E.tenella, E.maxima, E.praecox and E.necatrix there was not a the perfect match between the two methods, with the proportion of compatibility 45% [21].

In Sweden, described the polymerase chain reaction (PCR) had been adopted to detect, identify and distinguish between Eimeria species the causal agent of poultry coccidiosis by used of ITS1 region of the rDNA as a variable and perfect for differentiation between Eimerian species, so a proper primers were designed and led to diagnosed the species (E.acervulina, E.brunetti, E.necatrix and E.tenella) and this study concluded that the ITS1 region of the Eimerian species contain enough variation to design primers can be applied in the PCR technique to detect and distinguish between different species Which constitute excellent indicators of epidemiological studies in the future [5].

The present study used the PCR assay for diagnosis of Eimerian species in which PCR product that represent the amplified ITS1 region of rDNA were analyzed to study the DNA sequencing of three local Eimeria species and compare with global strains of Emiria that recorded in GenBank at the site NCBI data basE.

However, the molecule also possesses phylogenetically informative variable regions that are useful for determining relationships among species and these region represent the

ITS1 region which located in rDNA, so the results from the present study illustrate the percentage of similarity (98% – 99%) between local isolated E.tenella and E.tenella isolate Bareilly (JX853830.1), which refers to a highly match percentage in the DNA sequencing between the local and global strains that recorded in the NCBI data basE.

The Phylogenetic relationship tree analysis according to (MEGA 6) program from type (Test UPGMA tree) to compare between the local E.necatrix and global strains shows identical percentage (91% – 100%) with E.necatrix isolate Bareilly (JX853832.1) in the site NCBI – data base While the Phylogenetic relationship tree analysis of E.maxima comparsion with global strains shows identical percentage (98%) with E.maxima isolate Bareilly (JX853828.1).

The results of Multiple sequence alignment analysis of ITS1 region in the PCR product of five samples of species E.tenella (S1, S2, S3, S4 and S5) with global strains shows great affinity with E.tenella Australia isolate (AF446074.1), E.tenella China isolate (GQ153633), E.tenella U.K isolate (AF026388.1), E.tenella Turkey isolate (HQ680474.1), E.tenella India isolate (JX853830.1), E.tenella South Korea isolate (FJ447468.1) and E.tenella Egypt isolate (JQ060999.1).

While the phylogenetic tree analysis of five samples of the species E.tenella (locally isolation) with global strains shows a high percentage of similarity between the S1 (local strain) and E.tenella Australia isolate (AF446074.1), S2 with. E.tenella Turkey isolate (HQ680474.1) and E.tenella Egypt isolate (JQ060999.1), S3 with E.tenella China isolated (GQ153633.1), S4 with E.tenella USA isolate (AY779513.1) and E.tenella India isolate (JX853830.1) and S5 with E.tenella South Korea isolate (FJ447468.1) and E.tenella UK isolate (AF026388.1).

The comparison between local E.necatrix (S1, S2, S3, S4 and S5) and the global strains by useing of multiple sequence alignment analysis of ITS1 region of PCR product which appear a percentage of similarity between the local strains of E.necatrix and E.necatrix Sweden isolate (AF026385.1), E.necatrix India isolate (JX853832), E.necatrix China isolate (JN022588) and E.necatrix Australian isolate (AF446070.1) according to (MEGA 6) program.

Also the phylogenetic tree analysis of five samples of the species E.necatrix appeared a closely relation between the local samples (S1, S3) and E.necatrix Australia isolate (AF446074.1), while the similarity between (S4, S5) and E.necatrix China isolate (JN 022588.1) were great while the local S2 appear more closely with E.necatrix China Isolate (JN022588.1).

A multiple sequence alignment analysis was conducted for a comparison between the local samples of the species E.maxima and the global strains in which a percentage of similarity appear between the local samples and E.maxima USA isolate (FJ230371.1), E.maxima Turkey isolate (HQ680471.1), E.maxima Sweden isolate (AF065094.1), E.maxima South Korea isolate (HQ615990.1), E.maxima India isolate (JX853828.1), E.maxima China isolate (FJ449681.1) and E.maxima Australia isolate (AF44601.1).

The phylogenetic tree of five samples for the

species E.maxima were analyzed to compare with global strains of the same species and that analysis appeared a similarity between all the five samples with E.maxima Australia isolate (AF446061.1), E.maxima Turkey isolate (HQ 680471.1), E.maxima South Korea isolate (HQ615990.1), E.maxima India isolate (JX853828.1), E.maxima USA isolate (FJ230371.1) and E.maxima China isolate (FJ449681.1).

References

[1] Stucki, U., Braun, R.and Roditi, Exp Parasitol., **76**, 68 (1993).

[2] HD.Chapman, JR.Barta, D.Blake, A.Gruber, M. Jenkins, NC.Smith, X. Suo, and FM. Tomley,. Advances in parasitology, **83**, 93 (2013).

[3] S.Fernandez, A. C. Costa, A. M. Katsuyama, A. M. Madeira and A. Gruber, Parasitol. Res. **89**,437 (2003).

[4] DP.Blake, KJ.Billington, SL.Copestake, RD.Oakes, MA.Quail, KL.Wan, MW.Shirley and AL.Smith, PLoS Pathog, **7**, e1001279 (2011).

[5] B.Schnitzler, P.Thebo, F.Tomley, A.Uggla, and M. Shirley, Avian Pathology, **28**, 89 (2014).

[6] F.C. Velkers, A. Bouma, J.A. Stegeman and M.C. de Jong, Vaccine, **30**, 322 (2012).

[7] Lew, A.E., Anderson, GR., Minchin, CM., Jeston, PJ., Jorgensen, WK, Vet Parasitol. **112**, 33 (2003).

[8] Long,PL., Reid, WM., Research report., **404**, 1 (1982).

[9] Long, PL., Joyner, LP, J Protozool., **31**, 535 (1984).

[10] Meireles, MV., Roberto LO, Riera RF., Brazilian J Poult Sci., **6**, 249 (2004).

[11] Jenkins, M.C, A.K. Miska, A and S. KloppB., AVIAN DISEASES **50**,110 (2006)

[12] Morgan, JA., Morris, GM., Wlodek,BM.,Byrnes, R., Jenner, M., Constantinoiu, CC.,Anderson, GR., Lew-Tabor,AE., Molloy, JB., Gasser, RB., Jorgensen, WK, Mol Cell Probes., **23**, 83 (2009).

[13] Al-Mayah, Q., Sharhan H., M Sc thesis, College of Medicine, University of Babylon (2013).

[14] Tsuji,N., Kawazu,S., Ohta,M, Kamio T., Isobe,T., Shimura, K., Fujisaki, K, J Parasitol. **83**, 966(1997).

[15] Su, Y. C., A. C.,Fei and F. M. Tsai, Vet. Parasitol. **117**, 221 (2003).

[16] Nowzari, N., Dinparast,D. N., Rahbari,S.,Yakchali,B., Kazemi,B. and Moazeni,Jula. G., Vet. Parasitol., **128**, 59 (2014).

[17] Nematollahi, A., Moghaddam, GH., Farshbaf,P. R, Mun Ent Zool. **4**, 53 (2009).

[18] Williams, R. B, Int. J. Parasitol. **31**,1056(2001).

[19] Razmi,G.R., Kalideri A, Iran.Prevent Vet Med. **44**, 247 (2000).

[20] Velkers, F.C., A. Bouma, J.A. Stegeman and M.C. deJong, Vet.Parasitol., **187**, 63 (2012).

[21] Anita H., Anne,G., Per,T., Jens, G. Mattsson and Magne K., Avian Pathology.**37**, 161 (2014).

Large-basis shell model calculations of odd-A 63-73Ni isotopes

Fouad A. Majeed, Ali Obies Muhsen Almayyali and Fatima M. Hussain
Department of Physics College of Education for Pure Sciences, University of Babylon, Iraq.
Received Date: 15/Jun/2015
Accepted Date: 16/Aug/2015

الخلاصه

أجريت حسابات أنموذج القشرة بنطاق واسع لنظائر النوى $^{63-73}$Ni الفردية العدد الكتلي والواقعه في منطقة القشرة $f_{5/2}\,pg_{9/2}$ تم حساب مستويات الطاقة ذات التماثل الموجب والسالب وصولاً الى J=15/2 بأستخدام برنامج نموذج القشرة Nushellx@msu عن طريق توظيف التفاعلات المؤثرة jun 45 و jj44b. أجريت مقارنة بين الحسابات النظرية مع البيانات العملية المتوفرة حديثاً. تم الحصول على تطابق مقبول بين البيانات العملية والنتائج النظرية للنوى قيد الدراسه.

الكلمات المفتاحية

أنموذج القشرة، مستويات الطاقة، نيوشيل أكس.

Abstract

Large-scale shell model calculations for neutron-rich odd-A $^{63-73}$Ni isotopes have been performed in the lower $f_{5/2}\,pg_{9/2}$-shell region. The energy levels for positive and negative parity states up to J=15/2 are calculated by using the shell model code Nushellx@msu by employing the effective interactions jun 45 and jj44b. The theoretical calculations are compared with the most recent available experimental data. Reasonable agreement is obtained between the theoretical values and the experimental data for the selected isotopes under study.

Keywords

Shell model, energy levels, Nushellx.

1. Introduction

The shell model [1] has been used for many years to describe the structure of nuclei, especially those that are fairly light or moderately near closed shells. With the steady improvement of computers, the size of the model spaces that can be accommodated has grown, expanding the region of nuclei that can be treated. Neutron-rich nuclei in the A>>60 mass region have been the subject of many recent experimental and theoretical investigations [2].

Recently shell model with large-basis have been performed to study the energy levels and reduced transition probabilities ($B(E2_1^+;0 \rightarrow 2_1^+$ for even-even $^{66-76}$Ni isotopes by F. A. Majeed *et al*. [3]. Their results show reasonable agreement with the experimental data.

J. Diriken *et al*. [4] have studied in the nearby ^{67}Ni nucleus, -by performing *a* (*d*, *p*) -experiment in inverse kinematics employing a post-accelerated radioactive ion beam (RIB) at the REX-ISOLDE facility. The experiment was performed at energy of 2. 95 MeV/u using a combination of the T-REX particle detectors, the Miniball γ-detection array and a newly-developed delayed-correlation technique as to investigate μs-isomers. A comparison with extended shell model calculations and equivalent (^{3}*He*, *d*) studies in the region around ^{90}Zr highlights similarities for the strength of the negative-parity pf and positive-parity $g_{9/2}$ state.

The aim of the present work is to employ shell model calculations with large basis without imposing any restrictions, to study the low-lying energy levels of odd-A $^{63-73}$Ni nuclei. The calculations will be performed by using the shell model code Nushellx@msu [5] by employing the jun 45 [6] and jj44b [7] effective interactions, to test the ability of the present effective interactions to reproduce the experiment in this mass region.

2. Shell model calculations

Large-scale shell model calculations have been performed for neutron-rich odd-A $^{63-73}$Ni isotopes lies in the $f_{5/2}pg_{9/2}$ shell region. The calculations have been performed with the interactions jun 45 [6] and jj44b [7]. The jun 45 interaction is based on Bonn-C potential, the single-particle energies and two-body matrix elements was modified empirically so as to fit 400 experimental data out of 69 nuclei with A=63-69. In the fitting of jun 45 interaction the experimental data are taken around N=50. The jj44b interaction was obtained from a fit to about 600 binding energies and excitation energies with 30 linear combinations of the good J−T two-body matrix elements. For jj44b the energy data for the fit taken from nuclei with Z=28−30 and N=48−50. The single-particle energies for the $2p_{3/2}$, $1f_{5/2}$, $2p_{1/2}$ and $1g_{9/2}$ single-particle orbits employed in conjunction with the jun 45 interaction are -9. 8280, -8. 7087, -7. 8388, and -6. 2617 MeV respectively. In the case of the jj44b interaction they are -9. 6566, -9. 2859, -8. 2695, and -5. 8944 MeV, respectively. The core is ^{56}Ni, i. e. N=Z=28, and the calculations are performed in this valence space without truncation. The calculations have been performed using the shell-model code Nushellx@msu [5] on desktop computer dell precision workstation T7500 with xenon processor, cpu 2. 4 Hz, 4-cores, 84GB and 2TB hard disk.

3. Results and discussion

Fig.(1) presents the comparison of our theoretical work using jun 45 and jj44b effective interactions for positive and negative parity states for ^{63}Ni isotope. From this Fig. we noticed that jun 45 effective interaction correctly reproduce the ground-state spin of $1/2^-$. The jj44b interaction, however, fails to correctly reproduce the ground-state spin of $1/2^-$, although the three lowest-lying states of spin and parity $3/2^-$, $5/2^-$, and $1/2^-$ are calculated to lie within a range of only 110 keV, reflecting the close proximity of the neutron single-particle orbitals $2p_{3/2}$, $1f_{5/2}$, and $2p_{1/2}$ in the ^{63}Ni nucleus.

In general, the theoretical values are in good global agreement with the experimental data for both interactions. The spins $9/2^+$, $7/2^-$, $9/2^-$, $13/2^+$, $11/2^+$, and $7/2^+$ experimentally unconfirmed values at 1.291 MeV, 1.451 MeV, 1.451 MeV, 2.183 MeV, 2.183 MeV, and 2.573 MeV, respectively. Jun 45 predict these states at 1.258 MeV, 1.415 MeV, 1.474 MeV, 2.751 MeV, 2.849 MeV, and 2.559 MeV, respectively. The effective interaction jj44b predict these spins at 1.410 MeV, 1.261 MeV, 1.789 MeV, 2.875 MeV, 2.767 MeV and 2.469 MeV, respectively. Spins at $15/2^+$, $13/2^-$ and $15/2^-$ have been predicted by both jun 45 and jj44b effective interactions which have not been assigned experimentally.

The calculated low-lying energy levels are shown in Fig.(2) for ^{65}Ni isotope. The ground-state spin of $5/2^-$ could not be reproduced with jun 45 and jj44b effective interactions. The jun 45 effective interaction is closer to the experimental data and able to reproduce the correct order of the low lying states. The J^π values of $9/2^-$, $7/2^-$, $11/2^+$, $13/2^+$ and $15/2^+$ are not confirmed experimentally, jun 45 predict the values for these spin at 1.844 MeV, 1.287 MeV,

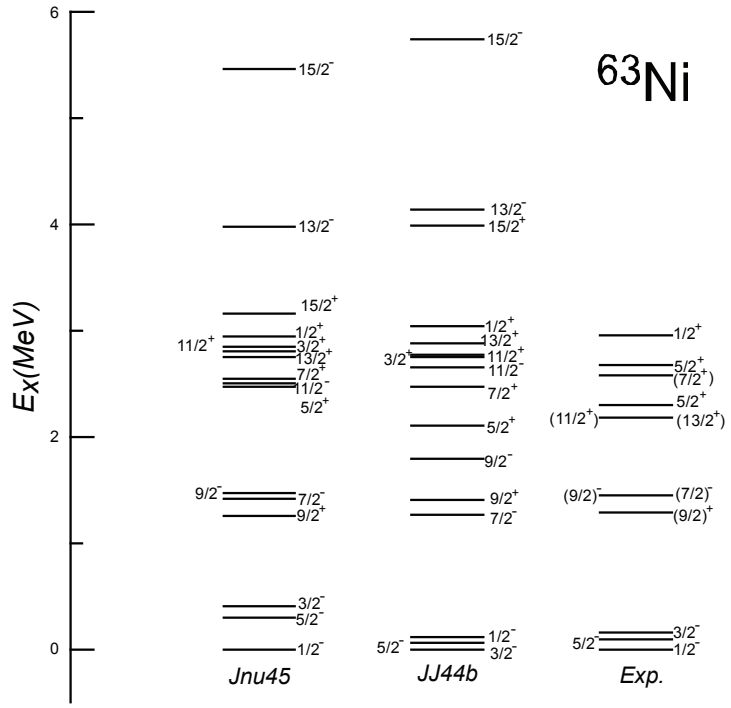

Fig.(1): Comparison of calculated and experimental low-lying spectra for ^{63}Ni isotope with jun 45 and jj44b effective interactions.

2.99 MeV and 2.841 MeV, respectively, while jj44b predict these states at 2.102 MeV, 1.610 MeV, 2.357 MeV, 2.351 MeV and 3.545 MeV respectively. The spin $7/2^-$ have been predicted lower than $9/2^+$ using jj44b effective interaction which is in reverse order compared with the experimental values, this crossover behavior might be attributed to the shape change from vibrational to rotational collectivity as the number of neutrons or protons increases from shell closure towards midshell. In general the agreement between theoretical calculations and the experimental data from jun 45 and jj44b is reasonable for low-lying levels, as seen in Fig.(2).

Fig.(3) displays the comparison between our calculations with the experimental data for ^{67}Ni isotope. The two interactions used in the present work are able to reproduce the ground state spin $1/2^-$. Both effective interactions are able to reproduce the correct ordering of the low-lying spins $5/2^-$ and $9/2^+$ and the predicated values with jj44b effective interactions are more in agreement with the experimental data than jun 45.

In Fig.(4), the calculated energy levels for ^{69}Ni obtained using jun 45 and jj44b effective interactions together with the experimental data are shown. The two interactions used in the present calculations are able to predict correct ground state spin as observed in experiment. The experimental values of ^{69}Ni isotope are all unconfirmed. Jun 45 and jj44b effective interactions are able to reproduce the correct sequence of the low-lying states $1/2^-$, $5/2^-$ and $9/2^+$. The calculation with jj44b are closer to the experimental values than jun 45 for these state. New high spins states have been assigned using jun 45 effective interaction these states are $11/2^-$, $15/2^-$, $1/2^+$ and $15/2^+$ with values 2.855 MeV, 3.403 MeV, and 3.008 MeV, respectively, while

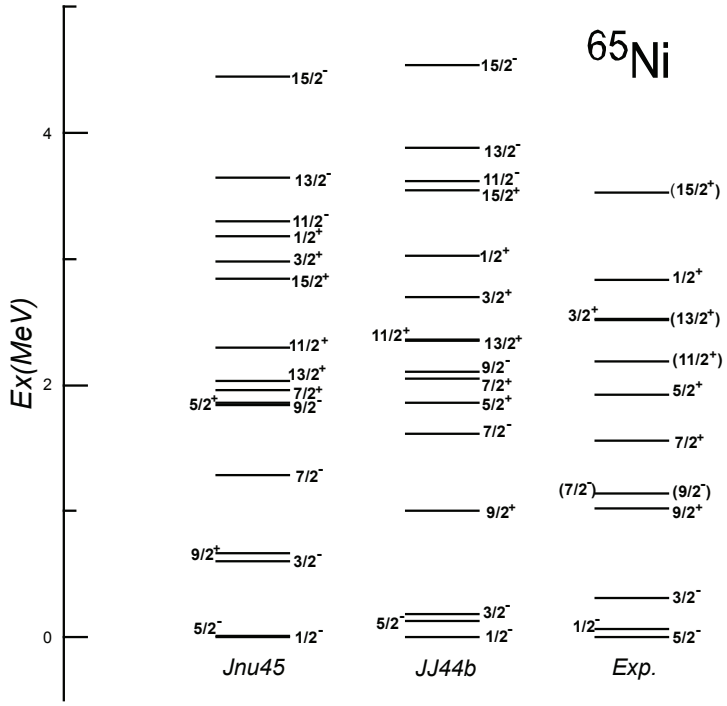

Fig.(2): Comparison of calculated and experimental low-lying spectra for ^{65}Ni isotope with jun 45 and jj44b effective interactions.

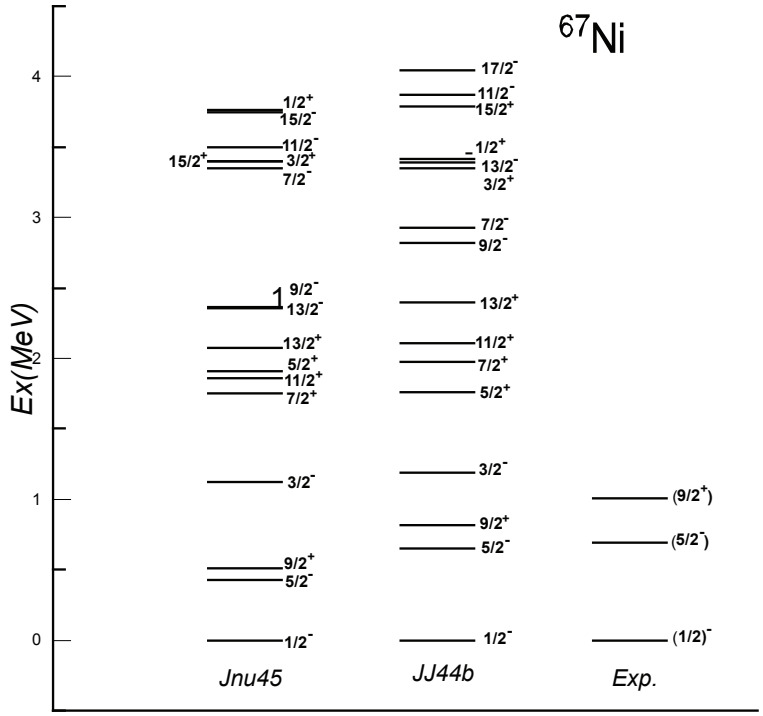

Fig.(3): Comparison of calculated and experimental low-lying spectra for ^{67}Ni isotope with jun 45 and jj44b effective interactions.

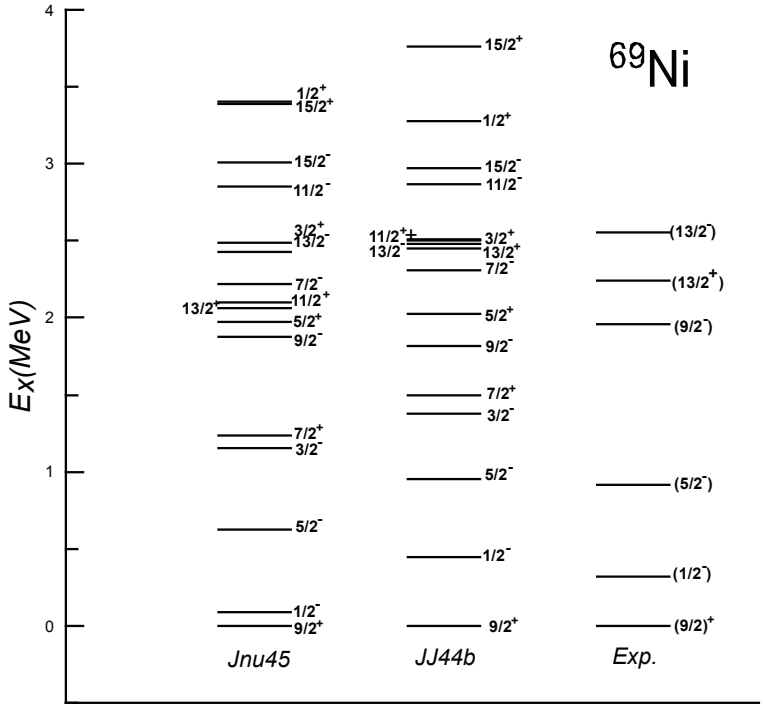

Fig.(4): Comparison of calculated and experimental low-lying spectra for ^{69}Ni isotope with jun 45 and jj44b effective interactions.

jj44b predict them at 2.870 MeV, 2.969 MeV, 3.275 MeV and 3.759 MeV, respectively.

The calculated low-lying energy levels for positive and negative parity states of ^{71}Ni and ^{73}Ni isotopes using jun 45 and jj44b effective interaction compared with the experimental data and is presented in Figs. (5) and (6), respectively. The ground state for both isotopes is correctly reproduced by using both effective interactions. The experimental data are unconfirmed for ^{71}Ni and ^{73}Ni isotopes. The ordering of the low-lying spin states for ^{71}Ni isotope are correctly reproduced by jj44b effective interaction, while ju45 predicts $1/2^-$ lower than $7/2^+$ which is in disagreement with the experimental data. The effective interaction jj44b reproduce the correct ordering of $7/2^+$ and $1/2^-$ states for ^{71}Ni isotope in comparison with the experimental data. The experimental data for the isotope ^{73}Ni is not available at the moment and once the observed experimental data are available one can judge which of the effective interactions used in the present work are more able to reproduce the experimental data.

4. Conclusion

The present work highlights the ability of the present shell model calculations for neutron-rich isotopes near ^{60}Ni and the challenges in the calculations due to high dimension of J-T scheme. In our work there is no restriction imposed on the valence nucleons and all bases were included in the calculations. A conclusion can be drawn that the effective interactions jun 45 and jj44b are adequate choice for nuclei lies in this mass region. The effective interactions jj44b is more consistent in reproducing the experimental data and the ordering of the low-lying spectra than jun 45 for the nuclei investigated in the present study.

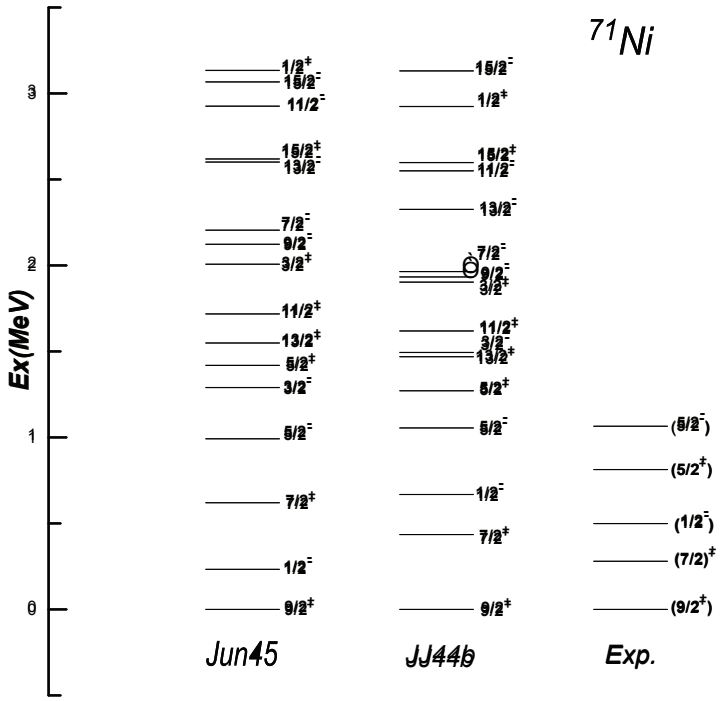

Fig.(5): Comparison of experimental and calculated low-lying spectra for ^{71}Ni isotope with jun 45 and jj44b effective interactions.

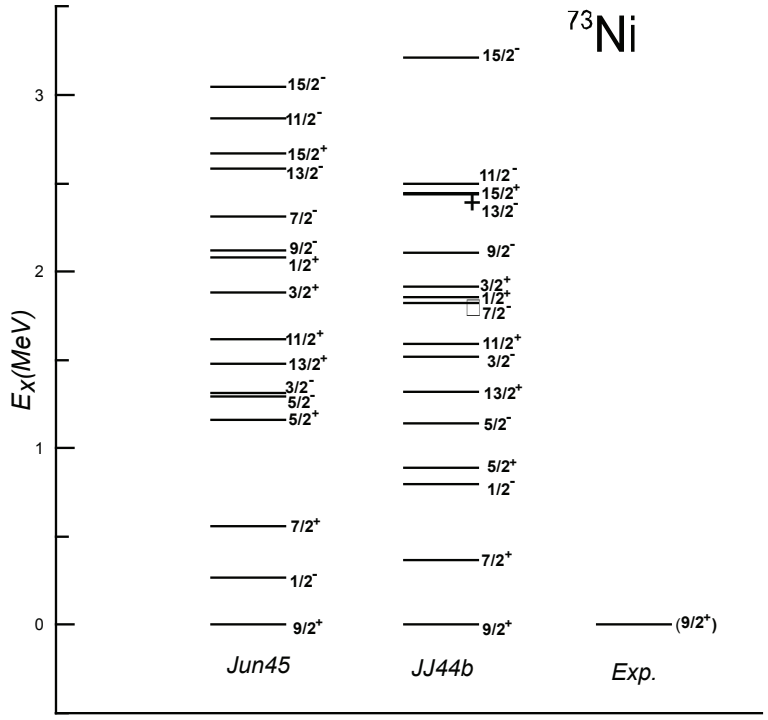

Fig.(6): Comparison of calculated and experimental low-lying spectra for ^{73}Ni isotope with jun 45 and jj44b effective interactions.

References

[1] M.G.Mayer, Phys.Rev.**75**, 1969 (1949).

[2] A.Albers *et al*., Phys.Rev.**C88**, 054314 (2013).

[3] F.A.Majeed, F.M.Hussain and A.O.M.Almayyali, Int.J.of Sci.Res.**11** (11), 2842 (2014).

[4] J.Diriken *et al*., Phys.Lett.**B 736**, 533 (2014).

[5] B.A.Brown, W.D.M.Rae, E.McDonald and M.Horoi, NuShellX@MSU,http://www.nscl.msu.edu/ brown/ resources/resources.html.

[6] M. Honma *et al*., Phys.Rev.C **80**, 064323 (2009).

[7] B.A.Brown (unpublished).

[8] ENSDF, Evaluated nuclear structure data file, database version 29-5-2015; accessed 13/3/2015.

Voltammetric characterization of polystyrene grafted with acrylonitrile electrode self modification with carbon nanotube (Psgacesmcnt)

*** Muhammed Mizher Radhi and ** Emad A. Jaffar Al-Mulla**
*** Department of Radiological Techniques, College of Health and Medical Technology, Middle Technical, University of Baghdad, Iraq**
**** Department of Chemistry, Faculty of Science, University of Kufa, Iraq**
Received Date: 5/Jun/2015
Accepted Date: 9/Jul/2015

الخلاصة

تم تصنيع قطب جديد مصنع من البولي ستيرين المطعم اكرلوناترال والمعدل بمادة الكاربون نانوتيوب وباستخدام اشعة كاما والعامل المساعد كبريتات الامونيوم الحديدية.

تم دراسة الصفات الكهروكيميائية للقطب المصنع حيث اعطى تحسيناً في اداءه وذلك عن طريق استخدام الكاربون نانوتيوب الذي يزيد في التوصيلية الكهربائية لمادة البوليمر المطعم اثناء استخدامه في جهاز الفولتامتري الحلقي. وقد تم تشخيص الصفات السطحية للقطب الجديد باستخدام SEM وAFM. وكذلك تم استخدام محلول $K_3Fe(CN)_6$ كمادة قياسية في جهاز الفولتامتري الحلقي في تشخيص الصفات الكهروكيميائية للقطب.

خواص التوصيل الكهربائي ل GPESMCNT درست في 1 مولاري من KCl وبتراكيز مختلفة ل [$K_3Fe(CN)_6$] وعند درجات حرارة مختلفة باستخدام تقنية CV.

وقد لوحظ أن القطب الجديد ساعد في تحسين أداء تقنية الفولتامتري الحلقي خاصة في استخدامه بتجربة القطب الدوار التي لا يمكن استخدام الأقطاب المعدلة فيه.

ان نتائج القياس اوضحت ان المادة النانوية لها اهمية في تركيبة البوليمرالمطعم برفع قيمة التيار الكهربائي لقمتي الاكسدة والاختزال للحديد Fe (II)/Fe (III) لمرت عديدة مقارنة مع الاقطاب التجارية مثل قطب الكاربون الزجاجي وقطب البلاتين وقطب الذهب.

الكلمات المفتاحية

قطب البولي ستيرين المطعم اكرلوناترال والمعدل بمادة الكاربون نانوتيوب، CNT جهاز الفولتا متري الحلقي.

Abstract

A novel self modification of grafted polystyrene-acrylonitrile working electrode with carbon nanotubes was success for fabrication from grafting polymer via gamma irradiation and ferrous

ammonium sulfate (FAS) as a catalyst. The electrochemical properties of the self modified grafted polymer with CNT (PSGACESMCNT) improved performance the working electrode at higher conducting surface was done through using in cyclic voltammetry (CV). Morphology of the surface of PSGACESMCNT was characterized by AFM and ASM. The characterization of electrocnductivity properties of PSGACESMCNT was studied in 1M of KCl with different concentration of K_3 $[Fe(CN)_6]$, at different scan rates, temperature, and different concentrations using CV technique. The new PSGACESMCNT improved performance the working electrode in CV at different techniques such as rotating disc electrode (RDE). also, the nanomaterials in the chain of grafted polymer was enhanced the redox current peaks of Fe (II)/Fe (III) multi times than at commercial working electrodes such as GCE, Pt-electrode, Au-electrode…. etc.

Keywords

grafted polymer electrode self modified, CNT, cyclic voltammetry, K_3 $[Fe(CN)_6]$.

1. Introduction

The modification of grafted polymer with nano-deposits such as CNT, C_{60} and activated carbon is very important for the scientists especially in the electrochemistry by cyclic voltammetric analysis field [1-5].

The unique chemical, physical, electronic (metallic or semiconducting) and high thermal properties of carbon nanotubes (CNTs) made them interesting materials for widespread application in the fields such as electrochemical sensors, biosensors, supports for heterogeneous metal catalysts in organic synthesis, fuel cells, semiconductors, batteries, random access memory cells, field effect transistor, field emission display, atomic force microscopy probes, microelectrodes, specific adsorbents to remove organic pollutants from water and waste water and as a potential drug carriers in cancer therapy [6-9].

Working electrodes must have electrically properties as conductor and electrochemically inert. Working solid electrode materials included platinum, gold and glassy carbon were used in cyclic voltammetry. Other materials (e. g., semi-conductors, for example ITO, indium-tin oxide, or conductive polymers or grafted polymer) are also used, for more specific applications [10, 11].

Electrochemical behavior of famotidine has been studied at composite polymer membrane working electrode. Cyclic voltammetric method has been developed for the determination of drug in pharmaceutical formulation. A well-defined anodic peak was observed for famotidine in the entire pH range. The current increases steadily with scan rate and concentration. This composite film showed good catalytic behavior, which includes a good current response. The result is compared with the glassy carbon electrode and it was found that the current with composite polymer electrode is of the order of 18. 60 mA whereas with glassy carbon electrode it was around 565. 00 μA [12].

Electrochemical study behavior of terthiophene and its corresponding polymer, which is obtained electrochemically as a film by Cyclic Voltammetry (CV) on platinum electrode. The analysis focuses essentially on the effect of two solvents acetonitrile and dichloromethane on the electrochemical behavior of the obtained polymer. The voltammograms show that the film of polyterthiophene can oxide and reduce in two solutions; in acetonitrile, the oxidation current intensity is more important than in dichloromethane. The impedance plots show the semicircle which is characteristic of charge-transfer resistance at the electrode/polymer interface at high frequency and the diffusion process at low frequency [13].

Grafted copolymer of polypyrrole has been synthesized by electrochemical polymerization of pyrrole in the presence of poly(para-chloromethylstyrene-co-styrene-co-pyrrolemethylstyrene). The produced copolymer exhibits an electrical conductivity comparable to that of polypyrrole. This measurement showed that copolymer has excellent thermal stability. The response mechanism of this compound to sense a selection of gases and vapors was investigated, by measuring its electrical conductivity by four-point probe method. This gas sensor may have advantages over the other sensors in its

ability to operate at room temperature, lower gas and vapous sensing concentration, suiTable solubility, stability in air, sufficient diffusion, and selectivity [14].

This review highlights the recent progress made in the area of thermoelectric (TE) applications of conducting polymers and related composites. Several examples of such materials and their TE properties are discussed. TE properties of new poly (2, 7-carbazole) derivatives are highlighted. References are also made to carbon nanotube/ polymer composites and their improved electrical and TE performance. Studies on polymer/ inorganic materials composites have also taken a step forward and have shown very promising TE properties [15].

In this work, grafted polymer was modified with carbon nanotubes to fabrication grafted polymer electrode self modified with carbon nanotubes. The new grafted polymer electrode was electrochemically characterization in K_3 [$Fe(CN)_6$] with KCl aqueous electrolyte by CV technique.

2. Experimental

2. 1. Synthesis of grafted polymer modified with carbon nanotubes (GP/CNT)

Polystyrene was grafted with acrylonitrile as a monomer and modified with nano- deposit (carbon nanotubes) and ferrous ammonium sulfate (FAS) as a catalyst using gamma-irradiation. The new grafted polymer modified with carbon nanotubes has been investigated and characterized [3].

2. 2. Instrument and Electroanalytical Methods

Electrochemical workstations of NuVant Systems Inc., USA (EZ stat series with potentiostat/ glvanostat driven by electroanalytical measuring software) were connected to a PC computer in order to perform cyclic voltammetry (CV), chronoamperometry (CC), and chronoamperometry (CA). An Ag/AgCl (3 M NaCl) and platinum wire (1 mm diameter) were used as the reference and counter electrodes, respectively.

The working electrode used in this study was grafted polymer electrode self modified with carbon nanotubes (PSGACESMCNT). The voltammetric experiments were carried out with K_3 [$Fe(CN)_6$] and KCl as supporting electrolyte. Solution was degassed with nitrogen gas for ten to fifteen minutes prior to recording the voltammogram.

2. 3. Reagents

All chemicals were analytical reagents or at spectroscopy grade purity. Also, solutions were prepared by double distilled water. It was used the supporting electrolyte solution of 1M KCl in aqueous media at room temperature.

2. 4. Fabrication the new polystyrene-acrylonitrile electrode self modified with CNT (PSGACESMCNT)

PSGACESMCNT has been fabricated from grafted polymer modified with carbon nanotubes. The diameter of electrode was 3 cm. A hole was done (1mm) to allow 1cm length of platinum wire out from other side of electrode. A piece of copper wire was joined with the platinum wire. All parts of fabricated electrode were covered with glassy tube and then fixed by epoxy resin as shown in Fig.(1).

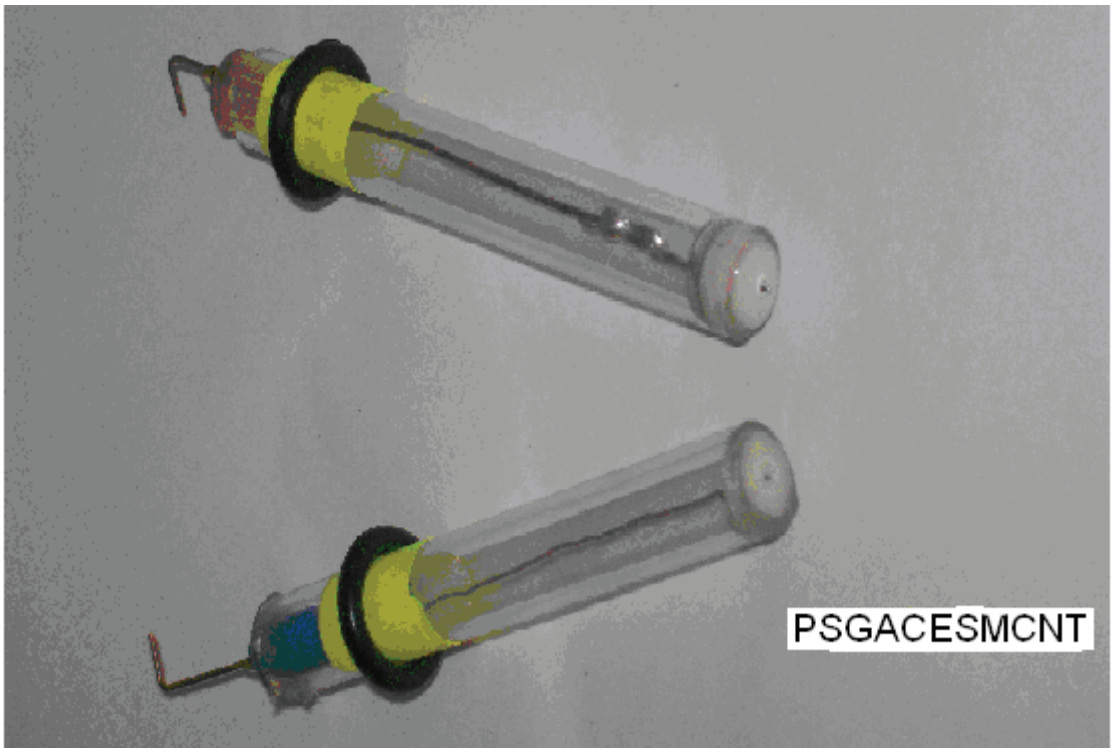

Fig.(1): PSGACESMCNT

3. Results and discussion

3. 1. Electrochemical properties

$K_3Fe(CN)_6$ solution is commonly used as a reference standard solution for the purpose of calibrating a voltammetric system in KCl aqueous solution. During the calibration process of an electroanalytical workstation (EZ stat) using glassy carbon electrode (GCE) and grafted polymer self modified with carbon nanotubes electrode (GPESMCNT) as working electrode. The current of Fe (II) / Fe (III) redox couple appears to be significantly enhanced by the PSGACESMCNT. The enhancement of oxidation-reduction current peaks +600 µA and -200 µA, respectively is comparison of GCE at very weak redox current peaks of +70 µA and -60 µA respectively as show in Fig.(2) and b.

3. 2. Effect of different scan rate

The effect of varying scan rates (SR) on the cyclic voltammograms using grafted polymer electrode self modified with CNT as working electrode in 1M KCl as a supporting electrolyte was studied with 1mM $K_3Fe(CN)_6$ over a scan rate ranging from 5 – 1000 mV/s. Oxidation and reduction currents of Fe (II)/Fe (III) couple increased with the scan rate due to heterogeneous kinetics and IR effect. Fig.(3) is a reasonably linear dependence of PSGA CESMCNT reduction current on the scan rate and is described by y=0. 48X – 1. 225, R^2 =0. 963. The slope of graph Log Ipc (reduction current) versus Log (SR) is 0. 48; which is significantly differ from the theoretical value of half for diffusion- controlled process, indicating presence of a complex. The relationship between oxidative potential and scan rate of PSGACESMCNT, shows a reduction peak

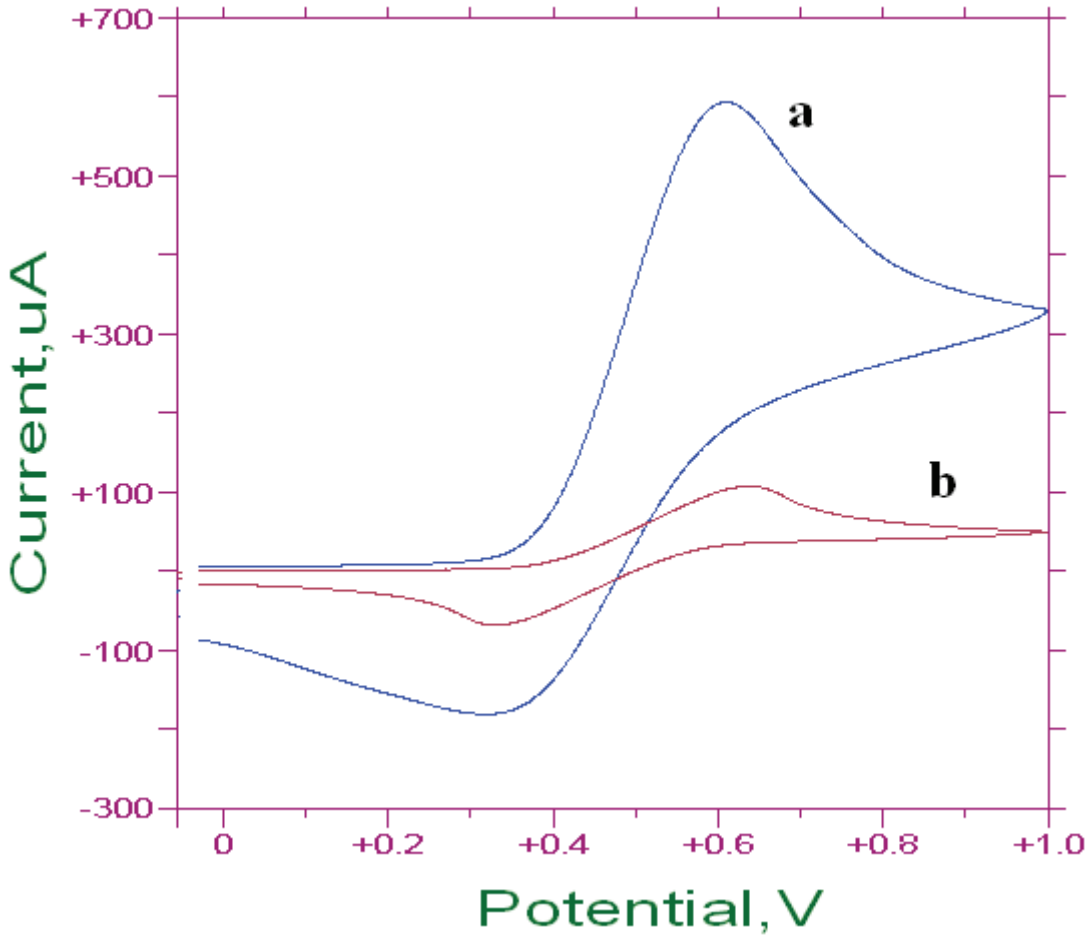

Fig.(2): cyclic voltammogram of K_3 ($Fe(CN)_6$) in 0. 1M KCl (SR=100 mV/sec) versus Ag/AgCl using (a) GPESMCNT and (b) GCE.

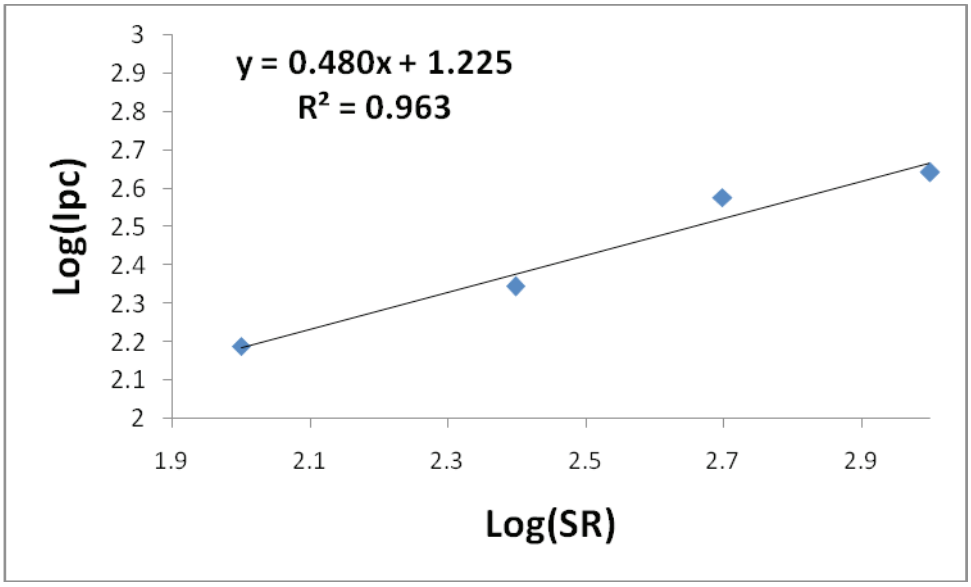

Fig.(3): Plot Log (Ipc) versus Log (SR) of 1mM $K_3Fe(CN)_6$ in 1M KCl at different scan rate (SR = 100, 250, 500, 1000 mV/sec) using PSGACESMCNT versus Ag/AgCl as reference electrode.

at 150 mV in low scan rate but increased more than 500 mV at high scan rate (Linearly with Y=0. 48X-1. 225 (R^2=0. 963). Surface intercepts process at zero current produces zero current potential (E0, 1) of 150 mV for the reduction of PSGACESMCNT.

3. 3. Effect of varying K3Fe(CN)6 concentration

Fig.(4) shows the linear current dependent on $K_3Fe(CN)_6$ concentration; observed at concentration range (5-10mM) which is described by the equation of y=18X+221. 2 with R^2=0. 984. The slope of the linear line for $K_3Fe(CN)_6$ showed that a considerably high sensitivity response of 18 µA/mM is readily obtained at GPESMCNT during cyclic voltammetry.

3. 4. Reproducibility

The potential cycling of the redox of PSGACESMCNT in 1mM $K_3Fe(CN)_6$ and 1 M KCl aqueous solution as a supporting electrolyte was carried out during cyclic voltammetry. Continuous potential cycling did not seem to affect the redox current of PSGACESMCNT as the faradic activity appears reproducible even after 15 cycles, reflecting the stability and reproducibility at the surface of PSGACESMCNT.

3. 5. Scanning electron microscopy (SEM) of GPE/CNT

Before electro-analysis polystyrene grafted acrylonitrile surface appears compact and nonporous. The uniformity of the grafted polymer surface slightly increases since occurrence of

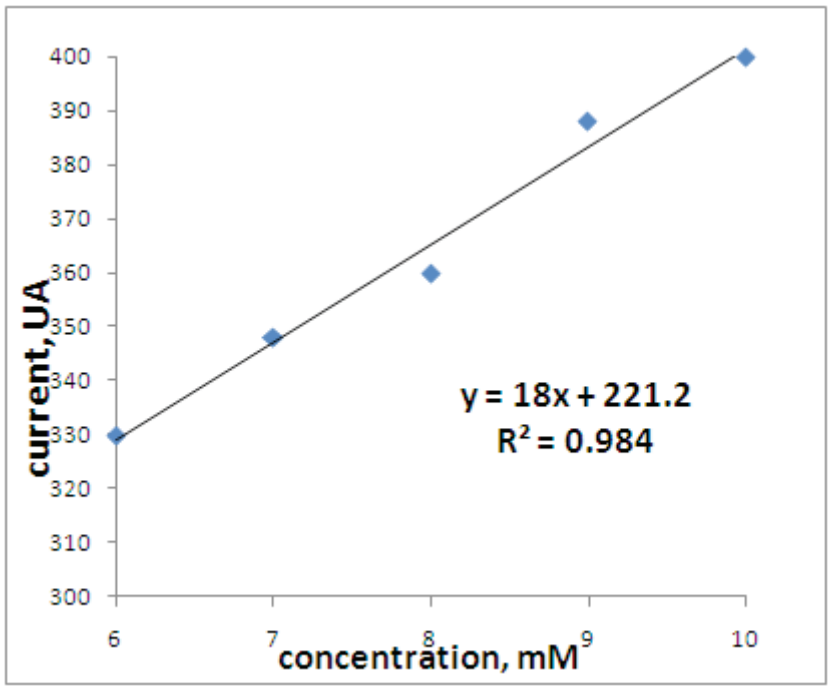

Fig.(4): plot cathodic current versus different concentration of at $K_3Fe(CN)_6$ in 1M KCl scan rate=100 mV/sec using PSGACESMCNT versus Ag/AgCl as reference electrode.

protrusion observed phase as shown in Fig.(5) (a). After modification with CNT, although many of the nano deposits with homogenous distribution of CNT still remain at about <1 μm as show in Fig.(5) (b).

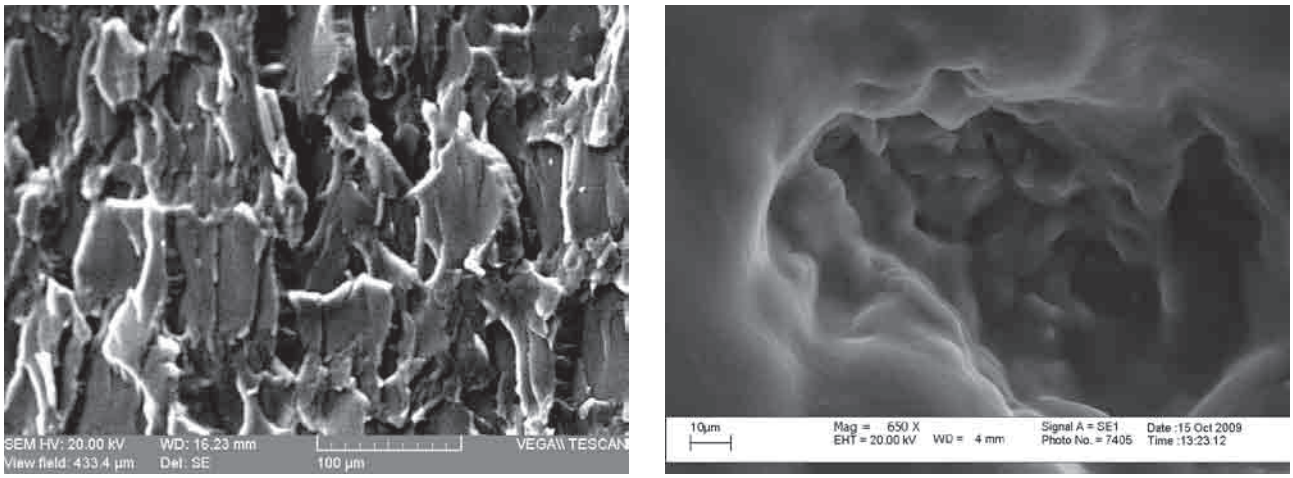

(b) **(a)**

Fig.(5): SEM of (a) polystyrene grafted acrylonitrile (b) polystyrene grafted acrylonitrile modified with CNT

3. 6. Atomic force microscopy (AFM)

The surface image of AFM in an area of 20 μm x 20 μm of the grafted polymer (polystyrene acrylonitrile) before and after modified with CNT as shown in Fig.(6). The surface of the electrode appeared to be compact and rough. According to AFM images, the average grain size and thickness of the film were estimated to be 11. 23 μm and 28. 69 μm, respectively.

4. Conclusions

A polystyrene grafted acrylonitrile Electrode self modified with CNT (PSGACESMCNT) has an extended potential working region as a compared with solid electrodes and classical modification electrodes. The stability of PSGACESMCNT as a working electrode was evaluated by using $K_3Fe(CN)_6$ in KCl electrolyte. Redox peaks of Fe(II)/Fe(III) obtained at PSGACESMCNT showed high current as compared with bar GCE. Electro-catalytic activity of GPESMCNT is therefore evident in this study. GPESMCNT was studied by redox process of $K_3Fe(CN)_6$ in KCl solution during cyclic voltammetry. The redox peaks potential shifts slightly to less negative value by about 100 mV for oxidative peak and 50 mV for reductive peak with current enhancement of about 3-5 folds. The sensitivity under conditions of cyclic voltammetry is significantly dependent on the concentration and scan rate. It is an excellent reproducibility of the current which provided a fabricated electrode has a property in experiment without cleaning.

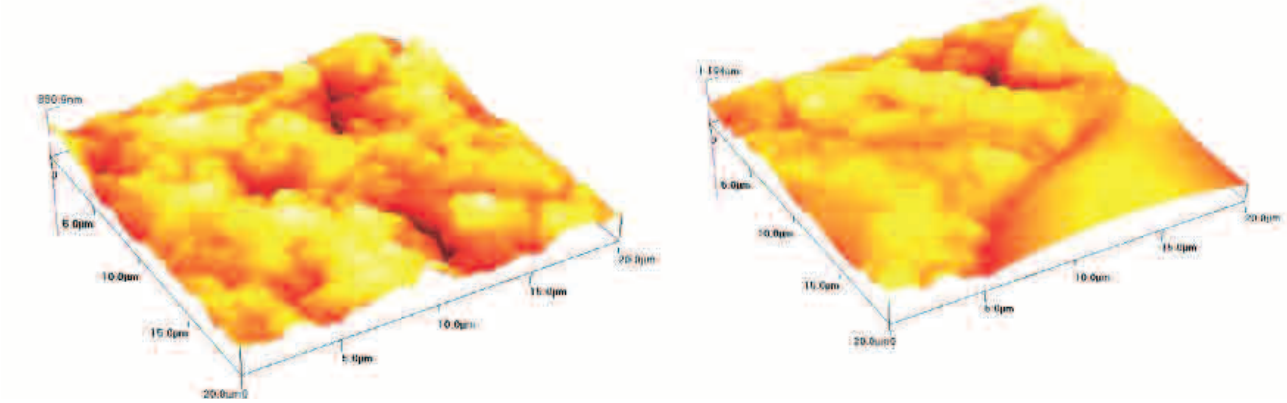

Fig.(6): AFM of Polystyrene grafted acrylonitrile

References

[1] W. T. Tan, M.M. Radhi, M.Z.B. Ab Rahman and A.B. Kassim, j. Appl. Sci. **10**,139 (2010).

[2] M. M. Radhi, W. T. Tan, and M. Z. Rahman,. Sci. Res. Ess. **7**, 790 (2012).

[3] M. M. Radhi, A. J. Haider, and Z. N. Jameel, Res. J. Chem, Sci. **2**, 1 (2012).

[4] A. Bhattacharya, and B.N. Misra, Prog. Polym. Sci. **29**, 767 (2004).

[5] D. Carlos, C. T. Maria, and J. Guoqian, Reac. Funct. Polym. **71**, 938 (2011).

[6] M. M. Radhi, and E. A. J. Al-Mulla, Rendiconti Lincei. **25**, 209 (2013).

[7] H. J. Lee, S. W. Han, Y. D. Kwon, L.S. Tan, and J. B. Baek, Carbon **46**,1850 (2008).

[8] W. Lu, N. Li, W. Chen, Y. Yao, Carbon **47**, 3337 (2009).

[9] L. Wang, D. Zhu, L. Duan, and W. Chen, Carbon **48**, 3906 (2010).

[10] A. A. Abdullah, E. A. J. Al-Mulla. And S. A. Aowda, Res. Chem. Intermed. **39**, 2817 (2013).

[11] M. M. Radhi, E. A. Jaffar Al-Mulla, and W. T. Tan, Res. Chem. Intermed. **40**, 179 (2014).

[12] D. C. Tiwari, R. Jain, and G. Sahu, Indian J. Chem, Tech. **15**, 472 (2008).

[13] M. M. Radhi, W. T. Tan, and A. Kassim, J. Chem. Eng. Japan. **43**, 927 (2010).

[14] S. H. Hoseini and A. A. Entezami, Iranian Polym. J. **14**, 101 (2005).

[15] N. Dubey and M. Leclerc, J. Polym. Sci. Part B: Polym. Phy. **49**, 467 (2011).

Measurement of the natural radiation of soil samples from official offices in the city of Baghdad (Al-Karkh)

Ali K. hasan and Masar E. Mahdi
Department of physics, College of education for girls, University of Kufa, Iraq
Received Date: 9/Jun/2015
Accepted Date: 4/Jul/2015

الخلاصة

اربع وعشرون نموذج جمعت من جانب الكرخ في مدينة بغداد لقياس مستوى النشاط الإشعاعي لهذه النماذج بإستخدام مطياف أشعة كاما – كاشف الجرمانيوم عالي النقاوة (HPGe) واستخدمة برنامج (GINE-2000) للكشف عن النظائر المشعة وقيم الفعالية الخاصة بها وقد وجده بأن الفعالية المحددة للنضير (^{214}Bi) او (^{214}Pb) كانت مكافئة لمستوى الفعالية للـ(^{238}U) عند Bq/kg, (13.88±0.69) بينما معدل القيمة للـ(^{228}Ac) او (^{212}Pb) كان (15.73±0.86) Bq/kgوالذي يكافئ الخاصة بـ(^{232}Th) ومعدل قيمة الفعالية للـ(^{40}K) كان Bq/kg (317.58±14.11) وللـ (^{137}Cs) هو Bq/kg (1.83±0.27) وإن معدل قيمة الجرعة الممتصة في الهواء وتأثير الجرعة السنوية لجانب الكرخ كانت $nGy.\ h^{-1}$ (29.80±1.50)و$\mu sv.\ y^{-1}$ (36.54±1.84) على التوالي.

الكلمات المفتاحية

كاشف الجرمانيوم عالي النقاوة برنامج (GINE-2000)، مستوى فعالية (^{238}U)، مستوى فعالية (^{232}Th).

Abstract

Twenty – four soil samples were collected from the official offices at Al-Karkh side in the city of Baghdad to measure the effective radiation doses of these samples using a gamma – ray spectrometer, by high purity germanium detector (HPGe). The detection of radionuclide and the values of specific activity were calculated by using (GINE-2000) program. It was found that the rate of specific activity of the nuclide (^{214}Bi or ^{214}Pb) was equivalent to the specific activity of (^{238}U) at (13.88±0.69) Bq/kg, while its average value for (^{228}Ac or ^{212}Pb) was (15.73±0.86) Bq/kg which is equivalent to the specific activity of (^{232}Th). The average value of specific activity of (^{40}K) was (317.58±14.11) Bq/kg and for (^{137}Cs) was (1.83±0.27) Bq/kg. Then the average value of the absorbed dose in air and the annual effect dose for Al-Karkh side were (29.80±1.50) $nGy.\ h^{-1}$ and (36.54±1.84) $\mu sv.\ y^{-1}$ respectively.

Keyword

Radiation, Gamma-Ray Spectrometer, Absorbed Does and Annual effective dose rate.

1. Introduction

Studies related to determine the radioactivity levels and the radionuclides distributions in the environment are of great importance. Because, many of the species an the surface of the ground are exposed to radiation, both from a natural mainly or an artificial radioisotope. Natural radioisotopes come mainly from terrestrial origin, such as ^{238}U, ^{232}Th and ^{40}K. The most dangerous artificial sources of radiation is ^{137}Cs [1]. The determination of the concentration of these radioisotopes in the soil enables us to study the background count rate. This study chosen the Karkh side of Baghdad, which contains several important governmental offices. This district was bombarded heavily during the (1991 – 2003) wars. Since these offices were located in a heavily populated residential neighboring the purpose of this study becomes obvious, i. e, to conclude the impact of the measurement results on the general public in this side of the capital.

2. Sample preparation

Twenty – four soil samples were collected from carefully selected officers in Al- Karkh side, using a small shovel. The soil surface was scrapped, then a hole of 40cm was drilled. The hole depth was ranging between 10 to 15 cm. A sufficient amount of soil was taken in plastic bottles. The samples were indexed with special reference number. The samples were carefully prepared by removing any possible strange objects such as gravels and plant roots, after being dried for 3-4 days by sunlight exposure to remove the moisture. Thus the samples became homogeneous and impurity free and ready for counting.

A suitable quantity of the well dried samples was taken and placed in Marinelli beakers (~500 ml). After washing it very well with diluted hydrochloric acid, then with distilled water, so, it was prepared for measurements.

Fig.(1) showed the official map of Baghdad, and the sampling sites are located.

Fig. (1): Map of Baghdad showing the sampling located

3. Materials and method

The sample was measured by a gamma – ray spectroscopy type (DSA2000) with (HPGe) detector as shown in (Fig. 2). The resolution at (1332 keV) ^{60}Co was (2. 2 keV), and relative efficiency was 40% using GENIE-2000 program to calculate the natural radioactivity [2].

In this study, gamma spectroscopy was used to determine the activities of ^{238}U, ^{232}Th, ^{40}K and ^{137}Cs. The gamma ray lines of 609 keV from ^{214}Bi and 352 keV gamma-rays from ^{214}Pb were used to determine the ^{238}U. The gamma ray lines of 583 keV from ^{212}Pb and 911 keV gamma rays from ^{228}Ac were used to determine the ^{232}Th. The activity of ^{40}K was evaluated using its 1460. 8 keV gamma ray line. The activity of ^{137}Cs was evaluated using its 661. 6 keV gamma-ray line [3].

The total air absorbed dose rate ($nGy.\ h^{-1}$) due to the mean activity concentrations of ^{238}U, ^{232}Th and ^{40}K (Bq/kg) can be calculated by using the formula [4]:

(1) D ($nGy.\ h^{-1}$) = 0. 429A_U + 0. 666A_{Th} + 0. 042A_k

where A_U, A_{Th} and A_K are the mean activity concentrations of ^{238}U, ^{232}Th and ^{40}K in (Bq/kg) respectively.

To estimate the Annual effective dose equivalent in air the conversion coefficient from absorbed dose in air to effective dose received by an adult had to be taken into consideration. This value is published in UNSCEAR and the outdoor occupancy factor of about (0. 2) [4,5]. The annual effective dose equivalent can be calculated by using the formula:

(2) AEDE ($\mu Sv\ y^{-1}$) = D ($nGy\ h^{-1}$) × 8760 (hy^{-1}) × 0. 2 × 00. 7 ($Sv\ Gy^{-1}$) × 10^{-3}

Fig. (2): A gamma-ray spectrometer type (DSA2000) with (HPGe) detectort

4. Results and discussion:

The activity concentrations of the radionuclides ^{238}U, ^{232}Th, ^{40}K and ^{137}Cs in 24 soil samples considered in the present study are shown in Table (1). Fig. (3) shown the activity (Bq/kg) of ^{238}U, ^{232}Th, ^{40}K and ^{137}Cs in the soil sample. The total air absorbed dose rate and the

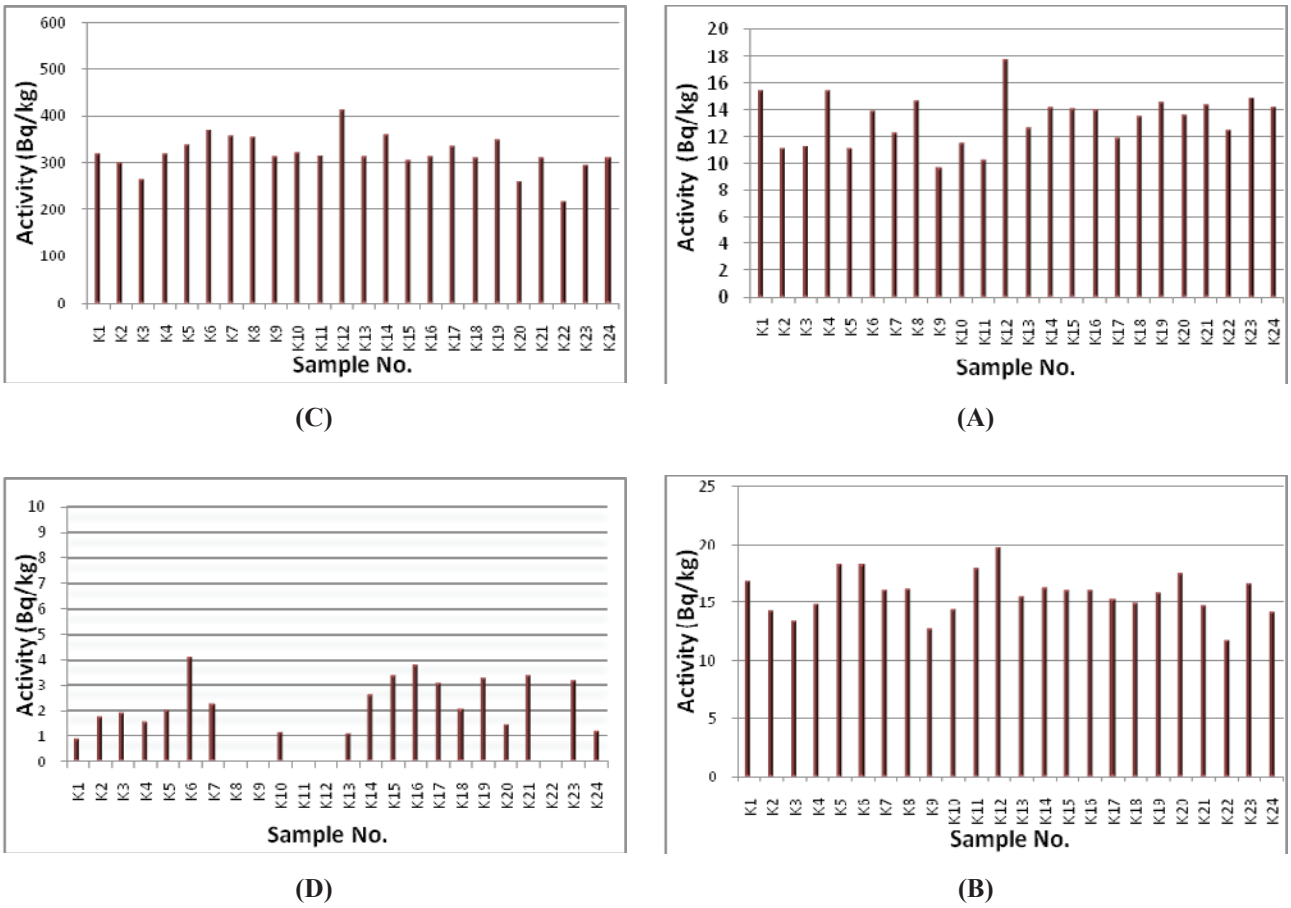

Fig. (3): Distributions of numbers of samples activity (Bq/ kg) of (A)^{238}U, (B) ^{232}Th, (C) ^{40}K and (D)^{137}Cs

annual effective dose equivalents from outdoor terrestrial gamma for 24 soil samples were calculated and presented in Table (2).

We can be seen from Table (1) the maximum value of ^{238}U is (17.70±0.87) *Bq/kg* in sample (K12), the minimum value is (9.77±0.46) *Bq/kg* in sample (K9), and the average rate of ^{238}U is (.13) 88±0.69*Bq/kg*. The maximum value of ^{232}Th is (19.77±0.92) *Bq/kg* in sample (K12), the minimum value is (11.71±0.29) *Bq/kg* in sample (K22), and the average rate of ^{232}Th is (15.73±0.86) *Bq/kg*. The maximum value of ^{40}K is (408.47±15.59) *Bq/kg* in sample (K12), the minimum value is (217.16±12.23) *Bq/kg* in sample (K22), and the average rate of ^{40}K is (317.58±14.11) *Bq/kg*. In addition, the maximum value of ^{137}Cs (4.07±0.44) *Bq/kg* in sample (K6), and appeared below the detection limit in samples (K8, K9, K11, K12, K22) and the average rate (1. 83 ± 0. 2) *Bq/Kg*.

The maximum value of the dose absorbed in air was (38.21±1.65) *nGy h*$^{-1}$ in sample (K12), the minimum value was (22.40±1.02) *nGy h*$^{-1}$ in sample (K22), and the average rate of the absorbed dose was (29.80±1.50) *nGy h*$^{-1}$. While after calculating the Annual effective dose equivalent in air of the sample found the maximum value was (46.86±2.02) *μSv y*$^{-1}$ in a sample (K12) and the minimum value was (27.47±1.25) *μSv y*$^{-1}$ in sample (K22),

Table (1): Activity Concentrations of radionuclide for each sample in (Bq/kg

Samples	Location	^{238}U	^{232}Th	^{40}K	^{137}Cs
K1	Health center (New Iraq)/ AL-Ghazaliya	15. 44±0. 79	16. 75±0. 83	318. 64±13. 50	0. 88±0. 21
K2	Pharmaceutical stores Al-Adil	13. 31±0. 71	14. 30±0. 98	297. 63±14. 79	1. 72±0. 30
K3	Hakim Hospital/Al-Shualla	11. 27±0. 29	13. 46±0. 94	264. 57±12. 18	1. 86±0. 24
K4	Conference Palace/ Garden Region	15. 42±0. 81	14. 83±0. 90	319. 42±13. 58	1. 54±0. 25
K5	National center for registration of displaced persons/ Al-harthiya	14. 46±0. 75	18. 31±1. 00	337. 57±15. 41	2. 00±0. 31
K6	Baghdad operation command/ AL-harthiya	13. 90±1. 00	18. 31±1. 12	368. 67±17. 16	4. 07±0. 44
K7	Engineers Association agricultural/AL-ma'mon	12. 30±0. 44	16. 03±0. 89	355. 69±15. 89	2. 27±0. 32
K8	Al-yarmuk Hospital/ AL-yarmuk	14. 61±0. 91	16. 16±0. 84	351. 59±14. 83	BDL
K9	Palace of Justice /AL-Huriya	9. 77±0. 46	12. 71±0. 86	310. 76±13. 22	BDL
K10	Mustansiriya University/ College of pharmacy	13. 14±0. 64	14. 41±0. 58	321. 61±13. 55	1. 18±0. 22
K11	Communication tower alm'amon	10. 71±0. 73	17. 98±0. 95	311. 99±15. 08	BDL
K12	President of court appeal al karkh	17. 70±0. 87	19. 77±0. 92	408. 47±15. 59	BDL
K13	Red crescent hospital/AL-Mansur	13. 77±0. 65	15. 51±0. 84	310. 71±13. 25	1. 1±0. 22
K14	Arab child hospital/AL-Aiskan	14. 15±0. 87	16. 29±0. 86	357. 15±14. 92	2. 59±0. 32
K15	Baghdad provincial council/ Al-karkh	14. 91±0. 70	16. 06±0. 83	302. 95±13. 63	3. 38±0. 47
K16	The Iraq state company railway/ Al-Alawi	14. 01±0. 80	16. 02±0. 89	311. 65±13. 30	3. 74±0. 47
K17	Directorate of education in Baghdad alkarkh/AL-Utaifiyya	11. 90±0. 82	15. 27±0. 83	334. 33±14. 48	3. 08±0. 358
K18	AL-Kazimiyah hospital/ AL-Kazimiyah	13. 59±0. 83	14. 89±0. 86	306. 95±13. 18	2. 08±0. 27
K19	Doura oil refinery/AL- Doura	14. 59±0. 79	15. 80±1. 08	347. 22±15. 27	3. 27±0. 62
K20	Secondary Ameriya for boys/ AL-Ameriya	13. 67±0. 95	17. 52±0. 67	258. 78±11. 48	1. 44±0. 28
K21	Secretariat of the council of ministers/Garden Region	14. 37±0. 78	14. 67±0. 82	308. 94±13. 16	3. 37±0. 35
K22	Health center/Al-Adil district	12. 43±0. 71	11. 71±0. 29	217. 16±12. 23	BDL
K23	Alakpal school girls primary/ Al-Baya	14. 95±1. 01	16. 55±1. 05	291. 29±15. 35	3. 18±0. 49
K24	AL-Diyar primary school mixed/ AL-Amal	14. 19±0. 86	14. 17±0. 80	308. 16±13. 59	1. 19±0. 22
Average	————————	13. 88±0. 69	15. 73±0. 86	317. 58±14. 11	1. 83±0. 27

*BDL:-Below the detection limit

Table (2): The dose rate ($nGyh^{-1}$) and AEDE ($\mu Sv.\ y^{-1}$) for the soil sample

Sample	D ($nGyh^{-1}$)	AEDE ($\mu Sv.\ y^{-1}$)
K1	31. 38±1. 47	38. 48±1. 80
K2	27. 95±1. 58	34. 28±1. 94
K3	25. 10±1. 27	30. 78±1. 56
K4	30. 17±1. 53	36. 96±1. 87
K5	32. 80±1. 64	40. 23±2. 02
K6	33. 90±1. 91	41. 58±2. 34
K7	31. 16±1. 46	38. 21±1. 80
K8	32. 05±1. 58	39. 31±1. 94
K9	25. 94±1. 33	31. 82±1. 64
K10	28. 98±1. 24	35. 54±1. 52
K11	29. 90±1. 59	36. 66±1. 95
K12	38. 21±1. 65	46. 86±2. 02
K13	29. 50±1. 40	36. 19±1. 72
K14	32. 18±1. 58	39. 47±1. 94
K15	30. 03±1. 43	36. 82±1. 76
K16	30. 00±1. 50	36. 78±1. 84
K17	29. 57±1. 52	36. 26±1. 87
K18	28. 86±1. 47	35. 39±1. 80
K19	31. 00±1. 71	38. 00±2. 1
K20	28. 56±1. 34	35. 03±1. 65
K21	29. 13±1. 44	35. 73±1. 77
K22	22. 40±1. 02	27. 47±1. 25
K23	29. 87±1. 79	36. 63±2. 20
K24	28. 70±1. 48	35. 19±1. 82
Average	29. 80±1. 50	36. 54±1. 84

5. Comparison with arab and international studies

Table (3) showed the comparison of the values for specific activity of radionuclides which had been calculated in the current study with the results of some Arab and international studies.

We can observed that all the values of specific activity of the current study were approaching the median value of previously studies [1, 6, 18] within the permissible limits in the world.

Table (3): The results of some studies for the Arab States and international as well as the results of the current study

Country	^{238}U	^{232}Th	^{40}K	Reference
Turkey (Istanbul)	21	37	342	[6]
Syrian	20	20	270	[7]
Kuwait	36	6	227	[8]
Mexico	23	19	530	[9]
Jordan	22	21	138	[10]
Nigeria	16. 2	24. 4	348	[11]
Cyprus	7. 1	5	104. 6	[1]
Egypt	13. 7	12. 3	1233	[12]
Pakistan	25. 8	49. 2	561. 6	[13]
Bangladesh	42	81	833	[14]
Vietnam	19. 6	31	346	[15]
Saudi Arabia (taif)	23. 8	18. 6	162. 8	[16]
western Serbia	60. 4±26. 2	49. 1±18. 5	379±108	[17]
Yemen (Juban)	44. 4±4. 5	58. 2±5. 1	822. 7±31	[18]
Baghdad (AL-Karkh)	±0. 6913. 88	±0. 86 15. 73	±14. 11317. 58	Current study

6. Conclusions:

We conclude from the above results:

The maximum value activity concentrations of the radionuclides (^{238}U, ^{232}Th, and ^{40}K) were observed in sample (K12), which represents the Presidency of the Court of Appeal Karkh side of Karkh side. It is likely that the reason for the rise in this site due to the terrorist bombing that targeted this site in 2010. The maximum value for the ^{137}Cs was observed in sample (K6), which represents the Baghdad Operations Command's area, in Harthiya however that value did not exceed the allowable global limit. There are some sites that were bombed such as secure communications tower and we noted a significant decrease in the values of specific activity in comparison with the observed values in previous studies for the same site. It is likely to be caused by a process of decontamination prior to the reconstruction of this site. Despite the high values of specific activity in some samples, all samples were within the allowable limit internationally and globally accepted and did not pose a threat to the people and other living species.

From these results we can be classified the Karkh side of Baghdad within regions radioactivity and does not constitute a danger to workers at these and near the sites.

References:

[1] M. Tzortzis, E. Svoukis and H. Tsetos, Radiation protection dosimetry, **109**, 217 (2004).

[2] Model DSA-2000 Digital Spectrum Analyzer, User's Manual, Canberra Industries, U.S.A (2000).

[3] J. Al-Jundi, Jordan. Radiat. Meas. **35**, 23 (2002).

[4] UNSCEAR, Report to general assembly, Annex B. "exposure from natural radiation sources", New York, United Nation, (2000).

[5] H. A. Al-Sulaiti, P. H. Regan, D. A. Bradley, M. Matthews, T. Santawamaitre and D. Malain, IX Radiation Physics and Protection Conference, Nasr City - Cairo, Egypt, 15-19 November (2008).

[6] L.S. Quindos, P.L. Femandez and J. Soto, Berlin. **87** (2), 365(1987).

[7] G.Karahan, and A. Bayulken, Journal of Environmental Radioactivity,**47**, 213(2000).

[8] H. R.Saad, and D.Al-Azmi, Applied Radiation and Isotopes, **56**, 991 (2002).

[9] F.Mireles, J. I. Davila, L. L. Quirino, J. F. Lugo, J. L. Pinedo and C. Rios, Health Physics, **84**, 368 (2003).

[10] J. Al-Jundyi, B. A. Al-Bataina, Y.Abu-Rukan and H.H.Shehadah, Radiation measurement, **36**,555 (2003).

[11] A.M.Arogunjo, I. P. Farai and A. Fuwape, Radiation Protection Dosimetry, **108,** 73 (2004).

[12] N.K.Ahmed and A.M. El-Arabi, Journal of Environmental Radioactivity, **84**, 51 (2004).

[13] N.Akhtar, M. Tufail, M. Ashraf and M. Iqbal, Pakistan Radiation Measurement. **39**, 11-14 (2004).

[14] M. I. Chowdhury, M. Kamal, M.N. Alam, Salaha Yeasmin and M.N. Mostafa, Radiation Protection Dosimetry Journal, **118**, 126 (2006).

[15] N. Q Huy, and T. V. Luyne, Radiation Protection Dosimetry, **118**, 331 (2006).

[16] A. El-Aydarous, Global Journal of Environmental Research, **1** (2), 49 (2007).

[17] G. Dugalic, D. Krstic, M. Jelic, D.Nikezic, B. Milenkovic, M. Pucarevic and T. Zeremski-Skoric, Journal of hazardous materials,**177**(1-3),697 (2010).

[18] A.I. Abd El-mageed, A.H.El-Kamel, A.Abbady, S.Harb A.M.Youssef, and I.I. Saleh, "Assessment of natural and anthropogenic radioactivity levels in rocks and soils in the environs of Juban town in Yemen", Tenth Radiation Physics and Protection Conference, Nasr City - Cairo, Egypt, 27-30 November (2010).

Influence of some additives on flammability and mechanical properties of modified polyester containing heterocyclic ring composites

Hilal M. Abdullah، Khalida A. Omran and Khawla I. AL-Musawi
Department of Chemistry، College of Education for pure Sciences-Ibn-AL-Haithem
University of Baghdad، Iraq
Received Date: 19/Jun/2014
Accepted Date: 16/Aug/2015

الخلاصة

في هذا العمل، تم دراسة تأثير خمسة أنواع من أملاح الفسفور اللاعضوية على تثبيط اللهوبية والخواص الميكانيكية (قوة الشد وقوة الانحناء) لراتنج البولي استر غير المشبع المحور المتشابك جزئيا والمتراكب مع الألياف الزجاجية، كذلك تم دراسة تأثير نوعين من الألياف الزجاجية (حصائر الألياف المقطعة وحصائر الألياف المحاكة) على تثبيط اللهوبية والخواص الميكانيكية للمتراكب. تم تحضير ألواح من الراتنج المحضر المتراكب بإضافة نسب مئوية (0.5, 1.0, 1.5, 2.0 و2.5%) من المضافات وبإبعاد (15×150×5) ملم مع ثلاثة طبقات من كل نوع من الألياف الزجاجية. أربعة طرق اختبار قياسية استخدمت لحساب تثبيط اللهوبية والخواص الميكانيكية وهي:

ASTM: D-2863, ASTM: D-635, ASTM: D-790 وASTM: D-638.

أن النتائج المستحصلة من هذه الاختبارات تشير إلى إن المضاف V يمتلك تأثيراً عالياً على تثبيط اللهوبية، حدوث إطفاء ذاتي (S.E) عند نسبة 1.5% وكذلك حدوث عدم أشتعال للعينة عند النسبة 2.5% للراتنج المتراكب مع الياف الزجاجية من نوع حصائر الياف المحاكة، وكذلك فأنه يظهر تأثيراً عالياً في خفض قيم الخواص الميكانيكية، لكن المضاف I يمتلك تأثير قليل على تثبيط اللهوبية ويظهر تأثيراً واطئاً على قيم الخواص الميكانيكية.

الكلمات المفتاحية

أملاح الفسفور اللاعضوية، المضافات، تثبيط اللهوبية، خواص ميكانيكية، البوليمرات المعدلة، البوليمر الحلقي الشاذ، المواد الأولية.

Abstract

In this work, the effect of five types of inorganic phosphors salts on flammability and mechanical properties (Flexural and Tensile) strength, of partially cross linked modified unsaturated polyester resin, were studied. Sheets of composites with different weight percentage of additives were prepared. Four standard test methods were used to measured the flame retardation and mechanical

properties, which are: ASTM: D-2863, ASTM: D-635, ASTM: D-790 and ASTM: D-638.

Results obtained from these tests indicated that, additive V has high efficiency as a flame retardant, self - extinguishing (S.E.) was occur at the percentage 1.5% and non - burning (N.B.) was occur at the percentage 2.5% for resin and showed high effect to reduce the values of the mechanical behaviors, but additive I has low effect on retard composition and low effect on the values of mechanical properties.

Keyword

Additives; Fire-retardant; Mechanical properties; Modified polymers; Modified polyester; Heterocyclic polymer; Composite material.

1. Introduction

A large number of synthetic polymeric materials were using in these days, with various different properties are available for medical applications and engineering matrices. Most of the common materials have sufficient mechanical stability and elasticity as well as desired stability towards degradation, and are non-toxic. [1, 4].

Heterocyclic polymers are linear high polymers comprising, heterocyclic rings, or groups of rings, linked together by one or more covalent bonds. As a group such polymers are often both mechanically rigid and inherently resistant to thermal degradation [5].

Modified polymers are widely used in the packaging industry because of their good barrier and mechanical properties, good chemical stability and processability, low costs and low toxicity. Polyethylene, polyethyleneterphthalate, polyamides and unsaturated polyester resins, are important classes of polymers with different properties [6]. When combining these polymers in multilayered structure, materials in which the favorable properties of both polymers are present can be obtained. However these polymers are not compatible and do not adhere to one another, which of course diminishes the performance of multilayered films [7].

Very wide applications for polymeric materials were extended to use them as composites that covered most aspects of life. So these materials have to modified in aspect of reducing the hazarded of heat and fire [8]. Different polymers vary in the rate of combustion and thus difference may depend on the degree of exposure to ignition source [9]. The process of combustion of polymeric materials by a heat source and a sufficient amount of oxygen of the atmosphere contains a series of physical and chemical changes that occur to both the polymer and the environment [10]. Many organic and inorganic phosphorus compounds are used as flame- retardants materials in polymeric compounds [11], Although the mechanism of action is less understood of the halogenated compounds [12], and often used phosphorus compounds synergistic with nitrogen and halogen compounds. Synergistic effect means, that using two or more of the flame - retardant materials with polymeric material for the purpose of increasing the efficiency of the disability, and in any case it is not necessary that all phosphorus compounds are flame - retardant with the same degree of efficiency, also the retarded of the flame is not linear function relative to the content of the phosphorus in the used material [13].

2. Experimental part

2. 1. Materials

a. All chemicals were used in this work analytical grade.
b. Flame-retardant; Mono ammonium phosphate, with purity 99%; Di ammonium phosphate, with purity 99.5%; Chlorinated rubber containing 72% chlorine in powder form; imported from MERCK Company.

2. 2. Standard tests

a. ASTM: D-2863: The measurement of limiting Oxygen Index (LOI), is widely used for measuring flammability of polymers [14].
b. ASTM: D-635: The measurement of rate of burning (R.B), average extent of burning

(A.E.B), average time of burning (A.T.B), Self-Extinguishing (S.E) and Non-Burning (N.B.) [15].

c. ASTM: D-790: The measurement of flexural strength, by three point method [16], with constant rate of displacement (crosshead speed) equal to 1 mm/Min., by using Instron-1122 instrument.

d. ASTM: D-638: The measurement of tensile strength [17], with constant rate of displacement (crosshead speed) equal to 1 mm/Min., by using Instron–1122 instrument.

2. 3. Flame-retardant materials

1. Monoammonium phosphate (additive I).
2. Diammonium phosphate (additive II).
3. Chlorinated rubber (additive III).
4. 50% from additive I+50% from additive III (additive IV).
5. 50% from additive II+50% from additive III (additive V).

2. 4. Preparation of modified resin

a. Preparation of hetero-cyclic monomer [18]

A mixture of (147 gm, 1.5 mole) from Maleic anhydride and (79.5 gm, 1.5 mole) from Sodium azide in a 500 ml three-necked flask equipped with a thermometer, a mechanical stirrer and reflux condenser; (80.35 gm, 1.5 mole) from Ammonium Chloride and (50 ml) THF, were added to the mixture. The mixture warmed carefully with an electric heating mantle to (60 °C); heating stopped after 3hr.; and then, the mixture was filtered and the solvent was evaporated to give a yellow crystal, (m.p.144-146 °C). Equation (1) represents that reaction. Fig.(1), represents the FT-IR spectrum of this monomer, were showed the following bands: at (3308) cm^{-1} due to υ (NH) cyclic, at (2850) cm^{-1} for υ (CH) aliphatic, at (1778) cm^{-1} for υ (C=O) anhydride group, and at (1635) cm^{-1} for υ (NH) group.

b. Preparation of the linear modified resin [19]

(172.5 gm, 1.5 mole) from the monomer was prepared in (a), were dissolved in (216 gm, 3 mole) from Glycerol in a 500 ml three-necked flask equipped with a mechanical stirrer, with stirred for 1hr. in room temperature until all monomer will be dissolve in Glycerol. (222 gm, 1.5 mole) from Phthalic anhydride were add to the mixture and warmed carefully with an electric heating mantle to (160 °C), for 1hr. until a clear liquor is formed. The mixture was heated to (220 °C), under reflux and about (50 ml) of toluene was then added carefully through the condenser, and the heating was stopped after 3hr., until no more water came off. The flask was allowed to cool down to room temperature. Equation (2), represents that reaction, and Fig. (2), represents the FT-IR spectrum of the linear modified resin, showed the following bands: at (3444)cm^{-1} due to the overlapping between υ (N-H) cyclic, υ (O-H) group and υ (CH) aromatic, at (2947-2885)

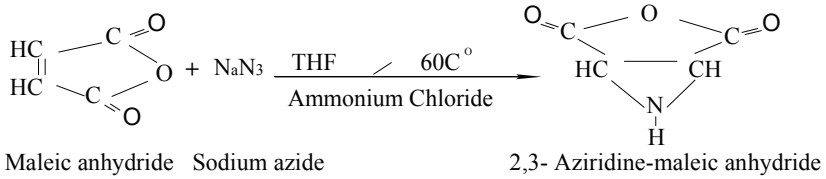

Maleic anhydride Sodium azide 2,3- Aziridine-maleic anhydride

Equation (1): Preparation of the hetero-cyclic monomer.

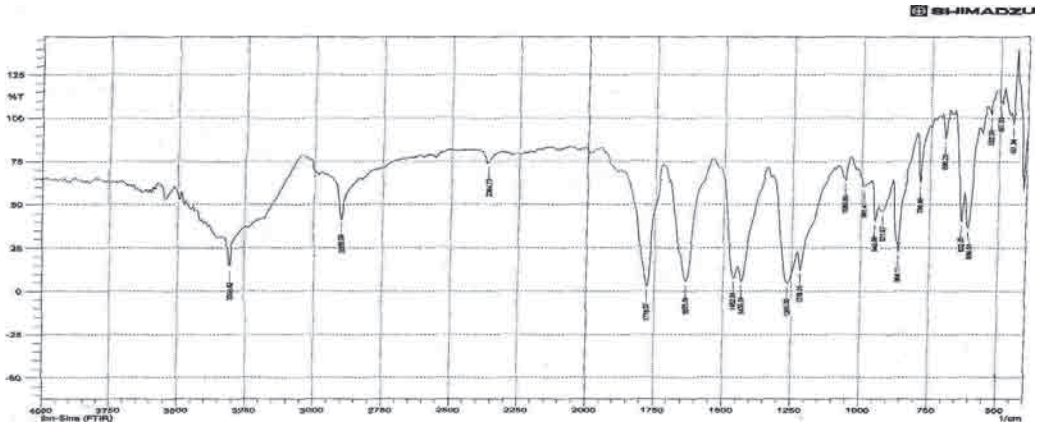

Fig. (1): The FT-IR spectrum of the prepared monomer.

Table (1): Physical properties of the modified resins after the addition of vinyl monomer.

Physical properties	Values
Molecular Weight ($\overline{Mn}$)	Around 2100 (gm/mole)
Solid content	46 %
Viscosity	17 poise
Gel time	13 min. at 25 ^{o}C
Acid Value	27
Density	1. 2 (gm/cm^3)

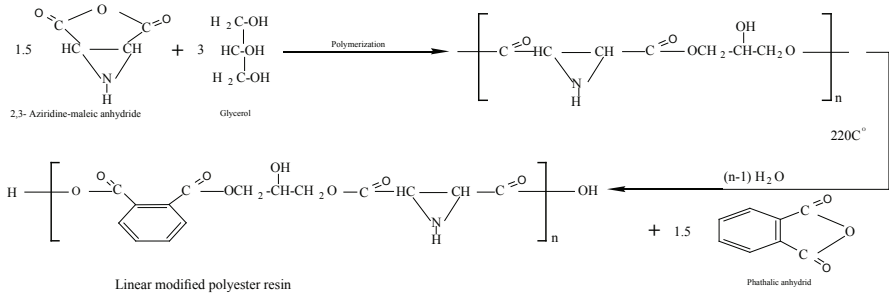

Equation (2): Preparation of the linear modified resin.

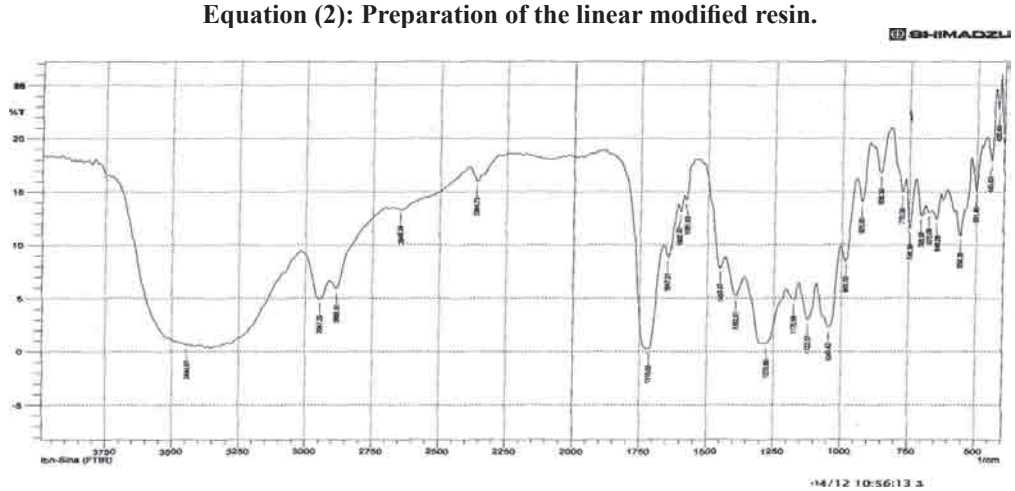

Fig. (2): The FT-IR spectrum of the linear modified resin.

Table (2): Mechanical properties of the prepared resin with additives

Type of tests	Tests of mechanical properties	Additives %					Additives
		Non	1. 0	1. 5	2. 0	2. 5	
Tensile Tests	Tensile Strength (σ_T) MPa	71	67	63	59. 6	53. 4	I
		71	65	61	57	52	II
		71	62. 7	57	54	49. 6	III
		71	60	55	50. 4	46	IV
		71	58. 4	53. 7	49	44. 8	V
	Young Modulus (E) GPa	3. 32	2. 97	2. 53	2. 39	1. 97	I
		3. 32	2. 75	2. 29	2. 10	1. 71	II
		3. 32	3. 52	2. 06	1. 85	1. 53	III
		3. 32	2. 36	1. 81	1. 64	1. 26	IV
		3. 32	2. 18	1. 59	1. 42	1. 05	V
Flexural Tests	Flexural strength (S_F) MPa	125	120. 6	115. 8	110. 3	106	I
		125	117	112	107	104	II
		125	114. 6	108. 9	105	101. 8	III
		125	112	106	102. 7	98. 1	IV
		125	109. 7	103. 7	99. 5	96	V
	Flexural Modulus (E_F) GPa	3. 19	2. 83	2. 35	1. 94	1. 47	I
		3. 19	2. 61	2. 14	1. 69	1. 22	II
		3. 19	2. 39	1. 86	1. 44	1. 05	III
		3. 19	2. 15	1. 64	1. 26	0. 82	IV
		3. 19	1. 87	1. 38	1. 02	0. 64	V

cm^{-1} for asymmetric and symmetric stretching vibrations of (CH) aliphatic, at (1716) cm^{-1} for υ (C=O) ester group, at (1643) cm^{-1} for υ (NH) group, and at (1581) cm^{-1} for υ (C=C) aromatic. The negative test of $NaHCO_3$ solution proves that the prepared modified polyester resin does not contain any un-reacted anhydride.

c. Preparation of Partially cross-linked modified resin [19]

(154. 5 gm, 0. 5 mole) from the linear resin, was prepared in (b), and mixed with (11.6 gm, 0.1 mole) from Fumaric acid in a 500 ml three-necked flask equipped with a mechanical stirrer and a thermometer, with stirred and warmed carefully with an electric heating mantle to (180 °C), under reflux and about (20 ml) of toluene was then added carefully through the condenser, and the heating was stopped after 1hr., until no more water came off. The flask was allowed to cool to (80 °C), and about (1.36×10^{-3} mole)

from Hydroquinone, and Cobalt Octoate (6%) as accelerator, were added with stirred. The flask was allowed to cool down approximately (35 ^{o}C), and added (216 gm, 2.08 mole) from Styrene monomer to the partially cross- linked modified resin and stirred for half hours until pourable syrup was formed. The viscosity and density of the prepared resins were calculated using, Brookfild digital viscometer instrument and Hydrometer instrument respectively, and the average number molecular weight ($\overline{Mn}$) was determined using the end group analysis method [20]. Equation (3), represents that reaction and Fig.(3), showed the FT-IR spectrum of the partially cross-linked modified resin; this chart appeared, the following bands: at (3437) cm^{-1} due to the overlapping between υ (N-H) cyclic, υ (O-H) group and υ (CH) aromatic, at (2943-2889) cm^{-1} for asymmetric and symmetric stretching vibration of (CH) aliphatic, at (1721) cm^{-1} for υ (C=O) ester group, at (1630) cm^{-1} for υ (NH) group, at (1578) cm^{-1} for υ (C=C) aromatic and at (1121) cm^{-1} for υ (C- O) ester.

The negative test of $NaHCO_3$ solution proves that the prepared modified polyester resin don't contain any un-reacted Fumaric acid, and Table (3), represents the physical properties measured of the prepared modified resin after addition of Styrene monomer. The addition of certain Molar percentage of Fumaric acid to the modified resin, this acid is linked by esterification process with two sets of hydroxyl dangling in two series of parallel polymer to formed a bridge between these two chains and the Fumaric acid containing double bond, this bond great benefit in cross linking with styrene monomer to formed the curing polymer, the formation of this bridge leads to reduce the number of hydroxyl groups in the polymer chains and this was confirmed by test of hydroxyl groups analysis. Using hydroxyl group analysis to determined the percentage of hydroxyl content of partially cross linked modified resin, by using, ASTM: D-2849. This standard test depends on two types of reaction (acetylation and phthalation) reactions; That test showed the percentage of hydroxyl content were decreasing from 218. 406%, to 48. 049%, with addition of the Fumaric acid to formed partially cross-linked modified resin.

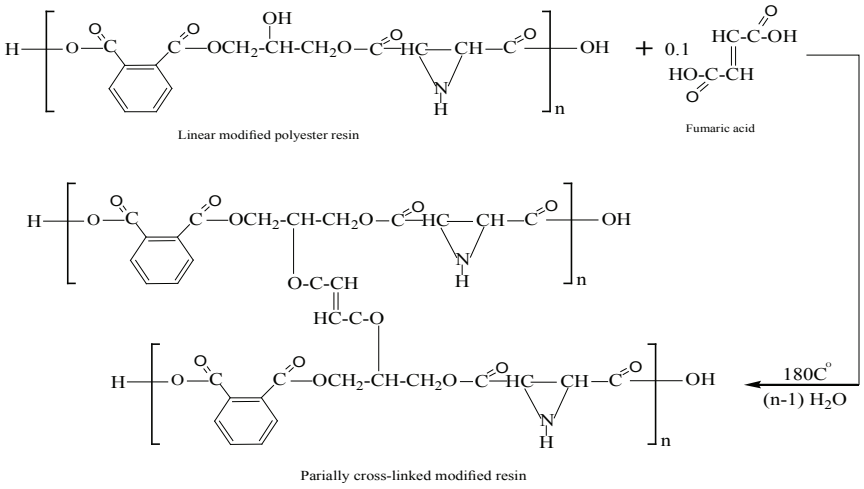

Equation (3): The partially cross-linked modified resin.

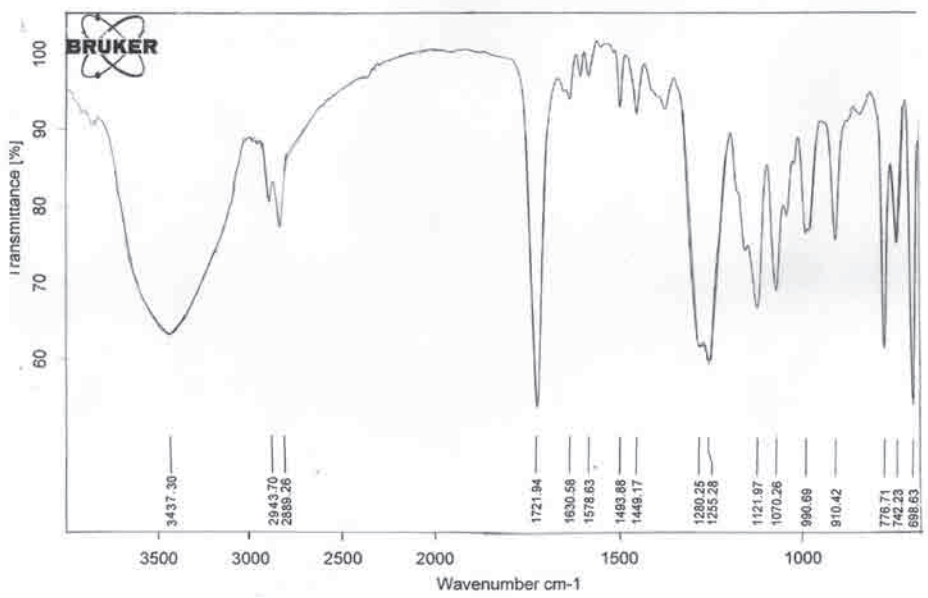

Fig. (3): The FT-IR spectrum of the partially cross- linked modified resin.

Table (3): The limiting Oxygen Index (LOI) of the partially modified resin with additives

% Additives	(LOI)				
	Non	1. 0	1. 5	2. 0	2. 5
I	20. 7	22. 65	23. 34	24. 03	24. 77
II	20. 7	22. 78	23. 63	24. 40	25. 32
III	20. 7	22. 95	23. 76	24. 56	25. 67
IV	20. 7	23. 14	24. 28	25. 32	26. 56
V	20. 7	23. 49	24. 75	26. 01	26. 83

2. 5. Preparation of polymeric specimens

The specimens of polymeric material containing additives, were prepared in dimensions (20 x 20 x 0. 5) cm; Two sheets were prepared from each percentage weight (1. 0, 1. 5, 2. 0 and 2. 5 %), of flame retardant materials (as additives) and using Methylethy lketone peroxide (MEKP) as a hardener. These sheets were cut as a samples according to ASTM standard were used in this study.

3. Results and Discussion:

3. 1. Mechanical Properties

The mechanical properties of polymers depend on many factors like molecular structure, types of branching, space distribution between main chains which contains molecular groups, and the percentage of cross linking density between these back-bone chains [21, 23].

Table (2), listed the values of Young Modulus and the maximum stress (Tensile strength) the values of Bending Modulus and the maximum stress (Flexural strength) for partially cross linked

modified resin with percentages (1. 0, 1. 5, 2. 0 and 2. 5 %) of additives; these results indicated that, increased in the percentages of additives will be decreased the behavior of mechanical properties of composite resin. This is attributed to the fact, when a stress is applied on the composite material, it will distribute on each of the matrix [24].

The result of tests obtain that, the behavior of the mechanical properties increased with increasing the percentage of additives [25]. The failure of the material under the mechanical tests, may result from the effect of stress of tensile strength, and shear together, in which the cracks appear in the positions of defects in which the stresses are concentrated, then, these cracks rapidly propagate after occurring the simple fracture [26, 27]. The results of mechanical properties tests for resin containing different weight percentage of additives, shown that the mentioned additives would lead to lower values. This reduction in the values of mechanical properties is attributed to influence of these additives on matrix, because the hard particles placed in brittle material lead to stress concentration in adjacent matrix [28]. Fig. (4), showed the stress-strain curve of prepared resin containing different percentage of additives, and Fig.(5), showed the stress-deflection curve of prepared resin containing different percentage of additives; these curves improved that behavior of mechanical properties of partially cross linked modified resin.

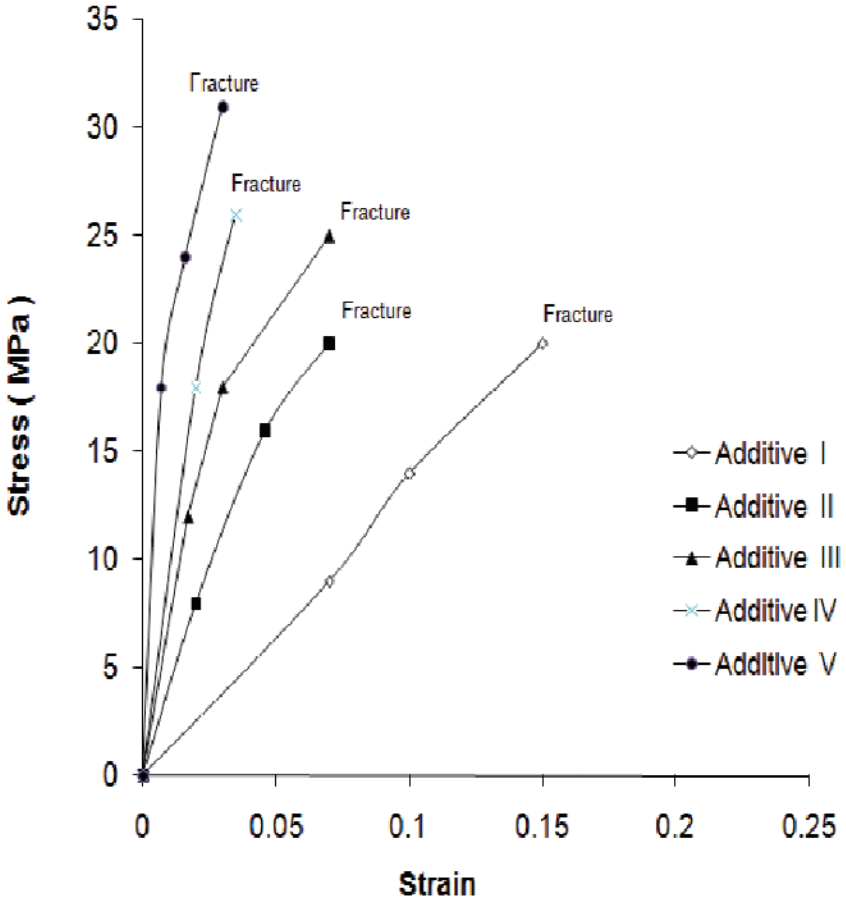

Fig. (4): Stress-strain curve of the prepared resin with additives.

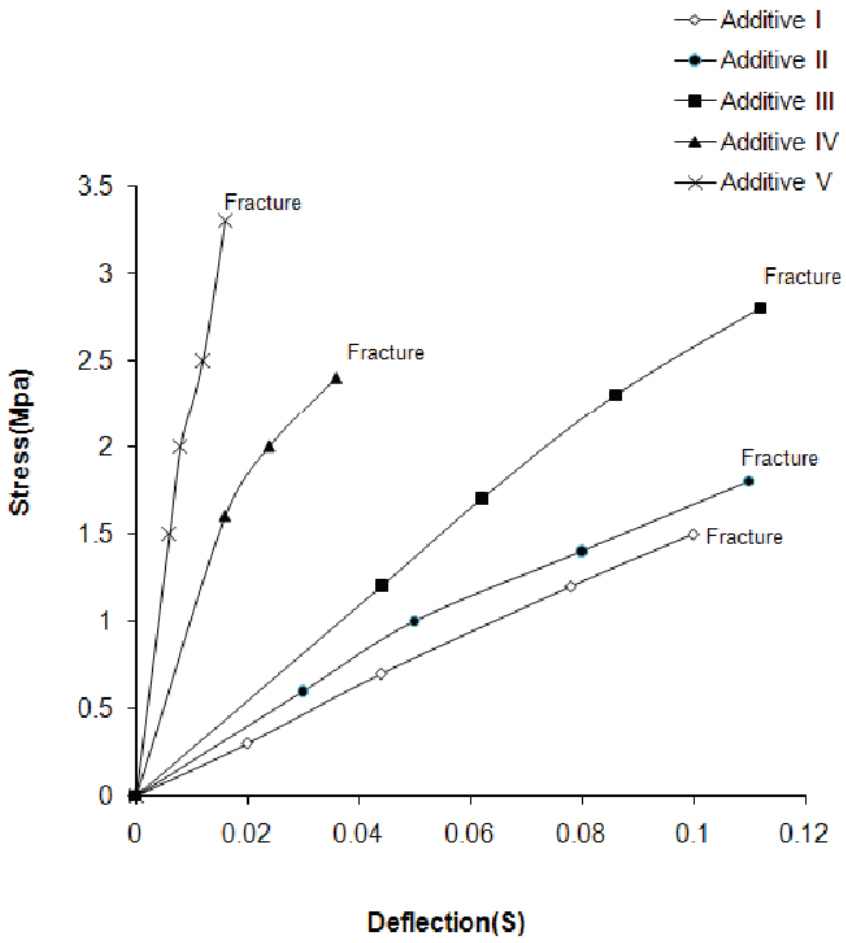

Fig. (5): Stress-deflection curve of the prepared resin with additives.

3. 2. Flammability Tests

Thermosetting polymer such as polyesters and epoxides, are generally less flammable than thermoplastic polymers, because of the difficulty of formed volatile flammable gases from highly cross-linked structures of the former and their greater tendency to the thermolze to the difficulty flammable char [29].

Table (3), listed the values of the limiting oxygen index (LOI), for partially cross linked modified resin with percentages (1.0, 1.5, 2.0 and 2.5%) of additives and Fig.(6), showed the behavior of reduced the flame. The oxygen concentration required to support a candle – like of prepared resin specimen was increased with increasing the weight percentages of additives. The efficiency of I, II, III, IV and V additives in the following order:

$$V > IV > III > II > I$$

The results obtained from that Table indicated that, the high efficiency of additive V (synergistically additive), in the weight percentage 1.5%, and decreased that effect (very weak efficiency) of additive I, in the weight percentage 1.0%; these results can be explained due to, presence of phosphor, nitrogen and chlorine elements in their structure, which have high effect on retard combustion. The free radicals were form from decomposition of material ($P^{\cdot}$, $N^{\cdot}$ and $Cl^{\cdot}$), will reacted rapidly with the free radicals of flame

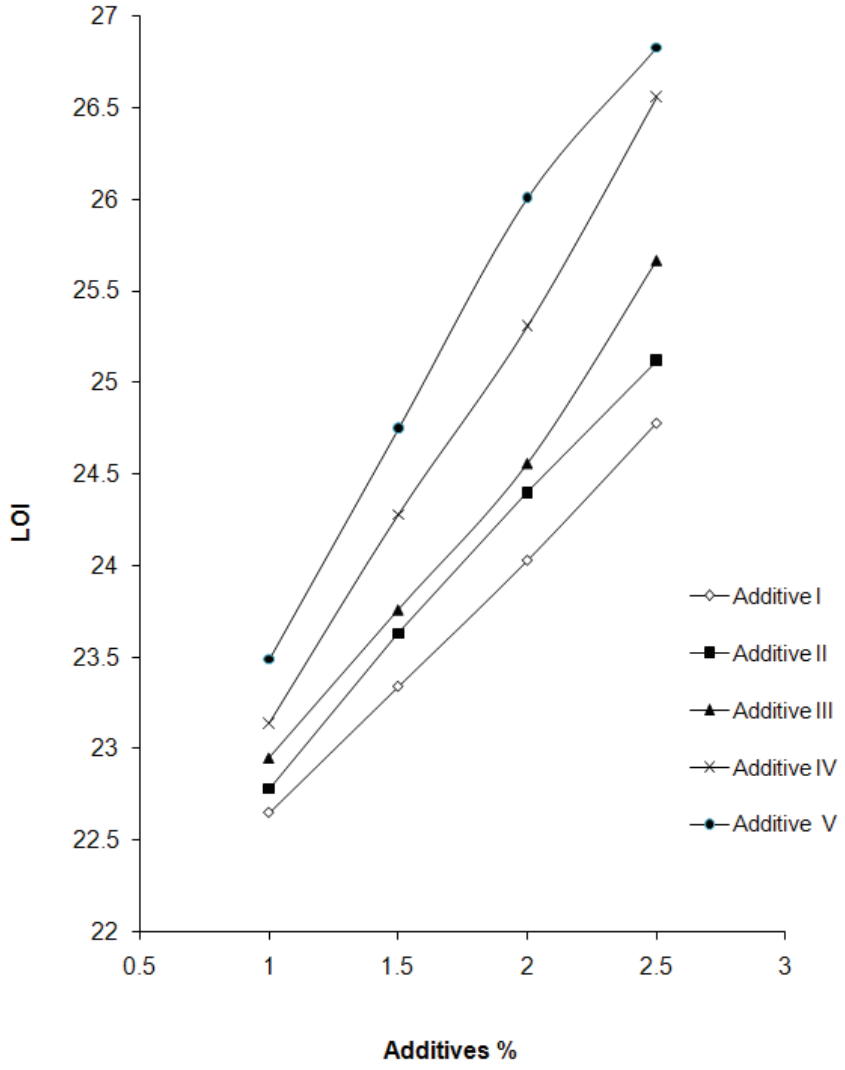

Fig. (6): Limiting oxygen index (LOI) of the prepared resin with additives.

chain, such as ($H^{\cdot}$, $O^{\cdot}$, $^{\cdot}OOH$, …, etc.) to form inert compounds like (HPO, NH_4, …, etc.) and work on inhibition of thermal decomposition will occur in flame front, because decreases of amount of generation heat and to formed a group from the non-flammable gases, such as (CO, CO_2, H_2O, …, etc.), thus will decreases from volatile materials flammable. The char will form as a result from the thermal decomposition of the specimen, it covered the polymer roof.

The rate of burning (R.B) of the with the additives has a continuous reduction with increasing the weight percentage of additives (inversely proportional), as in Table (4), listed the values of the rate of burning (R.B.), for partially cross linked modified resin with percentages (1.0, 1.5, 2.0 and 2.5%) of additives. Fig. (7), showed the flame speed curves of flame retardation for partially cross linked modified resin with additives. This results indicated that, the additive V has high efficiency on self-extinguishing (S.E) of prepared resin, especially in weight percentage 1.5% and Non-burning (N.B) occurring in percentage 2.0%.

Table (4): The rate of burning (R. B) of the prepared resin with additives

Additives % Test	Non	1. 0	1. 5	2. 0	2. 5	Additives
AEB (cm)	10. 0	9. 3	8. 7	8. 3	5. 6	I
	10. 0	8. 5	8. 0	7. 5	4. 4	II
	10. 0	8. 1	7. 4	6. 2	-	III
	10. 0	7. 5	6. 8	5. 6	-	IV
	10. 0	7. 0	6. 4	-	-	V
ATB (Min.)	7. 35	8. 23	8. 53	9. 76	10. 37	I
	7. 35	7. 80	8. 42	9. 38	9. 17	II
	7. 35	7. 71	9. 14	8. 61	-	III
	7. 35	7. 14	8. 83	11. 20	-	IV
	7. 35	7. 70	10. 34	-	-	V
R. B (Cm/Min.)	1. 36	1. 13	1. 02	0. 85	0. 54	I
	1. 36	1. 09	0. 95	0. 80	0. 48	II
	1. 36	1. 05	0. 81	0. 72	-	III
	1. 36	1. 01	0. 77	0. 50	-	IV
	1. 36	0. 91	0. 58	-	-	V
S. E	-	-	-	yes	yes	I
	-	-	-	yes	yes	II
	-	-	yes	yes	yes	III
	-	-	yes	yes	yes	IV
	-	-	yes	yes	yes	V
N. B	-	-	-	-	-	I
	-	-	-	-	-	II
	-	-	-	-	yes	III
	-	-	-	-	yes	IV
	-	-	-	yes	yes	V

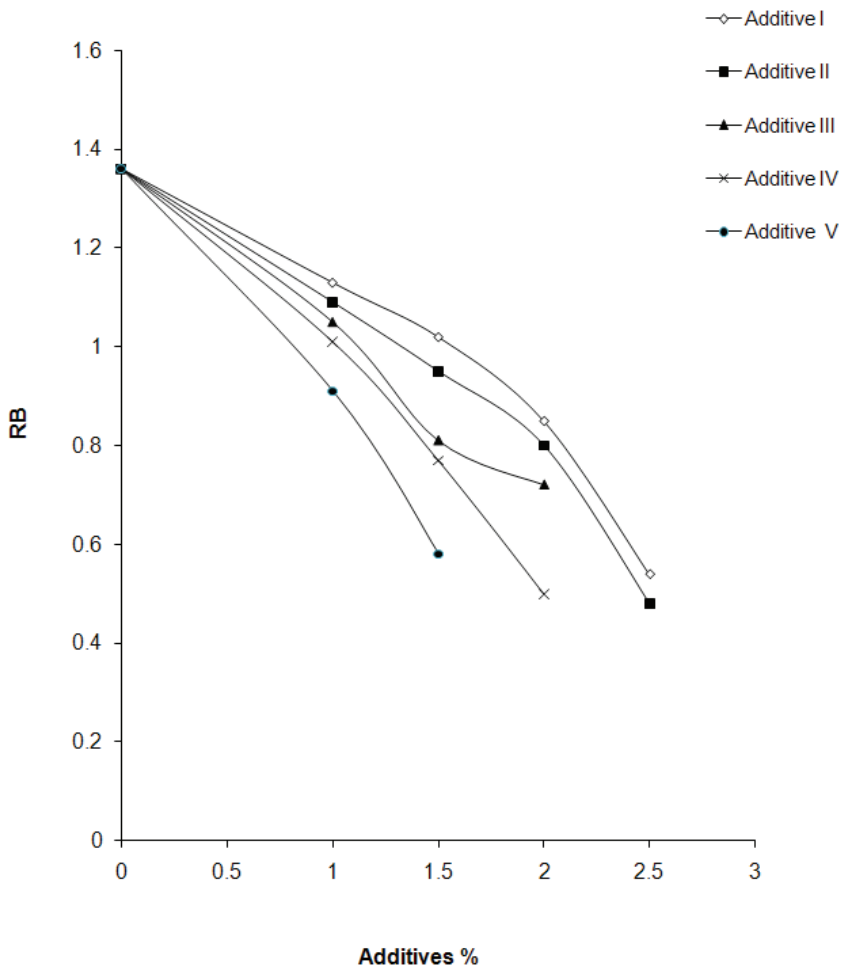

Fig. (7): Rate of burning (R. B.) of the prepared resin with additives.

Conclusions

The main conclusions of this work can be summarized as follows:

1. The efficiency of the flame retardation for additives was in the following order:

V >IV > III > II > I

2. Limiting oxygen index (LOI) was increased with increasing of weight percentage of additives, but the rate of burning (R. B) was decreased with increasing of weight percentage of additives.

3. Additive V has high effect on retard combustion for the composite, but it reduces the mechanical properties.

4. Additive I showed low effect on retard combustion for the composite, and it showed little effect on the values of mechanical properties comparing with additive V.

References

[1] R. Lebaron and K. Athanasiou, Tissue Eng, **6**,85 (2010).

[2] J. Hubbell, Curr Opin Biotechnol, **10**, 123 (1999).

[3] K. M. Shakesheff, S.M. Cannizzaro and R. Langer, J. Biomat. Sci. Polym. Ed.; **9**, 507(1998).

[4] D. L. Elbert and J. A. Hubbell, Annu. Rev. Mater. Sci., **26**, 365 (1996).

[5] M. V. Sreenivasa, A. N. Nagappa, and L. V. G. Nargund, Indian J. Heterocycl. Chem., **8**, 23 (2007).

[6] M.A. AL-Issa., T. Davis, M.Huglin and D.C. Vip, Polymer, 26 (12), 1869 (1985).

[7] A. Factor, J. Chem. Educ, **51**, 453 (1974).

[8] E. Hanss-Georg, An Introduction to Plastics,John Wiely andSons, NewYork, 24 (2003).

[9] S. Aslam, J.Mater.Sci., **32**, 2329 (1997).

[10] B. Parkyn, F.Lam and B.V. Clifton, Polyesters, Vol. II, London, 54 (1967).

[11] M. M. Hirschler, "Flame Retardant Mechanisms", 110, City University Press, London (1975).

[12] J. A. Albright and C. J. K.miec, J. Appl. polym., Sci., **22**, 2451 (1978).

[13] F.K.Antta, C.F.Cullis and M.M.Hirschler, Eur. Polym. J., **17**, 451 (1981).

[14] Annual Book of ASTM Standard, **8**, 1 (2011).

[15] Annual Book of ASTM Standard, Part-35 (2000).

[16] Annual Book of ASTM Standard, **8**, 4 (2001).

[17] Annual Book of ASTM Standard, 8, 1 (1989).

[18] F. Firrozi, K. Javidnia, M. Kamali, A. Foroumadi, and A. Shfiee, J.Heterocyclic Chem., **32**, 1235 (1995).

[19] S.A.Kassim, J.Al-Khafaji, A.H.Al-Dujili, and M.S.Al-Mahdawi, "Practical Industrial Chemistry", 1st.ed., University of Baghdad (1988).

[20] E. Lokensgard, Industrial Plastics, Thomson Delwar Learning, NewYork, **88**, (2013).

[21] Prudhomme R.E. and Abtal E., Macromolecular, 27 (20), 5780 (1994).

[22] Rosen B., Fracture Processes in Polymeric Solids, John Wiely and Sons,NewYork,41 (1964).

[23] Jaffer H.I., Thesis, University of Baghdad, College of Science, 87, (2000).

[24] G. Caminol, L.Costa and E.Casorati, J. Appl. polym., Sci., **35**, 1863 (1988).

[25] R. J.SchwarZ," Flame Retardants of Polymeric Materials", V.2, Eus. Kurgla, W.C. and papa, A.J. (1978).

[26] E. G.Cretize, J. Res Nartl, Bur., Stand., 74A,521 (1970).

[27] S. Chondhary, J.K Fink, Klederer, and H. A. Krassing, J. Appl. Polym. Sci, **34**, 863 (1987).

[28] L. Z. Xu, K. Jioo, S. S. Zhang, and S. P. Kuang, Bull-Korean Chem. Soc., **23**, 12 (2002).

[29] E. Hanss-Georg; Macromolecules; John Wiely and Sons; NewYork; Vol. 1, 16 (2005).

Iterated bivariate rayleigh distribution

Kareema Abed AL-Kadim, Afrah Sahim
Deparameter of Mathematics
College of Education for Pure Sciences, University of Babylon, Iraq
Received Date: 20/Jun/2015
Accepted Date: 9/Jul/2015

الخلاصة

ان توزيع رالي هو احد توزيعات الحياة وهو حالة خاصة من توزيع ويبل وله كثير من الاستخدامات في مجالات الحياة المختلفة، المالية، معالجة الإشارات والاتصالات. ان الصلات هي دوال تجمع دوال التوزيع الحدية والتي تعتبر متغيرات عشوائية ذات نوزيع منتظم على الفترة (1,0). فالصلة هي وسيله لبناء عوائل للتوزيعات الثنائية وهي مقباس للأعتمادية بين متغيرين لأنها تسمح لنا فصل تأثير الأعتمادية من تأثيرات التوزيعات الحدية.

في هذا البحث تم اشتقاق توزيع رالي الثنائي المكرر باستخدام مفهوم الصلات مع مناقشة بعض الخواص، على سبيل المثال دالة التوزيع، دالة الكثافة الأحتمالية، الدوال الشرطية، التوقع الشرطي، التباين المشترك ومعامل الأرتباط.

الكلمات المفتاحية

توزيع رالي، الصلات، توزيع ثنائي المتغيرين، دالة كثافة الإحتمالية الشرطية، المعامل المترابط، التوقع المشروط.

Abstract

The Rayleigh distribution is one of the lifetime distributions and a special case from Weibull distribution. It has widely used in many fields in real life, finance, signal processing, and communications. Copulas are functions that join their one-dimensional marginal distribution functions which are uniform on the interval (0,1). The copula is an important tool for constructing families of bivariate distributions and it is measure of dependence between two variables since it allows us to separate the effect of dependence from the effects of the marginal distributions.

In this paper, we derive iterated bivariate Rayleigh distribution using the concept of copula with discussion of some properties, like the cdf, pdf, conditional pdf's, conditional expectation, covariance and correlation coefficient.

Keywords

copulas, Rayleigh distribution, bivariate distribution, conditional probability density function, conditional expectation ,correlation coefficient.

1. Introduction

Rayleigh, [1] noted that the data about the wave heights, wave length, wave induce pitch, wave and heave motions of the ships follow the Rayleigh distribution which was derived from the bivariate normal distribution when the variables are independent with equal variances.

The concept of copula was established by Sklar A. [2] when he studied the relationship between a multidimensional probability function and its lower dimensional margins.

Quesada-Molina, J., J., Rodrguez-Lallena, J. A., and beda-Flores, M., [3] presented a theory of copulas with some of the results and various examples.

Abdel-Hady, D.,[4] has studied the generalized bivariate Rayleigh (GBR) distribution its the cumulative distribution function, the probability density function, the conditional distribution of the BGR distribution and the maximum likelihood estimator.

Zeng, X., Ren, J., Wang, Z., Marshall, S., Durrani, T., [5] derived new bivariate copulas for Exponential, Weibull and Rician distributions. They proved that the three copula functions of these distributions are equivalent, and also showed that the copula function of log-normal distribution is quivalent to the Gaussian copula.

Sarabia, J., M., Prieto F. and Jord V., [6] introduced three new classes of bivariate beta-generated distributions with main properties.

In this search we derive the iterated Bivariate Rayleigh distribution which can be used in the lifetime phenomena, like finance, signal processing, and communications

2. Some important concepts

2. 1. Rayleigh distribution [7]

The Rayleigh random variable has the distribution function as

$$F(x) = 1 - e^{-\frac{x^2}{2\sigma^2}}, \quad x \geq 0, \sigma > 0 \quad .(1)$$

And its probability density function is

$$f(x) = \frac{x}{\sigma^2} e^{-\frac{x^2}{2\sigma^2}}, \quad x \geq 0, \sigma > 0 \quad .(2)$$

Therefore the mean and the variance of X are as follows

$$E(X) = \sigma\sqrt{\frac{\pi}{2}}, \quad V(X) = \frac{4-\sqrt{\pi}}{2}\sigma^2$$

2. 2. Copula [3]

Definition 2. 2. 1: A concept of copula can be defined as a function C: [0, 1] $^2\rightarrow$ [0, 1] that satisfies the following:

a. C (u, 0) = 0 = C (0, v), and C (u, 1) = u and C (1, v) = v, for every u, v in [0, 1],

b. $C(u_2, v_2) - C(u_2, v_1) - C(u_1, v_2) + C(u_1, v_1) \geq 0$, for every u_1, u_2, v_1, v_2 in [0, 1] such that $u_1 \leq u_2$ and $v_1 \leq v_2$.

2. 3. Theorem [8]

Let be a joint distribution function with marginals F_1 and F_2. Then, there exists a copula C such that, for all $x, y \in [-\infty, \infty]$,

$$F(x, y) = C\big(F_1(x), F_2(y)\big) \quad .(3)$$

And the p. d, f, is

$$f(x, y) = c\big(F_1(x), F_2(y)\big) f_1(x) f_2(y) \quad .(4)$$

where f, f_1, f_2, and c be the density functions of F, F_1, F_2 and *C*, respectively.

3. Iterated F. G. M. bivariate rayleigh distribution [2]

The joint pdf, and cdf of "Iterated Bivariate Rayleigh Distribution", I BRD, using, (3), (4) which are as follows:

$$C(u_1, v_1) = u_1 v_1[1 + \alpha(1 - u_1)(1 - v_1) + \beta u_1 v_1(1 - u_1)(1 - v_1)] \quad .(5)$$

$$c(u_1, v_1) = 1 + \alpha(1 - 2u_1)(1 - 2v_1) + \beta u_1 v_1(2 - 3u_1)(2 - 3v_1)$$

$$\text{where } u_1 = F_1(x_1), v_1 = F_2(x_2) \text{and} -1 \leq \alpha \leq 1, -1 - \alpha \leq \beta \leq (3 - \alpha + \sqrt{9 - 6\alpha - 3\alpha^2})/2 \quad .(6)$$

That is, the cdf is

$$F(x_1, x_2) = F_1(x_1)F_2(x_2)\left(1 + \alpha(1 - F_1(x_1))(1 - F_2(x_2)) + \beta F_1(x_1)F_2(x_2)(1 - F_1(x_1))(1 - F_2(x_2))\right)$$

$$= \left(1 - e^{-\frac{x_1^2}{2\sigma_1^2}}\right)\left(1 - e^{-\frac{x_2^2}{2\sigma_2^2}}\right)\left[\left(1 + \alpha e^{-\frac{x_1^2}{2\sigma_1^2}} e^{-\frac{x_2^2}{2\sigma_2^2}}\right) + \beta\left(1 - e^{-\frac{x_1^2}{2\sigma_1^2}}\right)\left(1 - e^{-\frac{x_2^2}{2\sigma_2^2}}\right) e^{-\frac{x_1^2}{2\sigma_1^2}} e^{-\frac{x_2^2}{2\sigma_2^2}}\right]$$

$$= 1 - e^{-\frac{x_2^2}{2\sigma_2^2}} - e^{-\frac{x_1^2}{2\sigma_1^2}} + e^{-\frac{x_1^2}{2\sigma_1^2}} e^{-\frac{x_2^2}{2\sigma_2^2}} + \alpha(e^{-\frac{x_1^2}{2\sigma_1^2}} e^{-\frac{x_2^2}{2\sigma_2^2}} - e^{-\frac{x_1^2}{2\sigma_1^2}} e^{-\frac{x_2^2}{\sigma_2^2}} - e^{-\frac{x_1^2}{\sigma_1^2}} e^{-\frac{x_2^2}{2\sigma_2^2}} + e^{-\frac{x_1^2}{\sigma_1^2}} e^{-\frac{x_2^2}{\sigma_2^2}}) + \beta\left(e^{-\frac{x_1^2}{2\sigma_1^2}} e^{-\frac{x_2^2}{2\sigma_2^2}} - 2e^{-\frac{x_1^2}{2\sigma_1^2}} e^{-\frac{x_2^2}{\sigma_2^2}} - 2e^{-\frac{x_1^2}{\sigma_1^2}} e^{-\frac{x_2^2}{2\sigma_2^2}} + 4e^{-\frac{x_1^2}{\sigma_1^2}} e^{-\frac{x_2^2}{\sigma_2^2}} - 2e^{-\frac{3x_1^2}{2\sigma_1^2}} e^{-\frac{x_2^2}{\sigma_2^2}} + e^{-\frac{3x_1^2}{2\sigma_1^2}} e^{-\frac{x_2^2}{2\sigma_2^2}} + e^{-\frac{x_1^2}{2\sigma_1^2}} e^{-\frac{3x_2^2}{2\sigma_2^2}} - 2e^{-\frac{x_1^2}{\sigma_1^2}} e^{-\frac{3x_2^2}{2\sigma_2^2}} + e^{-\frac{3x_1^2}{2\sigma_1^2}} e^{-\frac{3x_2^2}{2\sigma_2^2}}\right) \quad .(7)$$

Fig.. (1) shows example of bivariate distribution (7)

The pdf is

$$f(x_1,x_2)=f_1(x_1)f_2(x_2)\left[1+\alpha\left(1-2F_1(x_1)\right)\left(1-2F_2(x_2)\right)\right.$$

$$\left.+\beta F_1(x_1)F_2(x_2)\left(2-3F_1(x_1)\right)\left(2-3F_2(x_2)\right)\right]$$

$$=\frac{x_1}{\sigma_1^2}\frac{x_2}{\sigma_2^2}e^{-\frac{x_1^2}{2\sigma_1^2}}e^{-\frac{x_2^2}{2\sigma_2^2}}+\alpha\left(4\frac{x_1}{\sigma_1^2}\frac{x_2}{\sigma_2^2}e^{-\frac{x_1^2}{\sigma_1^2}}e^{-\frac{x_2^2}{\sigma_2^2}}-2\frac{x_1}{\sigma_1^2}\frac{x_2}{\sigma_2^2}e^{-\frac{x_1^2}{\sigma_1^2}}e^{-\frac{x_2^2}{2\sigma_2^2}}-2\frac{x_1}{\sigma_1^2}\frac{x_2}{\sigma_2^2}e^{-\frac{x_1^2}{2\sigma_1^2}}e^{-\frac{x_2^2}{\sigma_2^2}}+\right.$$

$$\left.\frac{x_1}{\sigma_1^2}\frac{x_2}{\sigma_2^2}e^{-\frac{x_1^2}{2\sigma_1^2}}e^{-\frac{x_2^2}{2\sigma_2^2}}\right)+\beta\left(16\frac{x_1}{\sigma_1^2}\frac{x_2}{\sigma_2^2}e^{-\frac{x_1^2}{\sigma_1^2}}e^{-\frac{x_2^2}{\sigma_2^2}}-4\frac{x_1}{\sigma_1^2}\frac{x_2}{\sigma_2^2}e^{-\frac{x_1^2}{\sigma_1^2}}e^{-\frac{x_2^2}{2\sigma_2^2}}-4\frac{x_1}{\sigma_1^2}\frac{x_2}{\sigma_2^2}e^{-\frac{x_1^2}{2\sigma_1^2}}e^{-\frac{x_2^2}{\sigma_2^2}}+\right.$$

$$3\frac{x_1}{\sigma_1^2}\frac{x_2}{\sigma_2^2}e^{-\frac{3x_1^2}{2\sigma_1^2}}e^{-\frac{x_2^2}{2\sigma_2^2}}+3\frac{x_1}{\sigma_1^2}\frac{x_2}{\sigma_2^2}e^{-\frac{x_1^2}{2\sigma_1^2}}e^{-\frac{3x_2^2}{2\sigma_2^2}}-12\frac{x_1}{\sigma_1^2}\frac{x_2}{\sigma_2^2}e^{-\frac{3x_1^2}{2\sigma_1^2}}e^{-\frac{x_2^2}{\sigma_2^2}}-12\frac{x_1}{\sigma_1^2}\frac{x_2}{\sigma_2^2}e^{-\frac{x_1^2}{\sigma_1^2}}e^{-\frac{3x_2^2}{2\sigma_2^2}}+$$

$$\left.9\frac{x_1}{\sigma_1^2}\frac{x_2}{\sigma_2^2}e^{-\frac{3x_1^2}{2\sigma_1^2}}e^{-\frac{3x_2^2}{2\sigma_2^2}}+\frac{x_1}{\sigma_1^2}\frac{x_2}{\sigma_2^2}e^{-\frac{x_1^2}{2\sigma_1^2}}e^{-\frac{x_2^2}{2\sigma_2^2}}\right)$$

.(8)

Fig.(2): shows example of bivariate distribution And the conditional pdf is

$$f(x_1/x_2)=\frac{f(x_1,x_2)}{f(x_2)}$$

$$=\frac{x_1}{\sigma_1^2}e^{-\frac{x_1^2}{2\sigma_1^2}}+\alpha\left(4\frac{x_1}{\sigma_1^2}e^{-\frac{x_1^2}{\sigma_1^2}}e^{-\frac{x_2^2}{2\sigma_2^2}}-2\frac{x_1}{\sigma_1^2}e^{-\frac{x_1^2}{\sigma_1^2}}-2\frac{x_1}{\sigma_1^2}e^{-\frac{x_1^2}{2\sigma_1^2}}e^{-\frac{x_2^2}{2\sigma_2^2}}+\frac{x_1}{\sigma_1^2}e^{-\frac{x_1^2}{2\sigma_1^2}}\right)$$

$$+\beta\left(16\frac{x_1}{\sigma_1^2}e^{-\frac{x_1^2}{\sigma_1^2}}e^{-\frac{x_2^2}{2\sigma_2^2}}-4\frac{x_1}{\sigma_1^2}e^{-\frac{x_1^2}{\sigma_1^2}}-4\frac{x_1}{\sigma_1^2}e^{-\frac{x_1^2}{2\sigma_1^2}}e^{-\frac{x_2^2}{2\sigma_2^2}}+3\frac{x_1}{\sigma_1^2}e^{-\frac{3x_1^2}{2\sigma_1^2}}\right.$$

$$\left.+3\frac{x_1}{\sigma_1^2}e^{-\frac{x_1^2}{2\sigma_1^2}}e^{-\frac{x_2^2}{\sigma_2^2}}-12\frac{x_1}{\sigma_1^2}e^{-\frac{3x_1^2}{2\sigma_1^2}}e^{-\frac{x_2^2}{2\sigma_2^2}}-12\frac{x_1}{\sigma_1^2}e^{-\frac{x_1^2}{\sigma_1^2}}e^{-\frac{x_2^2}{\sigma_2^2}}+9\frac{x_1}{\sigma_1^2}e^{-\frac{3x_1^2}{2\sigma_1^2}}e^{-\frac{x_2^2}{\sigma_2^2}}+\frac{x_1}{\sigma_1^2}e^{-\frac{x_1^2}{2\sigma_1^2}}\right)$$

.(9)

Proposition 3. 1

If (X_1, X_2) ~IBRD (σ_1, σ_2), then

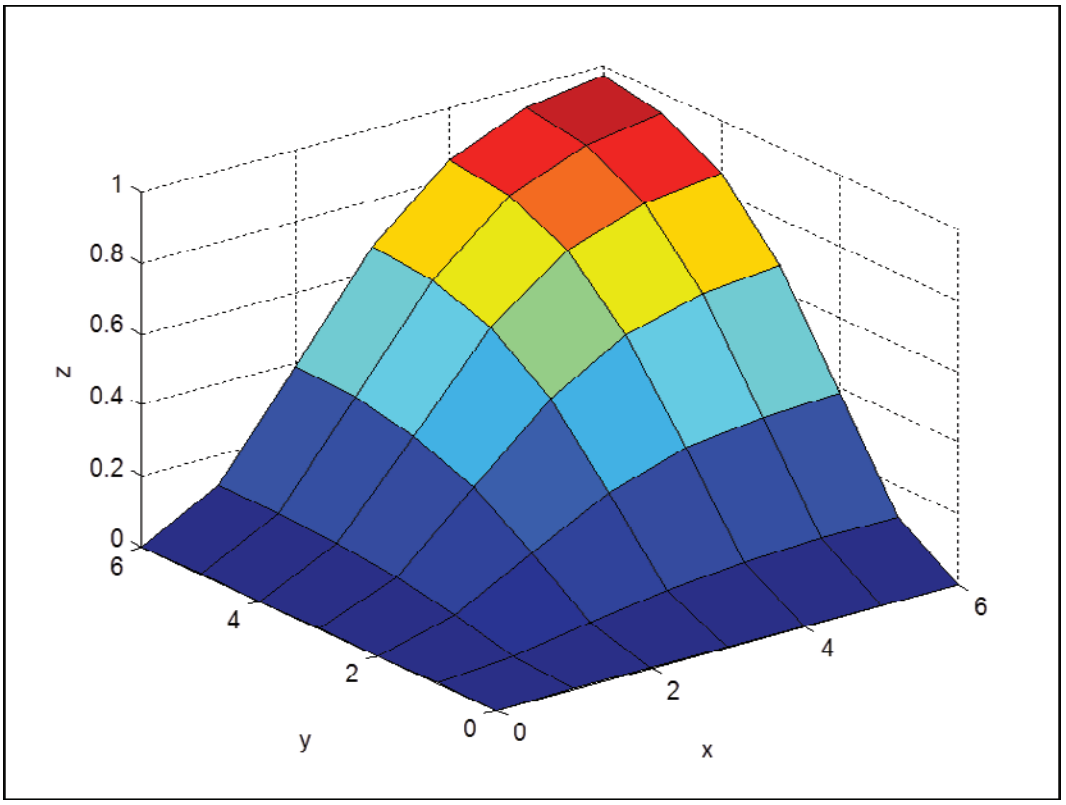

Fig.(1): Where

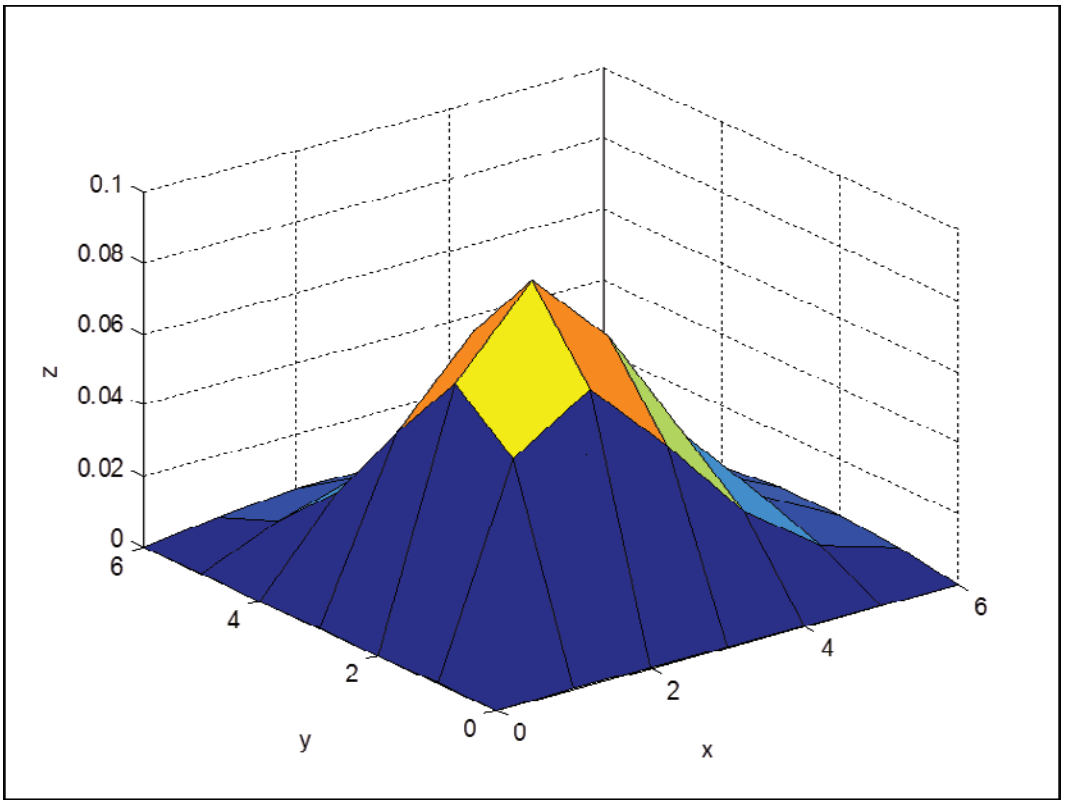

Fig.(2): Where

$$X_1 \sim R(\sigma_1) \text{and } X_2 \sim R(\sigma_2) \quad .1$$

$$E(X_1/X_2) = \gamma + \alpha\gamma\gamma_1 - 2\alpha\gamma\gamma_1 e^{-\frac{x_2^2}{2\sigma_2^2}} + \beta\gamma\gamma_2 - 4\beta\gamma\gamma_2 e^{-\frac{x_2^2}{2\sigma_2^2}} + 3\beta\gamma\gamma_2 e^{-\frac{x_2^2}{\sigma_2^2}} \quad .2$$

$$E(X_1X_2) = \gamma\lambda + \alpha\lambda\gamma\gamma_1^2 + \beta\lambda\gamma\gamma_2^2 \quad .3$$

$$\text{cov}(X_1, X_2) = \alpha\lambda\gamma\gamma_1^2 + \beta\lambda\gamma\gamma_2^2 \quad .4$$

$$\text{corr}(X_1, X_2) = \frac{\alpha\lambda\gamma\gamma_1^2 + \beta\lambda\gamma\gamma_2^2}{\sqrt{4 - 2\lambda - 2\gamma + \lambda\gamma}} \quad .5$$

Proof of (1)

$$f(x_1) = \int_0^\infty f(x_1, x_2)\, dx_2$$

$$= \frac{x_1}{\sigma_1^2} e^{-\frac{x_1^2}{2\sigma_1^2}} + \alpha\left(2\frac{x_1}{\sigma_1^2} e^{-\frac{x_1^2}{\sigma_1^2}} - 2\frac{x_1}{\sigma_1^2} e^{-\frac{x_1^2}{\sigma_1^2}} - \frac{x_1}{\sigma_1^2} e^{-\frac{x_1^2}{2\sigma_1^2}} + \frac{x_1}{\sigma_1^2} e^{-\frac{x_1^2}{2\sigma_1^2}}\right)$$

$$+ \beta\left(8\frac{x_1}{\sigma_1^2} e^{-\frac{x_1^2}{\sigma_1^2}} - 4\frac{x_1}{\sigma_1^2} e^{-\frac{x_1^2}{\sigma_1^2}} - 2\frac{x_1}{\sigma_1^2} e^{-\frac{x_1^2}{2\sigma_1^2}} + 3\frac{x_1}{\sigma_1^2} e^{-\frac{3x_1^2}{2\sigma_1^2}} + \frac{x_1}{\sigma_1^2} e^{-\frac{x_1^2}{2\sigma_1^2}}\right.$$

$$\left. - 6\frac{x_1}{\sigma_1^2} e^{-\frac{3x_1^2}{2\sigma_1^2}} - 4\frac{x_1}{\sigma_1^2} e^{-\frac{x_1^2}{\sigma_1^2}} + 3\frac{x_1}{\sigma_1^2} e^{-\frac{3x_1^2}{2\sigma_1^2}} + \frac{x_1}{\sigma_1^2} e^{-\frac{x_1^2}{2\sigma_1^2}}\right)$$

$$= \frac{x_1}{\sigma_1^2} e^{-\frac{x_1^2}{2\sigma_1^2}}$$

and f (x_2) is found similarly.

Proof of (2)

$$E(X_1/X_2) = \int_0^{\infty} x_1 f(x_1/x_2)dx_1$$

$$= \sigma_1\sqrt{\frac{\pi}{2}} + \alpha(\sigma_1\sqrt{\pi}e^{-\frac{x_2^2}{2\sigma_2^2}} - \frac{1}{2}\sigma_1\sqrt{\pi} - 2\sigma_1\sqrt{\frac{\pi}{2}}e^{-\frac{x_2^2}{2\sigma_2^2}} + \sigma_1\sqrt{\frac{\pi}{2}})$$

$$+ \beta\left(4\sigma_1\sqrt{\pi}e^{-\frac{x_2^2}{2\sigma_2^2}} - \sigma_1\sqrt{\pi} - 4\sigma_1\sqrt{\frac{\pi}{2}}e^{-\frac{x_2^2}{2\sigma_2^2}} + \frac{1}{\sqrt{6}}\sigma_1\sqrt{\pi} + 3\sigma_1\sqrt{\frac{\pi}{2}}e^{-\frac{x_2^2}{\sigma_2^2}}\right.$$

$$\left. - \frac{4}{\sqrt{6}}\sigma_1\sqrt{\pi}e^{-\frac{x_2^2}{2\sigma_2^2}} - 3\sigma_1\sqrt{\pi}e^{-\frac{x_2^2}{\sigma_2^2}} + \frac{3}{\sqrt{6}}\sigma_1\sqrt{\pi}e^{-\frac{x_2^2}{\sigma_2^2}} + \sigma_1\sqrt{\frac{\pi}{2}}\right)$$

$$= \gamma + \alpha\gamma\gamma_1 - 2\alpha\gamma\gamma_1 e^{-\frac{x_2^2}{2\sigma_2^2}} + \beta\gamma\gamma_2 - 4\beta\gamma\gamma_2 e^{-\frac{x_2^2}{2\sigma_2^2}} + 3\beta\gamma\gamma_2 e^{-\frac{x_2^2}{\sigma_2^2}}$$

$$\text{where } \gamma = \sigma_1\sqrt{\frac{\pi}{2}}\,, \gamma_1 = \frac{2-\sqrt{2}}{2}\,, \gamma_2 = \frac{\sqrt{3}-\sqrt{6}+1}{\sqrt{3}} \qquad .(10)$$

Then by the Same way, we get

$$E(X_2/X_1) = \lambda + \alpha\lambda\gamma_1 - 2\alpha\lambda\gamma_1 e^{-\frac{x_1^2}{2\sigma_1^2}} + \beta\lambda\gamma_2 - 4\beta\lambda\gamma_2 e^{-\frac{x_1^2}{2\sigma_1^2}} + 3\beta\lambda\gamma_2 e^{-\frac{x_1^2}{\sigma_1^2}}$$

$$\text{where } \lambda = \sigma_2\sqrt{\frac{\pi}{2}} \qquad .(11)$$

Proof of (3)

$$E(X_1X_2) = \int_0^{\infty} x_2 E(X_1/X_2)\, f(x_2)dx_2 \qquad .(12)$$

$$= \gamma\sigma_2\sqrt{\frac{\pi}{2}} + \alpha\gamma\gamma_1\sigma_2\sqrt{\frac{\pi}{2}} - \frac{1}{2}\alpha\gamma\gamma_1\sigma_2\sqrt{\pi} + \beta\gamma\gamma_2\sigma_2\sqrt{\pi} + \frac{1}{\sqrt{6}}\beta\gamma\gamma_2\sigma_2\sqrt{\pi}$$

$$= \gamma\lambda + \alpha\lambda\gamma\gamma_1^2 + \beta\lambda\gamma\gamma_2^2$$

Proof of (4)

$$\operatorname{cov}(X_1, X_2) = E(X_1X_2) - E(X_1)E(X_2) = \alpha\lambda\gamma\gamma_1^2 + \beta\lambda\gamma\gamma_2^2 \quad (13)$$

Proof (5)

$$\operatorname{corr}(X_1, X_2) = \frac{\operatorname{cov}(X_1, X_2)}{\sqrt{\operatorname{var}(X_1)\operatorname{var}(X_2)}} = \frac{\alpha\lambda\gamma\gamma_1^2+\beta\lambda\gamma\gamma_2^2}{\sqrt{4-2\lambda-2\gamma+\lambda\gamma}} \quad (14)$$

4. Conclusions

Copula function provides us with good tool to derive the extension of BRD (σ_1, σ_2), we denote it as IBRD (σ_1, σ_2), Therefore we present some of its properties, like the cdf, pdf, conditional pdf ′ s, conditional expectations and correlation.

References

[1] Rayleigh, L.,” On the resultant of a large number vibrations of the same pitch and of arbitrary phase”, Phil, Mag 10 (1880)

[2] Sklar, A., Fonctions de repartition et leurs marges, Publications of the Institute of Statistics, Universit´e de Paris 8, 229 (1959).

[3] Quesada-Molina, J., J., Rodrguez-Lallena, J. A., and beda-Flores,M., Matem. Garcı’a de Galdeano. **27**, 499 (2003).

[4] Abdel-Hady, D, Journal of Applied Sciences Research, **9**, 5403 (2013).

[5] Zeng, X., Ren, J., Wang, Z., Marshall, S., Durrani, T., Copulas for statistical signal processing (Part I): Extensions and generalization, Signal Processing 94, 691 (2014).

[6] Sarabia, J., M., Prieto, F., and Jord, V., Journal of Statistical Distributions and Applications (2014).

[7] Walck,C., Fysikum, Hand-book on STATISTICAL DISTRIBUTIONS for experimentalists (2007).

[8] Balakrishnan, N. and Lai C. -D., Continuous Bivariate Distributions, 2ed., springer (2009).

Study of the optical properties R6G doped polymer PVA for different thicknesses

Khawla J. Tahir and Hawraa H. Obeed
College of Science, University of Kerbala, Iraq.
Received Date: 8/Jun/2015
Accepted Date: 9/Jul/2015

الخلاصة

يهدف هذا البحث الى دراسة الخواص البصرية الخطية واللاخطية لصبغة الرودامين الليزرية في مذيب الميثانول لمختلف الاسماك من الصبغة والبوليمر (2, 4, 6, 8, 10, 29 مايكرومتر) في تركيز 1×10^{-6} مول/ لتر. وتم دراسة الخواص البصرية اللاخطية مثل معامل الانكسار اللاخطي ومعامل الامتصاص اللاخطي باستعمال تقنيه المسح على المحور الثالث في جزءين، الجزء الاول وضع فتحه امام الكاشف (الفتحة المغلقة) لايجاد معامل الانكسار اللاخطي، والجزء الثاني رفع الفتحة (الفتحة المفتوحة) لايجاد معامل الامتصاص اللاخطي، واستخدم طولين موجيين (532,1064) نانومتر.

الكلمات المفتاحية

الخواص البصرية الخطية واللاخطية لصبغة الرودامين، معامل الإنكسار الخطي واللاخطي، تقنية المسح على المحور الثالث، الفتحة المغلقة، الفتحة المفتوحة.

Abstract

This paper is aimed to study linear and nonlinear optical properties of polymer doped with laser dye R6G in solvent methanol of different thickness (2, 4, 6, 8, 10, 29 μm) in concentration ($1x10^{-6}$ mole/liter).

To study non-linear optical properties as refractive index (and absorption coefficient (β) by using Z-Scan technique in two parts, one part put aperture in front of the detector (close aperture) to find the non-linear refractive index, in second part remove the aperture (open aperture) to find non-linear absorption coefficient, and using two wavelength 532, 1064 nm.

Keyword

linear and nonlinear optical properties, dye R6G, non-linear refractive index, Z-Scan technique.

1. Introduction

Nonlinear optics is the interaction of light with materials. In the discovery of lasers with high intensity when they fall on the middle transparent there is a change in the optical properties such as refractive index, absorption, polarization, and this is called nonlinear properties [1]. To study the non-linear optical properties by using the simplest method is called Z-Scan technique a simple experiment and a sensitive method for measuring the sign and magnitude of the non-linear refraction and non - linear absorption for solids and liquids is Z-Scan technique developed by Sheik-Bahae et. al. in 1989 [2]. The data of experimental were recorded gradually through moving simple alone axis (z) and measuring the transmission of the samples in each position (z) [3], as shown in Fig.(1) [4].

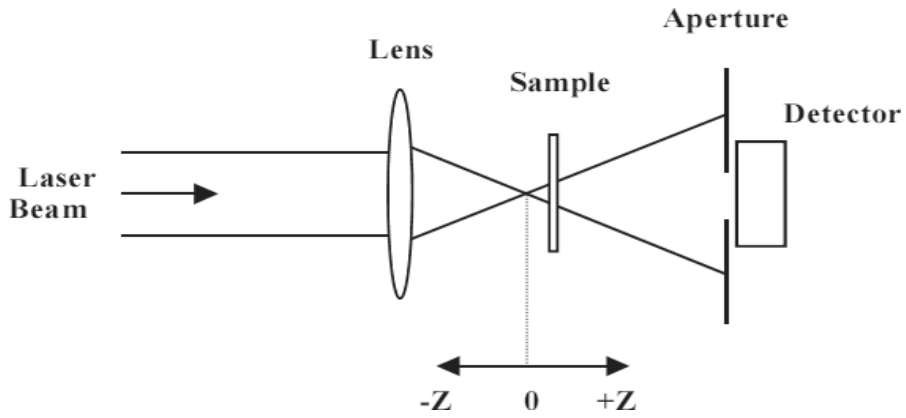

Fig.(1): Z-Scan set up There are two types of Z-Scan technique close aperture to calculate the non-linear refractive index in Fig.(2)

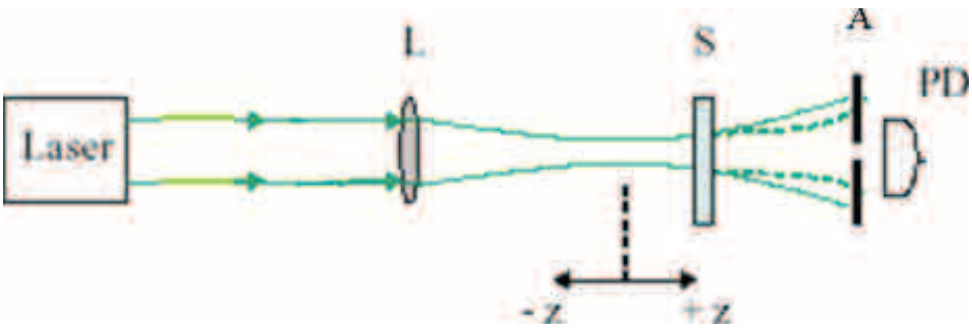

Fig.(2): Z-Scan technique close aperture [2]

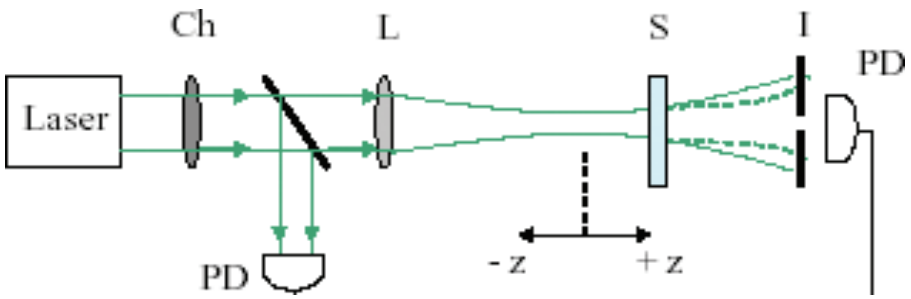

Fig.(3): Z-Scan technique open aperture [5]

And open aperture to determine the absorption coefficient in Fig.(3)

The rhodamines are based structurally on xanthenes [6] and the wavelength region (500-700 nm) and are generally efficient [7], R6G chloride have a high efficiency when used as an effective media in dye lasers, R6G chloride is a red powder has chemical formula C_{27} H_{29} CLN $2O_3$ with highly soluble and has characteristic molar mass (479.02 g/mole), the structure of R6G is shown in Fig.(4).

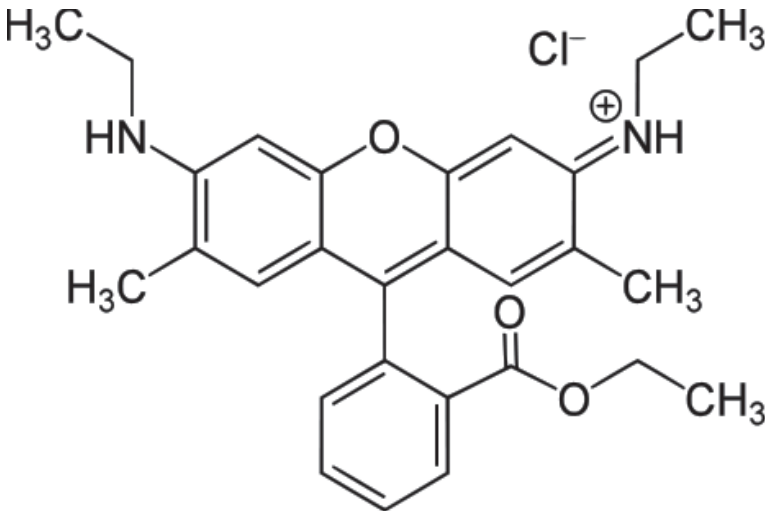

Fig.(4): the structure of R6G

Polyvinyl alcohol (PVA) is important polymeric materials and has many properties such as relative low cost, dielectric material and good charge storage capacity [8, 9], the structure of PVA in Fig.(5).

Table (1): Properties of PVA [11]

Appearance	White powder
Melting point	230
T g (dry film)	(75-85)
Stability to sunlight	Excellent

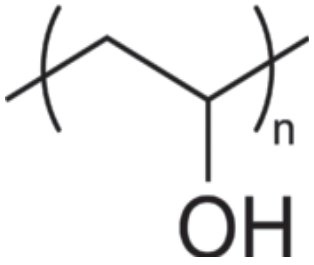

Fig.(5) polyvinyl alcohol [10]

2. Experimental

2. 1. Sample preparation

The powder of R6G dye is accurately weighted.

Solutions of concentrations ($1x10^{-4}$, $5x10^{-4}$, $1x10^{-5}$, $1x10^{-6}$ and $5x10^{-6}$ mole/liter) in methanol solvent were prepared by

$$w = \frac{Mw*V*C}{1000} \quad \ldots\ldots\ldots (1)$$

where

W: weight of the dissolved dye (gm)

Mw: molecular weight of the dye (479. 02 gm/mol)

V: the volume of the solvent (ml)

C: the dye concentration (mol/l)

The prepared solutions were diluted according to the following equation:

$$C_1 \chi V_1 = C_2 \chi V_2 \quad \ldots\ldots\ldots (2)$$

where

C_1: primary concentration

C_2: new concentration

V_1: the volume before dilution

V_2: the volume after dilution

Dye R6G doped polymer PVA

Dye doped polymer films were fabricated by casting method, the solution of the polymer is prepared by dissolving the amount of polymer (0. 7 gm in 10 ml of water solvent).

2. 2. Results and discussions:

To study the linear and nonlinear optical properties of the R6G and PVA films of different thicknesses.

2. 3. Spectra of absorption and fluorescence:

The Spectra of absorption and fluorescence for films R6G and PVA in methanol for different thickness (2, 4, 6, 8, 10, 29 μm) of the polymer ($1x10^{-6}$ mole/liter) concentration are shown in Fig.(6) and Fig.(7).

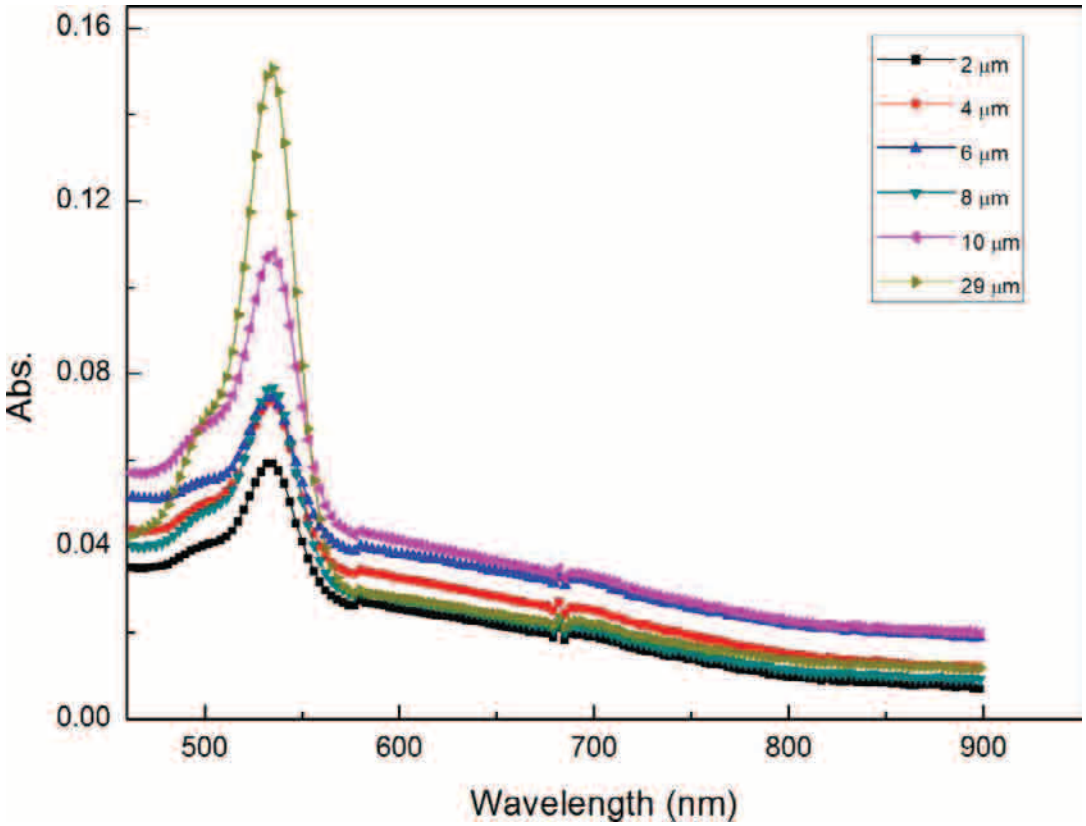

Fig.(6): spectra of Absorption for different thickness

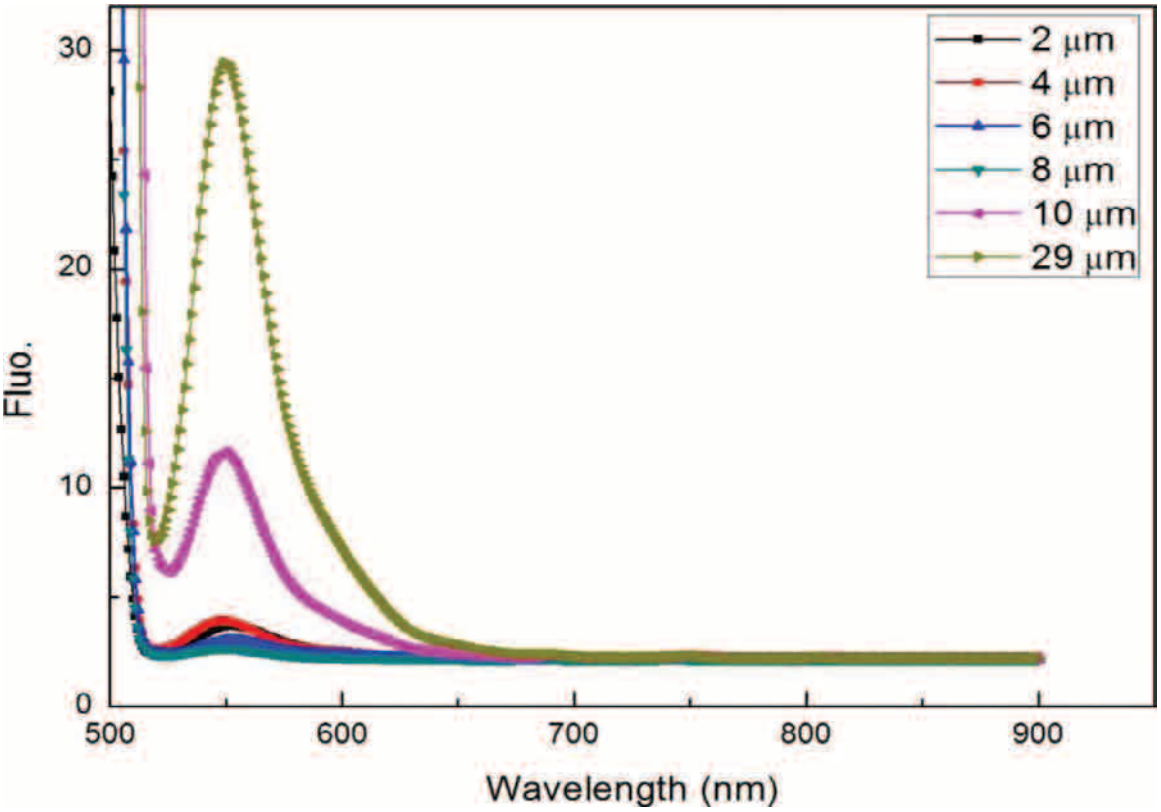

Fig.(7): spectra of Fluorescence for different thickness

2. 4. Linear 0ptical properties:

The linear absorption coefficient of R6G and PVA was determined for both wave lengths using the formulae [12].

$$\alpha_0 = \frac{1}{t} ln \frac{1}{T} \ldots\ldots\ldots (3)$$

Where (t) is the thickness of sample and T is the transmittance, and the extinction coefficient is obtained interns of the absorption coefficient,

$$K = \frac{\lambda \alpha_0}{4\pi} \ldots\ldots\ldots (4)$$

Table (2): Linear optical properties for R6G and PVA in different thickness and concentration (1x10-6 mole/liter).

t (µm)	T% 532 nm	α_0 cm^{-1}	n	T% 1064 nm	α_0 cm^{-1}	n	K × 10^{-7} 532 nm	K × 10^{-7} 1064 nm
2	87. 2634	681. 2	1. 7056	99. 689	15. 57	1. 0822	28853. 38	1318. 99
4	84. 4413	422. 78	1. 8187	99. 212	19. 78	1. 1342	17907. 56	1675. 63
6	84. 2724	285. 2	1. 8254	98. 915	18. 18	1. 1595	12080. 13	1540. 09
8	83. 913	219. 24	1. 8399	98. 689	16. 49	1. 1768	9286. 28	1396. 92
10	78. 1746	246. 23	2. 0769	98. 435	15. 77	1. 1949	10429. 49	1335. 93
29	70. 9455	118. 36	2. 4029	97. 714	7. 97	1. 241	5013. 34	675. 17

2. 5. Nonlinear optical properties:

Z-Scan technique close aperture to determine the T_p and T_v

Where T_p is the maximum transmittance and T_v is the minimum transmittance

The non-linear refractive index was measured by the formula [13]

$n_2 = \Delta\emptyset_0 / I_0 L_{eff} k$…….. (5)

where $\Delta\emptyset_0 = \Delta T_{p-v} / 0.406$. …….. (6)

Where $\Delta\emptyset_0$ is the nonlinear phase shift

$\Delta T_{P-V} = T_P - T_V$…….. (7) [13]

$k = \frac{2\pi}{\lambda}$…….. (8)

$I_0 = 2p / \pi w_0^2$…….. (9) [14]

I_0 is intensity of th laser beam at the focus (Z = 0)

P: power of laser beam

W_0: the beam radius at the focal point

$L_{eff} = (1-exp^{-\alpha_0 t}) / \alpha_0$……. (10) [13], L_{eff}:the effective length of the sample, t: is the sample thickness, α: linear absorption coefficient.

from the open aperture Z-scan data, the nonlinear absorption coefficient is estimated [13]

$\beta = \frac{2\sqrt{2}}{I L_{eff}} \Delta T$…….. (11)

Where ΔT is the one peak value at the open aperture Z-scan curve.

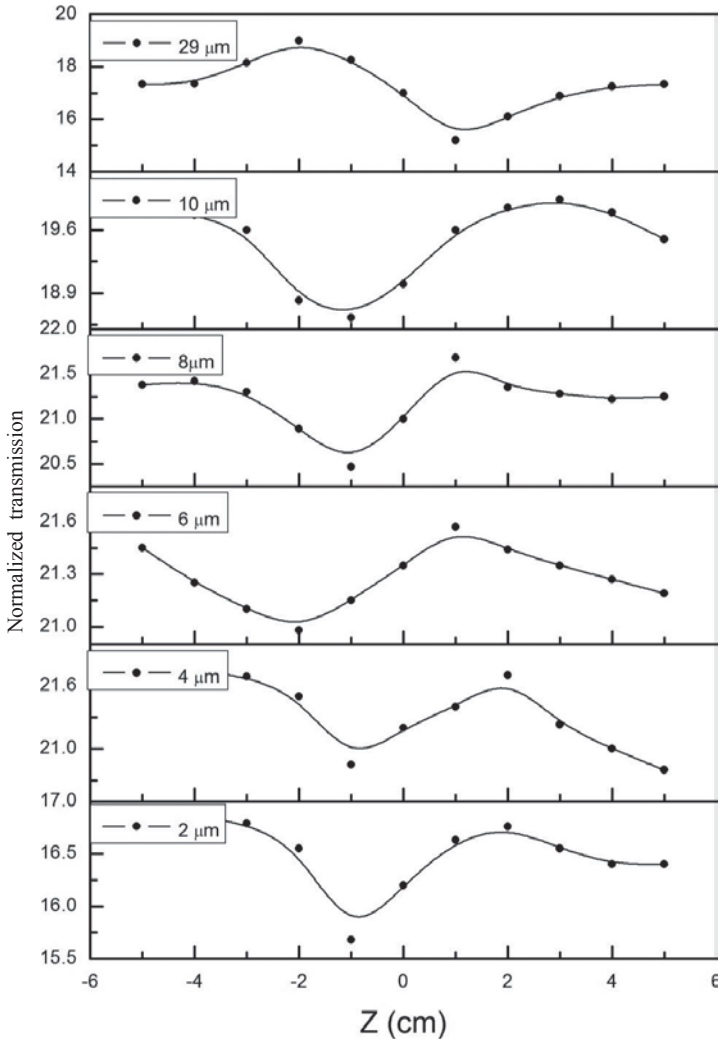

Fig.(8): Closed aperture Z-Scan for R6G and PVA in wavelength 532 nm in different thickness and concentration (1x10^{-6} mole/liter).

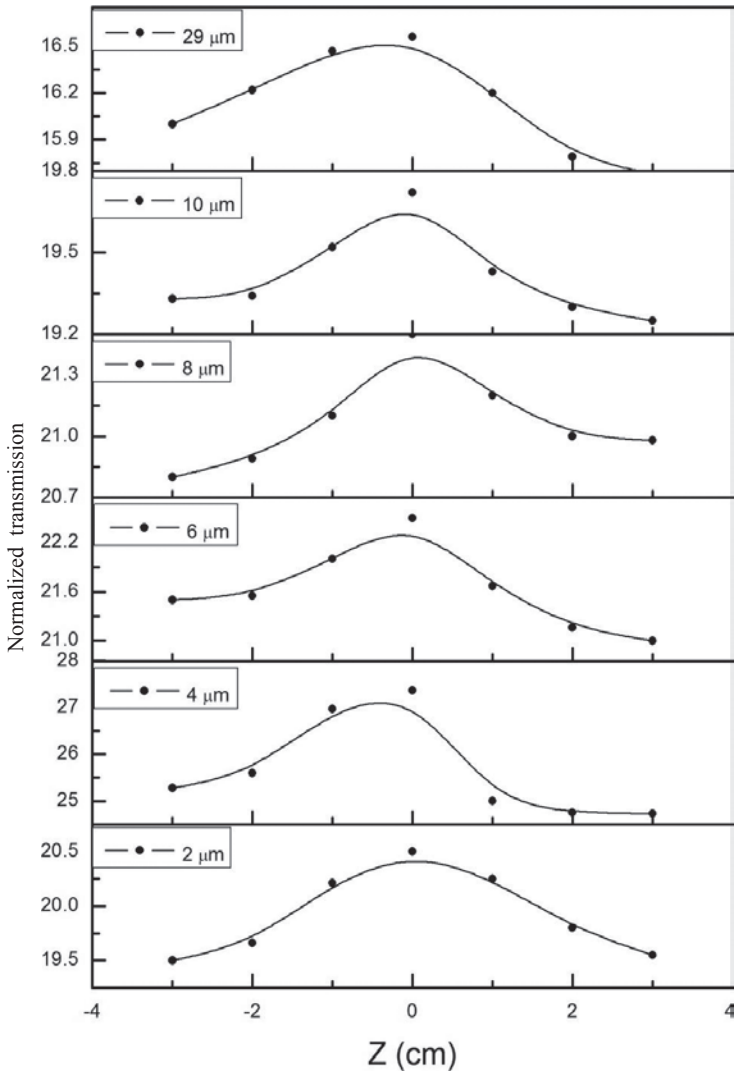

Fig.(9): Open aperture Z-Scan for R6G and PVA in wavelength 532 nm in different thickness and concentration (1x10^{-6} mole/liter).

Case 1: In $\lambda = 532$ nm and $I_0 = 49.147 \times 10^3\ mW/cm^2$

Table (3): The results of nonlinear optical properties for R6G and PVA by the Z- scan.

t(μm)	ΔT_{P-V}	ΔØ (Rad)	$n_2(\frac{cm^2}{mw}) \times 10^{-7}$	T_{max}	$\beta(\frac{cm^2}{mw})$
2	1.08	2.66	24.52	20.5	6.3
4	0.85	2.09	9.79	27.37	4.3
6	0.59	1.45	4.5	22.5	2.3
8	1.21	2.98	7	21.5	1.7
10	1.31	3.23	6.28	19.72	1.3
29	4	9.85	6.9	16.56	0.388

From this Table it can be shown that higher nonlinear refractive index (n_2) obtained when the thickness is (2μm), we also note that the non-linear absorption coefficient (β) increases with the decreasing of the thicknesses.

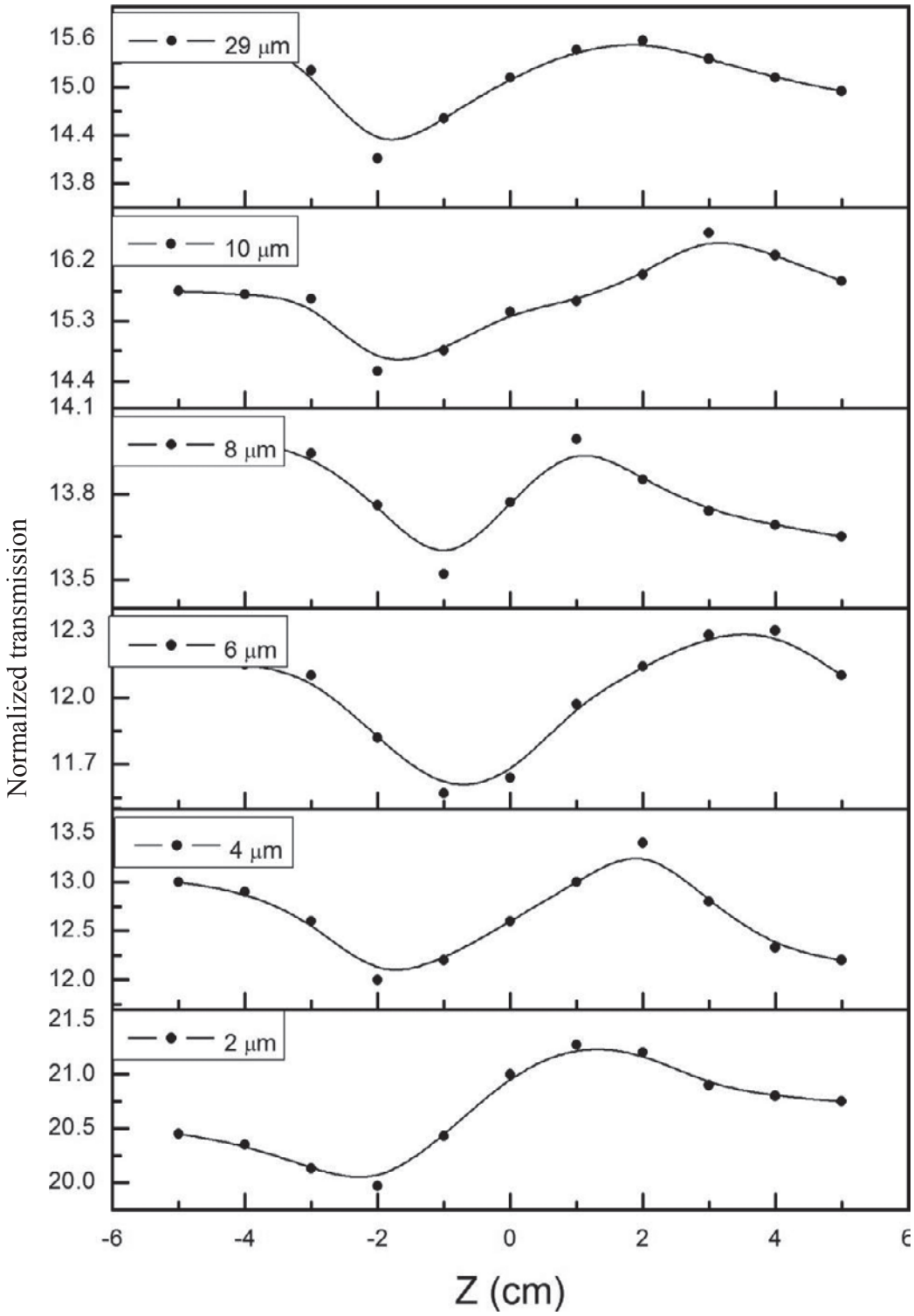

Fig.(10): closed aperture Z-Scan for R6G and PVA in wavelength 1064 nm in different thickness and concentration (1x10-6 mole/liter).

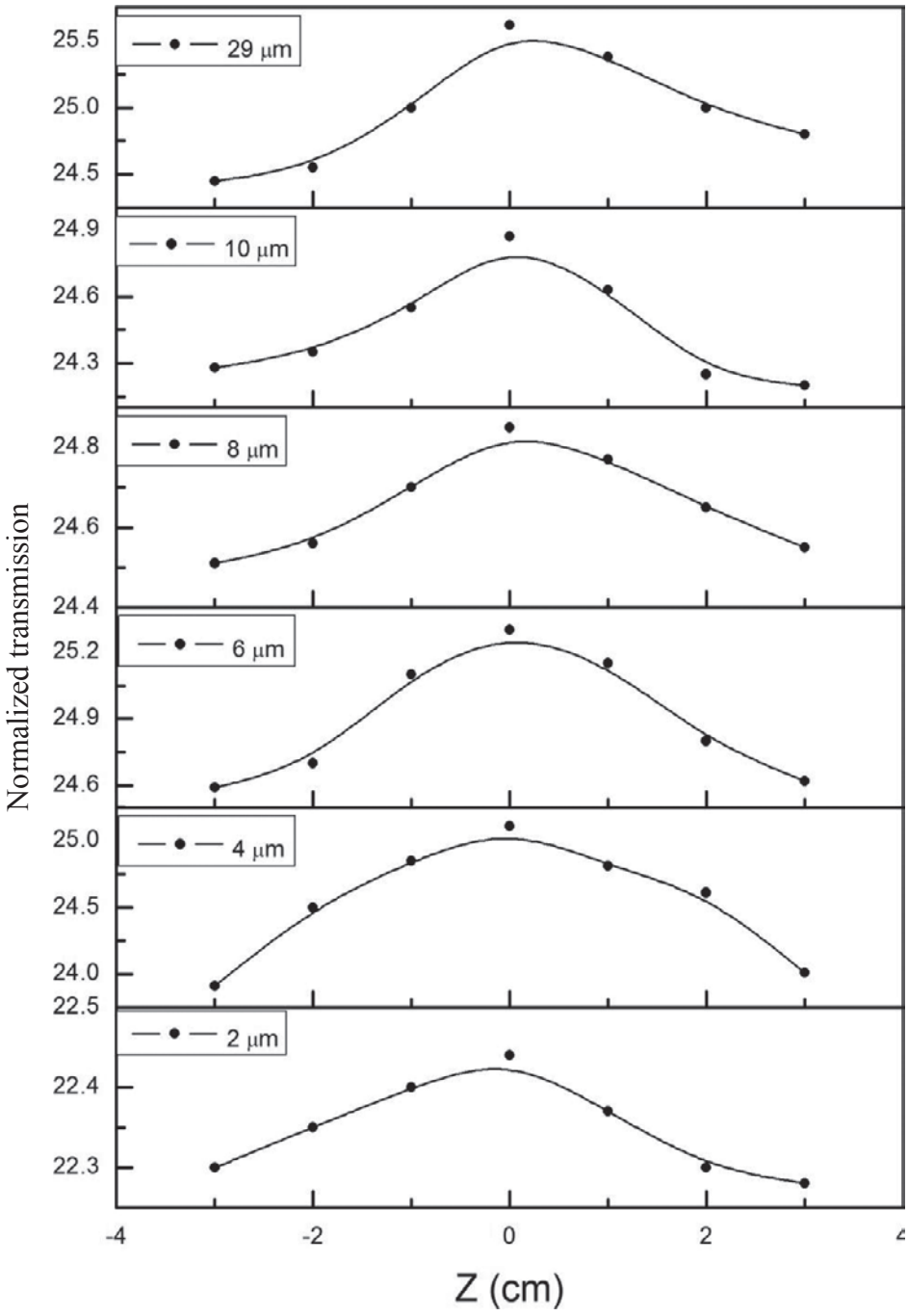

Fig.(11): open aperture Z-Scan for R6G and PVA in wavelength 1064 nm in different thickness and concentration (1x10^{-6} mole/liter).

Case 2: In $\lambda = 1046$ nm and $I_0 = 72.737 \times 10^3\ mW / cm^2$

Table (4): The results of nonlinear optical properties for R6G and PVA by the Z- scan.

t(μm)	ΔT_{P-V}	ΔØ (Rad)	$n_2(\frac{cm^2}{mw}) \times 10^{-7}$	T_{max}	$\beta(\frac{cm^2}{mw})$
2	1. 3	3. 2	37. 3	22. 44	4. 37
4	1. 2	2. 96	17. 3	25. 11	2. 5
6	0. 73	1. 8	7. 03	25. 3	1. 65
8	0. 47	1. 16	3. 4	24. 85	1. 22
10	2. 07	5. 1	11. 97	24. 87	0. 97
29	1. 47	3. 6	2. 9	25. 62	0. 35

This Table shows that the nonlinear refractive index (n_2) increases with the decrease of the thickness except when the value (t = 10μm), we also note that the non-linear absorption coefficient (β) increases with the decrease of the thickness.

From this Table shows that the energy gab increase with increasing the thickness.

Table (5): The results of E. g for different thickness

t(μm)	E. g
2	2. 1
4	2. 2
6	2. 21
8	2. 22
10	2. 23
29	2. 25

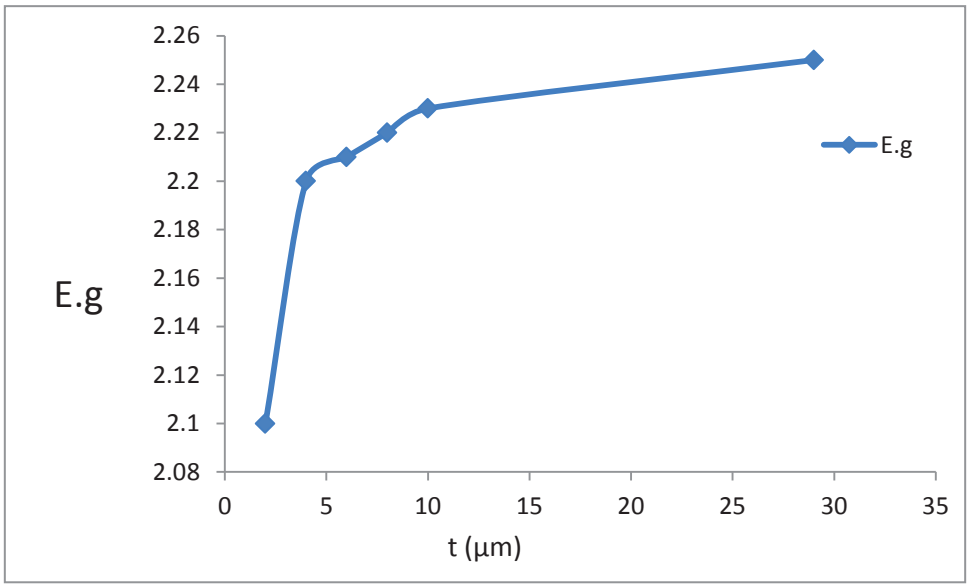

Fig.(12): Energy gab for different thicknesses

Reference:

[1] F. Trager, "Handbook of Lasers and Optics", springer (2007).

[2] E. W. Van Stryland,, Characterization Techniques and Tabulations for Organic Nonlinear Materials, 655-692 (1998).

[3] M. Sheik-Bahae, A. A. Said, D. J. Hagan, M. J. Soileau, and S. E. W. Van Stryl and, Technology and Applications Center New port Corporation (2007).

[4] D. J. Hagan, E. W. Van Stryland, Y. Y. Wu, T. H. Wei, M. Sheik-Bahae, A. Said, K. Mansour, J. Young and M. J. Soileau, Society of Photo-Optical Instrumentation Engineers, 1105 (1989).

[5] W. Wing-Kay Lam, M. sc thesis, Department of Electrical and Computer Engineering,University of Toronto (2003).

[6] Stryker H. I., Carney's P., N. J., United State Patent. 3767358, oct., 23 (1973).

[7] Schafer F. P., Drexhage K. H., et. al., Topics in Applied Physics, **1**, (1977).

[8] M. A. Schoondorp, E. J. Vorenkamp, and A. J. Schouten, Thin Solid Films **196**, 121 (1991).

[9] Garoff, S. R. Stephens, C. Hanson, and G. Sorenson, "Optics Quantum (1982).

[10] Whitmore, P. M. H. J. Robota, and C. D. Harris, J. Chem. Phys., **77**, 1560 (1982).

[11] Celanese, Celvol Polyvinyl Alcohol A Versatile High-Performance Poly. (2007).

[12] H. Ma and C. B. de Araujo, Appl. Phys. Lett, **66**, 1581 (1995).

[13] M. Sheik-Bahae, A. A. Said, T. H. Wei, D. J. Hagan, E. W. Van Stryland, IEEE J. Quant. Electron, **26**, 760–769 (1990).

[14] A. A. Nalda, J. Opt. Mater**., 19**, 2 (2002).

Spectroscopic properties of different concentration xanthene›s dye mixture (6G, 3GO, B and C) solution in chloroform

*** Ali H. Al-Hamdani, ** Slafa I. Ibrahim and *** Hussein Ali Hadi Al-Hamdani**
*** Laser and Optoelectronics Engineering Department, University of Technology, Iraq**
**** Energy and Fuel Research Center, University of Technology, Iraq.**
***** Electrical and Electronic Engineering Department, College of Engineering, University of Kerbala, Iraq**
Received Date: 13/Jul/2015
Accepted Date: 20/Jul/2015

الخلاصة

تم في هذا البحث دراسة طيف الامتصاص والفلورة ضمن المدى (700 – 400) نانومتر لمزيج من (رودامين 6G، رودامين 3GO، رودامين B، رودامين C) والتي تعود إلى عائلة الزانثين بنسبة (1:1:1:1)، حيث تمت إذابتها في الكلوروفورم لتحضير محاليل بتركيز ($1*10^{-4}$، و$7*10^{-5}$، $5*10^{-5}$، $3*10^{-5}$، $1*10^{-5}$، $5*10^{-6}$) مول\لتر بدرجة حرارة الغرفة.

نلاحظ إن شدة الامتصاص وعرض حزمة طيف الامتصاص، وحيود الحزمة تزداد بزيادة التركيز والتي تتوافق مع قانون بيير–لامبرت. الكفاءة الكمية لمزيج الرودامين المذاب في الكلوروفورم تم حسابه باستعمال التراكيز أعلاه وكانت كما يلي (58%, 68%, 76%, 94%, 71%, 70%) على التوالي. تم حساب زمن العمر الإشعاعي وكما يلي (1.44, 1.25, 0.99, 0.65, 0.18, 0. 08) نانوثانية على التوالي. كما تم حساب زمن عمر التألق وكما يلي (0.84, 0.86, 0.75, 0.61, 0.12, 0.05) نانوثانية على التوالي.

الكلمات المفتاحية

صبغات الزانثين، رودامين 6G، رودامين 3GO، رودامين B، رودامين C.

Abstract

In this research the absorption and fluorescence spectrum in the range (400-700) nm for (Rhodamine 6G, Rhodamine 3GO, Rhodamine B and Rhodamine C) mixture which belong to Xanthene family were studied in the ratio (1:1:1:1), it has dissolved in chloroform to prepare different concentration ($5*10^{-6}$, $1*10^{-5}$, $3*10^{-5}$, $5*10^{-5}$, $7*10^{-5}$, and $1*10^{-4}$) mole/L at room temperature.

We notice that the absorption intensity, bandwidth of absorption spectrum and stock shift are increased with increasing concentration, and this agree with Beer-Lambert law. The quantum efficiency of the dissolved Rhodamine mixture in chloroform has been calculated by using the

same above concentration and their results are as follows (70%, 71%, 94%, 76%, 68% and 58%) respectively. The radiative life time have been computed as given (0. 08, 0. 18, 0. 65, 0. 99, 1. 25, and 1. 44) nanosecond respectively. Fluorescent life time have been also computed as given (0. 05, 0. 12, 0. 61, 0. 75, 0. 86 and 0. 84) nanosecond respectively.

Keywords

Xanthene's dye, Rhodamine 6G, Rhodamine 3GO, Rhodamine B, Rhodamine C, Laser dye.

1. Introduction

Lasing dyes are generally defined as substances capable of emitting light when stimulated and typically have, as their lasing media, dye compounds composed of conjugated double bonds [1].

Xanthene dyes are those containing the xanthylium as chromophore with amino or hydroxy groups meta to the oxygen as the usual auxochromes. Rhodamines are commercially the most important amino xanthenes. The organic dye laser has found many applications in scientific research because of its unusual flexibility [2]. Many experimental and theoretical works concerning the spectral properties of xanthene dyes were done because of their great promising results in solar concentration and nonlinear optics device applications.

There are large amount of data about laser dyes from many authors, Alaverdyan1 R. B. and co-workers studied Luminescence spectrum thermal properties of Rhodamine 6G doped polymethyl metacrylate film sandwiched between cholesteric liquid crystal layers [3]. Kailasnath M. and co-workers studied the energy transfer and optical gain studies of FDS: Rh B dye mixture investigated under CW laser excitation [4]. Bahattab M. A. and co-workers studied Photostability of Liquid Mixture Based on Rhodamine 590 Dye in Vinyl Acetate Polymer Solution [5]. Ali B. R. studied the energy transfer in dye laser mixture (1-Fluorescien+1-Rh 6G) [6], Ali H. Al-Hamdani study the spectroscopic properties for Rodamine 3GO [7], Rodamine B [8] dissolved in chloroform, Fluorescein Sodium dye in Ethanol [9], mixture of R6g and Rc dissolved in chroform [10] and R6G doped PMMA [11].

In the present work we study spectral properties of (R6G, R3GO, RB and RC) which is efficient laser dye and covers the wavelength region from 500 to 700 nm.

2. Materials and methods:

Solutions of different concentrations of four dyes (R6G, R3GO, RB and RC) in chloroform solvent were prepared from given weight of dye powder, according to the following equation:

$$w = \frac{Mw \times V \times C}{1000} \ldots (1)$$

Where: W weight of the dissolved dye (gm), *Mw* molecular weight of the dye (gm/mol),

V the volume of the solvent (ml), C the dye concentration (mol/l).

The prepared solutions were diluted according to the following equation:

$$C_1 \chi V_1 = C_2 \chi V_2 \ldots (2)$$

Where: C_1 primary concentration, C_2 new concentration, V_1 the volume before dilution, V_2 the volume after dilution.

The spectrum of the molecular fluorescence F (ύ) gives the relative fluorescence intensity at wave-number (ύ), this is related to the quantum efficiency by the following equation [4].

$$q_{fm} = \int_0^\infty F(\acute{\upsilon})\, d\acute{\upsilon} \ldots (3)$$

In order to evaluate absolute quantum efficiency, we have to consider both the radiative and non-radiative processes taking place in the medium, therefore

$$q_{fm} = \frac{K_{fm}}{K_{fm} + \Sigma K_d} = \frac{K_{fm}}{K_{fm} + K_{IC} + K_{ISC}} \ldots (4)$$

Also Since $K_{fm} = 1/\tau_{fm}$ and $\tau_f = 1/(K_{fm} + \Sigma K_d)$

Therefore,

$$q_{fm} = \frac{\tau_f}{\tau_{fm}} = \int_0^{\infty} F(\acute{\nu})\, d\acute{\nu} \ldots (5)$$

Where, τ_{fm} is the radiation life time can be calculated using relation as follow,

$$\frac{1}{\tau_{fm}} = 2.88 \times 10^{-9}\, n^2\, (\nu'^2) \int \varepsilon(\nu)\, d\nu \ldots (6)$$

Where, **n** is refractive index of a medium, **ύ** is wave number at the maximum absorption, and **∫ε(ύ) d ύ** is the area under the absorption spectrum curve as a function of the wave number [4].

The measurements of the absorption spectra of the samples are taken by using a spectrophotometer (Metertech, SP8001, UV/VIS spectrophotometer), and the emission spectra taken by using (Spectrofluorometer-model SL174, Elico). Refractive index is taken by using Refractometer (Bellingham and Stanley Ltd, Tunbridgewells, ABBE60, England).

Xanthenes derivative dyes used in this work are:

1. Rhodamine 6G which also called Rhodamine 590, Basic Rhodamine Yellow, molecular formula $C_{28}\ H_{31}\ N_2\ O_3\ Cl$, molar mass (479. 02 g/mole).
2. Rhodamine B which also called Rhodamine 610, Basic Violet 10, molecular formula $C_{28}\ H_{31}\ N_2\ O_3\ Cl$, molar mass (479. 02 g/mole).
3. Rhodamine 3GO chloride; molecular formula $C_{26}\ H_{27}\ N_2\ O_3\ Cl$, molar mass (451. 02 g/mole).
4. Rhodamine C, molecular formula $C_{28}\ H_{31}\ N_2\ O_3\ Cl$, molar mass (479. 02 g/mole).

3. Results and discussion

The absorption and fluorescence spectral of dye mixtures at different concentrations in the ratio of (1R6G: 1R3GO:1RB:1RC) are shown in Table(1) and Fig. (2), (3), (4), (5), (6), (7), (8) and (9) respectively.

From these Figs. we can observed that absorption intensity at maximum wavelength is increased with increasing concentration of dye mixture and this is in agreement with Beer – Lambert law. Also it is noticed from Fig. (1) that the bandwidth of the absorption spectrum are increased with increasing concentration of dye mixture and these behaviors are due to the increase in concentration which produces an increase in number of molecules in volumetric unit which effect in the energy state.

From Table (2) one can observe that the radiative life time and fluorescence life time increase with increase in the concentration. The fluorescence life

Table (1): The wavelength at relative maximum intensity for absorption and Fluorescence of dye mixtures at different concentration in the ratio of (1R6G: 1R3GO: 1RB: 1RC).

Dye ratio	Conc. (mole/L)	Wavelength (ABSmax) nm	Absorption Intensity	Wavelength (Fmax) nm	Fluorescence Intensity
1:1:1:1	5*10-6	535. 76	0. 3069	547. 5	154
1:1:1:1	1*10-5	537. 12	0. 4912	549. 5	3371
1:1:1:1	3*10-5	535. 76	1. 1816	555. 5	3570
1:1:1:1	5*10-5	541. 55	2. 3673	575	1145
1:1:1:1	7*10-5	538. 66	2. 5044	577. 5	918
1:1:1:1	1*10-4	528. 42	2. 6157	583	531

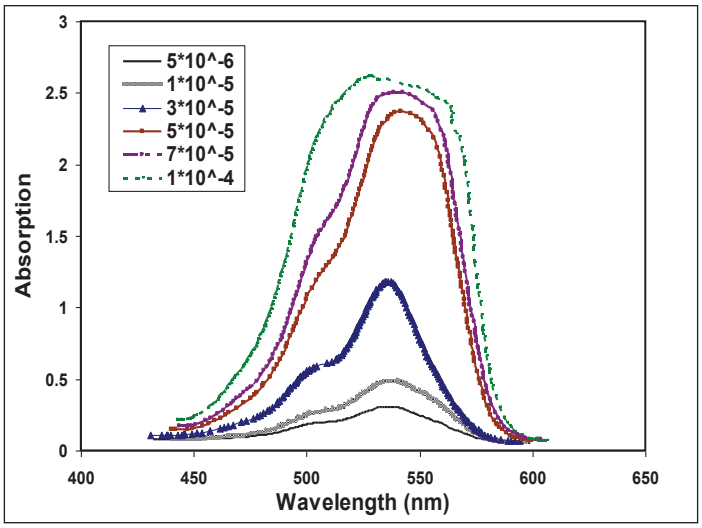

Fig. (1): Absorption spectrum for mixture of (1R6G: 1R3GO: 1RB: 1RC) at different concentration

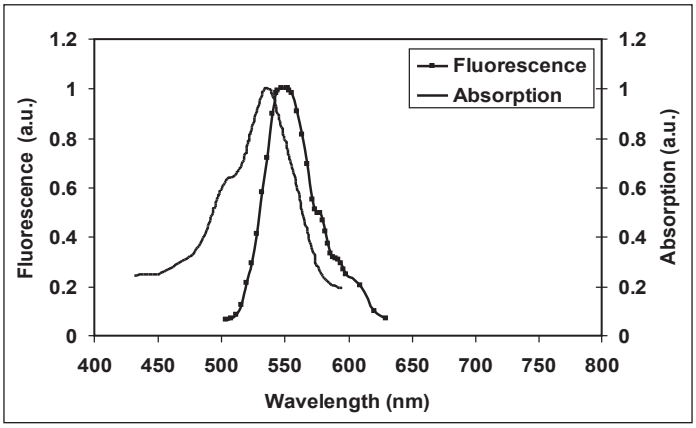

Fig. (2): Absorption and fluorescence spectrum for mixture of (1R6G: 1R3GO: 1RB: 1RC) at concentration ($5*10^{-6}$mole/L).

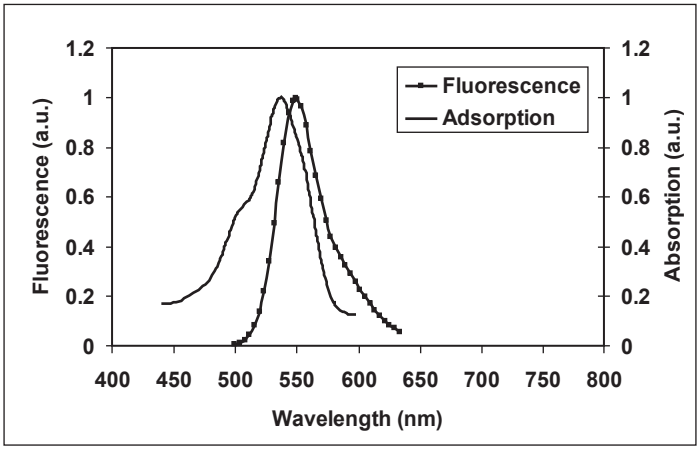

Fig. (3): Absorption and fluorescence spectrum for mixture of (1R6G: 1R3GO: 1RB: 1RC)at concentration ($1*10^{-5}$mole/L).

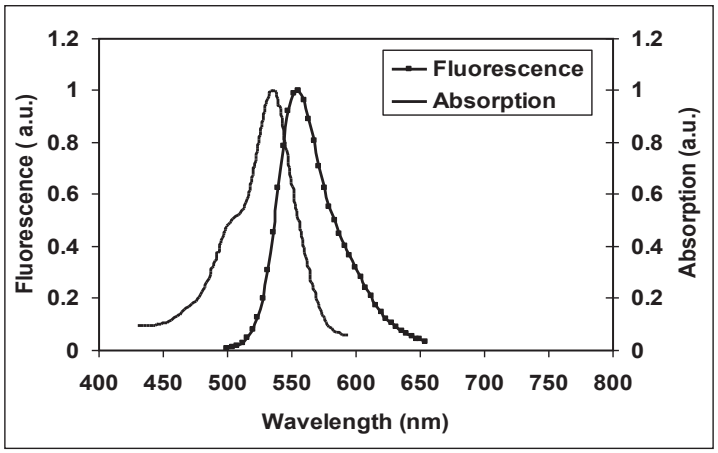

Fig. (4): Absorption and fluorescence spectrum for mixture of (1R6G: 1R3GO: 1RB: 1RC) at concentration ($3*10^{-5}$mole/L).

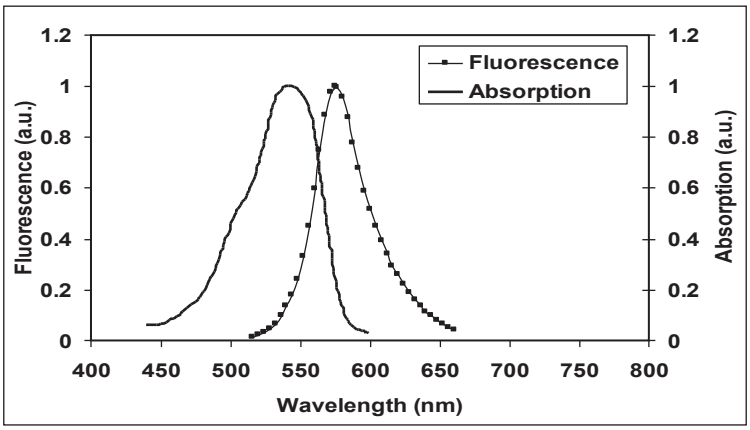

Fig. (5): Absorption and fluorescence spectrum for mixture of (1R6G: 1R3GO: 1RB: 1RC) at concentration ($5*10^{-5}$mole/L).

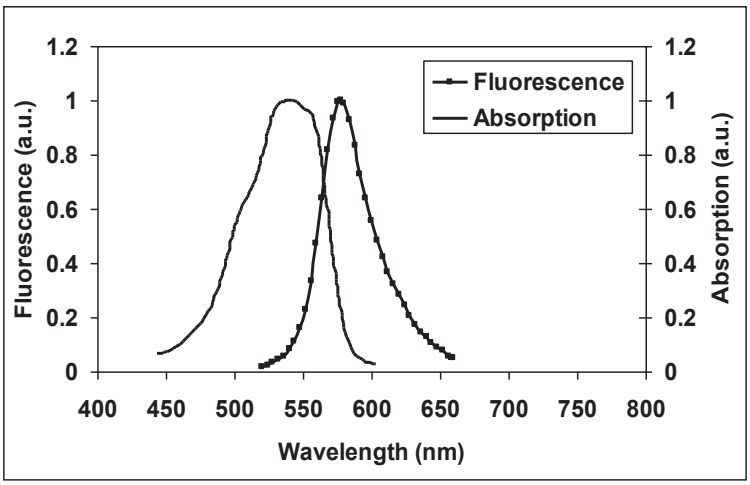

Fig. (6): Absorption and fluorescence spectrum for mixture of (1R6G: 1R3GO: 1RB: 1RC) at concentration ($7*10^{-5}$mole/L).

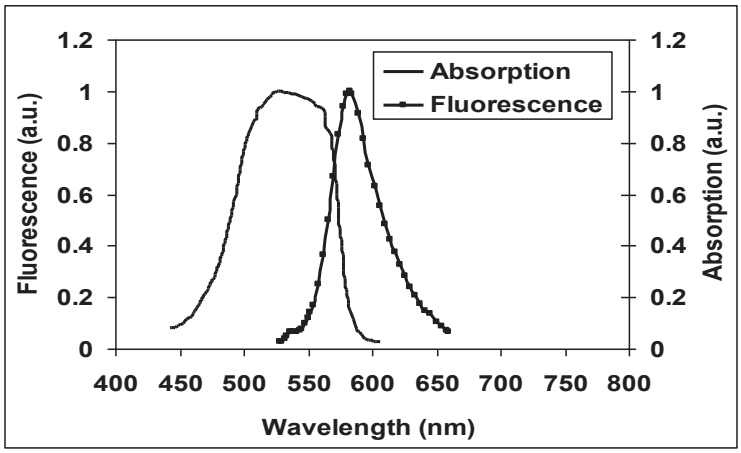

Fig. (7): Absorption and fluorescence spectrum for mixture of (1R6G: 1R3GO: 1RB: 1RC) at concentration ($1*10^{-4}$mole/L).

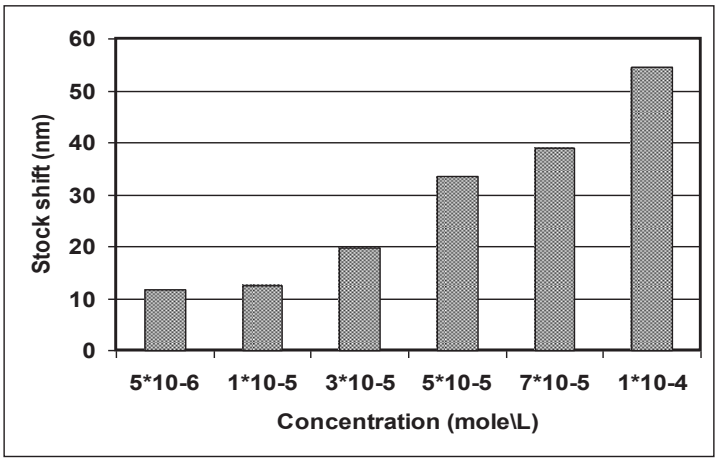

Fig. (8): The stock shift between absorption and fluorescence spectrum of samples.

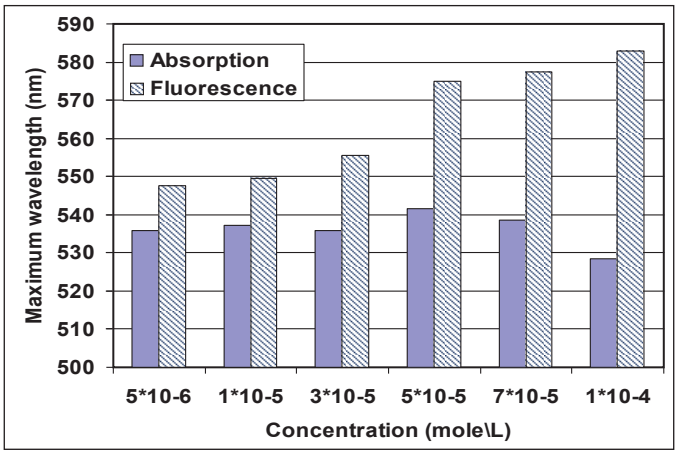

Fig. (9): The maximum wavelength of absorption and fluorescence spectrum of samples.

time was less than radiative life time because of non radiative processes. The results indicate that the best concentration was the lower one (3*10-5 mol/l) which quantum efficiency equal 94. 41% so this dyes concentration can be used to improve solar cell conversion efficiency. But since the other important parameter (stock shift) was small (only 19. 7 nm) which offer a small matching between the solar spectrum and silicon solar cell responsively. So one conclude that there is a large leakages in the collected data about dye properties and there is a great interest must focus on this filed.

Table (2): The stock shift, quantum efficiency yield, radiative emission probability, radiative life time, and fluorescence life time of dye mixtures at different concentration in the ratio of (1R6G: 1R3GO:1RB:1RC).

Conc. (mole/L)	Stock shift (nm)	Quantum efficiency %	Kfm	τfm (nsec)	τf(nsec)
5*10-6	11. 74	70. 39	12. 0052	0. 0832	0. 0586
1*10-5	12. 38	71. 1 2	5. 5416	0. 1804	0. 1283
3*10-5	19. 74	94. 41	1. 5225	0. 6568	0. 6173
5*10-5	33. 45	76. 22	1. 008	0. 9913	0. 7556
7*10-5	38. 84	68. 66	0. 7962	1. 2559	0. 8623
1*10-4	54. 58	58. 96	0. 6939	1. 441	0. 8496

References

[1] Dale R. Pfost,"Laser Tape Systems",United States Patent, No. 4, 523, 319, Jun. 11 (1985).

[2] Maeda, M. Laser Dyes" Properties of Organic Compounds for Dye Lasers" Academic Press, Orlando, Fla., (1984).

[3] Alaverdyan R.B., Dadalyan T K, Karapetyan A S, and Torosyan N S "Luminescence Spectrum Thermal Properties of Rhodamine 6G Doped Polymethyl Metacrylate film Sandwiched between Cholesteric Liquid Crystal Layers", International Symposium on Optics and its Applications (OPTICS2011), Journal of Physics :Conference Series 350 ((2012).

[4] G´omez.L., Cuppo F.L.S. and A. M. Figueiredo Neto, Brazilian Journal of Physics, **33** (2003).

[5] Bahattab M.A., Mohammad Ahmad M. and King T.A., International Journal of Pure and Applied Physics, **3**, 22 (2007).

[6] Ali B.R, International Journal of Application or Innovation in Engineering &Management, **2**, 525 (2013).

[7] Ali H. Al-Hamdani, Yasmeen Z. Dawood, Shafa Majeed Jaseem, International Review of Chemical Engineering (I.RE.CH.E.), **5** (2013).

[8] Ali H. Al-Hamdani, Rajaa Nader, Rafah Abdul Hadi, IOSR Journal of Research & Method in Education (IOSR-JRME), **4**, 68 (2014).

[9] Ali H. Al-Hamdani, Adnan F. Hassan, Faiz Salih Abbas, "The Effect of Concentration on Spectroscopic Properties of Fluorescein Sodium dye in Ethanol", **6**, 112 (2014).

[10] Ali H. Al-Hamdani, Shaima Khyioon, Rafa abdul Hadi, "Calculation the Quantum Efficiency of Mixture of Rhodamine (RC and R6G) dyes dissolved in Chloroform», 1st energy and Renewable energy conference, university of technology, Energy and Renewable Energies Technology Center, Baghdad, IRAQ (2013).

[11] Ali H. Al-Hamdani, Rafa, abdul Hadi, Raja Nader, Iraqi Journal of Physics, **12**, 59 (2014).

Computation of inheritance share in islamic law by an expert system using decision tables

Huda F. AL-Shahad and Zeina AbdAl-Retha
Department of Computer, Collage of Science, University of Kerbala, Iraq
Received Date: 2/Aug/2015
Accepted Date: 3/Sep/2015

الخلاصة

نظام الارث من الانظمة الاسلامية المهمة التي تهتم بتركة المتوفي وتوزيعها بالاعتماد على القران الكريم، يعتمد توزيع التركة على الحالة الاجتماعية للمتوفي وعلى درجة القرابة للورثة، يتناول هذا البحث استخدام فكرة جداول القرارات في توزيع الارث التي يمكن استخدامها من قبل القاضي او اي طرف مستفيد لتحديد الوارثين وكيفية توريث كل منهم وذلك حسب استحقاقه في قانون الاحوال الشخصية العراقي.

شملت هذه الجداول الورثة من الدرجة الاولى والثانية ولغرض تبسيط هذه الجداول فقد اخذ بنظر الاعتبار في تصميمها هيكلة هذه الجداول بحيث يشمل التصميم جدول رئيسي يتفرع الى جداول فرعية وهذه بدورها تتفرع الى جداول فرعية أخرى وهكذا حسب حالات التركة. هذه الجداول تستخدم كقاعدة معرفة للنظام الخبير حيث تستخدم المعلومات كحقائق ثابته.

الكلمات المفتاحية

نظام الخبير، ورثة، حصة تركة، قاعدة المعرفة، التراث.

Abstract

The legacy system is important Islamic sciences that are interested of the legacy of the dead and all deserve have enacted laws of the Book of Allah (Quran), it is depending on the social state of the dead and the relation of heirs with the dead. An origin of huge discussion, both inside and outside the Muslim group is the Islamic law of legacy. This research deals with the use of decision Tables in distribution of an inheritance that can use by the judge or anyone that need to know how to compute the share according to Iraqi Personal Status Law.

The Tables consist of the first and second relation heirs, for the purpose of simplifying these Tables were taking into consideration the organizing of these Tables. The main Table isolated into sub-Tables, which additionally branch out to other sub-Tables as legacy cases. The Tables are the knowledge base of the expert system that take the information on it and then make it as the fact in the rule base.

In this research the user input the information about the dead as an answer of expert questions, according to these answers the system moves to sub-decision Table. The decision Tables contain all the information that the user need, after the questions finish and the information use as the facts of the expert system then the share of the user appear according the Holy Quran.

Keywords

Expert System, Heirs, Inheritance Share, Knowledge Base, Legacy.

1. Introduction

Inheritance is the transmission the legacy of the dead person to the successor of the children or grandchildren or kinship. Upon the death of the person is the distribution of the estate (movable and immovable property of the deceased) to his heirs in accordance with the personal status law or by Iraqi views and jurisprudence own doctrine of the dead (within Islamic jurisprudence), which are referenced as appropriate.

The subject of inheritance is very large and complex, it depends on the social situation of inherited or dead and some neighborhoods on the degree of inheritors. Sometimes the shares are computed or distributed in a wrong way, so the idea of design the decision Tables and use it in expert system were simplified the way to distribute of the share in a perfect way [1].

An Artificial Intelligence System (AI) is found to solve many problems in life, it contains a special domain that is called expert system. An expert system is a machine program that simulates the judgment and conduct of a human or an association that has expert knowledge and experience in a specific field [2]. The way that prompts the advancement of expert system is unique in relation to that of accepted programming methods. The idea for expert system development come from the subject domain of AI, and obliges a flight from routine figuring practices and programming procedures [3].

2. Motivation

There are several attempts to mechanize some aspects of the distribution of inheritance and programmed on a computer. C. CRAIG, et. al explained in 1991 how can the children benefit from their parents' legacy by a design SELF prototype system that uses interpreting an object's parent as shared parts of the object. They deal with the unordered and ordered multiple inheritance and how to send it in unique sender path to simplify the work [4]. S. Nadia in 2003 showed the women's property and inheritance rights only, she discussed the complexity that the woman's face when the national law is growing so she suggested the development of strategy on women's rights in the United States to insure her share [5]. N. Zaini, et. al discussed in 2012 the distribution of Inheritance according two factors, Islamic low and the legacy of the dead. It takes the share in different Muslim community and compares it with the court and the challenge faced Sharia law. The research discusses the inheritance in three countries as a case study: Beaufort, Sabah and Malaysia [6].

In this research the idea of decision Tables was used for the purposes of calculating the distribution of the estate and heirs shares so as to help the judges in determining the rights of the heirs, according to his Iraqi al-Shara, the expert system uses these Tables as facts for calculating shares of heirs correctly.

The next section covers the expert system structure and information about each component and section 3 discusss the proposed system, the definition of decision Table and how to build it. In section 4 the result of the expert system is shown as a number of forms.

3. Methodology and components

The PC program that addresses and reasons with learning of any power subject with a point of view to handling issues or giving direction is an expert system.

Expert system needs to take care of issues

effective access to significant area knowledge base, and a thinking system to apply the information to the issues they are given. Typically, they will additionally need to have the capacity to clarify, to the users who depend on them, how they have arrived at their choices. They will for the most part expand upon the thoughts of knowledge representation, creation leads, hunt, et cetera, that we have effectively secured.

The expert system consists of four components knowledge base, Rule base, Inference Engine and user interface as shown in fig. 1 [7].

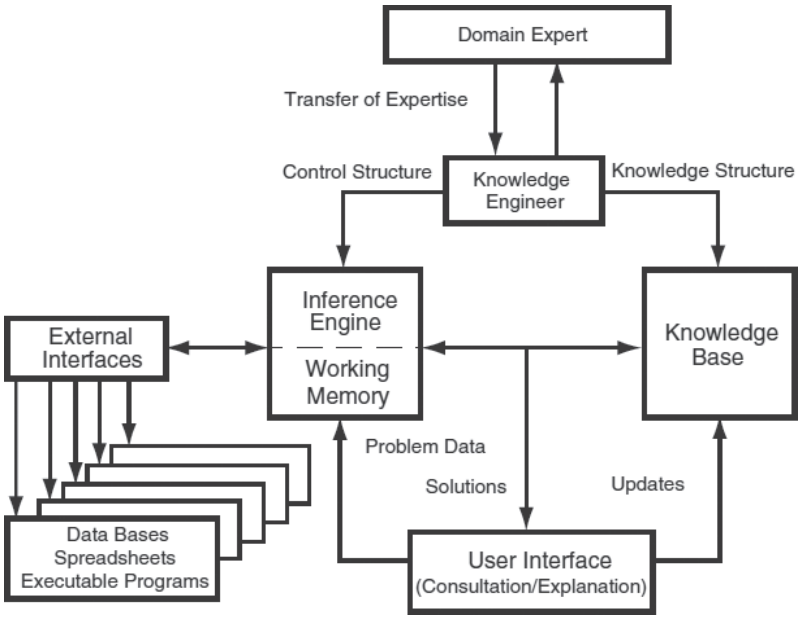

Fig. (1): Expert system components

3. 1. Knowledge base

The knowledge base contains the area particular information needed to solve the problem. The knowledge base is made by the knowledge engineer, who conducts a progression of meetings with the expert and arranges the learning in a frame that can be directly utilized by the framework. The knowledge engineer needs to have the learning of KBES (knowledge base of expert system) innovation and ought to know how to add to a specialist framework utilizing an improvement domain or expert system advancement shell. It is a bit much that the information designer be capable in the area in which the expert system is being produced. Be that as it may, a general learning and nature with the key terms utilized as a part of the area is constantly attractive, since this won't just help in better comprehension the space information however will likewise decrease the corresponding hole between the knowledge engineer and the expert. Before deciding on the structure of the knowledge base, the knowledge engineer ought to have a reasonable thought of diverse knowledge representation plans and the suitability of each under distinctive circumstances [2].

3. 2. Rule base

The rule base is the number of rules which represents the knowledge about the domain. The general type of a rule is:

If cond1

and cond2

and cond3

...

then action1, action2,...

The conditions cond1, cond2, cond3, etc. are evaluated based on what is the information known about the problem to be solved (i. e., the substance of the working memory). A few systems would permit disintersections in the precursors. For example, rules like the accompanying would be permitted [9].

If cond1

and cond2

or cond3

...

then action1, action2,...

3. 3. Inference engine

The actuation engine involves working precepts and principles. It uses a knowledge base to choose decisions. Following are the steps that are followed to produce the final output [diagnostic]. An understanding of the derivation standard idea is imperative to comprehend expert systems. The rules are entered as partitioned standards and it is the induction motor that uses them together to reach inferences. Since each one standard is a unit, principles may be erased or included without influencing different guidelines. One point of inference rules of surmising administers over conventional writing computer programs is that deduction rules use thinking which all the more nearly look like human thinking. Therefore, when a conclusion is drawn, it is conceivable to see how this conclusion was arrived at. Besides, on the grounds that the expert system employments. Learning in a structure like the expert, it may be simpler to recover this data from the expert [8].

3. 4. The user interface

The user interface is the method for correspondence between a user and the expert system critical thinking methods. A decent expert system is not exceptionally helpful unless it has a successful interface. It must have the capacity to acknowledge the inquiries or directions in a structure that the user enters and make an interpretation of them into working guidelines for whatever remains on the system. It likewise must have the capacity to decipher the replies, created by the system, into a structure that the user can comprehend, Careful consideration ought to be given to the screen outline so as to make the expert system seem “well disposed” to the user [9].

5. Proposed expert system and decision Table

The proposed expert system is designed to calculate the share of each person that relates to the dead in first degree relation such as son, daughter, wife, husband, father and mother. The fig. 2 shows the proposed steps of the system.

At the point when a Muslim dies, there are four duties which need to be performed. These are:

1. Payment of memorial service costs
2. Payment of his/her obligations
3. Execution his/her will
4. Distribution of remaining home amongst the beneficiaries as indicated by Sharia.

When the person is dead, the first task is to determine which of the relatives of the deceased are entitled to inherit and secondly, to determine the quantum share entitlement of each of the

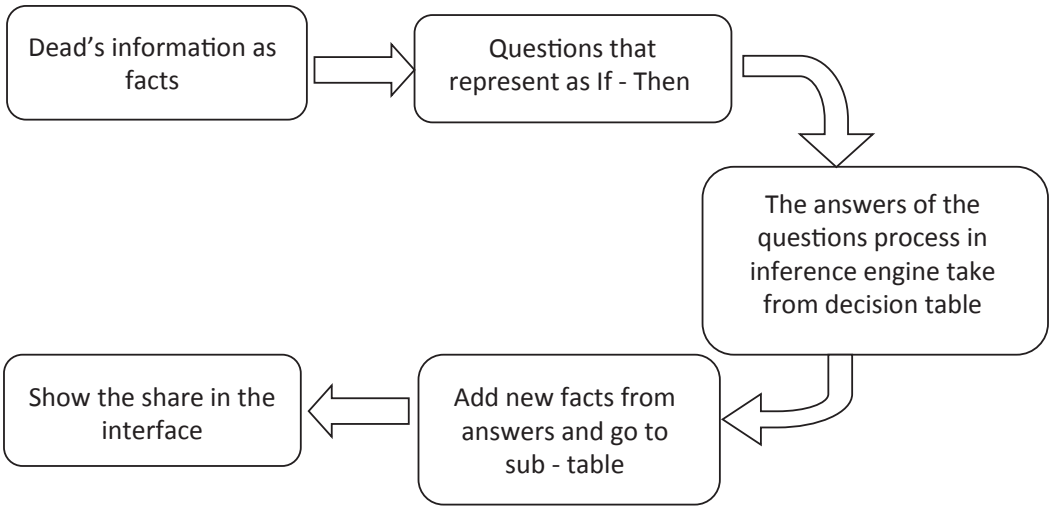

Fig. (2): Proposed system steps

heirs concerned. Muslim inherits from each other is proven from the Quran [10]:

"4:7 There is a share for men and a share for women from what is left by parents and those

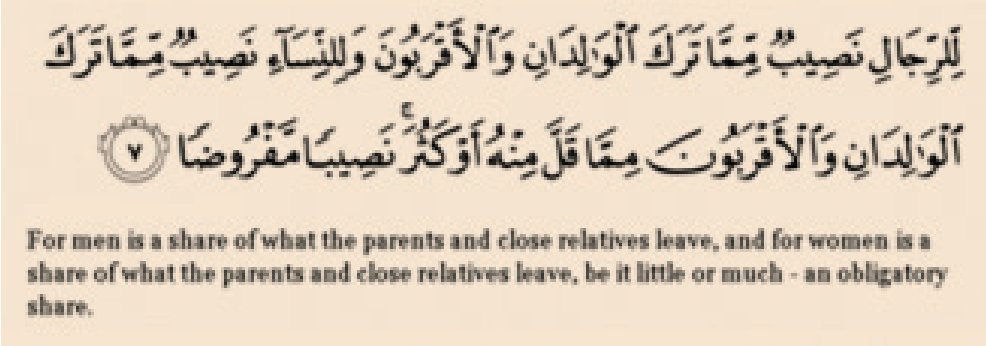
لِّلرِّجَالِ نَصِيبٌ مِّمَّا تَرَكَ ٱلْوَٰلِدَانِ وَٱلْأَقْرَبُونَ وَلِلنِّسَآءِ نَصِيبٌ مِّمَّا تَرَكَ
ٱلْوَٰلِدَانِ وَٱلْأَقْرَبُونَ مِمَّا قَلَّ مِنْهُ أَوْ كَثُرَ ۚ نَصِيبًا مَّفْرُوضًا ۝٧

For men is a share of what the parents and close relatives leave, and for women is a share of what the parents and close relatives leave, be it little or much - an obligatory share.

Fig. (3): An-Nisa

nearest related, whether, the property be small or large–a legal share. "[An-Nisa 4:7]

4. 1. Decision Table designed

Decision Table contains a set of condition's cases which produces a set of procedures to cover all possibilities it depends on the condition and it's answer requirement. The Table consists of two parts: First part, describe the conditions and range of cases that can be met by these conditions. The second part, describes all the measures that must be taken and selection of actions to be taken at the incidence of the different conditions. The number of rules in the Table covers all possibilities meeting the conditions and according to the relationship between the number of conditions and the number of rules 2x (where x is the number of conditions). In other words, each condition adds to the Table lead to double the number of rules, leading to the presence of a large number rules in the Table. For example, if the number of cases of the condition is 8 then there are 256 rules which affects the facility refer to the Table and uses it, therefore there were a number of methods to simplify the Table, including:

1. Combination rules: If the Table has two rules containing the same procedures and rules

were identical in terms except for one condition then these rule are integrated as a single rule.

2. Use a base of else rule: if there was several groups of cases of the condition lead to the same result, then the actions of these groups can be integrated into a single base using the base else rule.

4. 2. The use of Tables

Table inheritance is used to determine the heirs and their shares of the legacy by reference to the first Table and in the light of the condition of existing cases of the Table indicates a particular reference to the sub-Table and so on.

Example: the case of the fact that the dead is male, married, has no children, the wife, father and mother are alive, and has a number of brothers and sisters.

It is clear from the Table (1) that the case of example apply to the rule no. 5, and as a result track this rule sets the Table share a wife is ¼ from a legacy and then indicates reference to the sub-Table to find out the rest of the heirs quotas. When you return to the Table (2) shows the applicability of the rule of it (the mother alive, Grandma if she was alive or not, and the number of deceased brothers and sisters) in this rule sets the Table identifies the mother's share is 1/6 of the estate and the father rest of the estate after the share of wife and mother.

Table (1): Main information about dead

حالات الشرط	١	٢	٣	٤	٥	٦	٧	٨	٩	١٠	١١	١٢	١٣	١٤
المتوفى ذكر	ن	ن	–	–	ن	ن	–	–	ك	ك	ك	ك	–	–
المتوفى متزوج	ن	ن	ن	ن	ن	ن	ن	ك	ن	ن	ن	ن	ن	ك
لديه اولاد	ن	ن	ن	ن	ك	ك	ك	–	ن	ن	ك	ك	ك	–
الزوج على قيد الحياة	ن	ن	ك	ك	ن	ن	ك	–	ن	ن	ن	ن	ك	–
الاب على قيد الحياة	ن	ك	ن	ك	ن	ك	ن	ن	ن	ك	ن	ك	ك	ك
حصةالزوجة	٨\١ ت	٨\١ ت	–	–	٤\١ ت	٤\١ ت	–	–	–	–	–	–	–	–
حصة الزوج	–	–	–	–	–	–	–	–	٤\١ ت	٤\١ ت	٢\١ ت	٢\١ ت	–	–
حصص بقية الورثة	ج ١-١	ج ٢-١	ج ١-١	ج ٢-١	ج ٣-١	ج ٥-١	ج ٦-١	ج ٦-١	ج ١-١	ج ٢-١	ج ٣-١	ج ٥-١	ج ٧-١	ج ٧-١

Table (2): The branch table from main table

حالات الشرط	١	٢	٣	٤
الام على قيد الحياة	ن	ن	ك	ك
الجدة ام الام على قيد الحياة	–	–	ن	ك
للمتوفي عدد من الاخوة والاخوات	ن	ك	–	–
حصة الام	١\٦ ت	تستحق الام ثلث الباقي بعد نصيب احد الزوجين	–	–
حصة الجدة ام الام	–	–	١\٦ ت	–
حصة الاب	باقي التركة بعد نصيب احد الزوجين والام	باقي التركة بعد نصيب احد الزوجين والام	باقي التركة بعد نصيب احد الزوجين والجدة	باقي التركة بعد نصيب احد الزوجين

6. Results

In this research, we had taken kins only from first grade and second grade. The first Table has the information or questions about the dead (the sex, if married or not, has children or not... etc..) as shown in Fig. 3.

Fig. (3): Dead information

`When the user chooses the answers from the above Fig., other questions appear in a new form, the questions belongs to the children of the dead (if there is one son or more, one girl or more, if there

is any child dead and so on) the user is also must choose one of the three answers as shown in Fig. 4.

When the answering part is finished, the share must compute not only for the mother or father, but there is Ashab-ul-Furud (heirs with fixed shares) they must have their share, Fig. 5 shows

Fig. (4): Child's dead information

the share of them that appears as a message box in the program.

Finally, the share of everyone that stays alive will be computed and the user will use it in a simple way as shown in Fig. 6.

Many cases are taken in on this system, another

Fig. (5): Ashab-UL-Furud

case is if the dead doesn't have children and his mother is alive, so the share of her is 1/3 but if he has brothers then the share of her will be 1/6 and so on.

6. Conclusion

In general the use of the Table is much easier than read texts and on this basis the Table format

Fig. (6): Final share

was adopted in the announcement of the dates of trains and planes, as well as the idea of the multiplication Table in the course of primary schooling. Therefore the maturity of the heirs of the inheritance in the Tables according to the different cases of inheritance simplifies the calculation of the heir's rights and reduces from falling into the wrong distribution of inheritance and how much. These Tables provide ease of judges that make it an appropriate means within the reach of their hand, they can refer to it easily and using an expert system to compute the share made the process very simple and the result appears clearly without errors and in a fast way.

References

[1] Mohd R.,The Islamic Inheritance Law (FARAID): The Manifestatioin of Comprehensive Inheritance Management In Islam. National Convention of Faraid and Hibah, Malaysia (2008).

[2] Thomas P., Wealth and Inheritance in the Long Run Handbook of Income Distribution, Volume 2,. Elsevier B.V., London, UK. 1368 (2013).

[3] Durkin, J. Research Review, Ohio Journal of Science., **5**, 171 (1990).

[4] CRAIG C., David U., Bay-wei C. and Urs H., Parents are Shared Parts of Objects: Inheritance and Encapsulation in SELF. An International Journal, Kluwer Academic Publishers, California (1991).

[5] Nadia S., Women's Property and Inheritance Rights:Improving Lives in a Changing Time. International Center for Research on Women Academy for Educational Development U.S. (2003).

[6] Zaini N., Hayatullah L., Zuliza M. and Amir H., International Business Management, **6**, 228 (2012).

[7] Adedeji B., John Y., Fuzzy Engineering Expert Systems with Neural Network Application. John Wiley and Sons, New York. 289 (2002).

[8] Sasikumar M., A Practical Introduction to Rule Based Expert Systems. Narosa Publishing House, New Delhi (2007).

[9] Race A., Zahra A., Advances in Environmental Biology, **7** (8): 1460 (2013).

[10] The Nobil Quran, www.quran.com (2015).

Approximation of functions on unit sphere in terms of K-functional

Eman Samir Bhaya and Hind Ayad Shaker
Mathematics Department, College of Education, University of Babylon, Iraq
Received Date: 20/Jun/2015
Accepted Date: 22/Jul/2015

الخلاصة

قدمنا في هذا البحث مؤثرات معرفة على فضاء الدوال المعرقة على كرات الوحدة والتي تنتمي الى الفضاء Lp عندما p<1. باستخدام تلك المؤثرات قدمنا بعض النظريات المباشرة ونظريات اخرى معاكسة لها بدلالة الدالي K الذي يكون مكافئاً لمقياس نعومة تلك الدوال.

الكلمات المفتاحية

معرف المشغلات للدوال، فضاء الوحدة، بدلالة الدالي K.

Abstract

In this paper we introduce operators defined for functions from Lp for p<1 defined on unit sphere and then we are using to prove direct inequalities in terms of K-functional. Also we are to prove some propped related to these operator.

Keywords

operators defined for functions, unit sphere, K-functional.

1. Introduction

For R^d, the unit sphere U^{d-1} is given by

$$U^{d-1}=\{x=(x_1,\dots,x_d):|x|=(x_1^2+\cdots+x_d^2)^{1/2}=1\}$$

If $f\epsilon L_p(U^{d-1})$, p<1and the mapping $f: U^{d-1}\to R$, then let us define:

$$\|f\|_{L_p(U^{d-1})}=\|f\|_p:=\left(\int_{U^{d-1}}|f|^p\right)^{1/p}$$

And

$$L_p^n:=\{f:f\in L_p,\hat{f},\dots,f^{(n)}\in L_p\}\ ,\ p<1$$

For a function f(x) (x∈U^{d-1}), which is Lebesgue integrable on U^{d-1}, $d\geq 3$, the average on the cap of the sphere is given by [1]

$$B_t(f,y)=\frac{1}{\varphi(t)}\int_{\ell} f(x)d\sigma(x)\ ,t>0 \quad (1.1)$$

, where; ℓ={y: |y|=1, cost ≤ x .y ≤ 1, x, y ∈U^{d-1}} and x. y is the inner product in R^d is the measure on the sphere

$$\varphi(t)=\frac{2\pi^{(d-1)/2}}{\Gamma(\frac{d-1}{2})}\int_0^t sin^{d-2}u\,du$$

For a function f(x) (x∈U^{d-1}) which is integrable on U^{d-1}, the average on the rim of the cap S_t (f, y) is given by [1]

$$S_t(f,y)=\frac{1}{\Psi(t)}\int_{x.y=cost} f(x)d\gamma(x),t>0 \quad (1.2)$$

, where;

dγ (χ) is the measure (d-2 dimensional) of x on x. y = cost

$$\Psi(t)=\frac{2\pi^{(d-1)/2}}{\Gamma(\frac{d-1}{2})}\sin^{d-2}t$$

The Laplace – Beltrami operator on x∈U^{d-1} is given by

, where; $$\tilde{\Delta}f(x)=\Delta f(x/|x|) \quad (1.3)$$

$$\Delta f(x)=\frac{\partial^2}{\partial x_1^2}f(x)+\dots\dots\dots+\frac{\partial^2}{\partial x_d^2}f(x)$$

If $f\in L_p(U^{d-1})$, p<1, the K-functional can be defined as

$$K_r(f,\tilde{\Delta},t^{2r})_p^p = inf(\|f-g\|_p^p + t^{2r}\|\tilde{\Delta}^r g\|_p^p;$$

$$\tilde{\Delta}^r g \in L_p(U^{d-1}))$$

$$K(f,\tilde{\Delta},t^2)_p^p \equiv K_1(f,\tilde{\Delta},t^2)_p^p. \quad (1.4)$$

Using the definition of $B_t(f, x)$, for $B_t(f, x)$ is bounded operator, we get that

$$\|B_t(f,x)\|_{L_p(U^{d-1})} = \|B_t(f,x)\|_p \quad (1.5).$$

$$= \left\| \frac{1}{\varphi(t)} \int_{\ell} f(x)d\sigma(x) \right\|_p$$

$$\leq c(p)\|f\|_p$$

If $\tilde{\Delta}$ is the Laplace – Beltrami, for $\in L_p^2(U^{d-1})$, we get

$$\tilde{\Delta}B_t(f,x) = \Delta B_t(f(x)/|x|) \quad (1.6)$$

$$=$$

$$\frac{\partial^2}{\partial x_1^2} B_t(f(x_1))/|x| + \cdots\cdots\cdots + \frac{\partial^2}{\partial x_d^2} B_t(f(x_d))/|x|$$

$$=$$

$$\frac{\partial^2}{\partial x_1^2}\left(\frac{1}{\varphi(t)}\int_{\ell} f(x_1)d\sigma(x_1)\right)/|x| + \cdots + \frac{\partial^2}{\partial x_d^2}\left(\frac{1}{\varphi(t)}\int_{\ell} f(x_d)d\sigma(x_d)\right)/|x|$$

$$=\left(\frac{1}{\varphi(t)}\int_{\ell} \frac{\partial^2}{\partial x_1^2} f(x_1)d\sigma(x_1)\right)/|x| + \cdots +$$

$$\left(\frac{1}{\varphi(t)}\int_{\ell} \frac{\partial^2}{\partial x_d^2} f(x_d)d\sigma(x_d)\right)/|x|$$

$$= B_t(\Delta f(x)/|x|)$$

$$= B_t(\tilde{\Delta} f, x).$$

Then:

$$\tilde{\Delta}B_t(f,x) = B_t(\tilde{\Delta}f,x)$$

If the collection v_1,....., v_{d-1} is an orthonormal basis of the space orthogonal to x, the tangential gradient of f(x) is defined by [1]

$$grad_{tan}f(x) = \frac{\partial f(x)}{\partial v_1}, \dots\dots\dots, \frac{\partial f(x)}{\partial v_{d-1}}.$$

When $f \in L_p^1(U^{d-1})$, p<1

$$|grad_{tan}f(x)| = \max_{\xi \perp x} \left|\frac{\partial f(x)}{\partial \xi}\right|$$

2. Auxiliary Result

2. 1. Lemma [3]

Suppose $f(x) \in L_p^2$, and

$$B_t(f,x) = \frac{1}{\varphi(t)} \int_{\ell} f(x) d\sigma(x) \ , t>0$$

$$S_t(f,x) = \frac{1}{\Psi(t)} \int_{x.y=cost} f(x) d\gamma(x) \ ,t>0$$

$$\tilde{\Delta} f(x) = \Delta f(x/|x|) \quad for\ x \in U^{d-1}.$$

Then for x ∈ U^{d-1} and 0 <t <$\frac{\pi}{2}$, we have:

$$B_t(f,x) - f(x)$$

$$= \frac{1}{\varphi(t)} \int_0^t sin^{d-2}\theta \int_0^\theta sin^{2-d}\rho\ \varphi(\rho) B_\rho(\tilde{\Delta} f, x) d\rho\ d\theta$$

$$= \frac{1}{\varphi(t)} \int_0^t sin^{d-2}\theta \left\{\int_0^\theta sin^{2-d}\rho \int_{\ell} \tilde{\Delta} f(y) d\,\sigma(y) d\rho\right\} d\theta\ .$$

And

$$S_t(f,x) - f(x) =$$

$$= \frac{1}{\Psi(t)} sin^{d-2}t \int_0^t sin^{2-d}\theta\ d\theta \int_{\ell} \tilde{\Delta} f(y) d\sigma(y)$$

$$= \frac{1}{\Psi(t)} \int_0^t sin^{2-d}\theta\ \varphi(\theta) B_\theta(\tilde{\Delta} f, x)\ d\theta$$

2. 2. Lemma [1]

for $\xi \perp x$, $B_t(f,x)$ is given by

$$B_t(f,x) = \frac{1}{\varphi(t)} \int_{\Omega} \int_{-\kappa}^{\kappa} f(\upsilon + (x\cos\theta + \xi\sin\theta)\sqrt{1-|\upsilon|^2}) d\theta \, d\upsilon.$$

Where; $\varphi(t) = \frac{2\pi^{(d-1)/2}}{\Gamma_{(\frac{d-1}{2})}} \int_0^t \sin^{d-2} u \, du$

$\Omega = B_{x,\xi} \, sint = \{\upsilon : \upsilon . x = 0 \, , \upsilon . \xi = 0 \, , |\upsilon| \leq sint\}$,

$\kappa = \arccos(cost/\sqrt{1-|\upsilon|^2})$, then

$$\frac{\partial}{\partial \xi} B_t(f,x)$$

$$= \frac{1}{\varphi(t)} \int_{\Omega} \Big[f\Big(\upsilon + x\cos t + \xi\sqrt{1-|\upsilon|^2-\cos^2 t}\Big) \alpha(t,\upsilon) - f\Big(x + x\cos t - \xi\sqrt{1-|\upsilon|^2-\cos^2 t}\Big) \beta(t,\upsilon) \Big] d\upsilon$$

Where $\alpha(t, \upsilon)$ and $\beta(t, \upsilon)$ are close to 1 and arebounded by 1

2. 3. Lemma [4]

For $f \in L_\theta(U^{d-1})$, $1 \leq \theta \leq \infty$, there exsist $g \in L_{\grave{\theta}}(U^{d-1})$, such that $\frac{1}{\theta} + \frac{1}{\grave{\theta}} = 1$.

We have:

$$\begin{aligned} \left\| \tilde{\Delta} B_t B_\tau f \right\|_\theta - \varepsilon &\leq \left| \langle g, \tilde{\Delta} B_t B_\tau f \rangle \right| \\ &\leq \left| \langle g, B_t \tilde{\Delta} B_\tau f \rangle \right| \\ &\leq \left| \langle B_t g, \tilde{\Delta} B_\tau f \rangle \right| \\ &\leq \left| \langle grad_{tan} B_t g, grad_{tan} B_\tau f \rangle \right| \end{aligned}$$

Then

$$\left\| \tilde{\Delta} B_t B_\tau f \right\|_\theta - \varepsilon \leq \| grad_{tan} B_t g \|_{\grave{\theta}} \cdot \| grad_{tan} B_\tau f \|_\theta .$$

3. The main results

In this section we shall introduce our main result

3. 1. Theorem

For $B_t(f,x), S_t(f,x), K(f,\tilde{\Delta},t^2)$ are given by (1. 1), (1. 2), (1. 4) respectively, we have for p<1

$$\|f - B_t f\|_{L_{p(U^{d-1})}} \leq c(p)\, K(f, \tilde{\Delta}, t^2)_{L_p(U^{d-1})}$$

Proof: $\|f - S_t f\|_{L_{p(U^{d-1})}} \leq c(p)\, K(f, \tilde{\Delta}, t^2)_{L_p(U^{d-1})}.$

We choose $g \in L_p^2$

$$\|f-g\|_p^p + t^2\|\tilde{\Delta} g\|_p^p \leq 2\, K(f, \tilde{\Delta}, t^2)_p^p$$

$$\|B_t(f-g) - (f-g)\|_p^p \leq \|B(f-g)\|_p^p + \|f-g\|_p^p$$
$$\leq c\left[\|B(f-g)\|_p^p + \|f-g\|_p^p\right] \ , c < 1.$$

Then

$$\|B_t(f-g) - (f-g)\|_p^p \leq 2\|f-g\|_p^p$$

$$\|S_t(f-g) - (f-g)\|_p^p \leq \|S(f-g)\|_p^p + \|f-g\|_p^p$$
$$\leq c\left[\|S(f-g)\|_p^p + \|f-g\|_p^p\right], \text{c} < 1.$$

Then

$$\|S_t(f-g) - (f-g)\|_p^p \leq 2\|f-g\|_p^p.$$

Using Lemma2.1, we get

$$\|B_t g - g\|_p^p =$$

$$\left\|\frac{1}{\varphi(t)} \int_0^t sin^{d-2}\theta \{\int_0^\theta sin^{2-d}\rho \int_\ell \tilde{\Delta} g(y) d\sigma(y) d\rho\} d\theta\right\|_p^p$$
$$\leq c(p) t^2 \|\tilde{\Delta} g\|_p^p.$$

$$\|S_t g - g\|_p^p$$

$$= \left\|\frac{1}{\Psi(t)} sin^{d-2} t \int_0^t sin^{2-d}\theta d\theta \int_\ell \tilde{\Delta} g(y) d\sigma(y)\right\|_p^p$$

$$\leq c(p) t^2 \|\tilde{\Delta} g\|_p^p.$$

Then

$$\|f - B_t f\|_{L_p(U^{d-1})} \leq 2\|f-g\|_p^p + c(p) t^2 \|\tilde{\Delta} g\|_p^p$$
$$= c(p) K(f, \tilde{\Delta}, t^2)_{L_p(U^{d-1})}$$

$$\|f - S_t f\|_{L_p(U^{d-1})} \leq 2\|f-g\|_p^p + c(p) t^2 \|\tilde{\Delta} g\|_p^p$$
$$= c(p) K(f, \tilde{\Delta}, t^2)_{L_p(U^{d-1})}$$

3. 2. Theorem

If $L_p(U^{d-1})$, p<1, then $grad_{tan}\, B_{tf}$ is in $L_p(U^{d-1})$ and

$$\|grad_{tan} B_t f\|_{L_p} \leq \frac{c(p)\Psi(t)}{\varphi(t)} \|f\|_{L_p} \leq \frac{c(p)}{t} \|f\|_{L_p}$$

Proof:

By Lemma 2. 2 we get

$$\left|\frac{\partial}{\partial\xi}B_t(f,x)\right| =$$

$$\left|\frac{1}{\varphi(t)}\int_{\Omega}\left[f\left(v+xcost+\xi\sqrt{(1-|v|^2)-cos^2t}\right)\alpha(t,v)-\right.\right.$$

$$\left.\left.f\left(x+xcost-\xi\sqrt{(1-|v|^2)-cos^2t}\right)\beta(t,v)\right]dv\right|.$$

$$\leq\frac{2}{\varphi(t)}\{\int_{\Omega}\left|f(v+xcost+\xi\sqrt{(1-|v|^2)-cos^2t})\right|dv+$$

$$\int_{\Omega}\left|f(v+xcost+\xi\sqrt{(1-|v|^2)-cos^2t})\right|dv\}.$$

Since

$\int_{U^{d-1}}f(x)dx \leq [\ measure\ of\ U^{d-1}][\max_{x\in U^{d-1}}f(x)]$

, then

$$\left|\frac{\partial}{\partial\xi}B_t(f,x)\right| \leq \frac{2\psi(t)}{\varphi(t)}S_t(|f|,x).$$

$$|grad_{tan}B_t(f,x)| = \max_{\xi\perp x}\left|\frac{\partial}{\partial\xi}B_t(f,x)\right|.$$

Then we get , for $p<1$ *and* $f\in L_p^1(U^{d-1})$, that

$$\|grad_{tan}B_t(f,x)\|_{L_p} = \int_{U^{d-1}}(|grad_{tan}B_t(f,x)|^p dx)^{1/p}$$

$$= \int_{U^{d-1}}(\left|\max_{\xi\perp x}\frac{\partial}{\partial\xi}B_t(f,x)\right|^p dx)^{1/p}$$

$$\leq \int_{U^{d-1}}\left(\left|\frac{2\psi(t)}{\varphi(t)}S_t(|f|,x)\right|^p dx\right)^{1/p}$$

$$\leq \frac{2\psi(t)}{\varphi(t)}\|S_t(|f|,x)\|_{L_p},$$

since $\frac{2\psi(t)}{\varphi(t)} \leq \frac{c(p)}{t}$ *, then*

$$\|grad_{tan}B_t(f,x)\|_{L_p} \leq \frac{c(p)}{t}\left\|\frac{1}{\boldsymbol{\Psi}(t)}\int_{x.y=cost}f(x)d\boldsymbol{\gamma}(x)\right\|_{L_p}$$

$$\leq \frac{c(p)}{t}\|f\|_{L_p}$$

3. 3. Theorem

If $f \in L_p(U^{d-1})$, p<1. Then

$$\left\|\tilde{\Delta}^r B_{\tau_1} \cdots\cdots B_{\tau_{2r}} f\right\|_p \leq \frac{c_r(p)}{\tau_1 \ldots\ldots \tau_{2r}} \|f\|_p \quad , \quad p<1$$

Proof:

Since $\left\|\tilde{\Delta} B_t B_\tau f\right\|_p - \varepsilon \leq \left\|\tilde{\Delta} B_t B_\tau f\right\|_\theta - \varepsilon \quad , \theta \geq 1$

We choose g of in Lemma 2.3, then we get:

$\left\|\tilde{\Delta} B_t B_\tau f\right\|_p - \varepsilon \leq \|grad_{tan} B_t g\|_{\grave{\theta}} \cdot \|grad_{tan} B_\tau f\|_\theta$,

$\grave{\theta} \geq 1$, and $\frac{1}{\theta} + \frac{1}{\acute{\theta}} = 1$

$$\|grad_{tan} B_t g\|_{\grave{\theta}} = \left(\int_{U^{d-1}} |grad_{tan} B_t g|^{\acute{\theta}} \, dx \right)^{1/\acute{\theta}}$$

$$= \left(\int_{U^{d-1}} |grad_{tan} B_t g|^{\acute{\theta}+\frac{1}{\theta'}-\frac{1}{\theta'}} \, dx\right)^{\frac{1}{\theta'}+\acute{\theta}-\acute{\theta}}$$

$$\leq \left(\int_{U^{d-1}} |\mathrm{grad}_{\tan} B_t g|^{\acute{\theta}-\frac{1}{\theta'}} |\mathrm{grad}_{\tan} B_t g|^{\frac{1}{\theta'}} dx \right)^{\frac{1}{\theta'}-\acute{\theta}} \times$$

$$\left(\int_{U^{d-1}} |\mathrm{grad}_{\tan} B_t g|^{\acute{\theta}-\frac{1}{\theta'}} |\mathrm{grad}_{\tan} B_t g|^{\frac{1}{\theta'}} dx \right)^{\acute{\theta}}$$

Assume that $\frac{1}{\acute{\theta}} = q$, $so \quad \acute{\theta} = \frac{1}{q}$, $and \ q < 1$, then

$$\|\mathrm{grad}_{\tan} B_t g\|_{\acute{\theta}} \leq \left(\int_{U^{d-1}} |\mathrm{grad}_{\tan} B_t g|^{\frac{1}{q}-q} |\mathrm{grad}_{\tan} B_t g|^{q} dx \right)^{q-\frac{1}{q}}$$

$$\times \left(\int_{U^{d-1}} |\mathrm{grad}_{\tan} B_t g|^{\frac{1}{q}-q} |\mathrm{grad}_{\tan} B_t g|^{q} dx \right)^{\frac{1}{q}}$$

$$\leq c(q) \times \left(\int_{U^{d-1}} c(q) |\mathrm{grad}_{\tan} B_t g|^{q} dx \right)^{\frac{1}{q}}$$

$$\leq c(q) \|grad_{tan} B_t g\|_q, q<1 \qquad (1.\ 8).$$

And

$$\|grad_{tan}B_\tau f\|_\theta = \left(\int_{U^{d-1}} |grad_{tan}B_\tau f|^\theta dx\right)^{\frac{1}{\theta}}$$

$$= \left(\int_{U^{d-1}} |grad_{tan}B_\tau f|^{\theta+\frac{1}{\theta}-\frac{1}{\theta}} dx\right)^{\frac{1}{\theta}+\theta-\theta}$$

$$\leq \left(\int_{U^{d-1}} |grad_{tan}B_\tau f|^{\theta-\frac{1}{\theta}} |grad_{tan}B_\tau f|^{\frac{1}{\theta}} dx\right)^{\frac{1}{\theta}-\theta}$$

$$\times \left(\int_{U^{d-1}} |grad_{tan}B_\tau f|^{\theta-\frac{1}{\theta}} |grad_{tan}B_\tau f|^{\frac{1}{\theta}} dx\right)^{\theta}$$

Assume that $\frac{1}{\theta} = p$ so $\theta = \frac{1}{p}$ and $p < 1$, then

$$\|grad_{tan}B_\tau f\|_\theta$$

$$\leq \left(\int_{U^{d-1}} |grad_{tan}B_\tau f|^{\frac{1}{p}-p} |grad_{tan}B_\tau f|^p \, dx\right)^{p-\frac{1}{p}}$$

$$\times \left(\int_{U^{d-1}} |grad_{tan}B_\tau f|^{\frac{1}{p}-p} |grad_{tan}B_\tau f|^p \, dx\right)^{\frac{1}{p}}$$

$$\leq c(p) \times \left(\int_{U^{d-1}} c(p)|grad_{tan}B_\tau f|^p \, dx\right)^{\frac{1}{p}}$$

$\leq c(p)\|grad_{tan}B_\tau f\|_p$, p < 1 (1. 9).

From (1. 8), (1. 9), we get:

$\left\|\tilde{\Delta}B_t B_\tau f\right\|_p - \varepsilon \leq c(p,q)\, \|grad_{tan}B_t g\|_q \cdot \|grad_{tan}B_\tau f\|_p$

, where: p<1, q<1 and p + q=1

Let $\|g\|_q = c(q)$, and by Theorem 3.2 we get:

$$\left\|\tilde{\Delta}B_t B_\tau f\right\|_p - \varepsilon \leq \frac{c(q)}{t}\|g\|_q \cdot \frac{c(p)}{\tau}\|f\|_p$$

$$\leq \frac{c^2(q)\, c(p)}{t\tau}\|f\|_p.$$

Which, as is an arbitrary, implies our result for r=1.

Repetition of the above consideration implies.

$$\left\|\tilde{\Delta}^r B_{\tau_1} \cdots\cdots B_{\tau_{2r}} f\right\|_p \leq \frac{c_r(p)}{\tau_1 \cdots\cdots \tau_{2r}} \|f\|_p, \mathrm{p}<1$$

References

[1] W. Chen and Z. Ditzian,, Acta, Hungar. **75**, 165 (1997).

[2] E. Bhaya, On the constrained and un constrained approximation Ph. D. Thesis, Baghdad university, Iraq, (2003).

[3] Z. Ditzian and K. Runovskii, J. Approx.Theory, **7**, 113 (1999).

[4] V. H. Hristov and K. G. Ivanov, math. Balkanica (N.s.) **4**, 236 (1990).

[5] Yuan. Xu , Funk-Heck formula for orthogonal polynomials on spheres and on balls. Bull London Math, **505**, 447-457, (2001).

[6] Yuan. Xu, Orthogonal polynomials and summability in Fourier orthogonal series on spheres and on balls. Math. Proc. Cambridge Philos. Soc., **31**, 139-155, (2001).

[7] Yuan. Xu,Generalized classical orthogonal polynomials on the ball and on simplex. Constr. Approx., **17**, 383-412, (2001).

A Study of the surface diffuseness of inter-nucleus potential with quasi-elastic scattering for the $^{32,34}_{16}S + ^{208}_{82}Pb$ reactions

Khalid S. Jassim and Qasim J. Tarbool
Department of Physics, College of Education for pure Science, University of Babylon, Iraq
Received Date: 29/Jun/2015
Accepted Date: 8/Aug/2015

الخلاصة

تم انجاز دراسات حسابية دقيقة على معلمات الانتشار السطحي للجهد النووي ولتفاعل الايونات الثقيلة والتي تضمنت الانظمة باستخدام استطارة شبة مرنة بزاوية كبيرة عند طاقات حاجز الجهد والتي تكون قريبة من اعلى قيمة لحاجز كولوم.

حسابات القنوات المنفردة و الاقتران اخذت بنظر الاعتبار لاستبيان معلمات الانتشار للجهد النووي. وتم استخدام طريقة مربع كاي χ^2 لايجاد أفضل قيمة لمعلمات الإنتشار بالمقارنة مع القيم التجريبية.

معلمات الانتشار السطحي التي استبينت من حسابات قنوات الاقتران مع القذيفة الخاملة والهدف المهتز كانت تماما متوافقة مع القيمة القياسية والتي تكون 0.63 fm بينما حسابات القناة المنفردة تعطي قيم كبيرة وضمن المدى من 0.64 fm الى 0.65 fm.

الكلمات المفتاحية

معلمات الإنتشار السطحي للجهد النووي، الإستطارة شبه المرنة، القنوات المنفردة، القذيفة الخاملة والهدف المهتز.

Abstract

Precise systematic studies on the surface diffuseness parameter of the nuclear potential for the heavy-ion reactions involving the systems have been achieved by using large-angle quasi-elastic scattering at deep sub-barrier energies close to the Coulomb barrier height. The single-channel (SC) and coupled-channels (CC) calculations have been carried out to elicit the diffuseness parameter of the nuclear potential. The chi square method χ^2 has been used with a view to find the best fitted value of the diffuseness parameter in comparison with the experimental data. The surface diffuseness parameters have been elicited from the coupled-channels calculations with inert projectile and vibrational target are in complete agreement with the standard value which is (0.63 fm) while the single-channel calculations give to a certain extent larger values in the range from 0.64 fm to 0.65 fm.

Keywords

quasi-elastic scattering, Heavy-ion fusion reactions, deep sub-barrier energies, Coupled-channels calculations.

PACS number (s)

25. 70. Bc, 25. 70. Jj, 24. 10. Eq, 27. 70. + q

1. Introduction

Knowing of The nucleus-nucleus interaction potential is the main component in the analysis of nuclear reactions [1, 2] and it has been played a crucial role [3] so as to describe nucleus-nucleus collisions [4]. The nucleus-nucleus potential is the reason in the interaction energy of colliding nuclei [2, 5, 6], it has been used to estimate the cross sections of various nuclear reactions [1, 2], moreover, in deformed nucleus interaction the nucleus-nucleus potential rely on the orientation angle of the deformed nucleus relative to the beam direction [7, 9]. We can define the nucleus-nucleus potential as the sum of the nuclear potential $V_{N(r)}$ which is less defined and the Coulomb potential $V_{C(r)}$ which is well-known [1, 4]. By the precise description of the Coulomb or Rutherford scattering [4, 10]. The barrier height of the nucleus-nucleus reaction rely on the ratio between the nuclear and Coulomb potentials, that work at teeny distances between the surfaces of reactant nuclei [5]. Consequently, the nucleus-nucleus potential is consist from Coulomb and nuclear parts, so that long range repulsion Coulomb potential acts between the protons in nuclei while the nuclear interaction between nucleons [5], the nuclear part is commonly expressed by the Woods-Saxon (WS) form [11], which is discriminated by the deepness V_o, radius r_o, and diffuseness a parameters [12]. The fact that the WS form of a simple exponential had been exploited to research the surface characteristic of nuclear potential [13]. The WS potential has great importance in nuclear physics due to be considered reasonable potential [14]. The value of surface diffuseness parameter which was accepted, it is around 0. 63 fm has been used for accounts of elastic and inelastic scattering, which are sensitive fundamentally to the surface region of the nuclear potential [15]. We can study the nuclear potential through quasi-elastic scattering or fusion experimental data [10].

Quasi-elastic scattering can be defined as sum of elastic scattering, inelastic scattering and transfer reaction [16, 19], it is very well equivalent of the fusion reaction [16, 19, 20], which is defined as a reaction where two discrete nuclei integrate together to form compound system [21, 22]. Fusion and Quasi-elastic scattering are both considered extensive operations and are complementary to each other [13, 23, 24]. As a result, these interactions are subject to the same potential and share the same information about the mechanism of interaction, and both are sensitive to the channel coupling Impacts (due to collective inelastic excitements of the colliding nuclei) at energies near the Coulomb barrier [19, 20]. Experimentally, the measurement of quasi-elastic scattering more easier than that of fusion interaction, particularly at deep sub-barrier energies [13, 20]. As well as note that the scattering operation is sensitive fundamentally to the surface area of the nuclear potential, whilst the fusion reaction is also comparatively sensitive to the internal fraction [3, 15].

The experimental measurement process to large-angle quasi-elastic scattering cross sections are more efficient and easier than the fusion cross sections [10]. That the perversion of the rate of the quasi-elastic to the Rutherford cross sections from unity at deep sub-barrier energies provides a clear way to set the account of the surface

diffuseness parameter in the nucleus-nucleus potential [13]. Consequently, can be defined the diffuseness parameter as a landing of the nuclear potential and thus directly impacts on the barrier width and the coupling strong points which to first order rely on the derivative of the potential [25, 26]. It is one-component parameters of the WS potential, which is known downhill nuclear potential in the tailpiece area of Coulomb barrier [27, 29].

Coupling channel model is an ideal tool to reproduce the experimental data at the same time for several processes, such as elastic, inelastic scattering, particle transfers and fusion within a unified framework [21, 30]. The inter-nuclear potential is the most important component in the coupled-channels calculations [30], such that the nuclear potential affect the width of the barrier and the coupling strengths [26]. The channel coupling is caused by coupling of the internal degrees of freedom which are included the transfer reactions and the collective vibrational and rotational motions with the relative motion of the colliding nuclei [10, 12, 18]. In nucleus-nucleus collisions at deep sub-barrier energies near the Coulomb barrier, observed that the effect of coupling channels can be neglected, because reflection probability is nearly unity at such energies, however, this analysis would be acceptable for the spherical nuclei collisions [10, 12, 15]. The use of coupling channels accounts does not play an important role in determining the best value for the diffuseness parameters at deep sub-barrier energies, but the essential purpose of employ these accounts is to achieve the effects of some calculation inputs on the resulting diffuseness parameters. The excitation states of the colliding nuclei play an important role to perform coupled-channels calculations [31].

K. Washiyama et al. [15] had been performed study on the surface characteristic of nucleus-nucleus potential in heavy-ion reactions using large-angle quasi-elastic scattering at energies much less the Coulomb barrier. Consequently, single-channel was suitable potential model to describe these energies. They had concluded that systems which involve deformed target require the diffuseness parameter between 0. 8 fm and 1. 1 fm, whilst spherical nuclei systems require the diffuseness parameter of around 0. 60 fm.

K. Jassim et al. [4] have analyzed on the nuclear potential for heavy ion systems, namely ^{48}Ti, ^{54}Cr, and ^{64}Ni + ^{208}Pb systems by using large-angle quasi-elastic scattering at sub-barrier energies around the Coulomb barrier height.

This research aims to achieve the surface diffuseness parameters of inter-nucleus potential for the systems ${}^{34,32}_{16}S + {}^{208}_{82}Pb$ by using large-angle quasi-elastic scattering at deep sub-barrier energies close to the Coulomb barrier height and the single-channels and coupled-channels calculations were Conducted by using CQEL program which includes all orders of coupling and it is considered the latest version of computer code CCFULL [21]. The best fitted values of the diffuseness parameters in comparison with the experimental data have been obtained through the chi square method χ^2 [21].

2. Theory

The nucleus-nucleus potential is consist from two parts [5] nuclear part V_N which can be described well and fairly reasonable by the

Woods-Saxon (WS) form which is given by [10]:

$$V_N(r) = -\frac{V_0}{1+\exp\left[\frac{r-R_0}{a}\right]} .(1)$$

where R_0 is a radius parameter of the system,, vo, a and r_0 represent the potential depth, surface diffuseness parameter, and radius parameter, respectively, whilst r refers to the center -of-mass distance between the target nucleus of mass number A_T and the projectile nucleus of mass number A_P [26].

From another side, Coulomb part V_C between two spherical nuclei with regular charge density distributions and when they do not interfere is given by [10]:

$$V_c(r) = \frac{Z_P Z_T\ e^2}{r} .(2)$$

where Z_p and Z_T represent the atomic number of the projectile and target, respectively, r the distance between the centers of mass of the colliding nuclei [4, 33]. When the nuclei interfere, then the Coulomb potential is given by [32]:

$$V_c(r) = \frac{Z_P Z_T\ e^2}{2R_C}\left[3-\left(\frac{r}{R_c}\right)^2\right] .(3)$$

where R_c is the radius of the ball equivalent to the nuclei of the target and the projectile [4, 10].

The collision between two nuclei through the presence of coupling between the relative motion of the center of mass of the colliding nuclei $\vec{r} = (r, \hat{r})$ and the nuclear intrinsic motion ξ. The Hamiltonian for the system is giving by:

$$H(\vec{r}.\xi) = -\frac{\hbar^2}{2\mu}\nabla^2 + V(r) + H_0(\xi) + V_{coup}(\vec{r}.\xi) .(4)$$

where r refers to the center of mass distance between the colliding nuclei, μ is the reduced mass of the system while V (r) is the naked potential in the absence of the coupling where V (r) = V_N (r) + V_c (r), H_0 (ξ) represents the Hamiltonian for the intrinsic motion, Ccoup is the mentioned coupling [4]. The Schrodinger equation for the total wave function would be given by [4]:

$$\left(-\frac{\hbar^2}{2\mu}\nabla^2 + V(r) + H_0(\xi) + V_{coup}(\vec{r}.\xi)\right)\psi(\vec{r}.\xi) = E\psi(\vec{r}.\xi) .(5)$$

The internal degree of freedom ξ principally has a limited spin. We can write the coupling Hamiltonian in complications as [4]:

$$V_{coup}(\vec{r}.\xi) = \sum_{\lambda>0.\mu} f_\lambda\ (r) Y_{\lambda\mu}(\hat{r}).T_{\lambda\mu}(\xi) .(6)$$

$Y_{\lambda\mu}$ (r̂) refers to the spherical harmonics and $T_{\lambda\mu}$ (ξ) refers to the spherical tensors, which are built from the internal coordinate. The sum is taken over all values of excluding for λ = 0 since it is originally considered in V (r). The expansion basis for the wave function in equation (5) for a fixed total angular momentum J and its z-component M is defined as [4]:

$$\langle \vec{r}\,\xi|(nlI)JM\rangle = \sum_{m_l m_I}\langle l m_l I m_I|JM\rangle Y_{lm_l}(\hat{r})\,\varphi_{nIm_I}(\xi) .(7)$$

where l refers to the orbital, I represents the internal angular momenta, and represents the wave function for the internal motion which fulfills [4].

$$H_0(\xi)\,\varphi_{nIm_I}(\xi) = \epsilon_n\,\varphi_{nIm_I}(\xi) \quad .(8)$$

expanded with this basis as [4]:

The total wave function $\psi\ (r.\ \xi)$ has been

$$\psi(\vec{r}.\xi) = \sum_{n.l.I} \frac{u^J_{nlI}(r)}{r} \langle \vec{r}\,\xi | (nlI)JM \rangle \quad .(9)$$

The Schrödinger equation (equation (2)) can then be written as a group of coupled equations for $u_{nlI}{}^J(r)$ [4]:

$$\left[-\frac{\hbar^2}{2\mu}\frac{d^2}{dr^2} + V(r) + \frac{l(l+1)\hbar^2}{2\mu r^2} - E + \epsilon_n\right] u^J_{nlI}(r) + \sum_{ń.l'.Í} V^J_{nlJ;ń.l'.Í}(r) u^J_{ń.l'.Í}(r) = 0 \quad .(10)$$

Terms the coupling matrix elements is given by [4]:

$$V^J_{nlJ;ń.Í.Í}(r) = \langle JM\ (nlI) \left| V_{coup}(\vec{r}.\xi) \right| (ń.l'.Í)JM \rangle$$
$$= \sum_{\lambda} (-1)^{I-Í+l'+J} f_\lambda(r) \langle l \left|\left| Y_\lambda \right|\right| l' \rangle \langle nI \left|\left| T_\lambda \right|\right| n'I' \rangle \times \sqrt{(2l+1)(2I+1)} \begin{Bmatrix} I' & l' & J \\ l & I & \lambda \end{Bmatrix} \quad .(11)$$

The reduced matrix elements in equation (11) is defined by [4]:

$$\langle l_{ml} \left| Y_{\lambda\mu} \right| l'_{ml'} \rangle = \langle l'_{ml'}\ \lambda\mu \left| l_{ml} \right. \rangle \langle l \left|\left| Y_\lambda \right|\right| l' \rangle \quad .(12)$$

Since is freelance of the coefficient M, the coefficient has been suppressed as seen in equation (11). The equation (10) is called coupled-channels equations. For heavy-ion fusion interactions, these equations are commonly resolved using the incoming wave boundary conditions [4]

$$u^J_{nlI}(r) \sim \mathcal{T}^J_{nlI}\ exp\left(-1 \int_{r_{abs}}^{r} k_{nlI}\,(ŕ)dŕ\right) . r \leqslant r_{abs} \quad .(13)$$

$$\rightarrow \frac{i}{2}\begin{pmatrix} H_l^{(-)}(k_{nIr})\delta_{n,n_i}\delta_{l,l_i}\delta_{I,I_i} \\ +\sqrt{\frac{k_{nIi}}{k_{nI}}}\ S^J_{lI} H_l^{(+)}(k_{nIr}) \end{pmatrix} , r \longrightarrow \infty \quad .(14)$$

$$k_{nIr} = \sqrt{2\mu(E-\epsilon_{nI})}/\hbar^2 \ ,\ k_{nIi} = k = \sqrt{2\mu E/\hbar^2}$$

The local wave number is defined as [4]:

$$k_{nII}(r) = \sqrt{\frac{2\mu}{\hbar^2}\left(E - \epsilon_{nI} - \frac{l(l+1)\hbar^2}{2\mu r^2} - V(r) - V^J_{nlJ;nlJ}(r)\right)} \quad .(15)$$

Once we obtained the transmission coefficients the penetrability during the Coulomb barrier is given by:

$$P_{liIi}^{J}(E) = \sum_{n.l.I} \frac{k_{nlI}(r_{abs})}{k} |\mathcal{T}_{nlI}^{J}|^2 \quad .(16)$$

is the wave number for the entrance channel. The fusion cross section for unpolarized target is given by:

$$\sigma_{fus}(E) = \frac{\pi}{k^2} \sum_{JMli} \frac{2J+1}{2Ii+1} P_{liIi}^{J}(E) \quad .(17)$$

When the initial intrinsic spin = 0, then the initial angular momentum =J, with the coefficients and are suppressed in the penetrability, equation (17) then reads [4]:

$$\sigma_{fus}(E) = \frac{\pi}{k^2} \sum_{J} 2J+1\, P^{J}(E) \quad .(18)$$

where $P^{J}(E)$ is the penetrability which is affected now by the channel couplings. Unlike to the calculation of fusion cross sections, the calculation of quasi-elastic cross sections usually requires a large value of angular momentum so as to obtain converged results. The potential pocket at ($r = r_{abs}$) becomes superficiality or even disappears for such large angular momentum. Hence, the incoming flux in equation (13) cannot be correctly identified. Therefore, the quasi-elastic problem commonly performs the regular boundary conditions at the origin rather than using the incoming wave boundary conditions. When using the regular boundary conditions, a complex potential $V_N(r) = V_N^{0}(r) + iw(r)$, is needed to simulate the fusion reaction. Once the nuclear S-matrix in equation (11) is obtained, the scattering amplitude can then be calculated as [4]:

$$f_{lI}^{J}(\theta.E) = i\sum_{Jl} \sqrt{\frac{\pi}{kk_{nI}}}\, i^{J-l}\, e^{i[\sigma_J(E)+\sigma_l(E-\epsilon_{nI})]} \sqrt{2J+1}\, Y_{l0}(\theta) \left(S_u^{J} - \delta_{I.I_2}\delta_{l.l_2}\right) + f_c(\theta.E)\delta_{I.I_2}\delta_{l.l_2} \quad .(19)$$

σ_l is the Coulomb phase shift which is given by [4]:

$$\sigma_l = |\Gamma(l+1+i\eta)| \quad .(20)$$

While f_c is the Coulomb scattering amplitude which is given by [4]:

$$f_c(\theta.E) = \frac{\eta}{2k\sin^2\left(\frac{\theta}{2}\right)} e^{\left[-i\eta \ln\left(\sin^2\left(\frac{\theta}{2}\right)\right)+2i\sigma_0(E)\right]} \quad .(21)$$

η is the Summerfield parameter, which is given by, we can be evaluated the differential cross section by using equation (19) [4]

$$\frac{d\sigma_{qel}(\theta.E)}{d\Omega} = \sum_{JlI} \frac{k_{nI}}{k} |f_{lI}^{J}(\theta.E)|^2 \quad .(22)$$

we can be evaluated the Rutherford cross section by using equation (21) [4]

$$\frac{d\sigma_R(\theta.E)}{d\Omega} = |f_c(\theta.E)|^2 = \frac{\eta^2}{4k^2} csc^4\left(\frac{\theta}{2}\right) \quad .(23)$$

3. Procedure

The single-channel and coupled-channels calculations have been carried out using CQEL program, which is considered the latest version of computer code CCFULL [21]. This code solves the Schrödinger equation and the coupled equations exactly [33]. The chi square method χ^2 was considered normalization factor between the theoretical calculation and the experimental data to avoid systematic errors in the present work where the data with $d\sigma_{qel}/d\sigma_R>1$ were excluded from the fitting proceedings [4, 12] This calculations were made using a WS form for the nuclear potential, which is consists of real and an imaginary components [4, 12]. The values supposed for the parameters of the imaginary part (w = 30 MeV, r_w = 1. 0 fm and a_w = 0. 1 fm) result in trivial strength in the surface region [24]. The imaginary potential was used to account for the rather small internal absorption from barrier penetration [12]. The imaginary part of the potential remained inside the Coulomb barrier, the results were insensitive to variations of the imaginary potential parameters [4, 12] The Woods-Saxon (WS. The parameters of the real potential were researched to get the best fit to the experimental data, so it were reproduced for all interactions [4, 12] The Woods-Saxon (WS. The radius parameter r0 is taken to be 1. 2 fm, while the values of potential depth V0 depended on the diffuseness parameter are taken to be 62. 5 MeV and 80. 5 MeV for the ${}^{32}_{16}S+{}^{208}_{82}Pb$ and ${}^{32}_{16}S+{}^{208}_{82}Pb$ systems, respectively. The radius of the target was taken as $R_T = r_T A^{1/3}$ such that r_T = 1. 16 fm while for the projectile $R_p = r_p A^{1/3}$ so r_p = 1. 22 fm. The calculations are performed at scattering angle of $\theta_{lab.} = 170^\circ$ for the ${}^{32}_{16}S+{}^{208}_{82}Pb$ system, while $\theta_{lab.} = 159^\circ$ for the ${}^{32}_{16}S+{}^{208}_{82}Pb$ system [34, 37]. The experimental data of the quasi-elastic cross sections at deep sub-barrier energies for all systems were taken from the Ref. [36, 37]. We find that the deep sub-barrier region can be defined in this way corresponds to the region where $d\sigma_{qel}/d\sigma_R \geq 0.95$ for ${}^{32}_{16}S+{}^{208}_{82}Pb$ reaction, $d\sigma_{qel}/d\sigma_R \geq 0.93$ for ${}^{32}_{16}S+{}^{208}_{82}Pb$ reaction. We analysis and plot the calculated ratio of the quasi-elastic to the Rutherford cross sections as functions of the center of mass energies, in order to make sure that the calculations are properly consistent according to the available experimental data [24].

4. Results

4. 1. The ${}^{32}_{16}S+{}^{208}_{82}Pb$ reaction

This reaction involve spherical nuclei for both projectile ${}^{34,32}_{16}S$ and target ${}^{208}_{82}Pb$ [15]. The characteristics of the single-quadruple phonon excitation for each nucleus are shown in the Table (1), where β, ħω, J, π, and λ are the deformation parameter of the phonon state, excitation energy, angular momentum, parity and vibration mode respectively. [31]

Table (1): The characteristics of the single- quadruple phonon excitation for the nuclei.

Spherical Nuclear	β_0	ħω (MeV)	J^π	λ
${}^{32}_{16}S$	0.312	2.2303	2^+	2
${}^{208}_{82}Pb$	0.0553	4.0854	2^+	2
${}^{34}_{16}S$	0.252	2.1276	2^+	2

In the $^{32}_{16}S + ^{208}_{82}Pb$ system, the diffuseness parameter have been discussed in four states, in the first state we considered the projectile $^{32}_{16}S$ as well as target $^{208}_{82}Pb$ as inert nuclei (SC), while in the second state we considered the target nucleus $^{208}_{82}Pb$ is vibrational coupling with deformation parameter β_0= 0. 0553 to the state 2^+(4. 0854 MeV), while the projectile nucleus $^{32}_{16}S$ is inert, the third state, we assumed that the projectile nucleus $^{32}_{16}S$ is vibrational coupling to the state 2^+ with deformation parameter β_0= 0.312 (2.2303 MeV), while the target $^{208}_{82}Pb$ is inert, in the last state we assumed that projectile $^{32}_{16}S$ as well as target $^{208}_{82}Pb$ nuclei are vibrational coupling to the state 2^+. We used single-quadruple phonon excitation for the projectile and target nuclei which were vibrational excited. The values of the diffuseness parameters (a) have been obtained from SC and CC analysis, as well as others parameters of WS potential (radius r_0 and depth potential v_0) and the values of χ^2 fitting between experimental and theoretical data for the $^{32}_{16}S + ^{208}_{82}Pb$ reaction were shown in Table (2).

By observing the results in Table (2), we find that the better suitable value diffuseness parameter which have obtained from SC analysis (where the projectile $^{32}_{16}S$ and target $^{208}_{82}Pb$ nuclei are inert) is 0. 65 fm with χ^2=0. 178, this result considered very near for standard value a = 0. 63 fm, and represented by the hard line in Fig.(1) (a), while the dashed line represents the single-channel accounts with the diffuseness parameter is 0.55 fm was drawn for the comparison.

The better suitable value of the diffuseness parameter which have obtained from CC analysis (where we assumed that the projectile $^{32}_{16}S$ as inert with vibrational coupling for target $^{208}_{82}Pb$ nucleus) is 0.63 fm with χ^2=0.120, this result considered fully compatible with the standard value 0.63 fm, this is illustrated clearly through preview the hard line in Fig.(1) (b), The dot-dashed line in Fig. (1) (b) represents the result which obtained from CC analysis (where we assumed that the target as inert with vibrational coupling for projectile nucleus) with diffuseness parameter is 0.62 fm and χ^2=0.126, the dashed line in Fig.(1) (b)

Table (2): parameters of WS potential a, r_0 and v_0 and values of χ^2 fitting between experimental and theoretical data for different types reactions when the excited nuclei at vibrational excitation state with single-quadruple phonon.

Type of reaction	a (fm)	r0 (fm)	V0 (MeV)	χ2
SC (Inert + Inert)	0. 65	1. 2	62. 5	0. 178
CC (Inert + Vib.)	0. 63	1. 2	62. 5	0. 120
CC (Vib. + Inert)	0. 62	1. 2	62. 5	0. 126
CC (Vib. + Vib.)	0. 61	1. 2	62. 5	0. 112

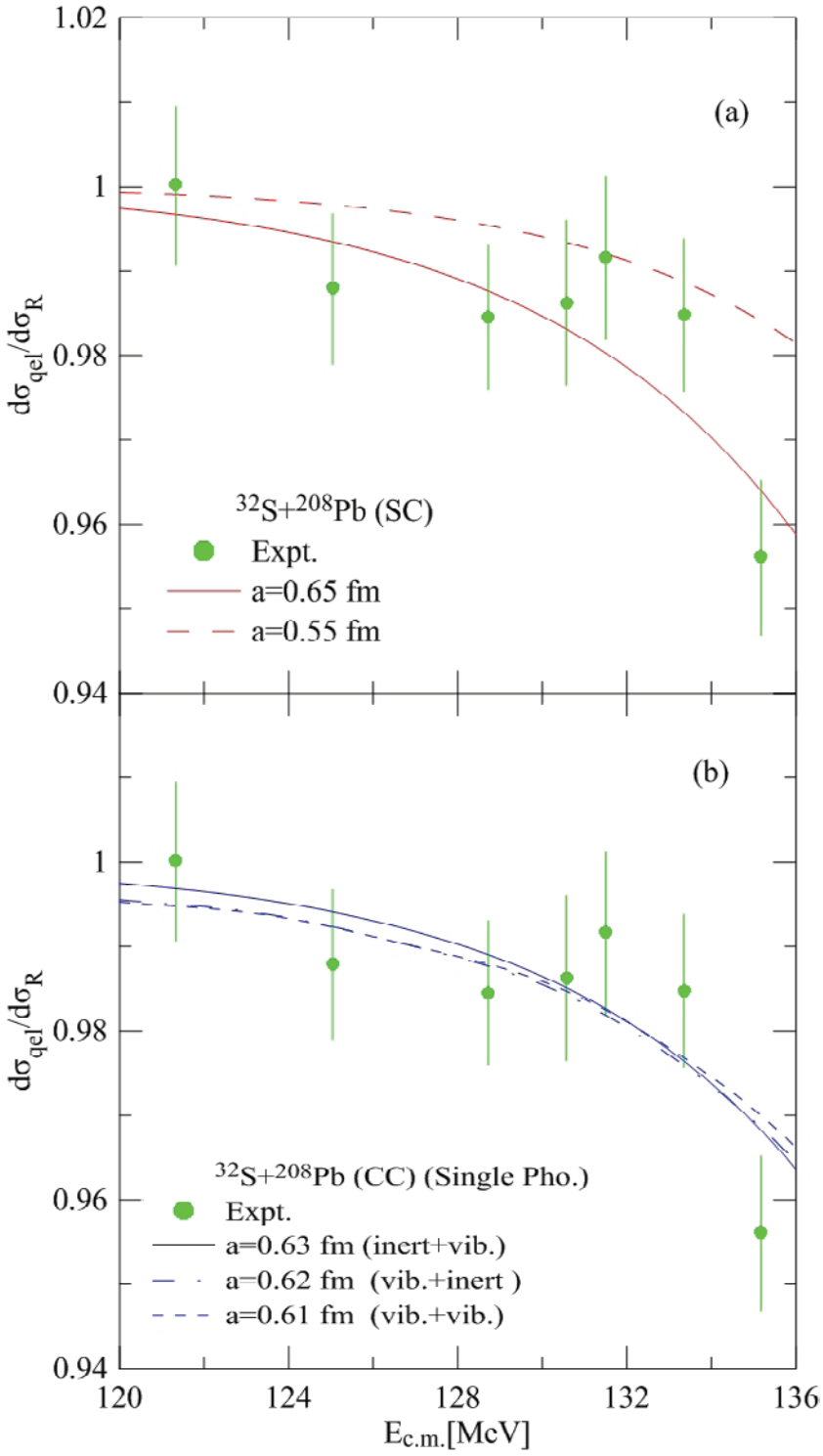

Fig.(1): Comparison of single-channel and different types of coupled-channels accounts with experimental data [15] (Referred to as points with error bars) for the system. In the upper panel (a) the hard and dashed lines represent the results of SC analysis at a = 0. 65 fm (represents the better suitable value of diffuseness parameter) and a = 0. 55 fm respectively, while the hard, dashed and dot-dashed lines in the lower panel (b) represent the results of CC analysis at a=0. 63 fm, a=0. 61 fm and a=0. 62 fm respectively

represents the result which got from CC analysis with collective vibrational excitations of the colliding nuclei (where the projectile $^{32}_{16}S$ and target nuclei are vibrational coupling to the state 2^+) with diffuseness parameter is 0. 61 fm and χ^2=0.112. The hard lines in Fig.(2) shows, the $d\sigma_{qel}/d\sigma_R$ at The best fitted diffuseness parameter is 0.63 fm, with χ^2=0.120 using a coupled-channel calculation at deep sub-barrier energies. In this reaction, we assumed that projectile $^{32}_{16}S$ is inert whilst the target $^{208}_{82}Pb$ is vibrational coupling to the state 2^+.

The dashed line in Fig.(2) shows the better suitable value of the diffuseness parameter for the $^{32}_{16}S+^{208}_{82}Pb$ reaction got from SC account is 0. 65 fm, with χ^2=0.178, we assumed that the projectile and target as inert nuclei.

In the $^{34}_{16}S+^{208}_{82}Pb$ system, the diffuseness parameter have been discussed in four states, in the first state we considered the projectile $^{34}_{16}S$ as well as target $^{208}_{82}Pb$ as inert nuclei, while in the second state we considered target nucleus $^{208}_{82}Pb$ is vibrational coupling with deformation parameter β_0=0. 0553 to the state 2^+(4.0854 MeV), while the projectile nucleus $^{34}_{16}S$ is inert, as to for the third state we assumed that the projectile nucleus $^{34}_{16}S$ is vibrational coupling to the state 2^+ with deformation parameter β_0= 0.252 (2.1276 MeV), while the target $^{208}_{82}Pb$ is inert, in the last way we assumed that projectile $^{34}_{16}S$ as well as target $^{208}_{82}Pb$ nuclei are vibrational coupling to the state 2^+. We used single-quadruple phonon excitation for the projectile and target nuclei which were vibrational excited. The values of the diffuseness parameters have been obtained from SC and CC analysis, as well as others parameters of WS potential (radius r_0 and depth potential v_0) and the values of χ^2 fitting between experimental and theoretical data for the $^{34}_{16}S+^{208}_{82}Pb$ reaction were shown in Table (3).

By observing the results in Table (3), we find

Table (3): parameters of WS potential a, r_0 and v_0 and values of χ^2 fitting between experimental and theoretical data for different types reactions when the excited nuclei at vibrational excitation state with single-quadruple phonon.

Type of reaction	a fm	r_0 fm	V_0 MeV	χ^2
SC (Inert + Inert)	0. 64	1. 2	94	0. 557
CC (Inert + Vib.)	0. 63	1. 2	94	0. 499
CC (Vib. + Inert)	0. 62	1. 2	94	0. 523
CC (Vib. + Vib.)	0. 62	1. 2	94	0. 560

that the better suitable value of the diffuseness parameter which have obtained from SC analysis (where the projectile $^{32}_{16}S$ and target $^{208}_{82}Pb$ nuclei are inert) is 0. 64 fm with χ^2=0. 557, this result considered very near to the accepted value of a = 0. 63 fm, and represented by the hard line in Fig.(3) (a), the dashed and dotted lines in Fig. (3) (a) represented the SC analysis with values of diffuseness parameter are 0. 66 fm and 0. 6 fm respectively, which were drown for the comparison.

The better suitable value of the diffuseness parameter which have obtained from CC analysis (where we assumed that the projectile $^{34}_{16}S$ as inert

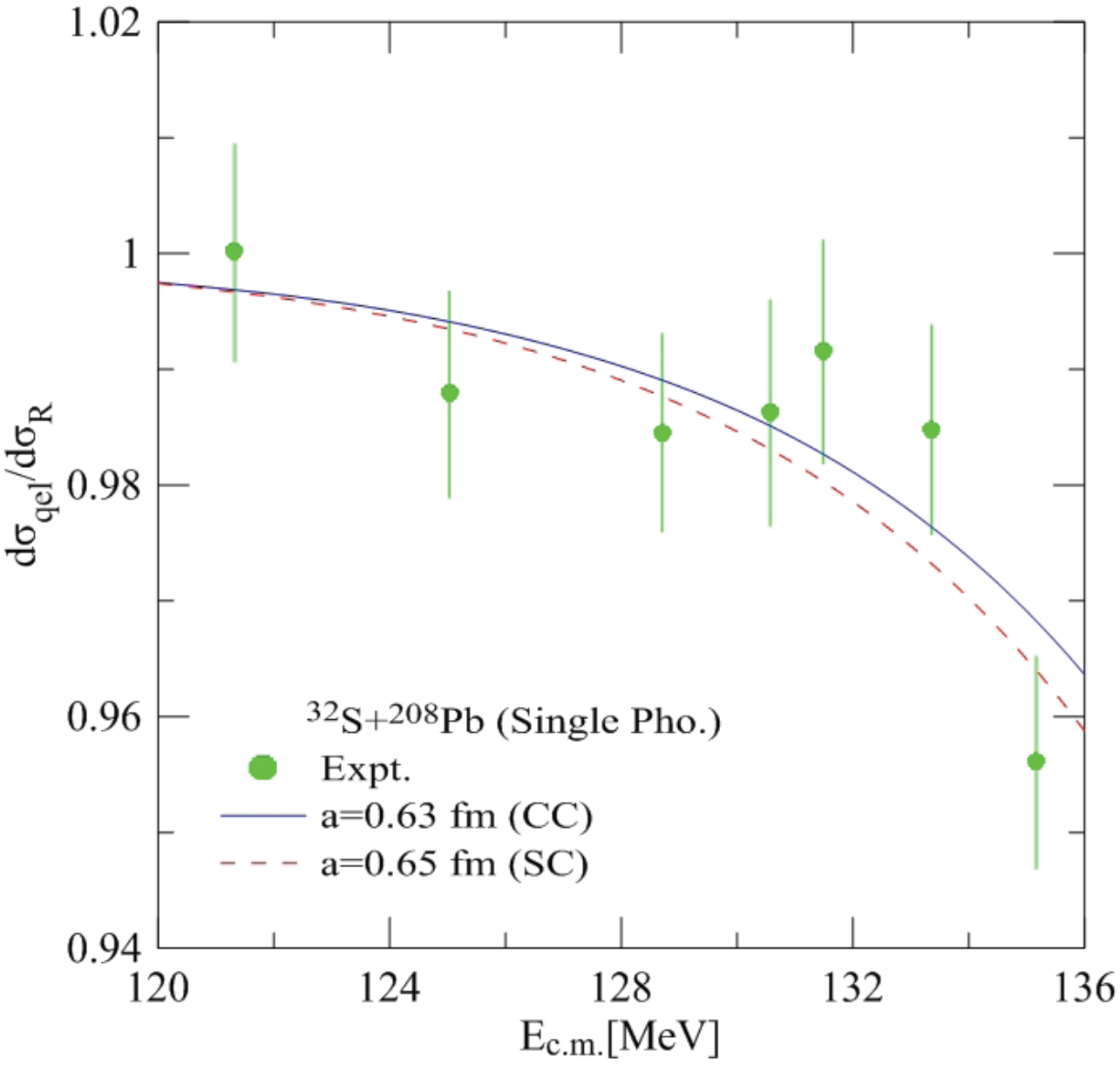

Fig.(2): Comparison of single and coupled-channels accounts for the better suitable value of the diffuseness parameter with experimental data [15] (Referred to as points with error bars) for the system. The hard line represents the results got from a coupled-channel analysis at a = 0. 63 fm, while the dashed line represents the single-channel analysis at a = 0. 65 fm.

with vibrational coupling for target $^{208}_{82}Pb$ nucleus) is 0. 63 fm with χ^2=0. 499, this result considered fully compatible with the standard value 0. 63 fm, this is illustrated clearly through preview the hard line in Fig.(3) (b), The dashed line in Fig. (3) (b) represents the result which obtained from CC analysis (where we assumed that the target as inert with vibrational coupling for projectile nucleus with diffuseness parameter a= 0. 62 fm and χ^2=0.523, the dashed line in Fig.(3) (a) represents the result which got from CC analysis with collective vibrational excitations of the

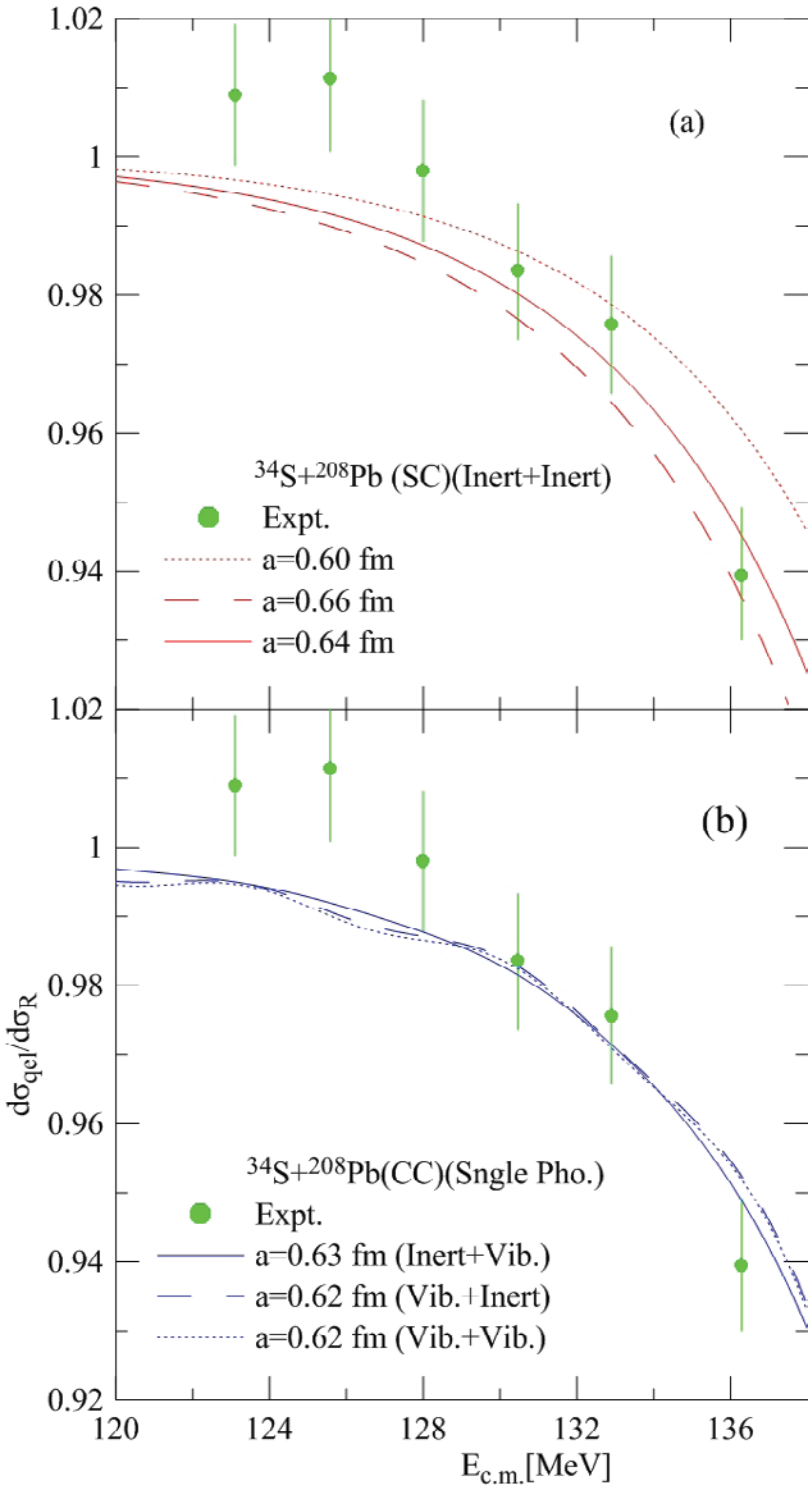

Fig.(3): Comparison of single-channel and different types of coupled-channels accounts with experimental data [15] (Referred to as points with error bars) for the system. The hard, dashed and dotted lines in the upper panel (a) represent the results of SC analysis at a=0. 64fm, a=0. 66 fm and a=0. 6 fm respectively while the hard, dashed and dotted lines in the lower panel (b) represent the results of CC analysis at a=0. 63 fm, a=0. 62 fm and a=0. 62 fm respectively.

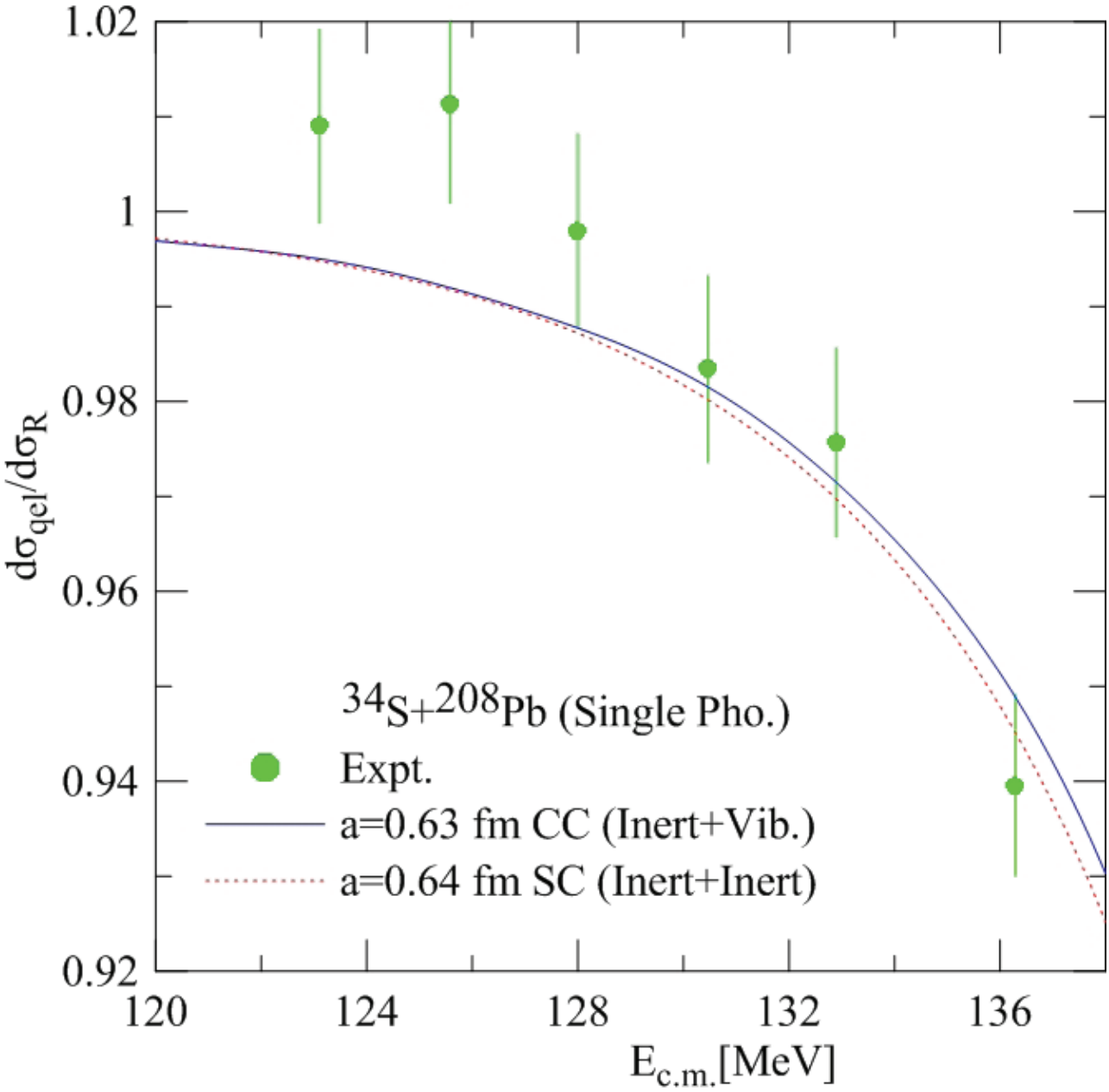

Fig.(4): Comparison of single and coupled-channels accounts for the better suitable value of the diffuseness parameter with experimental data [15] (Referred to as points with error bars) for the system. The hard line represents the results got from a coupled-channel analysis at a = 0. 63 fm, while the dotted line represents the single-channel analysis at a = 0. 64 fm.

colliding nuclei (where the projectile $^{32}_{16}S$ and target $^{208}_{82}Pb$ nuclei are vibrational coupling together to the state 2^+) with diffuseness parameter is 0.62 fm and χ^2=0.560.

We can comparison between the better suitable value of the diffuseness parameter which have obtained from SC and CC analysis in Fig.(3) (c), such that the hard line in Fig.(3) (c) represents the CC analysis (with inert Projectile and vibrational target) at diffuseness parameter

is 0.63 fm with χ^2 =0.499 was drawn for the comparison with dotted line which is represented the SC analysis at diffuseness parameter is 0. 64 fm with χ^2 =0.557.

Fig.(4) (a) shows property of the nuclear potential V_N at the surface region as a function of the distance r between the center of mass of the projectile and the target for the ${}^{32}_{16}S + {}^{208}_{82}Pb$ system, where the largest diffuseness parameter a=0. 65 fm (represents by the dashed line) which is resulted from SC analyses makes the nuclear potential to become more spread out comparison with the accepted value (represents by the hard line), while the Fig.(4) (b) clears characteristic of the nuclear potential V_N at the surface region as a function of the distance r between the projectile and the target for the ${}^{34}_{16}S + {}^{208}_{82}Pb$ system, where the largest diffuseness parameter is 0.64 fm (represents by the dashed line) compared to diffuseness parameter 0.63 fm (represents by the hard line) which were obtained from single-channel and coupled channel analyses respectively, makes too the nuclear potential to become more spread out [31].

The property of the nuclear potential V_N at the surface region as a function of the distance between the center of mass of the projectile and the target are shown in Fig.(5), where in the upper panel (a) the best fitted value of the diffuseness parameter which have obtained from CC analysis a=0. 63 fm (represents by the solid line), the dashed line represents the better suitable value of the diffuseness parameter which have obtained from SC analysis at a=0. 65 fm for the system ${}^{32}_{16}S + {}^{208}_{82}Pb$, while the sold line in the lower panel (b) represents the better suitable value of the diffuseness parameter which have obtained from CC analysis at a=0.63 fm, the dashed line represents the better suitable value of the diffuseness parameter which have obtained from SC analysis a=0. 64 fm for the system ${}^{32}_{16}S + {}^{208}_{82}Pb$.

5. Conclusions

Through micro methodology analyzes of the results, we found that the method of large-angle quasi-elastic scattering at deep sub-barrier energies close to the Coulomb barrier height is ideal tool for studying the surface property of Inter- nucleus potential for the spherical systems referred to in this research. Single-channel analyzes fits to experimental data gives diffuseness parameters 0. 65 fm and 0. 64 fm for the systems ${}^{32}_{16}S + {}^{208}_{82}Pb$ and ${}^{34}_{16}S + {}^{208}_{82}Pb$ respectively, does not differ much from the best fitted value of the diffuseness parameter which have obtained from CC analysis (with inert projectile and vibrational target) a= 0.63 fm which are in complete agreement with the standard value a= 0.63 fm. All coupling channels accounts gave values close to the standard value of the diffuseness parameter.

6. Acknowledgments

We thank Dr. Muhammad Zamrun and Dr. Mohd Lukman (Department of Physics, University of Malaya) for providing us with the (CQEL) code.

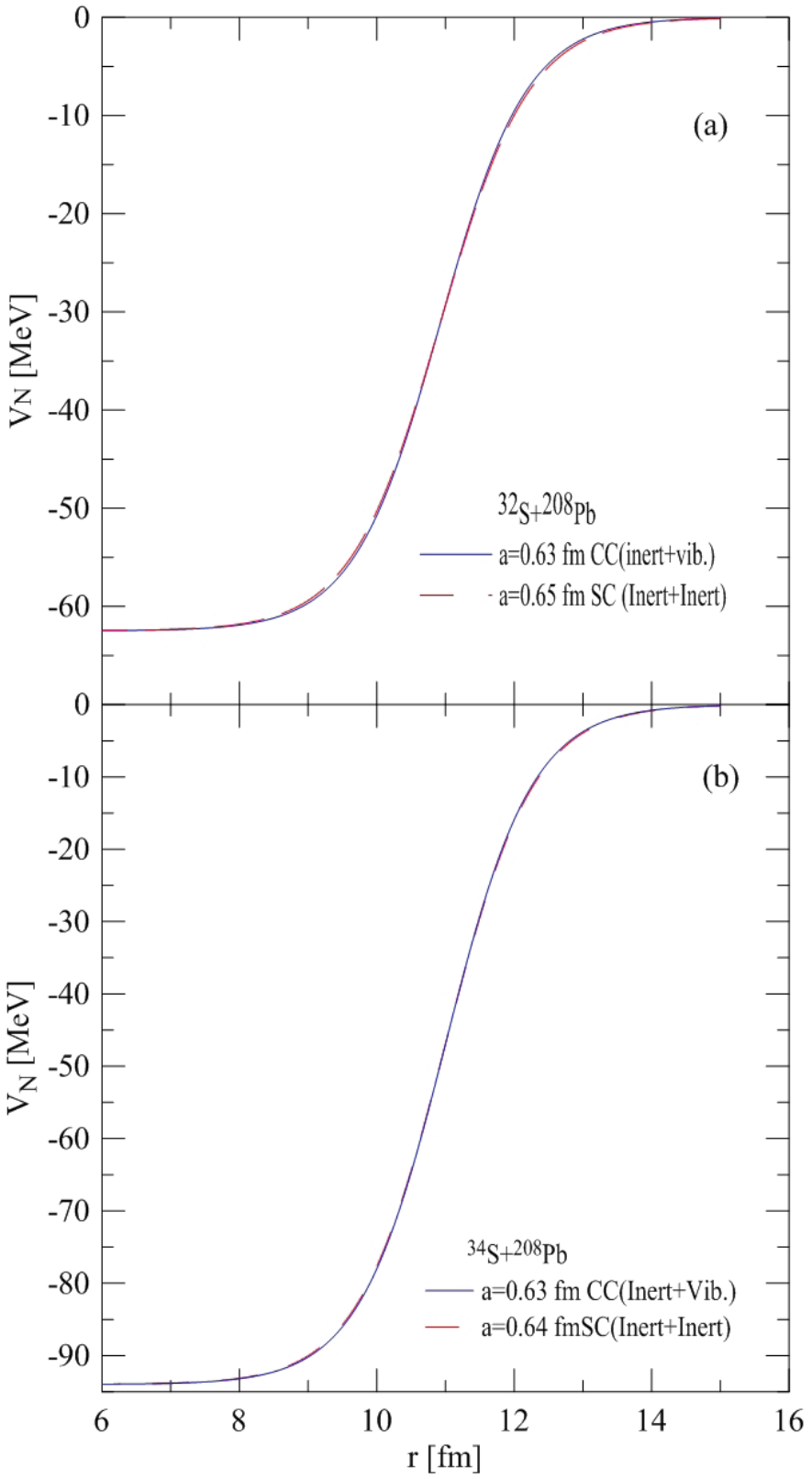

Fig.(5): Show the property of the nuclear potential V_N (MeV) at the surface region as a function of the distance r (fm) between the center of mass of the projectile and the target. The upper panel (a) for system and the lower panel (b) for thesystem.

References

[1] V.Y. Denisov, arXiv preprint nucl-th/0310019 (2003).

[2] R. Bass, Nuclear Reactions with Heavy Ions, Springer-Verlag, Berlin (1980).

[3] K. Hagino, and Y. Watanabe, arXiv preprint arXiv: 0706.2526 (2007).

[4] K. Jassim et al., IJSR, **3**(9): 1514-1518 (2014).

[5] V.Y. Denisov, and V. Nesterov (2006).

[6] G.R. Satchler, Direct nuclear reactions, "Clarendon Press" (1983).

[7] K. Hagino, arXiv preprint nucl-th/0611015 (2006).

[8] C.Y. Wong, Phys. Rev. Lett., **31** (12), 766 (1973).

[9] T. Rumin, K. Hagino, and N. Takigawa, Phys. Rev. C. **63** (4), 044603 (2001).

[10] M.I. Ibrahim, M. Zamrun, and H.A. Kassim, Phys. Rev C. **87** (2), 024611(2013).

[11] C. Berkdemir,A. Berkdemir, and R. Sever, Phys. Rev C. **72** (2), 027001 (2005).

[12] L. Gasques et al., Phys. Rev C**. 76** (2), 024612 (2007).

[13] K. Hagino et al., Phys. Rev C**. 71** (4), 044612 (2005).

[14] M. Pahlavani, J. Sadeghi, and M. Ghezelbash, Applied sciences, **11**, 106-113 (2009).

[15] K. Washiyama, K. Hagino, and M. Dasgupta, Phys. Rev C. **73** (3), 034607 (2006).

[16] M. Zamrun et al., Phys. Rev. C. **77** (3), 034604 (2008).

[17] G. Kaur et al. in Proceedings of the DAE Symp. onNucl. Phys (2014).

[18] K. Hagino, in Nuclear Physics Trends (2006).

[19] K. Hagino, and K. Washiyama, Probing internucleus potential with large-angle quasi-elastic scattering.arXiv preprint nucl-th/0605017, (2006).

[20] K. Hagino, and N. Rowley, Phys. Rev C. **69** (5), 054610 (2004).

[21] K. Hagino, N. Rowley, and A. Kruppa, Computer Physics Communications, **123** (1), 143-152 (1999).

[22] M. Beckerman, Physics Reports**, 129** (3), 145-223 (1985).

[23] D. Monteiro et al., Phys. Rev C. **76** (2), 027601 (2007).

[24] C. Lin et al., Phys. Rev. C. **79** (6), 064603 (2009).

[25] M. Dasgupta et al., Annual Review of Nuclear and Particle Science, **48** (1), 401-461 (1998).

[26] M. Dasgupta et al., Progress of Theoretical Physics Supplement **154**, 209-216 (2004).

[27] M. Singh, S.S. Duhan, and R. Kharab.in Proceedings of the DAE Symp. onNucl. Phys (2011).

[28] L. Canto et al., Physics reports, **424** (1), 1-111 (2006).

[29] A. Stefanini et al., Phys. Rev. C. **73** (3), 034606 (2006).

[30] K. Hagino et al., arXiv preprint nucl-th/0110065 (2001).

[31] M.L.B.I.I brahim, Ph.Dthesies, Department of Physics, University of Malaya Kuala Lumpur (2012).

[32] P. Fröbrich, and R. Lipperheide, Theory of Nuclear Reactions, Clarendon Press (1996).

[33] R. Naik, Studying Fusion Reactions for Effect of P (CN) on Heavy Nucleus Formation and for Nuclear Structure Effects. ProQuest, Oregon State University (2007).

[34] K. Washiyama, K. Hagino, and M. Dasgupta, Phys. Rev. C.**73** (3) (2006).

[35] S. Yusa, K. Hagino, and N. Rowley, Phy. Rev. C. **85** (5), 054601 (2012).

نمووحاصل الذرة الصفراء .Zea mays L. مجلة جامعة كربلاء.9 (علمي): 184 - 190.

[8] Rzodkiewiez, P. and W. Schapaugh. 2006. Evaluation of Soybean Varieties for Iron-deficiency Chlorosis. Keeping up with Research 140. K. State University.

[9] Page, A. I., R. H. Miller and D. R. Keeney. 1982. Methods of Soils analysis Part 2. Chemical and microbiological properties.Amer. Soc. Agron. Midison. Wisonsin. USA.

[10] Papanicoluon, E.P. 1976. Determination of cation exchange capacity of calcareous soils and their percent base saturation, Soil Sci. 121: 65 - 71.

[11] Black, C.A. 1965. Methods of Soil analysis, Amer. Soc. of Agron. Inc. USA.

[12] Richards, L.A. 1954. Diagnosis and improvement of Saline and Alkaline Soils. USDA. Hand book 60. USDA, Washington DC.

[13] Jackson, M.L., 1973. Soil Chemical Analysis. 2nd Edn., CRC Press, Baton Rogue, FL.

[14] Tandon, H.L.S. 1995. Methods of Analysis of soils, plants, fertilizers. India. New Delhi.

[15] Sujatha, S. 2005. Effect of Sources, level and methods of boron application on production, yield attributes and yield of maize (Zea Mea L.) Madras Agric., J. 92 (7-9): 479 - 483.

[16] Shamsi, K. and S. Kobraee. 2009. Effect of plant density on the growth, yield and yield components of three soybean varieties under climatic condition of Kermanshah, Iran. J. of Animal and plant Sci.2 (2): 96 - 99

[17] Barney, G. 2007. Manganese nutrition of Glyphosate -Resistant and conventional soybeans better crops. Vol.9-1No (4).

[18] Taiz, L. and E. Zeiger. 2010. Plant Physiology. 5th (ed.), Sianauer Associates, Sunderland, UK: p 629 g.

[19] Hu, H. and P.H. Brown. 1997. Absorption of boron by plant roots. Plant Soil. 193: 49 - 58.

[20] Tisdale, S.L., J.L. Havlin, W.L. Nelson W.L. and J.D. Beaton. 2005. Soil Fertility and Fertilizers. 5th Editions. USA.

[21] ديفلين، روبرت وفرانسيس ويذام. 1998. فسيولوجيا النبات. ترجمة محمد محمود شراقي، عبد الهادي خضر،علي سعد الدين سلامة ونادية امل. كلية الزراعة. جامعة الزقازيق. مصر.

[22] إدريس، محمد حامد. 2009. فسيولوجيا النبات. موسوعة النبات. مركز سوزان مبارك الاستكشافي العلمي في القاهرة - مصر.

مقاومة ظروف التربة لا سيما في حالة عدم توافر العناصر الغذائية أوانخفاض جاهزيتها بسبب ارتفاع تركيز الكلس فيها جدول (1) ذوالتاثير السلبي في مقدار جاهزية العناصر الصغرى لا سيما عنصري المنغنيز والبورون [6]،مما أدى إلى إعطاء نموأفضل انعكس في هذه الصفات عن طريق زيادة في البناء المعماري للجذور وثم زيادة انتقال المواد الغذائية المصنعة من المصدر إلى المصب والذي انعكس ايجابا على الحاصل ومكوناته [15, 16]. ويرجع تفوق معاملات الرش بالمنغنيز والبورون على عدم الرش في جميع الصفات المدروسة إلى أهمية هذين العنصريين كعناصر أساسية تدخل في تركيب الإنزيمات ومنشطة لإنزيمات أخرى،فضلا عن مساهمتهما في زيادة بناء الكلوروفيل والبروتين واختزال النترات والاشتراك في عملية نقل السكريات وغيرها والتي انعكست ايجابيا في زيادة النمووالحاصل لجميع الأصناف قيد الدراسة [17 ,18 ,19 ,20].كما ويرجع السبب في تفوق المستوى 50 + 50 ملغم. لتر$^{-1}$ إلى زيادة جاهزية المنغنيز والبورون نتيجة لإضافتهما بهذا المستوى فادى ذلك إلى زيادة نشاط الفعاليات الحيوية داخل النبات ومنها التمثيل الضوئي ومن ثم انتقال نواتجه إلى الحبوب، لأن هذه الحبوب بعد فترة من نشوئها تصبح هي المصب الدائم في النباتات وان الجزء الأكبر من نواتج التمثيل سواء كانت حديثة التكوين أومخزونة فإنها تؤدي إلى زيادة وزن الحبوب أثناء مرحلة امتلائها والذي انعكس ايجابا فيما بعد على الحاصل الاقتصادي [21, 22].

ان الدراسة الحالية تبين اهمية التغذية الورقية بالمغذيات الصغرى (المنغنيز والبورون) سيما تحت ظروف الترب الكلسية والتي يقل فيها جاهزية جميع العناصر الصغرى عدا المولبدنم، وتوضح تفوق الصنف بحوث 106 في اغلب الصفات مقارنة بالأصناف الاخرى قيد الدراسة كما توصي بضرورة استعمال التوليفة (50+50 ملغم. لتر$^{-1}$) من المنغنيز والبورون خلطا مع بعضهما بغية الحصول على افضل النتائج في النمووالحاصل الاقتصادي لمحصول الذرة الصفراء.

المصادر

[1] السعيدي، عثمان حسين ومحسن عويد فرحان وفيصل غازي احمد. 1993. دراسة قياسية للعوامل المؤثرة على عرض الذرة الصفراء في العراق (للفترة 73 1989) مجلة زراعة الرافدين 25 (2): 5 - 10.

[2] سعد لله، حسين احمد وياكار محمد الجباري وعدنان خلف محمد ومنير الدين فائق عباس ونويل زيا هيد و1998. استجابة تراكيب وراثية من لذرة الصفراء الى مستويات التسميد والكثافة النباتية. مجلة الزراعة العراقية، 3 (2): 4 - 150.

[3] Mengel, K.M., and E.A. Kirkby. 1987. Principles of Plant Nutrition. 3rd. ed. Int. potash. Inst. Bern، Switzerland.

[4] الجميلي، إسماعيل احمد سرحان. 2009. تأثير الكثافات النباتية ومواعيد إضافة السماد البوتاسي في نمووحاصل صنفين من فول الصويا Glycine max (L.) Merrill. رسالة ماجستير. قسم المحاصيل الحقلية.كلية الزراعة. جامعة الانبار.

[5] الدليمي، بشير حمد عبد الله ورسمي محمد الدليمي وعماد محمود البدراني. 2007. استجابة صنفين من فول الصويا Glycine max (L.) Merrill للتغذية الورقية بالبورون والتسميد النتروجيني. مجلة الانبار للعلوم الزراعية. 5 (2): 44 - 65.

[6] ابوضاحي، يوسف محمد ومؤيد احمد اليونس. 1988. دليل تغذية النبات. وزارة التعليم العالي والبحث العلمي -جامعة بغداد- كلية الزراعة.

[7] الموسوي، احمد نجم ويوسف ابوضاحي 2012. تاثير تجزئة السماد البوتاسي وتجزئة اضافته للتربة والرش في

جدول (9) تأثير التغذية الورقية بالمنغنيز والبورون في حاصل الحبوب (طن.هـ$^{-1}$) لثلاث اصناف تركيبية من الذرة الصفراء.

الأصناف	مستويات (المنغنيز + البورون) ملغم. لتر$^{-1}$			المتوسط
	0	25+25	50 +50	
المها	6.105	7.155	7.621	6.960
بحوث 106	6.589	7.977	8.352	7.639
5012	6.243	7.337	7.942	7.174
المتوسط	6.312	7.489	7.971	7.257
أ. ف.م. 0.05 %	الأصناف = 0.26 32		المغذيات = 0.2632	التداخل = 0.4533

طن.هـ$^{-1}$ وبذلك اختلف معنويا عن الصنف 5012 بينما اختلف الصنفان معنويا عن الصنف المها الذي أعطى اقل متوسط للوزن الجاف بلغ 6.641 طن.هـ$^{-1}$. بينت نتائج الجدول أيضا وجود اختلافات معنوية بين مستويات المنغنيز والبورون في متوسط هذه الصفة. إذ أعطت النباتات المرشوشة بالمستوى 50 + 50 ملغم. لتر$^{-1}$ أعلى متوسط لهذه الصفة بلغت 8.395 طن.هـ$^{-1}$ وبذلك تفوق معنويا على النباتات غير المرشوشة (معاملة المقارنة) وكذلك النباتات التي رشت بالمستوى 25 + 25 ملغم. لتر$^{-1}$ والتي أعطت 6.063 و7.184 طن.هـ$^{-1}$ لكل منهما على التوالي. حصل تداخل معنوي بين الأصناف ومعدل رش المنغنيز والبورون في صفة وزن المادة الجافة. ويتضح من الجدول إن وزن المادة الجافة قد ازداد معنويا في جميع الأصناف عند رشها بتركيزي المغذيات الصغرى مقارنة مع المعاملة بدون رش، ولكن الزيادة كانت أكثر وضوحا عند الرش بالتركيز 50 + 50 ملغم. لتر$^{-1}$. وقد تميز الصنف بحوث 106 المرشوش بهذه المعاملة بمعدل عال لوزن المادة الجافة بلغ 8.775 طن. هكتار$^{-1}$ بالمقارنة مع الرش بالمغذيين للصنف المها والتي سجلت 5.375 طن. هكتار$^{-1}$.

11. المناقشة

تباينت التراكيب الورثية قيد الدراسة فيما بينها في جميع الصفات ويلاحظ تفوق الصنف بحوث 106 على الصنفين المها و5012 في جميع الصفات وقد يعود السبب في ذلك إلى القابلية الوراثية العالية للصنف بحوث 106 في استغلال الظروف البيئية المحيطة به واستخدامها في عملية التمثيل الضوئي وكذلك كفاءة هذا الصنف في

جدول (10) تأثير التغذية الورقية بالمنغنيز والبورون في وزن المادة الجافة(طن.هـ$^{-1}$) لثلاث اصناف تركيبية من الذرة الصفراء.

الأصناف	مستويات (المنغنيز + البورون) ملغم. لتر$^{-1}$			المتوسط
	0	25+25	50 +50	
المها	5.375	6.563	7.986	6.641
بحوث 106	6.842	7.667	8.775	7.761
5012	5.972	7.323	8.426	7.240
المتوسط	6.063	7.184	8.395	7.214
أ. ف.م. 0.05 %	الأصناف = 0.5151		المغذيات = 1.1343	التداخل = 2.2433

لقد أثرت التغذية الورقية بالمنغنيزوالبورون معنويا في وزن 500 حبة. إذ أوضح الجدول نفسه أيضا إن إضافة هذه المغذيات مخلوطة مع بعضها بالمستويين 25+25 ملغم. لتر$^{-1}$ و50+50 ملغم. لتر$^{-1}$ رشا على الأوراق قد تفوقا بأعلى متوسط فأعطيا 84.00 و88.66 غم على التوالي والذي يلاحظ فيه تفوق المستوى الاخير معنويا في هذه الصفة. ولكنهما اختلفا بشكل معنوي عن معاملة المقارنة (بدون رش) التي أعطت اقل متوسط لهذه الصفة بلغ 78.33 غم. أما التداخل فيلاحظ تفوق معاملة الرش 50+50 من المنغنيز والبورون خلطا لصنف بحوث 106 في اعطاء اعلى قيمة لهذه الصفة بلغت 91.33 غم مقارنة مع معاملة عدم الرش مع الصنف المها والذي سجل 77.33 غم.

جدول (8) تأثير التغذية الورقية بالمنغنيز والبورون في وزن 500 حبة لثلاث اصناف تركيبية من الذرة الصفراء.

الأصناف	مستويات (المنغنيز+البورون) ملغم. لتر$^{-1}$			المعدل
	0	25+25	50 +50	
المها	77.33	82.33	86.00	81.88
بحوث 106	79.67	85.67	91.33	85.55
5012	78.00	84.00	88.67	83.55
المتوسط	78.33	84.00	88.66	83.66
أ. ف.م. 0.05 %	الأصناف = 1.135		المغذيات = 1.135	التداخل = 2.763

9. حاصل الحبوب (طن.هكتار$^{-1}$)

تعد هذه الصفة أهم مقياس حقلي يعطي التقييم النهائي للعمليات الزراعية فقد أشارت نتائج جدول (9) إلى وجود تأثير معنوي للأصناف في حاصل الحبوب. إذ أعطى الصنف بحوث 106 أعلى متوسط لهذه الصفة مقداره 7.639 طن. هكتار$^{-1}$ متفوقا بذلك معنويا عن الصنف 5012 الذي اعطى 7.174 طن. هكتار$^{-1}$ بينما أعطى الصنف المها أقل متوسط لهذه الصفة 6.960 طن. هكتار$^{-1}$. أثرت التغذية الورقية بالمنغنيز والبورون معنويا في صفة حاصل الحبوب. إذ بينت النتائج أن إضافة المنغنيز والبورون رشا على الأوراق بالمستوى 50 + 50 ملغم. لتر$^{-1}$ مخلوطة مع بعضها أعطت أعلى متوسط 7.971 طن. هكتار$^{-1}$ تلتها معاملة إضافة هذه المغذيات بالمستوى 25 + 25 ملغم. لتر$^{-1}$ التي أعطت 7.489 طن.هكتار$^{-1}$، أما معاملة المقارنة (بدون رش) فقد أعطت اقل متوسط لهذه الصفة بلغ 6.312 طن.هكتار$^{-1}$. حصل تداخل معنوي بين الأصناف ومعدل رش المنغنيز والبورون في صفة حاصل الحبوب. ويتضح من الجدول نفسه إن حاصل الحبوب قد ازداد معنويا في جميع الأصناف عند رشها بتركيزي المغذيات الصغرى مقارنة مع المعاملة بدون رش، ولكن الزيادة كانت أكثر وضوحا عند الرش بالتركيز 50 + 50 ملغم. لتر$^{-1}$. وقد تميز الصنف بحوث 106 المرشوش بهذه المعاملة بمعدل عال لحاصل الحبوب 8.352 طن. هكتار$^{-1}$ مقرنة مع اقل معدل للتداخل بين تراكيز الرش والاصناف والذي سجل في معاملة عدم الرش مع الصنف المها والذي بلغ 6.105 طن. هكتار$^{-1}$.

10. وزن المادة الجافة (طن.هـ$^{-1}$)

يبين الجدول (10) إن الصنف بحوث 106 قد تفوق معنويا بإعطاء اعلى متوسط لوزن المادة الجافة بلغ 7.761

جدول (6) تأثير التغذية الورقية بالمنغنيز والبورون في عدد الصفوف.عرنوص$^{-1}$ لثلاث اصناف تركيبية من الذرة الصفراء.

الأصناف	مستويات (المنغنيز+البورون) ملغم. لتر$^{-1}$			المعدل
	0	25+25	50 +50	
المها	13.00	17.33	18.00	16.11
بحوث 106	14.67	18.67	20.00	17.78
5012	13.33	18.00	19.67	17.00
المتوسط	13.66	18.00	19.22	16.96
أ. ف.م. 0.05 %	الأصناف = 0.513		المغذيات = 1.113	التداخل = 2.463

للأصناف في عدد الحبوب.صف$^{-1}$. إذ أعطى الصنف بحوث 106 أعلى متوسط لهذه الصفة مقداره 43.39 حبة متفوقا بذلك معنويا عن الصنف 5012 الذي اعطى 43.07 حبة بينما أعطى الصنف المها أقل متوسط لهذه الصفة 42.65 حبة. أثرت التغذية الورقية بالمنغنيز والبورون معنويا في صفة عدد الحبوب.صف$^{-1}$. إذ بينت النتائج إلى أن إضافة المنغنيز والبورون رشا على الأوراق بالمستوى 50 + 50 ملغم. لتر$^{-1}$ مخلوطة مع بعضها أعطت أعلى متوسط 43.94 حبة تلتها معاملة إضافة هذه المغذيات بالمستوى 25+25 ملغم. لتر$^{-1}$ التي أعطت 43.25 حبة، أما معاملة المقارنة (بدون رش) فقد أعطت اقل متوسط لهذه الصفة بلغ 41.91 حبة.

حصل تداخل معنوي بين الأصناف ومعدل رش المنغنيز والبورون في صفة حاصل الحبوب. ويتضح من الجدول إن هذه الصفة قد ازدادت معنويا في جميع الأصناف عند رشها

جدول (7) تأثير التغذية الورقية بالمنغنيز والبورون في عدد الحبوب.صف$^{-1}$ لثلاث اصناف تركيبية من الذرة الصفراء.

الأصناف	مستويات (المنغنيز +البورون) ملغم. لتر$^{-1}$			المتوسط
	0	25+25	50 +50	
المها	41.45	42.95	43.55	42.65
بحوث 106	42.35	43.49	44.35	43.39
5012	41.95	43.33	43.94	43.07
المتوسط	41.91	43.25	43.94	43.04
أ. ف.م. 0.05%	الأصناف 0.281		المغذيات = 0.632	التداخل = 0.953

بتركيزي المغذيات الصغرى مقارنة مع المعاملة بدون رش، ولكن الزيادة كانت أكثر وضوحا عند الرش بالتركيز 50 + 50 ملغم. لتر$^{-1}$. وقد تميز الصنف بحوث 106 المرشوش بهذه المعاملة بمعدل عال بلغ 44.35 حبة فيما كانت اقل قيمة مسجلة لمعاملة عد الرش بالمغذيات لصنف المها وبلغت 41.45 حبة.

8. وزن 500 حبة

توضح نتائج جدول (8) وجود اختلافات معنوية بين الأصناف في وزن 500 حبة إذ أعطى الصنف بحوث 106 أعلى متوسط لهذه الصفة 85.55 غم متفوقا بذلك معنويا عن الصنف 5012 الذي أعطى 83.55 غم وكذلك الصنف المها والذي اعطى اقل متوسط لهذه الصفة بلغ 81.88 غم.

5. طول العرنوص

أظهرت نتائج جدول (5) وجود فروق معنوية بين الأصناف في متوسط هذه الصفة، إذ أعطى الصنف بحوث 106 أعلى متوسط بلغ 25.20 سم ولم يختلف معنويا عن الصنف 5012 الذي أعطى 24.92 سم إلا أن كليهما اختلفا معنويا عن الصنف المها الذي أعطى اقل متوسط لهذه الصفة 24.67 سم. كما يلاحظ إن إضافة المنغنيز والبورون بالمستوى 50 ملغم. لتر$^{-1}$ لكل منهما مخلوطة مع بعض رشا على الأوراق قد أعطى أعلى متوسط بلغ 25.59 سم والذي لم يختلف معنويا عن معاملة إضافة هذه المغذيات بالمستوى 25 ملغم. لتر$^{-1}$ لكل منهما والتي أعطت 25.12 سم غير إن كليهما اختلفا معنويا عن معاملة المقارنة التي أعطت اقل معدل لهذه الصفة 24.08 سم. أما التداخل بين الأصناف والرش بالمنغنيز والبورون فقد تفوقت معاملات الرش بالمغذيين معنويا على جميع معاملات عدم الرش واعطت معاملة الرش بالمنغنيز والبورون (50+50) لصنف بحوث 106 اعلى طول للعرنوص بلغ. 0026 سم فيما كانت اقل قيمة مسجلة في معاملة عدم اضافة المغذيين لصنف المها وبلغت 23.85 سم.

جدول (5) تأثير التغذية الورقية بالمنغنيز والبورون في طول العرنوص لثلاث اصناف تركيبية من الذرة الصفراء.

الأصناف	مستويات (المنغنيز+البورون) ملغم. لتر$^{-1}$			المتوسط
	0	25+25	50 +50	
المها	23.85	24.94	25.22	24.67
بحوث 106	24.27	25.34	26.00	25.20
5012	24.12	25.09	25.57	24.92
المتوسط	24.08	25.12	25.59	24.93
أ. ف.م. 0.05 %	الأصناف = 0.387	المغذيات = 0.574	التداخل = 1.478	

6. عدد الصفوف.عرنوص$^{-1}$

توضح نتائج جدول (6) وجود اختلافات معنوية بين الأصناف في عدد الصفوف.عرنوص1- إذ أعطى الصنف بحوث 106 أعلى متوسط لهذه الصفة 17.78 متفوقا بذلك معنويا عن الصنف 5012 الذي أعطى 17.00 وكذلك الصنف المها والذي اعطى اقل متوسط لهذه الصفة بلغ 16.11.

أثرت التغذية الورقية بالمنغنيز والبورون معنويا في عدد الصفوف.عرنوص$^{-1}$ إذ أوضح الجدول نفسه أيضا إن إضافة هذه المغذيات مخلوطة مع بعضها بالمستويين 25 + 25 ملغم. لتر$^{-1}$ و50 + 50 ملغم. لتر$^{-1}$ رشا على الأوراق قد تفوقا بأعلى متوسط فأعطيا 18.00 و19.22 على التوالي والذي يلاحظ فيه تفوق المستوى الاخير معنويا في هذه الصفة. ولكنهما اختلفا بشكل معنوي عن معاملة المقارنة (بدون رش) التي أعطت اقل متوسط لهذه الصفة بلغ 13.66. أما التداخل فيلاحظ تفوق معاملة الرش 50 + 50 من المنغنيز والبورون خلطا لصنف بحوث 106 في تسجيل اعلى قيمة لهذه الصفة بلغت 20.00 فيما اعطت معاملة عدم الرش بالمغذيات لصنف المها اقل قيمة بلغت 13.00.

7. عدد الحبوب.صف$^{-1}$

اظهرت نتائج جدول (7) إلى وجود تأثير معنوي

3. 2. ارتفاع العرنوص

يبين الجدول (3) إن الصنف بحوث 106 قد تفوق معنويا بأعطاء اعلى متوسط لارتفاع العرنوص بلغت 73.0 سم ولم يختلف معنويا عن الصنف 5012 بينما اختلف الصنفان معنويا عن الصنف المها الذي أعطى اقل متوسط لارتفاع العرنوص بلغ 64.4 سم. بينت نتائج الجدول أيضا وجود اختلافات معنوية بين مستويات المنغنيز والبورون في متوسط هذه الصفة. إذ أعطت النباتات المرشوشة بالمستوى (50 + 50) ملغم. لتر$^{-1}$ أعلى متوسط لهذه الصفة بلغت 77.9 سم وبذلك تفوق معنويا على النباتات غير المرشوشة (معاملة المقارنة) وكذلك النباتات التي رشت بالمستوى (25 + 25) ملغم. لتر$^{-1}$ والتي أعطت 57.3 سم و71.6 سم لكل منهما على التوالي. أما التداخل فكان تأثيره معنويا في متوسط هذه الصفة وقد اعطى الصنف بحوث 106 وعند معاملة الرش (50 + 50) اعلى معدل بلغ 81.5 سم فيما كانت اقل قيمة مسجلة في معاملة عدم الرش وعند الصنف المها وبلغت 54.5 سم.

الأصناف	مستويات (المنغنيز+البورون) ملغم. لتر$^{-1}$			المتوسط
	0	25+25	50+50	
المها	54.5	64.3	74.6	64.4
بحوث 106	60.2	77.3	81.5	73.0
5012	57.2	73.3	77.6	69.3
المتوسط	57.3	71.6	77.9	68.9
أ. ف.م. 0.05%	الأصناف = 4.56		المغذيات = 5.43	التداخل =8.33

4. عدد الاوراق بالنبات

لم تظهر الأصناف اختلافات معنوية في عدد الاوراق بالنبات جدول (4). بينما اثر الرش بالمنغنيز والبورون تأثيراً معنويا في متوسط هذه الصفة. إذ أعطت معاملة إضافة هذه المغذيات بالمستوى 50 + 50 ملغم. لتر$^{-1}$ رشا على الأوراق اعلى معدل لعدد الاوراق بالنبات بلغ 12.95 ورقة والذي لم يرتق لمستوى المعنوية مع معاملة الإضافة بالمستوى 25 + 52 ملغم. لتر$^{-1}$ والتي أعطت معدلا اقل بلغ 12.31. أما معاملة المقارنة (بدون رش) فقد أعطت اقل معدل لهذه الصفة بلغ 11.36 ورقة. أما التداخل فلم يكن له تأثير معنوي في متوسط هذه الصفة.

جدول(4) تأثير التغذية الورقية بالمنغنيز والبورون في عدد الاوراق بالنبات لثلاثة اصناف تركيبية من الذرة الصفراء.

الأصناف	مستويات (الحديد + المنغنيز) ملغم. لتر$^{-1}$			المتوسط
	0	50+50	50 +50	
المها	11.20	12.20	12.57	11.99
بحوث 106	11.53	12.43	13.50	12.48
5012	11.37	12.30	12.80	12.15
المتوسط	11.36	12.31	12.95	12.21
أ. ف.م. 0.05%	الأصناف = غ. م		المغذيات = 0.639	التداخل = غ. م

هيئة سماد يوريا (N 46%) وبمقدار 320 كغم N. هكتار$^{-1}$. كما تمت إضافة السماد البوتاسي دفعة واحدة عند الزراعة على هيئة كبريتات البوتاسيوم (K2SO4 41.5% K) وبمقدار 160 كغم K. هكتار$^{-1}$. فيما اضيف السماد الفوسفاتي على هيئة سوبر فوسفات (P21%) بمقدار 120 كغم K. هكتار$^{-1}$ [7]. تم تهيئة ارض التجربة من حراثة وتنعيم وتسوية وتمريز ثم قسمت إلى وحدات تجريبية وبابعاد (4×4 م^2) للوحدة التجريبية الواحدة مع ترك فواصل بين القطاعات والمعاملات ضمن القطاع الواحد وبعرض م^2. أعطيت رية التعيير وبعدها زرعت البذور وبواقع ثلاث بذور في كل جورة وعلى مروز المسافة بينها 75 سم وبمسافة 25 سم بين جورة واخرى. وبعد الزراعة مباشرة تم ري التجربة رية خفيفة واستمرت عملية الري حسب حاجة النبات للماء، ثم خفت النباتات الى نبات واحد بعد اكتمال عملية البزوغ للإبقاء على كثافة نباتية 53333 نبات. هكتار$^{-1}$ (7). تم تحديد عشرة نباتات بصورة عشوائية عند الحصاد من المرزين الوسطيين لكل وحدة تجريبية عند النضج لدراسة الصفات التالية:

ارتفاع النبات، ارتفاع العرنوص، عدد الاوراق، وزن 500 حبة، طول العرنوص، عدد الحبوب/ بالصف، عدد الصفوف / العرنوص، الوزن الجاف وحاصل الحبوب.

3. النتائج والمناقشة

3. 1. ارتفاع النبات

أظهرت النتائج المعروضة في جدول (2) وجود فروق معنوية بين الأصناف في متوسط قيم هذه الصفة، إذ أعطى الصنف بحوث 106 أعلى متوسط بلغ 172.3 سم ولم يختلف معنويا عن الصنف 5012 الذي أعطى ارتفاع للنبات بلغ 168.9 سم إلا أن كليهما اختلفا معنويا عن الصنف المها الذي أعطى اقل متوسط لهذه الصفة 164.6 سم. كما يلاحظ إن إضافة المنغنيز والبورون بالمستوى 50 ملغم. لتر$^{-1}$ لكل منهما مخلوطة مع بعض رشا على الأوراق قد أعطى أعلى متوسط بلغ 176.6 سم، الذي لم يختلف معنويا عن معاملة إضافة هذه المغذيات بالمستوى 25 ملغم. لتر$^{-1}$ لكل منهما والتي أعطت 171.3 سم غير إن كليهما اختلفا معنويا عن معاملة المقارنة التي أعطت اقل معدل لهذه الصفة 156.3 سم. أما التداخل بين الأصناف والرش بالمنغنيز والبورون فقد تفوقت معاملات الرش بالمغذيين معنويا على جميع معاملات عدم الرش واعطت معاملة الرش بالمنغنيز والبورون (50 + 50) لصنف بحوث 106 اعلى ارتفاع للنبات بلغ 180.5 سم.

جدول (2) تأثير التغذية الورقية بالمنغنيز والبورون في ارتفاع ثلاث اصناف تركيبية من الذرة الصفراء.

الأصناف	مستويات (المنغنيز+البورون) ملغم. لتر$^{-1}$			المتوسط
	0	25+25	50 +50	
المها	152.5	167.9	172.6	164.3
بحوث 106	160.2	176.3	180.5	172.3
5012	156.2	173.9	176.7	168.9
المتوسط	156.3	171.3	176.6	
أ. ف.م. 0.05 %	الأصناف = 3.87		المغذيات = 5.57	التداخل = 8.78

جدول (3) تأثير التغذية الورقية بالمنغنيز والبورون في ارتفاع العرنوص لثلاث اصناف تركيبية من الذرة الصفراء..

تربة كلسية مصنفة ضمن مجموعة الترب العظمى Typic Torrifluvent ذات نسجه مزيجه غرينية والمبين صفاتها في جدول (1).استخدمت التجربة العاملية بتصميم القطاعات العشوائية الكاملة وبثلاثة مكررات. العامل الأول ويمثله الأصناف (المها وبحوث 106و5012). العامل الثاني ثلاثة مستويات من الرش بالمنغنيز والبورون كتغذية ورقية على شكل كبريتات المنغنيز ((MnSO4.4H2O 26% Mn وحامض البوريك (H3BO3) B17%، رشت اصناف التجربة بعد شهر من الإنبات وبتركيزين الأول هو25 ملغم. لتر$^{-1}$ والثاني 50 ملغم. لتر$^{-1}$ لكل من المنغنيز والبورون مخلوطة مع بعضها. أما معاملة المقارنة فقد رشت بالماء فقط. وتم رش كل مستوى حتى البلل التام لأوراق النبات في وقت الصباح الباكر باستخدام مرشة يدوية سعة 20 لتر. سمدت التجربة بالسماد النتروجيني بثلاث دفعات متساوية، الأولى عند الزراعة والثانية عند مرحلة الاستطالة أما الدفعة الثالثة أضيفت عند ظهور النورات الذكرية على

جدول (1) بعض الصفات الكيميائية والفيزيائية لتربة الدراسة قبل الزراعة.

الصفة		القيمة	وحدة القياس	المصدر
درجة التفاعل pH1:1		7.6	–	(9)
التوصيل الكهربائي Ec 1:1		2.9	ديسي سيمنز.م$^{-1}$	
المادة العضوية		9.2	غم.كغم$^{-1}$	(11)
الايونات الموجبة	Ca^{+2}	13.8	سنتيمول شحنة.كغم$^{-1}$	(9)
	Mg^{+2}	10.9	سنتيمول شحنة.كغم$^{-1}$	
	Na^{+}	8.2	سنتيمول شحنة.كغم$^{-1}$	
	K^{+}	0.19	سنتيمول شحنة.كغم$^{-1}$	(12)
الايونات السالبة	HCO_3^{-}	3.6	سنتيمول شحنة.كغم$^{-1}$	(11)
	SO_4^{-2}	12.9	سنتيمول شحنة.كغم$^{-1}$	(11)
	CO_3^{-}	Nil	–	(13)
	Cl^{-}	16.5	سنتيمول شحنة.كغم$^{-1}$	(14)
الكلس الكلي		247.2	غم.كغم$^{-1}$ تربة	(12)
النتروجين الجاهز		37.1	ملغم.كغم$^{-1}$	(9)
الفسفور الجاهز		14.8	ملغم.كغم$^{-1}$	
البوتاسيوم الجاهز		170.3	ملغم.كغم$^{-1}$	(14)
المنغنيز الجاهز		3.48	ملغم.كغم$^{-1}$	(9)
البورون الجاهز		1.12	ملغم.كغم$^{-1}$	(9)
مفصولات التربة	الرمل	101	غم.كغم^{1}	(11)
	الغرين	653	غم.كغم$^{-1}$	
	الطين	246	غم.كغم$^{-1}$	
صنف النسجة		مزيجة غرينية	–	

1. المقدمة

الذرة الصفراء (Zea mays L.) من المحاصيل المهمة اقتصاديا في العالم وتتبع العائلة النجيلية Poaceae وتعد من أهم المحاصيل التابعة لهذه العائاة بحيث تأتي بعد الحنطة والرز من حيث الأهمية الاقتصادية، وهي من المحاصيل ثلاثية الغرض بحيث تزرع لغرض الحصول على الحبوب والعلف والزيت، كما تعد أحد المحاصيل الاستراتيجية ذات الأهمية المتزايدة في الصناعات الغذائية لما توفره من أساسيات الأمن الغذائي البشري من جهة فضلاً عن كونها من المحاصيل الإستراتيجية التي توفر الأعلاف الخضراء لمشاريع الثروة الحيوانية من جهة اخرى [1]. وعلى الرغم من الأهمية الكبيرة لهذا المحصول إلا أن معدل إنتاجية وحددة المساحة في العراق لايزال منخفضاً مقارنة بالإنتاج العالمي، إن هذا التدني في معدل الإنتاج بوحدة المساحة يدعونا للبحث بجدية عن جميع الوسائل الممكنة لزيادة الحاصل من خلال استخدام الأساليب الحديثة في الزراعة للارتقاء بواقع الإنتاج، حيث تتحقق زيادة في نمو محصول الذرة الصفراء كأي محصول آخر عن طريق خدمة التربة والمحصول إذ أعطي اهتماما كبيرا بإنتاج البذور وتحسين نوعيتها، ويمكن تحقيق ذلك من خلال زراعة الأصناف الجيدة فضلا عن العديد من العمليات الزراعية والتي يأتي في مقدمتها التسميد [2].

تهتم الدراسات في مجال تقييم أصناف الذرة الصفراء من حيث إنتاجية البذور والنوعية وفق البيئات التي تزرع فيها الأصناف ومدى استجابتها لعوامل خدمة المحصول ومنها إضافة الأسمدة الكيمياوية بطرائق إضافة متنوعة، ومن الأمور المهمة في عملية الإنتاج هوأن تزرع الأصناف التي لها القدرة على تثبيت وخزن الطاقة الشمسية للاستفادة منها في عمليات الإنتاج، اذ تتباين هذه الأصناف في كثير من صفات النموالإنتاجية ونوعية الحاصل واستجابتها لإضافة المغذيات [3]. لاختبار مجموعة أصناف من المحصول لابد من زراعتها بمدى واسع من المتغيرات البيئية ومن ثم تأخذ الأصناف ذات التكيف العالي لهذه المتغيرات على حساب الأصناف الأخرى. ويمكن الحصول على حاصل جيد من البذور عندما يكون هناك توافق بين الصنف والظروف البيئية والعمليات الزراعية [4]، وان تفوق الصنف في حاصل البذور يدل على كفاءته العالية في استغلال هذه العوامل لخدمة عملية التمثيل الضوئي ومن ثم تحويل نواتجه إلى حاصل اقتصادي [5]. لم يكن الصنف هوالعامل الوحيد الذي يؤدي إلى زيادة إنتاجية المحصول بل هناك عوامل أخرى ومنها إضافة المغذيات الصغرى. اغلب الترب العراقية ذات تفاعل يميل للقاعدية والتي تؤثر في جاهزية بعض العناصر الغذائية الصغرى للنبات لاسيما عنصري المنغنيز والبورون [6]، فالنبات يحتاج إلى تجهيز دائم بهذه المغذيات وبالصورة الجاهزة لكي ينموويتطور ويكمل دورة حياته لان هذه العناصر لها دور مهم داخل النبات وتؤدي وظائف عديدة فيه من خلال مشاركتها في عملية الأكسدة والاختزال والتنفس وتكوين الكلوروفيل [8]، لذا فإن إضافة عنصري المنغنيزوالبورون رشا على الأوراق هوبهدف الحصول على أعلى إنتاجية وبأفضل نوعية من المحصول.

2. المواد وطرائق البحث

نفذت تجربة حقلية في الموسم الخريفي لعام 2013 في احد الحقول الزراعية التابعة إلى قضاء ابوغريب – بغداد في

(المها، بحوث 106 و5012). طبقت تجربة عاملية بتصميم القطاعات العشوائية الكاملة بثلاثة مكررات. اظهرت النتائج تفوق الصنف بحوث 106 في صفات ارتفاع النبات، ارتفاع العرنوص، طول العرنوص، عدد الصفوف.عرنوص$^{-1}$، عدد الحبوب.صف$^{-1}$ وزن 500 حبة، حاصل الحبوب وحاصل المادة الجافة فأعطى (172.3 سم، 73.0 سم، 25.20 سم، 17.78صف، 43.39 حبة، 85.55 غم، 7.639 طن.هـ$^{-1}$، 7.761 طن.هـ$^{-1}$) لكل منها على التوالي. أثرت التغذية الورقية بالمنغنيز والبورون مخلوطة مع بعضها رشا على الأوراق تأثيرا معنويا في جميع الصفات المدروسة وتفوقت المعاملة 50 + 50 ملغم. لتر$^{-1}$ في جميع الصفات قيد الدراسة في حين لم تؤثر معاملة 25 + 25 ملغم. لتر$^{-1}$ معنويا في صفات ارتفاع النبات وعدد الاوراق/ نبات وطول العرنوص. كما اثر التداخل بين الأصناف ومستويات رش المنغنيز والبورون تأثيرا معنويا في جميع الصفات اذ تفوقت معاملة الصنف بحوث 106 مع الرش بالمستوى 50 + 50 ملغم. لتر$^{-1}$ من المنغنيز والبورون مخلوطة مع بعضهما أعلى القيم لتلك الصفات. توصي الدراسة الحالية بضرورة استخدام التغذية الورقية لا سيما بعنصري المنغنيز والبورون لما لها من تأثير معنوي في نمووحاصل اصناف الذرة الصفراء وكذلك استخدام صنف اباء 106 تحت ظروف الترب الكلسية.

الكلمات المفتاحية

الذرة الصفراء، الرش بالمنغنيز، البورون، التربة الكلسية، النمووالحاصل.

استجابة ثلاثة تراكيب وراثية من الذرة الصفراء (Zea mays L.) للتغذية الورقية بالمنغنيز والبورون تحت ظروف التربة الكلسية في بعض صفات النمووالحاصل

* عباس علي العامري، * رزاق لفتة اعطية، ** احمد نجم الموسوي و* حميد عبد خشان الفرطوسي
* قسم المحاصيل الحقلية، كلية الزراعة، جامعة كربلاء، العراق
** قسم علوم الحياة، كلية التربية للعلوم الصرفة، جامعة كربلاء، العراق

تاريخ الإستلام: 10/May/2014
تاريخ قبول النشر: 16/Aug/2015

Abstract

A field experiment was applied in the field (Baghdad/Abu Ghraib) in the calcareous soil, in a silt loam soil during the autumn season of 2013. To study the effect of three combinations of spraying boron and manganese (0,25 + 25 and 50 + 50 mg. Liter^{-1}) in the growth and yield of three genotypes of maize are (AL-Maha, Bohoth 106 and 5012). the experiment was laid in Randomized Complete Block Design with three replications.

Results showed superiority Bohoth 106 in plant height, ear length, no. row. ear^{-1}, no. grains row^{-1}, weight of 500 grain, grain yield and yield of dry matter (172.3 cm, 73.0 cm, 25.20 cm, 17.78 row, 43.39 bead, 85.55 g, 7.639 tons.h^{-1}, 7.761 tons.h^{-1}) for each of them, respectively. foliar application of Manganese and Boron mixed was affected significant on all characters, treatment 50 + 50 mg. L^{-1} was significant in all characters under study but they did not significant up with 25 + 25 mg. Liter^{-1} in plant height and number of leaves. plant^{-1} and the length of ear. The effect of introduction between the categories and levels of manganese, boron spray significant effect in all the qualities treatment of Class Bohoth 106 with spray level 50 + 50 mg. Liter^{-1} of manganese, boron blended with the highest values for each of these characters.

Keywords

corn, foliar application, boron, manganese, growth and yield.

الخلاصة

اجريت تجربة حقلية في تربة كلسية مصنفة ضمن مجموعة الترب العظمى Typic Torrifluvent ذات نسجة مزيجة غرينية أثناء الموسم الخريفي لعام 2013 في محافظة بغداد منطقة ابوغريب. بهدف دراسة تأثير ثلاثة توليفات من الرش بالبورون والمنغنيز هي (25 + 25،0و50 + 50 ملغم. لتر$^{-1}$) في نمووحاصل ثلاثة تراكيب وراثية من الذرة الصفراء هي

ilton D. S., "Analysis of the K-40 levels in soil using gamma spectrometry", Journal of Brazilian archives of biology and technology, Vol. 48, PP. 221-228 (2005).

[17] Hamid B., Chowdhry I. and Islam M.,"Study of the nature radionuclides concentration in area of elevated radiation protection and dosimetry", Journal of Radiation Protection Dosimetry, Vol.98, No. 2, PP. 227-230, (2002).

[18] Singh S., Rani A. and Mahajan R. K., "226 Ra, 232Th and40 K Analysis in Soil Samples from Some Areas of Punjab and Himachal Pradesh,India Using Gamma Ray Spectrometry ", Journal of Radiation Measurements, Vol. 39,No.4,PP. 431-439, (2004).

[19] Yousef M. I. and Abu EI-Ela, "Natural Radioactivity Levels in Surface Soil of Kitchener Drain in the Nile Delta of Egypt", Journal of Nuclear and Radiation Physics, Vol. 2, No.1, PP.61-68, (2007).

[20] محمد قاسم خضير وعبد الرضا حسين صبر،"قياس مستوى الاشعاع الطبيعي في التربة السطحية في مناطق منتخبة من محافظة البصرة"، مجلة ابحاث البصرة - العلميات،العدد40، الجزء 3،ص88-96، (2014).

[21] كوثر حسن عبيس، "قياس ودراسة النشاط الاشعاعي الطبيعي لنماذج من التربة للدوائر الرسمية في محافظة القادسية"، رسالة ماجستير، جامعة الكوفة، (2012).

[22] United Nations Scientific Committee on the Effects of Atomic Radiation, "Sources and Effects of Ionizing Radiation", Report to General Assembly, United Nations, New York, (1993).

[10] Okeyode I. and Oluseye A.,»Studies of the Terrestrial outdoor Gamma Dose Rate Levels in Ogun-Osun River Basins Development Authority Headquarters, Abeokuta, Nigeria «, Journal of Physics International, Vol. 6,No. 1,PP.1-8, (2010).

[11] Harb S. R., "On the human radiation exposure as derived from the analysis of natural and man-made radionuclides in soil", Ph.D. thesis, Hanover University, Germany, (2004).

[12] Vosniakos F., Zavalaris K. and Papaligas T., "Indoor concentration of natural radioactivity and the impact to human health", Journal of Environ. Protect. Ecol., Vol. 4, No. 3, PP. 733-737 (2003).

[13] Beretka J. and Mathew P.J., "Natural radioactivity of Australian building materials, industrial wastes and by-products", Journal of Health Physics, Vol. 4 No. 8, PP. 87-95 (1985).

[14] Mirjana B. and Scepan S., "Radioactivity of sand from several renowned public beaches and assessment of the corresponding environmental risks ",Journal of the Serbian Chemical Society,Vol.74,No.4,PP.461-470, (2009).

[15] Papadopoulos A., Christofides G., Koroneos A., Papadopoulou L., Papastefanou C. and Stoulos S.," Natural radioactivity and radiation index of the major plutonic bodies in Greece", Journal of Environmental Radioactivity, Vol. 12, No. 4,PP:227-238, (2013).

[16] Jose A., Jorge J., Cleomacio M., Sueldo V. and Rom-

الجدول (4) معدل تركيز الفعالية النوعية للثوريوم -232، لليورانيوم -238 وللبوتاسيوم -40 لبعض الدراسات السابقة

ت	موقع الدراسة	معدل تركيز الفعالية النوعية ($Bq.Kg^{-1}$)			المصدر
		^{232}Th	^{238}U	^{40}K	
1	كوستاريكا	11	46	140	[11]
2	تايلاند	51	114	230	
3	نيجيريا	25	30	370	
4	كازخستان	60	37	300	
5	ماليزيا	82	66	310	
6	بنغلادش	19	24	360	[17]
7	الهند	87	57	143	[18]
8	مصر	5.83	9.07	44.81	[19]
9	البصرة	41.1	11.9	499.2	[20]
10	النجف الاشرف	12.10	23.59	60.68	[9]
11	مركز محافظة القادسية	20.55	1.917	262.43	[21]
12	نواحي محافظة القادسية	29.84	3.82	421.15	
13	المدى العالمي	(7-50)	(15-50)	(100-700)	[22]
14	مدينة نيبور الأثرية	1.058	9.703	636.054	الدراسة الحالية

References المصادر

[1] Tzortzis M. Svoukis, E. and Tsetos H.,"Comprehensive Study of Natural Gamma Radioactivity Levels and Associated Dose Rates from Surface Soils in Cyprus", Journal of Radiation Protection Dosimetry,Vol.(109), No.(3),PP:217-224,(2004).

[2] Iqbal M., Tufail M. and Mirza S., "Measurement of Natural Radioactivity in Marble Found in Pakistan Using a Nal(Tl) Gamma-Ray Spectrometer ",Journal of Environmental Radioactivity, Vol.(51), No.(2),PP:255-265,(2000).

[3] غلن فريدريك نول، "كشف وقياس الإشاعات"، ترجمة مريم مختار عتيق، دار الكتب الوطنية، ليبيا، (2006).

[4] Maher O. and Abu Saleh R.," radiation measurements in soil in the middle of Gaza-strip using nuclear track detectors CR-39 ," Journal Al-Aqsa University,Vol10., pp).2006) ,273-280 .

[5] United Nations Scientific Committee on the Effects of Ionizing Radiation Report, «Sources and Effects of Ionizing Radiation››, United Nations, New York, (2000).

[6] محمد صفوت السيوفي،"فيزياء الطب النووي"، دار النشر للجامعات، القاهرة، (2010).

[7] Gilmore G. and Heminngway J., "Practical gamma-ray spectrometry", 1st Edition, John Wiley & Sons, New York, (1995).

[8] قحطان رشيد صالح، "الكشاف الأثـري في العراق"، دار الكتب، العراق، (1987).

[9] Heiyam N., Ali K. and Hussein J., " Measurement Natural Radioactivity in Soil Samples from Important historical locals in Alnajaf Alashraf city, Iraq", Journal of Advances in Chemistry, Vol.(8), No.(1), PP:1472-1478, (2014).

- كما وجدت أعلى قيمة لمعامل الخطورة الخارجي H_{ex} كانت $Bq.Kg^{-1}$ (0.175) في نموذج رقم (9) قرب مقبرة المدينة، وأقل قيمة كانت $Bq.Kg^{-1}$ (0.140) في نموذج رقم (25) بالقرب من بناية مركز حماية المدينة الأثرية وكان معدل هذه القيم $Bq.Kg^{-1}$ (0.163).
- كما وجدت أعلى قيمة للجرعة الممتصة في الهواء كانت nGy/h (34.174) في نموذج رقم (9) قرب مقبرة المدينة، واقل قيمة كانت nGy/h (27.071) في نموذج رقم (25) بالقرب من بناية مركز حماية المدينة الأثرية وكان معدل هذه القيم nGy/h (31.648).
- وكانت أعلى قيمة للجرعة الفعالة السنوية الداخلية هي mSv/yr (1.006) في نموذج رقم (9) قرب مقبرة المدينة، وأقل قيمة كانت mSv/yr (0.797) في نموذج رقم (25) بالقرب من بناية مركز حماية المدينة الأثرية وكان معدل هذه القيم mSv/yr (0.926).
- اما الجرعة الفعالة السنوية الخارجية كانت أعلى قيمة mSv/yr (0.251) في نموذج رقم (9) قرب مقبرة المدينة، وأقل قيمة كانت mSv/yr (0.199) في نموذج رقم (25) بالقرب من بناية مركز حماية المدينة الأثرية وكان معدل هذه القيم mSv/yr (0.233).
- نلاحظ من خلال المناقشة أنه أعلى قيم تكون في المواقع الاثرية التي لم يكن فيها أي تغير في تربتها ومحمية مثل موقع البرج المدرج ومقبرة المدينة الأثرية وغيرها من المواقع الأثرية أما أقل قيم كانت في مواقع تم أنشاؤها منذ مدة زمنية ليست بعيدة حيث تم وضع طبقات من التراب مثل الموقع القريب من الشارع العام ومركز حماية المدينة الأثرية.

6. مقارنة النتائج مع دراسات سابقة
Compare the results with previous studies

يوضح الجدول (4) معدل بعض الدراسات المحلية والعربية والعالمية ومقارنتها بالدراسة الحالية، حيث أجريت في السنوات السابقة عدد من الدراسات لحساب النشاط الإشعاعي الطبيعي للنويدات المشعة طبيعيا في التربة من خلال حساب تر كيز الفعالية النوعية لليورانيوم –238 وللثوريوم –232 والبوتاسيوم –40.

7. الاستنتاجات Conclusions

وجد أن قيم النشاط الإشعاعي النوعي العائد لنظير الثوريوم ^{232}Th ونظير اليورانيوم ^{238}U ونظير البوتاسيوم ^{40}K توزعت على نسب متفاوتة بالنسبة لمدينة نيبور (نفر) الاثرية وهي ضمن المدى المسموح به عالميا. وإن أغلب نتائج معاملات الخطورة الاشعاعية لكل من مكافئ الراديوم ومعامل تركيز الفعالية ومعامل الخطورة الداخلي والخارجي والجرعة الممتصة والجرعة الفعالة للنماذج التربة كانت ضمن الحد المسموح به عالمياً، ماعدا زيادة طفيفة للجرعة الفعالة السنوية الداخلية في نموذجين وهي لا تشكل خطراً ملحوظاً ونعتقد سبب ارتفاعها نتيجة الاخطاء العشوائية في القياس. يمكن تصنيف مدينة نيبور (نفر) الاثرية في محافظة القادسية ضمن المناطق التي يكون فيها النشاط الإشعاعي الطبيعي ضمن الحدود المسموح بها وذلك اعتمادا على هذه النتائج ولا تشكل خطراً على البشر (الموظفين والسياح) والساكنين بالقرب من هذه المنطقة.

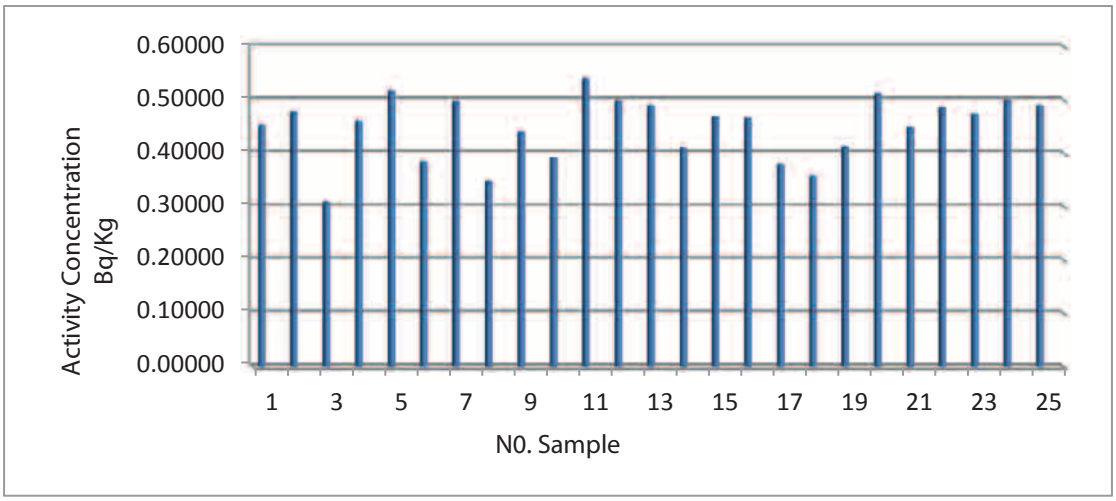

شكل **(8)** تركيز الفعالية النوعية ^{235}U

5. المناقشة Discussion

- أعلى قيمة للفعالية النوعية للثوريوم ^{232}Th كانت (0.0281.293±) $Bq.Kg^{-1}$ في نموذج رقم (16) الواقع بالقرب من البرج المدرج، وأقل قيمة كانت $Bq.Kg^{-1}$ (0.065±0.006) في نموذج رقم (3) قرب الشارع العام المبلط وكان معدل هذه القيم $Bq.Kg^{-1}$ (1.058).
- وبالنسبة لليورانيوم ^{238}U فأن أعلى قيمة للفعالية النوعية $Bq.Kg^{-1}$ (11.691±0.298) كانت في نموذج رقم (11) نهاية بقايا بناء المدينة الاثرية، وأقل قيمة كانت $Bq.Kg^{-1}$ (0.225±6.672) في نموذج رقم (3) قرب الشارع العام المبلط وكان معدل هذه القيم $Bq.Kg^{-1}$ (9.703).
- أما أعلى قيمة للفعالية النوعية للبوتاسيوم ^{40}K كانت $Bq.Kg^{-1}$ (701.469±4.383) في نموذج رقم (14) الواقع بين منطقة الغابات المحيطة بالمدينة وتل الصخرة، وأقل قيمة كانت $Bq.Kg^{-1}$ (514.982±4.425) في نموذج رقم (25) قرب بناية مركز حماية المدينة الأثرية وكان معدل هذه القيم $Bq.Kg^{-1}$ (636.054).
- وكان لليورانيوم ^{235}U أعلى قيمة للفعالية النوعية $Bq.Kg^{-1}$ (0.53876) كانت في نموذج رقم (11) نهاية بقايا بناء المدينة الأثرية، وأقل قيمة كانت $Bq.Kg^{-1}$ (0.30747) في نموذج رقم (3) قرب الشارع العام المبلط وكان معدل هذه القيم $Bq.Kg^{-1}$ (0.44716).
- وأن أعلى قيمة لمكافئ الراديوم Ra_{eq} كانت $Bq.Kg^{-1}$ (64.808) في نموذج رقم (9) قرب مقبرة المدينة، وأقل قيمة كانت $Bq.Kg^{-1}$ (51.865) في نموذج رقم (25) بالقرب من بناية مركز حماية المدينة الأثرية وكان معدل هذه القيم $Bq.Kg^{-1}$ (60.158).
- بالنسبة لمعامل تركيز الفعالية I_γ فكانت أعلى قيمة له $Bq.Kg^{-1}$ (0.540) في نموذج رقم (9) قرب مقبرة المدينة، وأقل قيمة كانت $Bq.Kg^{-1}$ (0.425) في نموذج رقم (25) بالقرب من بناية مركز حماية المدينة الأثرية وكان معدل هذه القيم $Bq.Kg^{-1}$ (0.499).
- وأعلى قيمة لمعامل الخطورة الداخلي H_{in} كانت $Bq.Kg^{-1}$ (0.201) في نموذج رقم (9) قرب مقبرة المدينة، وأقل قيمة كانت $Bq.Kg^{-1}$ (0.165) في نموذج رقم (3) قرب الشارع العام المبلط وكان معدل هذه القيم $Bq.Kg^{-1}$ (0.189).

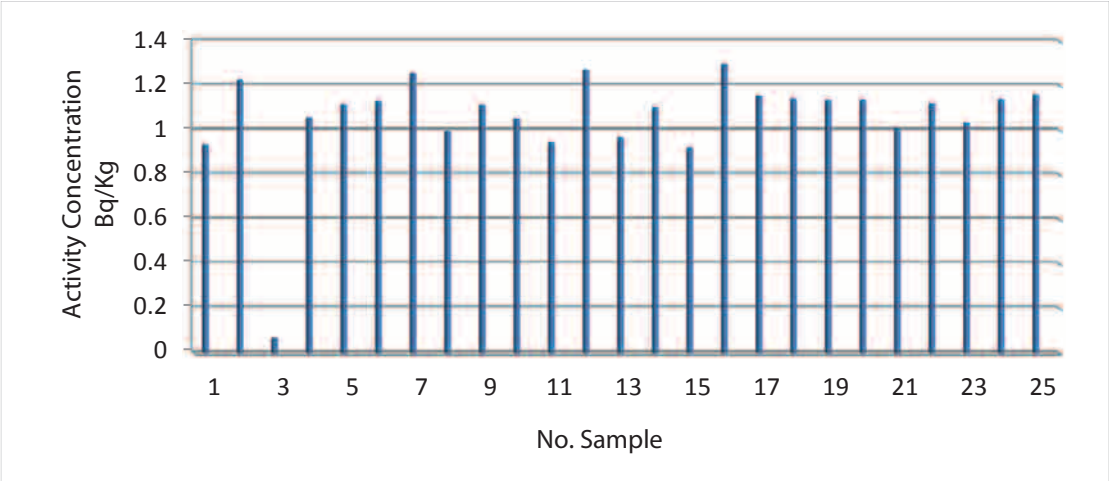

شكل (5) تركيز الفعالية النوعية ^{232}Th

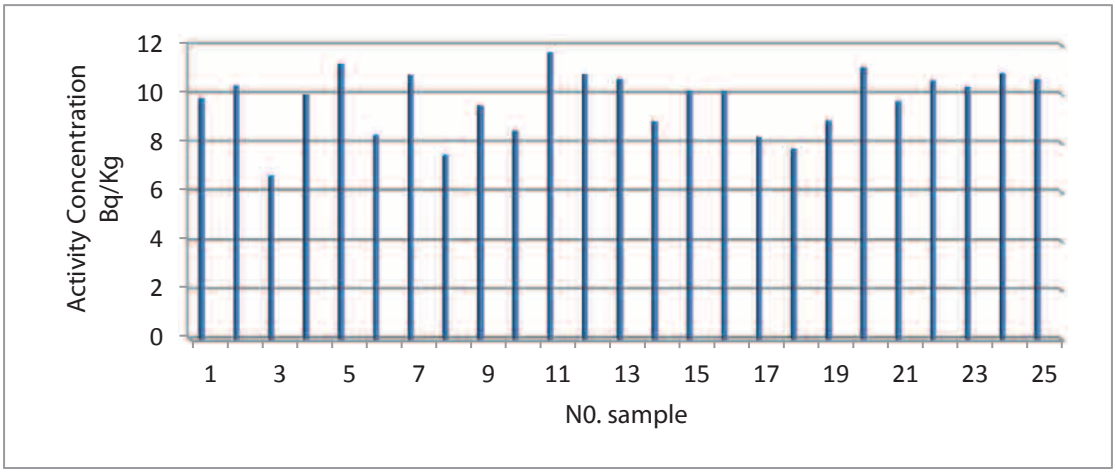

شكل (6) تركيز الفعالية النوعية ^{238}U

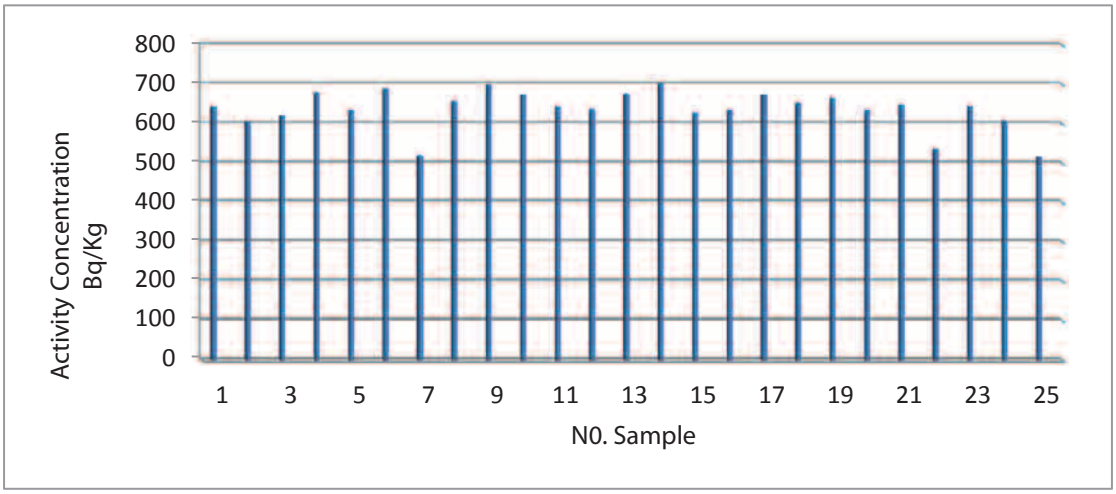

شكل (7) تركيز الفعالية النوعية ^{40}K

جدول (3) قيم معاملات الخطورة لكل من تركيز مكافئ الراديوم (Ra_{eq}) ومعامل تركيز الفعالية (I_γ) ومعامل الخطورة الداخلي (H_{in}) والخارجي (H_{ex}) وقيم كل من الجرعة الممتصة في الهواء والجرعة الفعالة السنوية الداخلية والخارجية.

No. Sample	Ra_{eq} ($Bq.Kg^{-1}$)	I_γ ($Bq.Kg^{-1}$)	Hazard Index ($Bq.Kg^{-1}$)		Absorbed Dose Rate (nGy/h)	Annual Effective Dose (mSv/y)	
			H_{in}	H_{ex}		Indoor	Outdoor
1S	60.578	0.503	0.190	0.164	31.886	0.939	0.235
2S	58.614	0.484	0.186	0.158	30.737	0.905	0.226
3S	54.482	0.458	0.165	0.147	28.965	0.853	0.213
4S	63.615	0.528	0.199	0.172	33.501	0.986	0.247
5 S	61.542	0.508	0.197	0.166	32.270	0.950	0.237
6 S	62.860	0.525	0.192	0.170	33.212	0.978	0.244
7S	52.489	0.430	0.171	0.142	27.382	0.806	0.201
8S	59.504	0.498	0.181	0.161	31.479	0.927	0.232
9 S	64.808	0.540	0.201	0.175	34.174	1.006	0.251
10 S	61.826	0.516	0.190	0.167	32.651	0.961	0.240
11 S	62.401	0.515	0.200	0.169	32.722	0.963	0.241
12 S	61.553	0.508	0.195	0.166	32.286	0.950	0.238
13 S	63.929	0.530	0.201	0.173	33.634	0.990	0.247
14 S	64.425	0.538	0.198	0.174	34.019	1.001	0.250
15 S	59.774	0.495	0.189	0.161	31.427	0.925	0.231
16 S	60.710	0.503	0.191	0.164	31.881	0.938	0.235
17 S	61.673	0.515	0.189	0.167	32.573	0.959	0.240
18 S	59.460	0.497	0.181	0.161	31.414	0.925	0.231
19 S	61.700	0.514	0.191	0.167	32.536	0.958	0.239
20 S	61.490	0.508	0.196	0.166	32.248	0.949	0.237
21 S	60.971	0.506	0.191	0.165	32.097	0.945	0.236
22 S	53.269	0.438	0.172	0.144	27.844	0.820	0.205
23 S	61.212	0.507	0.193	0.165	32.178	0.947	0.237
24 S	59.188	0.488	0.189	0.160	31.022	0.913	0.228
25 S	51.865	0.425	0.169	0.140	27.071	0.797	0.199
Max.	64.808	0.540	0.201	0.175	34.174	1.006	0.251
Min.	51.865	0.425	0.165	0.140	27.071	0.797	0.199
Ave.	60.158	0.499	0.189	0.163	31.648	0.926	0.233
W.Ave.	370	1≤	1≤	1≤	55	1	1

جدول (2) تركيز الفعالية النوعية (^{232}Th، ^{238}U، ^{40}K، ^{235}U)

No. Sample	(Bq.Kg^{-1}) Specific Activity Concentrations			
	^{232}Th	^{238}U	^{40}K	^{235}U
1S	0.935±0.24	9.804±0.273	642.458±4.195	0.45180
2S	1.223±0.027	10.334±0.280	604.827±4.394	0.47622
3S	0.065±0.006	6.672±0.225	619.736±4.120	0.30747
4S	1.056±0.025	9.963±0.275	677.637±4.308	0.45912
5 S	1.113±0.026	11.214±0.292	633.440±4.165	0.51677
6 S	1.128±0.026	8.317±0.251	687.901±4.341	0.38327
7S	1.252±0.027	10.766±0.286	519.153±4.438	0.49613
8S	0.994±0.024	7.506±0.239	657.271±4.243	0.34590
9 S	1.112±0.026	9.515±0.269	697.921±4.372	0.43848
10 S	1.051±0.025	8.469±0.253	673.900±4.296	0.39028
11 S	0.942±0.24	11.691±0.298	641.483±4.192	0.53876
12 S	1.269±0.027	10.789±0.286	636.269±4.491	0.49719
13 S	0.967±0.024	10.592±0.283	675.145±4.300	0.48811
14 S	1.102±0.026	8.871±0.259	701.496±4.383	0.40880
15 S	0.919±0.023	10.137±0.277	627.969±4.147	0.46714
16 S	1.293±0.028	10.099±0.277	633.831±4.483	0.46539
17 S	1.153±0.026	8.211±0.250	673.397±4.602	0.37839
18 S	1.1410.026±	7.741±0.242	650.988±4.223	0.35673
19 S	1.1330.026±	8.909±0.260	665.056±4.578	0.41055
20 S	1.1350.026±	11.085±0.290	634.021±4.484	0.51083
21 S	1.0060.024±	9.697±0.271	647.643±4.525	0.44687
22 S	1.1200.026±	10.524±0.282	534.833±4.486	0.48498
23 S	1.0320.025±	10.266±0.279	642.918±4.196	0.47309
24 S	1.1390.026±	10.820±0.286	607.08±4.402	0.49862
25 S	1.1600.026±	10.592±0.283	514.982±4.425	0.48811
Max.	1.293±0.028	11.691±0.298	701.496±4.383	0.53876
Min.	0.065±0.006	6.672±0.225	514.982±4.425	0.30747
Ave.	1.058	9.703	636.054	0.44716
W.Ave.	45	33	420	——

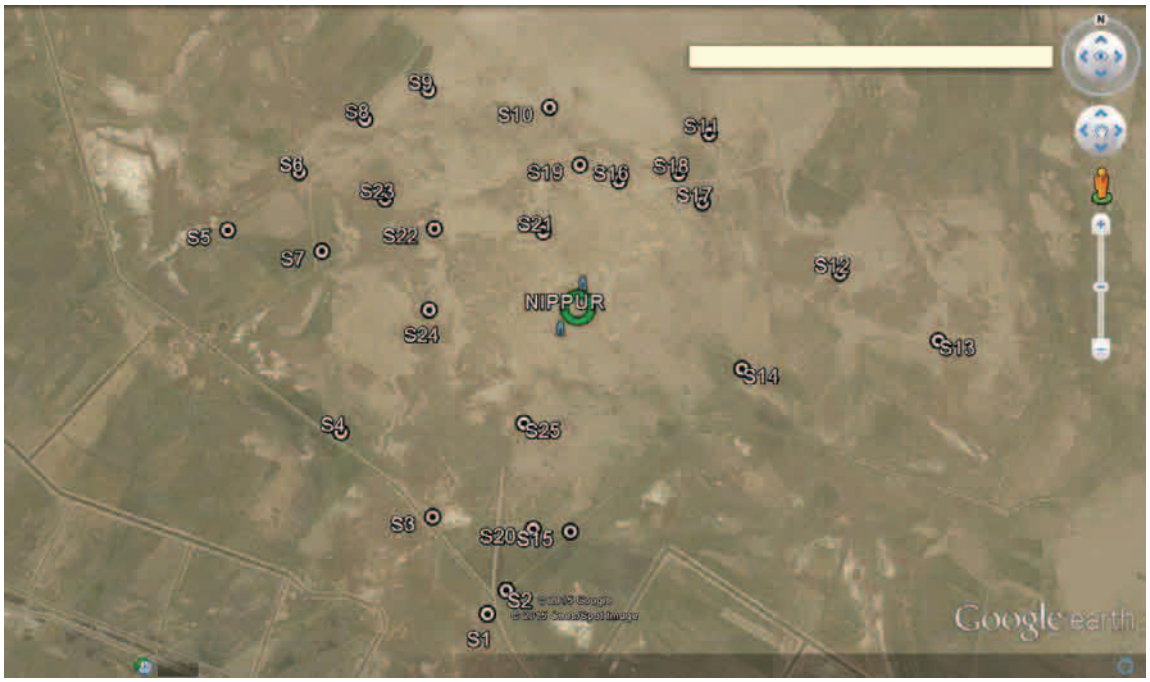

شكل **(3)** خارطة مدينة نيبور (نفر) الأثرية موضح عليها مواقع جمع النماذج

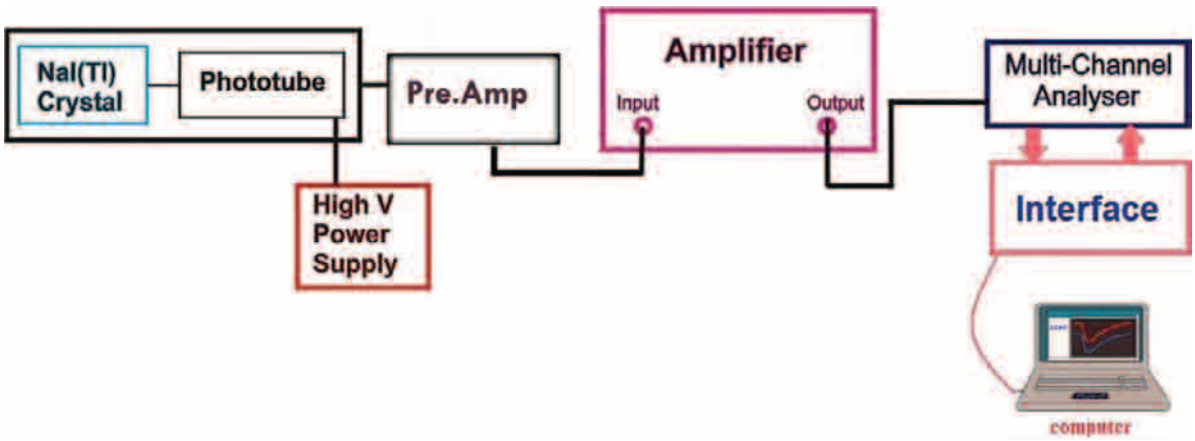

شكل **(4)** منظومة كاشف يوديد الصوديوم المطعم بالثاليوم **NaI(Tl) ("3×"3)**

4. النتائج Results

يوضح الجدول رقم (2) تركيز الفعالية النوعية للنويدات المشعة في التربة بعمق 15cm باستخدام المعادلات (1و2) بعد معايرة المنظومة مسبقا باستخدام عناصر قياسية لذلك وايجاد الكفاءة لكل عنصر من خلال منحني الكفاءة، والجدول رقم (3) يبين نتائج معاملات الخطورة المقاسة في هذا البحث للمنطقة المدروسة بالاعتماد على المعادلات من معادلة رقم (3) الى معادلة رقم (9) كما تم مقارنة النتائج المتحصل عليها مع المعدل العالمي (Worldwide Average) المسموح به [5]، والأشكال من (5) الى (8) توضح التفاوت بالقيم المتحصل عليها لتركيز الفعالية النوعية للنويدات المشعة.

شكل (1) خارطة العراق محدد فيها موقع مدينة نيبور(نفر) الأثرية

شكل (2) خارطة محافظة القادسية محدد فيها مدينة نيبور(نفر) الأثرية

جدول (1) قيم إحداثيات المواقع

Site number	Position	
	Latitude (°N)	Longitude (°E)
S1	32°06′47.5″	45°13′34.2″
S2	32°06′50.9″	45°13′37.5″
S3	32°07′01.8″	45°13′24.4″
S4	32°07′14.4″	45°13′07.9″
S5	32°07′45.3″	45°12′46.8″
S6	32°07′54.3″	45°12′59.5″
S7	32°07′42.0″	45°13′03.9″
S8	32°08′02.6″	45°13′11.3″
S9	32°08′07.2″	45°13′22.8″
S10	32°08′04.5″	45°13′45.0″
S11	32°08′00.3″	45°14′14.08″
S12	32°07′38.6″	45°14′37.4″
S13	32°07′28.3″	45°14′54.8″
S14	32°07′24.0″	45°14′19.5″
S15	32°06′59.6″	45°13′48.8″
S16	32°07′52.9″	45°13′57.6″
S17	32°07′49.5″	45°14′12.7″
S18	32°07′54.0″	45°14′08.5″
S19	32°07′55.4″	45°13′50.5″
S20	32°03′00.0″	45°13′42.2″
S21	32°07′45.0″	45°13′43.9″
S22	32°07′45.5″	45°13′24.2″
S23	32°07′50.1″	45°13′15.2″
S24	32°07′33.0″	45°13′23.4″
S25	32°07′15.8″	45°13′40.5″

حيث ان 8760 يشير الى عدد ساعات السنة.

بعد اختيار منطقة الدراسة مدينة نيبور (نفر) الأثرية في محافظة القادسية لدراسة النشاط الاشعاعي الطبيعي لنماذج من التربة تم جمع (25) نموذج بعمق 15cm، وثبتت إحداثيات المواقع باستعمال جهاز تحديد المواقع (G.P.S.) والجدول رقم (1) يبين قيم الإحداثيات المسجلة للمواقع التي تم أخذ النماذج منها والاشكال (1 و2 و3) تبين خارطة مدينة نيبور على خارطة العراق وعلى خارطة محافظة القاسية والمنطقة المدروسة موضح عليها ارقام النماذج باستخدام برنامج Google Earth على التوالي ثم يتم الحفر واستخراج العينة ووضعها في أكياس من مادة البولي أثيلين بسعة (2Kg)، وترقيمها حسب الموقع ثم تنقل الى مكان التهيئة والقياس.

لقياس النشاط الإشعاعي للنماذج يجب أن تكون التربة خالية من الرطوبة لأن قياس الفعالية النوعية يعتمد على وزن النموذج، وللتخلص من هذه الرطوبة يجب ان تجفف النماذج بتعريضها لأشعة الشمس لمدة من 2 الى 4 يوم تقريباً بمنطقة مكشوفة بحيث تصل الى وزن ثابت وبعد ذلك طحنت العينات ثم غربلت باستخدام مشبك ذي ثقوب صغيرة جداً تقريبا (0.5mm) لإزالة الحصى وجذور النباتات العالقة بها للحصول على تربة متجانسة خالية من الشوائب ثم يتم وضعها في أكياس بلاستيكية ثم ترك العينة لمدة شهر لغرض الوصول الى حالة التوازن،ثم أخذ (1Kg) لكل نموذج ونضعها داخل اسطوانة القياس Marinelli Beaker بعدها يتم القياس بوضع النموذج امام بلورة الكاشف المعايرة مسبقا والمحكمة العزل بواسطة درع رصاصي ويقاس كل انموذج لفترة 36000Sec (10h).

تم قياس النشاط الإشعاعي الطبيعي للنويدات الباعثة لأشعة كاما بالاستناد على قوة الاختراق العالية لأشعة كاما في المواد باستخدام منظومة العد والتحليل الإلكترونية المستخدمة في الكشف عن الأشعة النووية المتكونة من منظومة كاشف يوديد الصوديوم المطعم بالثاليوم NaI(Tl) (3"×3") والمجهز من شركة (Alpha Spectra Inc.-12I12/3,) المزود بمحلل متعدد القنوات ((MCA (ORTEC–Digi Base)) الذي يحتوي على 4096 قناة يربط بوحدة تسمى (ADC (Analog to Digital Convertor تساعد المحلل على تحويل النبضة القادمة الى أعداد رقمية، وإن القياسات النووية وتحليلها يتم بواسطة برنامج حاسوبي يسمى (MAESTRO-32) في داخل المختبر إذ يتم ربط أجزاء المنظومة كما في الشكل (4).

قبل القياس يجب معايرة المنظومة ويقصد بالمعايرة ايجاد العلاقة الخطية بين سعة النبضة الخارجة من الكاشف وطاقة اشعة كاما الساقطة على بلورة الكاشف [17]، ويستخدم لمعايرة طيف اشعة كاما مصادر قياسية معروفة الطاقة والشدة والغرض من تعدد المصادر هوالحصول على طيف لطاقات تستخدم في مجال البحث، وقد استخدمنا في بحثنا هذا مصادر قياسية هي (^{22}Na، ^{137}Cs، ^{54}Mn، ^{65}Zn، ^{60}Co) وإن قابلية فصل الطاقة للكاشف NaI(Tl) المستعمل في القياس هي (6.4%) بالنسبة للسيزيوم ^{137}Cs، ان التدريع المستخدم في المنظومة هوعبارة عن درع من الرصاص سمكه 5cm وطوله 20cm يحيط بالبلورة مع غطاء سمكه 5cm وقطره 22cm وكذلك تم تغطية الجزء السفلي التي تمثل قاعدة الكاشف وحامل الكاشف بالدرع ايضاً.

وهومعامل يستخدم لحساب الخطورة الناشئة عن إشعاع كاما المقترن مع النويدات الطبيعية المشعة (^{238}U، ^{232}Th، و^{40}K) في العينة المدروسة ويحسب من المعادلة الاتية [15,14]:

$$I_\gamma = \frac{A_U}{150} + \frac{A_{Th}}{100} + \frac{A_k}{1500} \quad (4)$$

3. 3. معامل الخطورة الخارجي (External Hazard Index (H_{ex})

المخاطر الخارجية تمثل المخاطر المتأينة من اشعاع كاما الطبيعي والهدف من ذلك هوالتأكد من عدم تجاوز الجرعة المؤثرة من هذه الاشعة الحدود المسموح بها ويحسب معامل الخطورة من المعادلة الآتية [16,14]:

$$H_{ex} = \frac{A_U}{370} + \frac{A_{Th}}{259} + \frac{A_k}{4810} \quad (5)$$

4. معامل الخطورة الداخلي (Internal Hazard Index (H_{in})

ان استنشاق جسيمات الفا المنبعثة من النظائر القصيرة العمر مثل الرادون والثورون التي تكون مصاحبة بأشعة كاما بطاقات مختلفة والذي يمكن التعبير عنه بدلالة معامل الخطورة الداخلي (H_{in}) ويحسب بالمعادلة الآتية [17]:

$$H_{in} = \frac{A_U}{185} + \frac{A_{Th}}{259} + \frac{A_k}{4810} \quad (6)$$

ومقدار المخاطر الداخلية يفضل أن يكون أقل من الواحد في البيئة المثالية للحصول على فرصة العمل السالم للأعضاء التنفسية ولمعيشة الأفراد.

3. 5. نسبة الجرعة المتصة في الهواء Absorbed Dose Rate in Air (*AD*)

يمكن حساب النسبة الكلية للجرعة المتصة في الهواء بدلالة تراكيز النوى الأرضية من خلال المعادلة الآتية [14]:

$$AD\ (nGy/h) = 0.462\ A_U + 0.621\ A_{Th} + 0.0417\ A_K \quad (7)$$

حيث ان (0.462، 0.621 و0.0417) هي عوامل التحويل عن النويدات المشعة التي تحدث بشكل طبيعي [9].

3. 6. الجرعة الفعالة السنوية The Annual Effective Dose

من اجل حساب الجرعة الفعالة السنوية يجب ان نأخذ بنظر الاعتبار (معامل التحويل من الجرعة المتصة الى الجرعة الفعالة وعامل الانشغال الداخلي)، ولحساب الجرعة المؤثرة للعنصر الباعث لأشعة كاما في الهواء فأن UNSCER 2000 قد نشرت ثابت التحويل 0.7 *Sv/Gy* كعامل للتحويل من الجرعة المتصة في الهواء إلى الجرعة الفعالة السنوية المستلمة من قبل البالغين واستخدم 0.80 وهونسبة الوقت الذي يقضى في الداخل و00.2 هونسبة الوقت الذي يقضى في الخارج، ومن هذه البيانات وجد ان الجرعة الفعالة السنوية تحسب كالآتي [16,14]:

$$\text{Indoor}\ (mSv/y) = AD\ (nGy/h) \times 10^{-6} \times 8760\ h/y \times 0.80 \times 0.7\ Sv/Gy \quad (8)$$

$$\text{Outdoor}\ (mSv/y) = AD\ (nGy/h) \times 10^{-6} \times 8760\ h/y \times 0.20 \times 0.7\ Sv/Gy \quad (9)$$

السومرية الكبيرة، اذ كانت في منتصف الألف الثالث قبل الميلاد مركزاً دينياً وثقافياً لبلاد سومر تقع هذه المدينة على بعد (35Km) تقريباً الى الشمال الشرقي لمدينة الديوانية مركز محافظة القادسية، وعلى بعد (10Km) تقريباً من قضاء عفك التابع لمحافظة القادسية في وسط العراق [8] وتقدر مساحة المنطقة المدروسة تقريباً ($25Km^2$).

3. المواد وطرائق العمل Methods and materials of work

عند توازن اليورانيوم ^{238}U مع ولائده المشعة وكذلك الثوريوم ^{232}Th وولائده باعتبار إن فعالية جميع عناصر السلسلتين الإشعاعيتين في حالة توازن لذلك من الممكن أن يُحسب تركيز عنصر في أي سلسلة بدلالة تركيز عنصر آخر، حيث تنبعث مجموعة من أشعة كاما يمكن تمييز عائدتها، فقد تم حساب تركيز الفعالية لكل من ^{232}Th من خلال حساب تركيز الفعالية لنويدة الثاليوم ^{208}Tl المشعة بطاقة 2614.511 KeV و^{238}U من خلال حساب تركيز الفعالية لنويدة البزموث ^{214}Bi بطاقة مقدارها 1764.539KeV وايضا يحسب تركيز نويدة البوتاسيوم ^{40}K المشعة بطاقة 1460.822KeV ويمكن حساب تركيز الفعالية النوعية من خلال المعادلة [10,9]:

$$A = \frac{N_{net}}{\varepsilon . I_\gamma . m . t} \pm \frac{\sqrt{N_{net}}}{\varepsilon . I_\gamma . m . t} [Bq . kg^{-1}] \quad (1)$$

اذ N_{net} صافي المساحة تحت منحني القمة الضوئية (Area under photo-peak)

ε الكفاءة المحسوبة للخط الكامي عند طاقة معينة

I_γ معامل تركيز الفعالية

m كتلة النموذج (Kg)

t زمن القياس (sec).

إن نسبة اليورانيوم ^{238}U هي 99.25% من اليورانيوم الطبيعي بينما تبلغ نسبة اليورانيوم ^{235}U (0.72%) من نسبة اليورانيوم الطبيعي الموجود في التربة فقد تم تقدير تركيز الفعالية لليورانيوم A_{U-235} من خلال العلاقة بينه وبين تركيز الفعالية لليورانيوم A_{U-238} وفق المعادلة الاتية [11].

$$A_{u-235} = \frac{A_{u-238}}{21.7} \quad (2)$$

بالاعتماد على تراكيز الفعالية لكل من الثوريوم ^{232}Th واليورانيوم ^{238}U والبوتاسيوم ^{40}K فقد تم حساب عدة معاملات للخطورة الاشعاعية وهي:

3. 1. مكافئ الراديوم (Radium Equivalent (Ra_{eq})

قيمة التركيز المكافئ لعنصر الراديوم (Ra_{eq}) الذي يستخدم لتقدير خطر التركيز المتسبب من فعالية ^{238}U و^{232}Th و^{40}K بوحدات $Bq.Kg^{-1}$ يحسب من المعادلة الاتية [13,12]:

$$Ra_{eq}\ (Bq.kg^{-1}) = A_U + 1.43\ A_{Th} + 0.077\ A_K \quad (3)$$

حيث ان A_k, A_{Th}, A_U تركيز الفعالية لليورانيوم وللثوريوم والبوتاسيوم على التوالي، وإن أعلى قيمة لـ Ra_{eq} يجب أن يكون أقل من الحد المسموح به عالميا $Bq.Kg^{-1}$ (370) [14].

3. 2. معامل تركيز الفعالية (Activity Concentration Index (I_γ)

1. المقدمة Introduction

الاشعاع يشمل الجسيمات المشحونة وغير المشحونة وهوينبعث من المواد الموجودة في الارض ويأتي مع الاشعة الكونية وينبعث ايضا في التجارب النووية والعلاج الطبي ويقسم الى نوعين احدهما طبيعي المنشئ والثاني صناعي، والنشاط الاشعاعي هوظاهرة طبيعية والعناصر المشعة طبيعيا في البيئة ينبعث منها انواع مختلفة من الاشعاع المؤين واغلبية تلك العناصر تنتمي الى احدى سلاسل الانحلال الاشعاعي الطبيعي [2,1] العناصر المشعة موجودة منذ خلق الارض وهي تمتلك اعمار نصفية مقدرة بمئات الملايين من السنين وهذه تقارب عمر الارض [3] تحوي القشرة الأرضية كميات صغيرة من اليورانيوم والثوريوم والراديوم فضلاً عن العديد من النظائر المشعة الأخرى بضمنها البوتاسيوم، وتمثل المواد المشعة الطبيعية واحدة من أهم مصادر تعرض الإنسان للإشعاع وبالرغم من أن هذه المواد تحوي على مستويات واطئة من الخلفية الإشعاعية الطبيعية فان الجرعة التراكمية يمكن أن تكون عالية [4] إذ إن التعرض للإشعاع الذي يتسلمه الإنسان من المصادر الطبيعية هواكبر بكثير من الجرعة الإشعاعية من المصادر الصناعية [5] عندما يتعرض الكائن الحي للإشعاعات المؤينة فأنها تتفاعل أولاً مع الجزيئات التي تكون المادة الخلوية (الماء، البروتينات، الاحماض الامينية، الانزيمات، الدهون، ...) ولهذا تحدث الاصابة أولاً على المستوى الجزيئي تستحث التغيرات على هذا المستوى تغيرات في التركيب البنائي للمكونات الخلوية مما يؤثر في أدائها الوظيفي أوحتى قد يؤدي الى تدميرها، تحدث الاصابة الاشعاعية للنسيج أوالعضوالبشري نتيجة تأثيرات غير مباشرة على مكونات الخلية أونتيجة تفاعل مباشر مع المركبات العضوية الحساسة للخلية [6] من خلال حساب تركيز الفعالية النوعية للنويدات المشعة في التربة كذلك يمكن حساب معاملات الخطورة وهناك وسائل وطرق مختلفة ابتكرت لقياس التركيز النوعي لأشعة كاما حيث تحسب الكميات المتواجدة في التربة للعناصر المشعة ومنها كاشف يوديد الصوديوم المطعم بالثاليوم Na(Tl) وهواشهر الطرق المستخدمة بسبب كفاءته العالية [7,3].

هدف هذه الدراسة هوتقدير مستوى تراكيز الفعالية النوعية للنويدات المشعة طبيعيا (NORM) من الثوريوم ^{232}Th، اليورانيوم ^{238}U، البوتاسيوم K^{40} واليورانيوم ^{235}U بأخذ عينات من التربة من مواقع مختلفة لمدينة نيبور (نفر) الاثرية في محافظة القادسية في وسط العراق من أجل تقييم مستوى الخلفية الاشعاعية التي تنشأ منها ورسم خارطة للإشعاع للمنطقة المدروسة في هذا العمل لتكون جزء من الخارطة الاشعاعية لمحافظة القادسية، وتتكامل مع الدراسات الحالية والمستقبلية، وكذلك حساب قيمة مكافئ الراديوم ومعامل تركيز الفعالية وكذلك معاملات الخطورة الداخلية والخارجية ونسبة الجرعة الممتصة في الهواء والجرعة الفعالة السنوية الداخلية والخارجية المؤثرة على صحة الانسان ثم مقارنة النتائج المتحصل عليها للنماذج المقاسة مع المعدل العالمي المسموح به.

2. المنطقة المدروسة The area studied

مدينة نيبور (نفر) الاثرية هي احدى الحواضر

الخلاصة

لدراسة النشاط الاشعاعي لتربة مدينة نيبور (نفر) الاثرية في محافظة القادسية اختير 25 موقعاً لأخذ العينات من المدينة وأجريت القياسات الطيفية باستعمال منظومة كاشف يوديد الصوديوم المنشط بالثاليوم NaI (Tl) الذي أبعاده ("3×"3) للفترة من 5/1/2015 الى 30/3/2015.

وجد أن الفعالية النوعية لكل من الثوريوم ^{232}Th، اليورانيوم ^{238}U، البوتاسيوم ^{40}K واليورانيوم ^{235}U في النماذج المدروسة تتراوح بين Bq/Kg (0.065±0.006) الى Bq/Kg (1.293±0.028) وبمعدل Bq/Kg (0.058) وBq/Kg (6.672±0.225) الى Bq/Kg (11.691±0.298) ومعدل Bq/Kg (9.703) وBq/Kg (514.982±4.425) الى Bq/Kg (701.496±4.383) وبمعدل Bq/Kg (636.054) وBq/Kg (0.30747) الى Bq/Kg (0.53876) وبمعدل Bq/Kg (0.44716)، على التوالي. كما حسب مكافئ الراديوم وكان يتراوح بين Bq/Kg (51.865) الى (64.808) Bq/Kg وبمعدل Bq/Kg (60.158)، ومعامل تركيز الفعالية (I_γ) فكان بين Bq/Kg (0.425) الى Bq/Kg (0.540) وبمعدل Bq/Kg (0.499)، واما معامل الخطورة الداخلي يتراوح بين Bq/Kg (0.165) الى Bq/Kg (0.201) وبمعدل Bq/Kg (0.189)، كما حسب معامل الخطورة الخارجي وكانت قيمته تتراوح بين Bq/Kg (0.140) الى /Bq (0.175) Kgوبمعدل Bq/Kg (0.163)، إما قيم الجرعة الممتصة في الهواء فقد تراوحت من nGy/h (27.071) الى (34.174) nGy/h وبمعدل nGy/h (31.648)، أما قيم الجرعة الفعالة السنوية الداخلية كانت بين mSv/y (0.797) الى (1.006) mSv/y وبمعدل mSv/y (0.926) والجرعة الفعالة السنوية الخارجية كانت بين mSv/y (0.199) الى mSv/y (0.251) وبمعدل mSv/y (0.233).

ومن مقارنة النتائج العملية مع النتائج المحسوبة عالميا وجد أن مستويات الإشعاع للنماذج المدروسة تقع ضمن الحدود المسموح بها.

الكلمات المفتاحية

طيف أشعة كاما، نشاط اشعاعي، معاملات الخطورة الاشعاعية، كاشف NaI(Tl).

دراسة النشاط الإشعاعي الطبيعي لنماذج من تربة مدينة نيبور (نفر) الأثرية في محافظة القادسية، العراق

عامر موسى كاظم و هيام ناجي هادي
قسم الفيزياء، كلية التربية للبنات، جامعة الكوفة، العراق
تاريخ الإستلام: 9/Jun/2015
تاريخ قبول النشر : 8/Aug/2015

Abstract

To study the radioactivity of soil of Nippur (Nepher) archaeological city in Qadsiyah governorate, 25 locations have been selected to take samples from this city, The gamma rays spectral measurements were done for all samples by using Iodide Sodium activated by Thallium NaI (Tl), its dimension (3"×3") for the period from 5/1/2015 to 30/03/2015.

The quality activity for Thorium ^{232}Th,Uranium ^{238}U, Potassium ^{40}K and Uranium ^{235}U in the studied samples is between (0.065) Bq/Kg to (1.293) Bq/Kg and average (1.058) Bq/Kg, (6.672) Bq/Kg to (11.691) Bq/Kg and average (9.703) Bq/Kg, (514.982) Bq/Kg to (701.496) Bq/Kg and average (636.54) Bq/Kg and (0.30747) Bq/Kg to (0.53876) Bq/Kg and average (0.44716) Bq/Kg respectively. The equivalent Radium is calculated and ranged between (51.865) Bq/Kg to (64.808) Bq/Kg and average (60.158) Bq/Kg, and the activity concentration index (I_γ) is founded between (0.425) Bq/Kg to (0.540) Bq/Kg and average (0.499) Bq/Kg, the internal risk coefficient is founded between (0.165) Bq/Kg to (0.201) Bq/Kg and average (0.189) Bq/Kg and external risk coefficient is calculated and its value ranged between (0.140) Bq/Kg to (0.175) Bq/Kg and average (0.163) Bq/Kg. The values of absorbed dose in air is ranged from (27.071) nGy/h to (34.174) nGy/h and average (31.648) nGy/h, the values of effective annual internal dose is between (0.797) mSv/y to (1.006) mSv/y and average (0.926) mSv/y and the effective dose of the annual external dose is between (0.199) mSv/y to (0.251) mSv/y and average (0.233) mSv/y.

The results comparison with internationally and it is found that the levels of radiation for samples studied within the permissible limits globally.

Key wards

Gamma ray spectrometry, natural radioactivity**,** dangers radioactive indexes, detector Na (Tl).

15	دراسة النشاط الإشعاعي الطبيعي لنماذج من تربة مدينة نيبور (نفر) الأثرية في محافظة القادسية،العراق	**عامر موسى كاظم** **هيام ناجي هادي** قسم الفيزياء، كلية التربية للبنات جامعة الكوفة، العراق.
31	استجابة ثلاث تراكيب وراثية من الذرة الصفراء (Zea mays L.) للتغذية الورقية بالمنغنيز والبورون تحت ظروف التربة الكلسية في بعض صفات النموالحاصل	* **عباس علي العامري** * **رزاق لفتة اعطية** ** **احمد نجم الموسوي** * **حميد عبد خشان الفرطوسي** * قسم المحاصيل الحقلية، كلية الزراعة، جامعة كربلاء، العراق. ** قسم علوم الحياة، كلية التربية للعلوم الصرفة، جامعة كربلاء، العراق.

كلمة العدد

الحمد لله رب العالمين، وازكى السلام وأعظم التسليم، على سيدنا محمد واله الطيبين الطاهرين الأكرمين. أما بعد:

فحقيق بمنتسبي مركز العميد الدولي للدراسات والبحوث العلمية التابع للعتبة العباسية المقدسة أن يسعدوا بمسألتين: إحداهما، إنتساب هذا المركز لسيدنا العباس بن علي بن أبي طالب صلوات الله عليهم أجمعين، وما في هذا الإنتساب من روح ومعاني، يجعل ما يصدر من هذا المركز متوضئا بهذا النور الإلهي المنبعث من شجرة آل محمد شجرة طوبى وشجرة الحقيقة التي أصلها ثابت وفرعها في السماء.

والمسألة الأخرى هي التنافس الشريف في ذات البحث والمعرفة بين منتسبي مركز العميد، وماينجم من هذا المركز من عطاء علمي مختلف في ألوانه متشابه في أهدافه وفي روح بحثه عن المعرفة العلمية.

من هنا تأتي مجلة الباهر لتكون فخر منجزات هذا المناخ العلمي الذي أريد له أن يكون مهوى أفئدة الباحثين عن البحث المستقل بعيدا عن الخطوط الحمراء (ضرة) المعرفة المجردة المنتجة.

يصدر هذا العدد ومعه يكبر حلم أن يكون لهذه المجلة العلمية، وهو ما مخطط له بأن تكون من مجلات الخط الأول في إمتلاكها معامل ارتباط وسمعة علمية لايني القائمون عليها يسعون لترصينها، والفوز بأسباب بلوغها الاهداف المنشودة.

ختاما.. تفتح المجلة أبوابها لكل باحث جاد ترتفع همته لأن يرى المنجز البحثي لأبناء أمته، يزاحم بمنكبيه المنجز البحثي لأقرانه من باحثي العالم، وليس هذا مستحيلا لمن يستحضر تاريخا مشرفا لأمتنا قوامه التطور العلمي المستنير....

وأخر دعوانا أن الحمد لله رب العالمين وصلى الله على محمد واله الطيبين الطاهرين.

الهيئة الاستشارية والتحريرية

بسم الله الرحمن الرحيم

جمهورية العراق
وزارة التعليم العالي والبحث العلمي
دائرة البحث والتطوير

Republic of Iraq
Ministry of Higher Education & Scientific Research
Research & Development

الرقم : ب ت ٤ / ٤٠٢١
التاريخ : ٢٠١٥/٠٥/١٨

No:
Date:

العتبة العباسية المقدسة / مركز العميد للدراسات والبحوث

م / مجلة الباهر

السلام عليكم ورحمة الله وبركاته...

استنادا الى الية اعتماد المجلات العلمية الصادرة عن مؤسسات الدولة، وبناءً على توافر شروط اعتماد المجلات العلمية لأغراض الترقية العلمية في "**مجلة الباهر** "الصادرة عن مركزكم تقرر اعتمادها كمجلة علمية محكمة ومعتمدة للنشر العلمي والترقية العلمية .

... مع التقدير

أ.د. غسان حميد عبد المجيد
المدير العام لدائرة البحث والتطوير
٢٠١٥/٥/ ١٨

نسخة منه الى//
- مكتب السيد المدير العام / إشارة الى موافقة سيادته بتاريخ ٢٠١٥/٥/١٧/ للتفضل بالاطلاع ... مع التقدير .
- قسم الشؤون العلمية/ شعبة التأليف والنشر والترجمة
- الصادرة

www.rddiraq.com
Emailscientificdep@rddiraq.com

18. تخضع البحوث لتقويم سري لبيان صلاحيّتها للنشر ولا تعاد البحوث الى أصحابها سواء أقبِلت للنشر أم لم تقبل وعلى الآليه الآتية:

أ. يبلّغ الباحث بتسلّم بحثه أثناء مدّة أقصاها أسبوعان من تاريخ التسلّم.

ب. يخطر أصحاب البحوث المقبولة للنشر بموافقة هيأة التحرير على نشرها.

ت. البحوث التي يرى المقّومون وجوب إجراء تعديلات أو إضافات عليها قبل نشرها تعاد الى أصحابها مع الملاحظات المحددة كي يعملوا على إعدادها نهائيا للنشر.

ث. يبلغ الباحث في حال الإعتذار عن نشر بحثه.

ج. يمنح كل باحث نسخة واحدة من العدد الذي نشر فيه بحثه.

19. يراعى في أسبقية النشر:

أ. البحوث المشاركة في المؤتمرات التي تقيمها جهة الإصدار.

ب. تاريخ تسلم رئيس التحرير للبحث.

ت. تاريخ تقديم البحوث التي يتم تعديلها.

قواعد النشر في المجلة

مثلما يرحب العميد أبو الفضل عليه السلام بزائريه من أطياف الإنسانية، تُرحب مجلة الباهر بنشر البحوث العلمية على وفق الشروط الاتية:

1. تنشر المجلة البحوث العلمية في مجالات العلوم المتنوّعة التي تلتزم بمنهجية البحث العلمي وخطواته المتعارف عليها عالميا ومكتوبة بإحدى اللغتين العربية أو الانكليزية التي لم يسبق نشرها.
2. أن تحتوي الصفحة الاولى من البحث على عنوان البحث واسم الباحث او الباحثين وجهة العمل ورقم الهاتف باللغتين العربية والانكليزية والبريد الالكتروني مع مراعاة عدم ذكر اسم الباحث أو الباحثين في صلب البحث أو اية اشارة إلى ذلك.
3. ترسل البحوث على الموقع الالكتروني للمجلة albahir.alkafeel.net من خلال ملء إستمارة إرسال البحوث.
4. ضرورة كتابة خلاصة البحث وعنوانه باللغتين العربية والانكليزية.
5. ملء التعهد الخاص بالمجلة الذي يتضمن حقوق النشر الخاصة بمجلة الباهر العلمية ومراعاة شروط الامانة العلمية في كتابة البحث.
6. يطبع البحث على ملف word وعدم استعمال scan في الاشكال البيانية.
7. اعداد الصفحة (2 سم للجهات الاربع للصفحة).
8. يكون نوع الخط Time new roman وحجم الخط لعنوان البحث الرئيس (16غامق) اما العناوين الثانوية (14غامق) بينما مادة البحث (14).
9. نوع الفقرة single مسافة بادئة خاص (بلا) قبل النص:(.) بعد النص (.) تباعد الاسطر (مفرد) قبل النص (.) بعد النص(.).
10. عدم استعمال الاطارات و الزخارف.
11. يتم ذكر المصادر في البحث باتباع اسلوب الترقيم بحسب اسبقية ذكر المصدر وتذكر المصادر في نهاية البحث.
12. تكون الرسوم ملونة واضحة مع مراعاة وضعها في مربع نص ووضعها في نهاية البحث.
13. تكتب الهوامش ان وجدت في نهاية البحث قبل المصادر.
14. لاتتجاوز عدد الصفحات 25 صفحة.
15. يمنح البحث مكافأة مالية في حال قبوله للنشر.
16. أن لا يكون البحث قد نشر سابقاً وليس مقدما إلى أية وسيلة نشر أخرى وعلى الباحث تقدم تعهد مستقل بذلك.
17. تعبر الأفكار المنشورة في المجلة عن آراء كاتبيها ولا تعبّر بالضرورة عن وجهة نظر جهة الإصدار ويخضع ترتيب البحوث المنشورة لموجبات فنية.

الترقيم الدولي
ردمد: ٢٣١٢-٥٧٢١
ردمد الالكتروني ٢٣١٣-٠٠٨٣
رقم الإيداع في دار الكتب و الوثائق العراقية ١٩٩٦ لسنة ٢٠١٤
كربلاء المقدسة - جمهورية العراق

Tel: +964 032 310059
Mobile: +964 760 235 5555
http://albahir.alkafeel.net
Email: albahir@alkafeel.net

جمهورية العراق
ديوان الوقف الشيعي

البصائر

مجلة فصلية محكمة
تختص بالعلوم الطبيعية والهندسية

تصدر عن
العتبة العباسية المقدسة
مركز العميد الدولي للبحوث والدراسات

مجازة من
وزارة التعليم العالي والبحث العلمي
معتمدة لأغراض الترقية العلمية

السنة الأولى، المجلد الأول، العددان الأول والثاني
شعبان ١٤٣٦ هـ، حزيران ٢٠١٥ م

جمهورية العراق

ديوان الوقف الشيعي

البصائر

ردمد
٢٣١٢-٥٧٢١
ردمد الإلكتروني
٢٣١٣-٠٠٨٣

مجلة فصلية محكمة تختص بالعلوم الطبيعية والهندسية

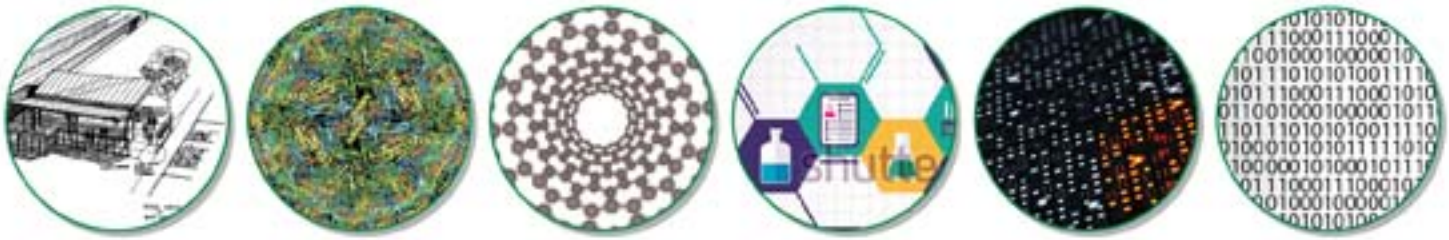

The influence of some additives on flammability and mechanical properties of modified polyester containing heterocyclic ring composites

Molecular and bioinformitic analysis of ITS1 region of three Eimeria species in Kerbala and Babylon provinces , Iraq

Spectroscopic Properties of Different Concentration Xanthene's Dye Mixture (6G, 3GO, B & C) Solution in Chloroform

Computation of inheritance share in Islamic Law by an expert system using Decision Tables

السنة الأولى – المجلد الأول – العددان الأول والثاني
شعبان ١٤٣٦ هـ - حزيران ٢٠١٥ م